DESCRIPTIONS, PETROLOGY, PHOTOGRAPHS, AND PHOTOMICROGRAPHS OF CORE FROM THE GREEN RIVER FORMATION, SOUTH-CENTRAL UINTA BASIN, UTAH

by

S. Robert Bereskin, Bereskin and Associates, Salt Lake City, Utah, and

Craig D. Morgan and Kevin P. McClure, Utah Geological Survey, Salt Lake City, Utah

Miscellaneous Publication 04 - 2
Utah Geological Survey
a division of
2004 Utah Department of Natural Resources

DESCRIPTIONS, PETROLOGY, PHOTOGRAPHS, AND PHOTOMICROGRAPHS OF CORE FROM THE GREEN RIVER FORMATION, SOUTH-CENTRAL UINTA BASIN, UTAH

by

S. Robert Bereskin, Bereskin and Associates, Salt Lake City, Utah, and

Craig D. Morgan and Kevin P. McClure, Utah Geological Survey, Salt Lake City, Utah

Cover photo: Federal 2-33 well (NW1/4NE1/4, section 33, T. 8S., R. 16E., SLBLM), Duchesne County Utah. Box 2 of 3 with core from 5657 to 5667 feet from the Travis interval in the Green River Formation. Core is housed at the Utah Geological Survey Core Research Center. Core description by S. Robert Bereskin is available in Appendix A. Photographed by Tom Dempster, Utah Geological Survey.

ISBN 1-55791-702-7

Miscellaneous Publication 04 - 2
Utah Geological Survey
a division of
2004 Utah Department of Natural Resources

STATE OF UTAH
Olene S. Walker, Governor

DEPARTMENT OF NATURAL RESOURCES
Robert Morgan, Executive Director
UTAH GEOLOGICAL SURVEY
Richard G. Allis, Director

For publications, contact
Natural Resources Map/Bookstore
1594 W. North Temple
tel. 801-537-3320
toll-free 1-888-UTAH MAP
http:\\geostore.utah.gov
email geostore@utah.gov

To contact the Utah Geological Survey
1594 W. North Temple, Ste 3110
Salt Lake City, UT 84116
tel. 801-537-3300
http:\\geology.utah.gov

CONTENTS

TABLE

ILLUSTRATIONS

ABSTRACT

Anastamosing, low-gradient, distributary channel deposits in the lower and middle members of the Eocene Green River Formation are the primary oil reservoirs in the south-central portion of the Uinta Basin, Utah. The Eocene depocenter was situated along the fluctuating southern shoreline of Lake Uinta, where complex deposits of the marginal-lacustrine environment were commonly laid down.

The Green River Formation contains several fining-upward sequences that can be recognized in outcrop, core, and well logs. Each sequence is about 60 to 120 feet (18–36 m) thick and consists of strata typically 30 to 35 feet (9–11 m) thick that were deposited during multiple lake-level fluctuations. The subaerial to subaqueous channels commonly possess an erosional base and exhibit a fining-upward character. Bedding features commonly range from large-scale trough and planar cross-bedded (or lamination) facies at the base, to a climbing ripple facies near the uppermost bed boundary. The best reservoir quality is typically within the laminated to cross-stratified facies, and the poorest reservoir quality is within the climbing ripple facies which usually possesses more deleterious micas and/or detrital clays.

Diagenesis exerts a major control on reservoir quality. Some sandstone beds were cemented early by an iron-poor calcite cement, which was often later leached resulting in good reservoir quality rock with secondary intergranular porosity (up to 20 percent) and permeability (10 to 100 millidarcies [md]). Without early calcite cementation, reservoir quality was often reduced by intense compaction, silicic and iron-rich carbonate cements, and authigenic clays.

INTRODUCTION

The Utah Geological Survey (UGS) led a four-year study of the lower and middle members of the Eocene Green River Formation in the south-central Uinta Basin, Utah (figure 1). The Green River is a highly oil-productive formation consisting of lacustrine and marginal-lacustrine rocks deposited in and around Paleocene- to Eocene-aged Lake Uinta. The objectives of the study were to increase both primary and secondary hydrocarbon recovery through improved characterization of fluvial-deltaic lacustrine reservoirs, thereby preventing premature abandonment of producing wells.

We examined core from wells that produce oil from the Green River Formation in the south-central Uinta Basin, informally referred to as the Monument Butte area (table 1). Appendix A presents detailed descriptions and graphical displays of each core. We included graphical representations of any density, neutron, resistivity, and gamma-ray logs that were run over the cored interval, and porosity and permeability curves for core that had plug analysis data. We also photographed selected core and thin sections: the photographs can be accessed by using the bookmarks or by clicking on the hyperlinks right of the depth column in the conventional core description. The hyperlink labels are: (1) Box, (2) Cp, and (3) TS.

Box = core box photograph, usually containing 5 to 18 feet (1.5–5.5 m) of core per box.

Cp = core photograph, a core piece, typically 12 inches (30 cm) or less, selected to show detailed bedding features.

TS = thin section photomicrograph.

Numerous whole and slabbed cores were available from the Utah Geological Survey Core Research Center in Salt Lake City. After an initial foot-by-foot analysis of 21 cores we made thin sections from sidewall and whole core material, and selected samples for scanning electron microscopy (SEM). Corresponding well logs and routine core analysis data were obtained for the cored intervals. In some cases, we used archived thin sections and/or thin section descriptions from graduate theses for petrographic interpretation when the original core could not be found.

In addition to descriptions of the basic mineralogy, lithology, and textural and structural characterisitics of the Green River Formation, this report also describes the complex forms of

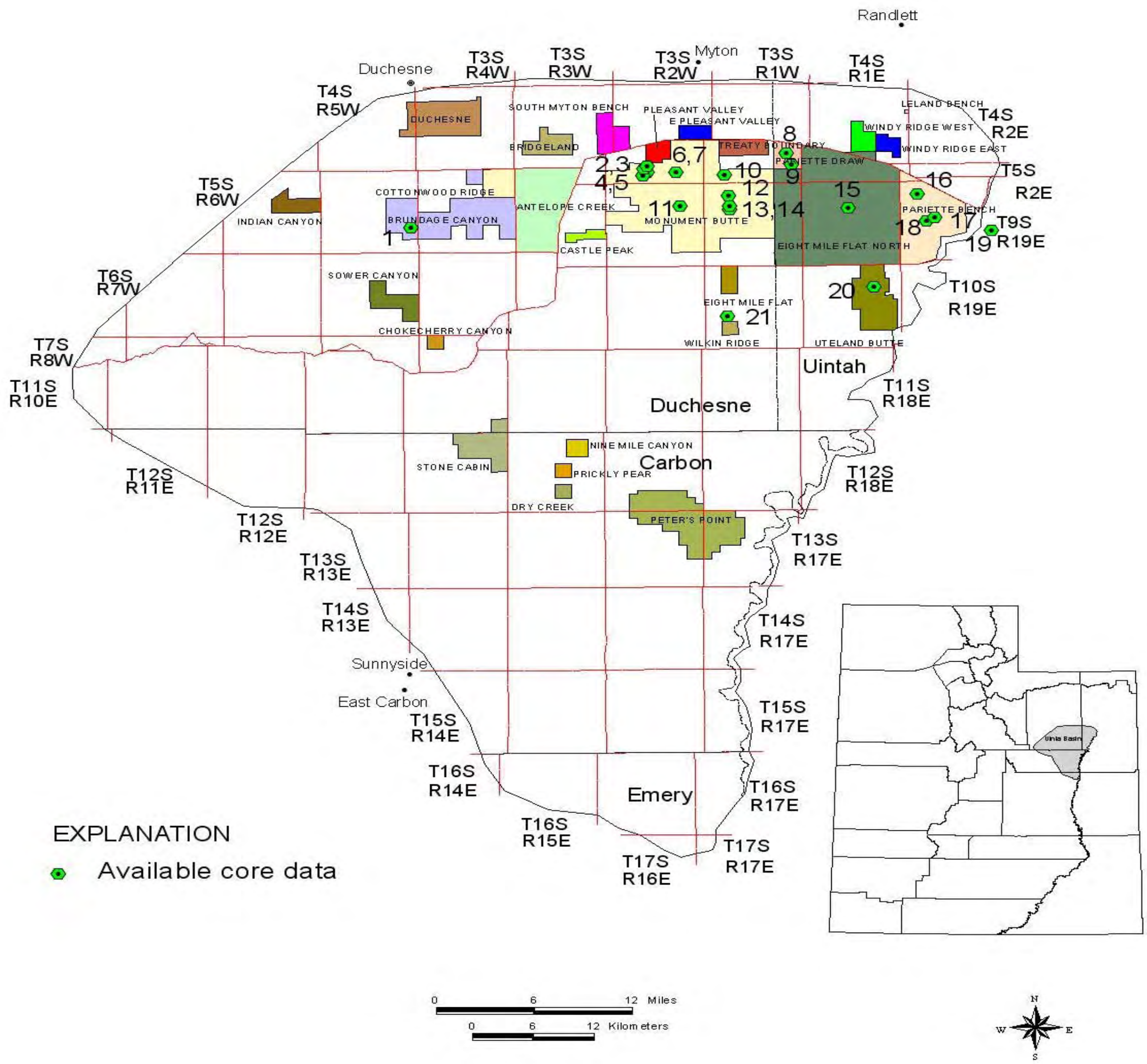

Figure 1. *Map of study area showing oil field boundaries and the location of wells with core described in this report. Numbers next to the core symbols refer to the map number in table 1.*

Table 1. *Location and cored interval data of the well core examined for this study and described in appendix A.*

MAP NUMBER[1] (figure 1)	WELL NUMBER	API NUMBER[2]	LOCATION Sec., T., R.[3]	CORED INTER-VAL (feet)	CORRELATION IN-TERVAL[4] (figure 2)
1	Ute Tribal 2-25	43-013-31833	25, T5S, R5W Uinta Base Line and Meridian	5527-5596	Castle Peak
2	Travis 14A-28	43-013-30792	28, T8S, R16E	5550-5646	Travis
3	Travis 10-28	43-013-30856	28, T8S, R16E	5586-5603	Travis
4	Federal 2-33	43-013-30749	33, T8S, R16E	5647-5676	Travis
5	Federal 6-33	43-013-30747	33, T8S, R16E	5596-5616	Monument Butte
6	Federal 6-35	43-013-30752	35, T8S, R16E	5026-5048	Monument Butte
7	Monument Federal 3A-35	43-013-31738	35, T8S, R16E	4993-5022	Monument Butte
8	Federal 23-24	43-047-32710	24, T8S, R17E	5325-5363	Monument Butte
9	Federal 23-25	43-047-32529	25, T8S, R17E	5145-5185	Monument Butte
10	State 6-32	43-013-30748	32, T8S, R17E	5042-5053	Monument Butte
11	Federal 33-11J	43-013-31451	11, T9S, R16E	4840-4870 5158-5207 5370-5424	Monument Butte Travis Travis
12	Allen 34-5	43-013-30721	5, T9S, R17E	4995-5045	Travis
13	Federal 33-8	43-013-31427	8, T9S, R17E	4632-4660 5440-5470	Monument Butte Castle Peak
14	Paiute 34-8	43-013-30778	8, T9S, R17E	4050-4129	Beluga
15	Pariette 5	43-047-10298	9, T9S, R18E	5407-5457	Castle Peak
16	Pariette 6	43-047-10873	5, T9S, R19E	4454-4487 4867-4894 5046-5080	Beluga Travis Travis
17	State 13-16J	43-047-31128	16, T9S, R19E	4238-4328 5350-5385	Monument Butte Uteland Butte
18	Federal 15-17	43-047-31002	17, T9S, R19E	4255-4306	Monument Butte
19	Federal 15-24B	43-047-32420	24, T9S, R19E	4738-4817	Castle Peak
20	Island 16	43-047-31505	11, T10S, R18E	4690-4812	Uteland Butte
21	Desert Springs 11-20-10-17	43-013-32088	20, T10S, R17E	4970-5030 5100-5150	Uteland Butte Uteland Butte

[1] Map number refers to numbers found on figure 1.
[2] API number is the American Petroleum Institute numbering system.
[3] Location: Sec. = section, T. = township, R. = range; all are SLBLM unless noted otherwise.
[4] Correlation interval: nomenclature from figure 3.

diagenesis that subsequently modified the sediment after deposition. Diagenesis usually involved compaction and cementation, dissolution of materials, and infilling of primary or secondary pores by authigenic clays or other minerals.

GEOLOGIC SETTING

The Uinta Basin is a topographic and structural trough encompassing an area of more than 9,300 square miles (14,900 km^2) in northeast Utah (figure 2). The basin is sharply asymmetrical, with a steep north flank bounded by the east-west-trending Uinta Mountains, and a gently dipping south flank.

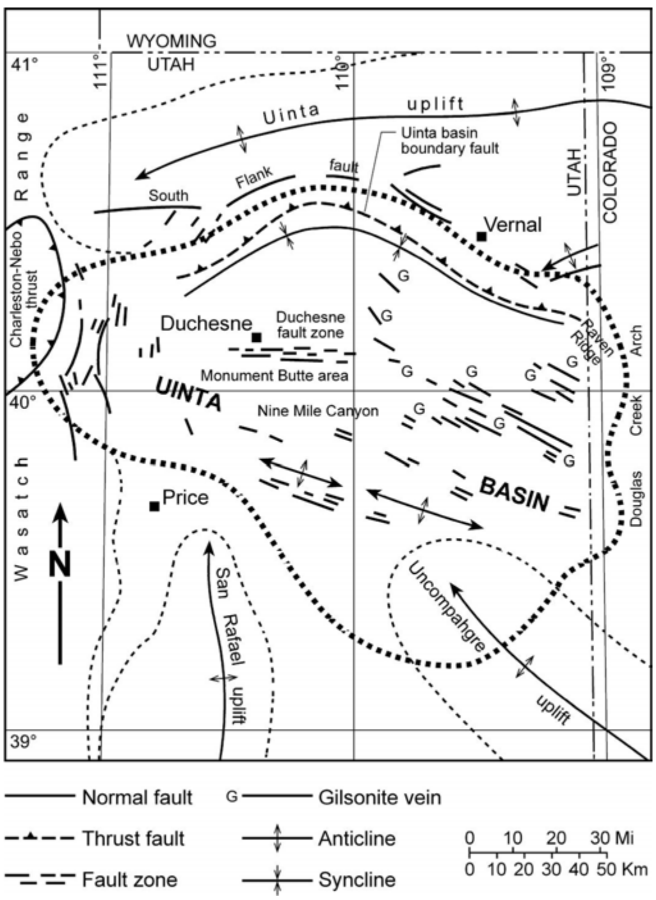

Figure 2. Major structural features, surface faults, and gilsonite veins in and around the Uinta Basin. Modified from Chidsey and Laine (1992).

The Uinta Basin formed in Late Cretaceous (Maastrichtian) time, creating a large area of internal drainage, which was filled by ancestral Lake Uinta during the Paleocene and Eocene. Deposition in and around Lake Uinta consisted of open- to marginal-lacustrine sediments that make up the Green River Formation. Alluvial redbed deposits that are laterally equivalent to, and intertongue with, the Green River make up the Colton (Wasatch) Formation.

More than 450 million barrels of oil (72 million m^3) have been produced from the Green River and Colton Formations in the Uinta Basin. The Cedar Rim, Altamont, Bluebell, and Red Wash fields produce oil from the northern-sourced deposits of Lake Uinta, whereas the fields in the Monument Butte area (Duchesne, Brundage, Sowers, Antelope Creek, Uteland Buttes, and Monument Butte fields [figure 1]) produce from southern-sourced deltaic deposits of the middle and lower members of the Green River. The southern shore of Lake Uinta was often very broad and flat, which allowed large transgressive and regressive shifts in the shoreline in response to climatic and tectonic-induced rise and fall of the lake. The cyclic nature of Green River deposition in the south-central Uinta Basin resulted in numerous stacked deltaic deposits. Distributary-mouth bars, distributary channels, and nearshore bars are the primary producing sandstone reservoirs in the area.

Some of the stratigraphic nomenclature commonly used in the Monument Butte area is shown in figure 3 and is discussed in detail by Morgan and Bereskin (2003), Morgan and others (2003) who divided the middle and lower members of the Green River Formation into five intervals, each having distinct reservoir properties based on regional correlations and examination of cores and surface exposures. The intervals have been named after representative oil fields or water-flood units in the south-central Uinta Basin. In stratigraphically ascending order, the five intervals are: (1) Uteland Butte, (2) Castle Peak, (3) Travis, (4) Monument Butte, and (5) Beluga. Each interval consists of one or more potential reservoir beds having similar paleodepositional history, petrology, and diagenesis.

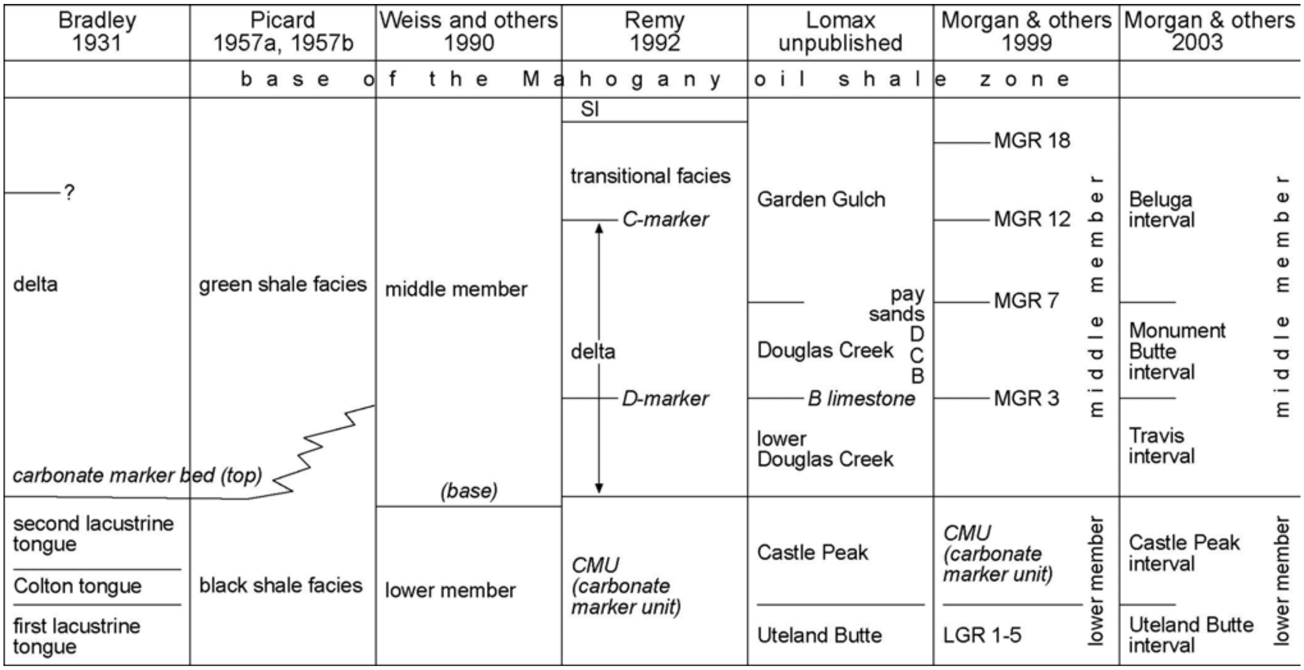

Figure 3. *Comparative nomenclature used for the Green River Formation (below the Mahogany oil shale zone) in the central Uinta Basin.*

ROUTINE CORE ANALYSES

We gathered routine core analysis data (porosity, permeability, grain density, and fluid saturation) for many of the cores described, as well as from core that was not available to us (appendix B). Porosity and permeability data are typically cross plotted to identify the relationship between the two. In wells for which core data are not available, the porosity is determined from well logs, and the permeability is determined from the porosity/permeability cross-plot data set. The porosity and permeability data were plotted, and best-fit slopes were determined for the entire data set and for data from each of the intervals (Morgan and others, 2000). The porosity/permeability slope for each interval is very similar except for the carbonate beds in the Uteland Butte interval (figure 4).

The porosities determined from the core samples were compared to porosities calculated by averaging the density log and neutron log porosity values, and to the density log porosity alone (Morgan and others, 2000). The density log porosities more closely matched the core-derived porosities. Porosity determined from the density well log is a function of the grain density of the rock. Typically, porosities in the Monument Butte area were calculated from density log data assuming a grain density of 2.68 grams/cubic centimeter (g/cm^3). Plotting the grain density values from all of the core data shows the majority of the samples have a grain density of 2.66 g/cm^3 except for the carbonate beds in the Uteland Butte interval, where most of the samples have a grain density of 2.75 to 2.76 g/cm^3 (Morgan and others, 2000). The higher grain density (2.68 versus 2.66 g/cm^3) can result in an overestimate of the log porosity by about 1 percent.

DEPOSITIONAL ENVIRONMENTS

Ryder and others (1976) described the major facies for the Green River Formation as: (1) alluvial, (2) marginal lacustrine, and (3) open lacustrine. Other important papers describing the depositional environments of the Green River include Bradley (1931), Picard (1955, 1957a, 1957b), Jacob (1969), McDonald (1972), Fouch (1975), Fouch and Dean (1982), Colburn and others (1985), Oleson (1986), Little (1988), Fouch and others (1992), Remy (1992), and

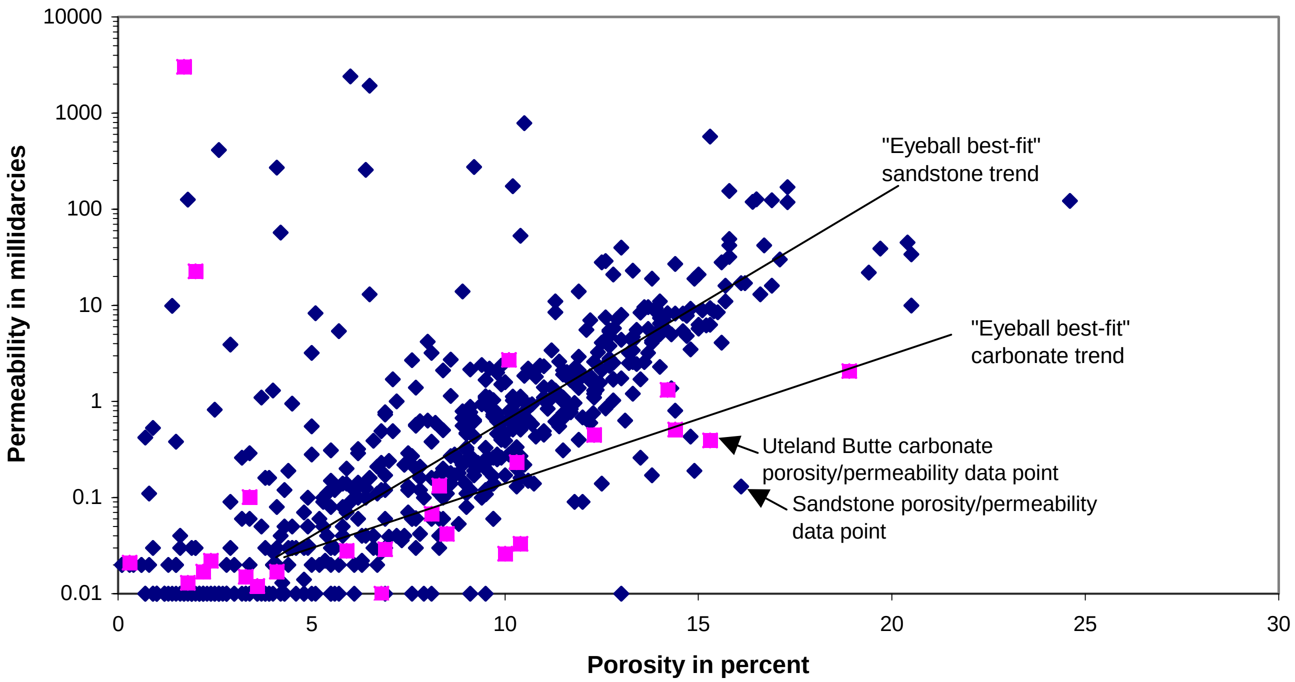

***Figure 4**. Cross plot of porosity and permeability routine core analyses data (appendix B). The "eyeball best fit" lines represent the general trend of the data. Note the difference in slope between the sandstone and carbonate trends.*

Keighley and others (2002). The Green River Formation core we studied consisted of sedimentary materials derived from the south or southeast that were shed northward toward the open lacustrine setting (Ryder and others, 1976). Most of the petroleum reservoir rock, which was the primary focus of this study, was deposited in the marginal-lacustrine facies along or near the fluctuating southern shoreline of ancestral Lake Uinta. Some core consisted of rock deposited in the open-lacustrine facies, but none is from the alluvial facies.

Marginal Lacustrine Facies

Ryder and others (1976) define the marginal-lacustrine facies as "composed of gray-green calcareous claystone, channel-form sandstone, and grain- to mud-supported carbonate units. The dominant depositional environments are interpreted to be lake-margin carbonate flat, deltaic, and interdeltaic." The marginal lacustrine facies is located between the alluvial Colton Formation and the distal open-lacustrine facies.

Lake-margin Carbonate Flat

The lake-margin carbonate flat or mud-flat lithology is recognized by its persistent laminated structure, mud cracks, diastemic surfaces, gently discordant strata, and by abundant accumulations of compacted thin-shelled pelecypods. The dark and light laminations reflect not only variations in organic content, but also discrete shell-rich and shell-poor laminations. Many such laminations strongly resemble the micro-irregularities of algal stromatolites having very low-amplitude, convex-upward, and undulatory laminations.

Very finely crystalline dolostones containing some rip-ups and subtle soft-sediment deformation were deposited in the mud-flat environment. These dolostones appear similar to the primary or penecontemporaneous dolostones deposited in paralic marine environments.

Deltaic

The deltaic distributary system interpretation of some of the core is based on sedimentary structures typical of channel deposition as well as the numerous rip-ups and multiple scours, many of which involve sand-on-sand contacts, lending evidence to superposed or imbricated channeling. Some distributary sandstone beds are subaqueous and display abundant dewatering phenomena, while others contain root casts, associated coal seams, mud-cracked horizons, and penecontemporaneous dolomites indicative of proximity to subaerial conditions. Changes in sedimentary structures do not always imply different and distinct sedimentary environments, but in many cases, a single depositional environment of varying sediment load and stream velocity. Also, lake level and water chemistry can affect the sedimentary structures as well (Oleson, 1986). As a result, a distributary system can exhibit variability in sedimentary structures such as: (1) scours and rip-ups, (2) steep cross-bedding, (3) planar laminations, (4) wavy laminations, (5) distinct current ripples, (6) megascopically structureless, (7) ripple laminae in phase, and more rarely, (8) ripple-drift or climbing ripples (figure 5).

Fining-upward sequences were identified in both core and open-hole logs, initiating with discernible scour and rip-ups composed of dolomitic mudstone, carbonate allochems, and organic debris. The very fine to medium-grained sandstones fine upward and pass through moderate-angle trough cross-bedding, to low-angle cross-lamination, to planar or wavy lamination, and in some cases, to poorly sorted sandstone with abundant ripple-drift lamination. Complete fining-upward sequences are comparatively rare, and likely represent streams of initial vigorous velocity, whose downcutting capabilities wane with time.

Typically, the distributary channel sequences consist of planar to wavy lamination, both with or without channel lags, some current ripples and small-scale cross-lamination, and are less frequently structureless or even initially ripple-drift laminated. Climbing ripples are usually found in the upper portion of the fining-upward sequence and probably represent deposition in the waning stages of a periodic flood. Such deposits likely occur when suspended load is laid down as flow velocities decrease, perhaps in a single, relatively abrupt phase. Sometimes the climbing ripple facies are isolated beds or in a stratigraphic position not associated with a clear fining-upward sequence, and are interpreted as interdistributary deposits.

Interdeltaic

Interdeltaic deposits include medium gray molluscan wackestones in which fresh water pelecypods and/or turriform gastropods accumulated as mostly broken and/or disarticulated materials. These deposits commonly underlie the grain-supported ostracodal or oolitic packestones or grainstones in part of a shallowing-upward parasequence. These wackestones possess little to no porosity and are not considered good reservoirs.

Open-Lacustrine Facies

Ryder and others (1976) defined the open-lacustrine facies as consisting "primarily of mud-supported carbonate and claystone units with minor amounts of sandstone and siltstone. Kerogen and other organic compounds produce shades of gray and brown. The open-lacustrine rock assemblages were deposited away from terrigenous clastic influxes either near the center of the lake or in nearshore settings." Typically, mudstones and shales comprise most of this facies and are not good reservoirs. As a result, the open-lacustrine facies is rarely cored. Dark-gray to black, organic-rich mudstones/shales are common in the lower member and the Travis interval of the middle member of the Green River Formation, and gray-green mudstones are found above the Travis interval. The contact between the two mudstones is transitional and varies laterally. A pronounced color change may be related to a profound change in the chemistry of the lake associated with changes in depth and/or circulation. The open-lacustrine facies includes distal argillaceous dolomite or limestone. In some cases, nonreservoir mudstones contain scattered phosphatic debris, mostly from vertebrate and modest ostracod accumulations. Both the dark gray to black mudstones and argillaceous carbonates are excellent petroleum source rocks and are typically oil prone.

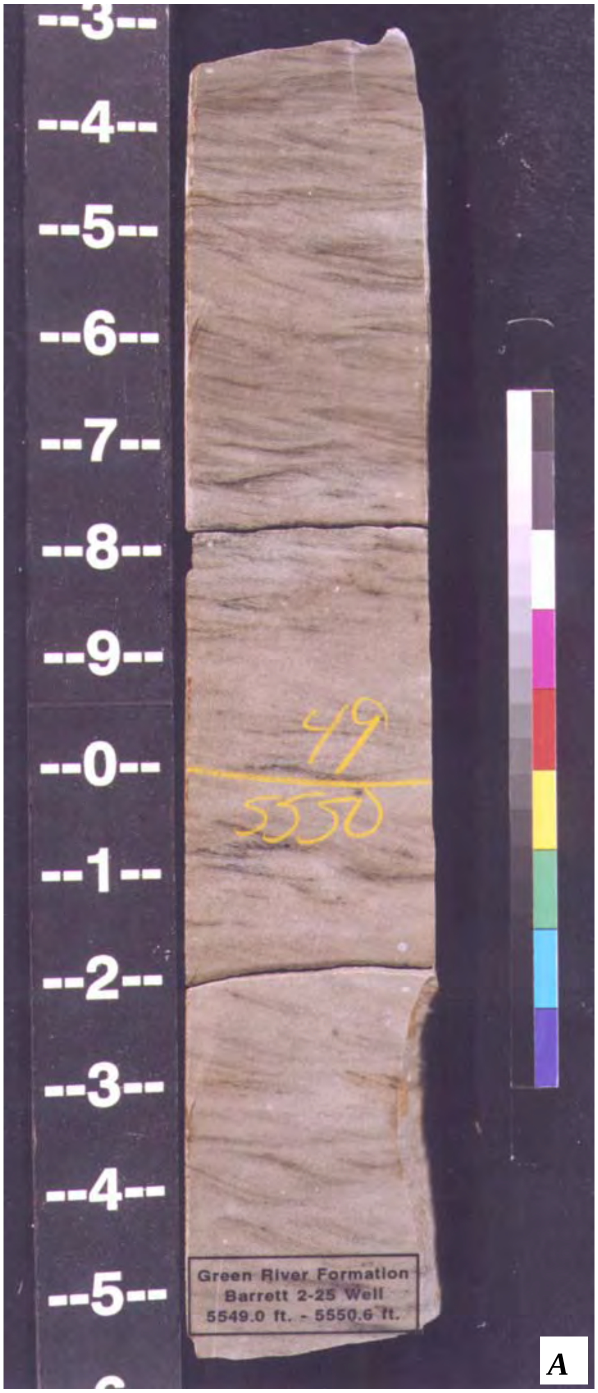

Figure 5. *Sedimentary structures typical of distributary-channel deposition. (A) Showing climbing ripples and/or ripple-drift lamination in upper portion of distributary channel, from Ute Tribal 2 – 25 well, section 25, T. 5 S., R., 5 W., Uinta Base Line and Meridian, 5,549.0 to 5,550.6 feet; see map number 1 on figure 1 and table 1. (B) From bottom to top: (1) planar lamination to cross-lamination, (2) possible large-scale rippling, and (3) wavy lamination to irregular small-scale ripples at top, from Pariette 5 well, section 9, T. 9 S., R. 18 E., SLBLM, 5,408.5 to 5,409.5 feet; see map number 15 on figure 1 and table 1 (vertical scales in tenths of a foot).*

In the Monument Butte area, the Travis interval often consists of thick (100 to 200 feet [30–60 m]) sandstone and siltstone beds within the open-lacustrine black shale facies of Picard (1957b). Lutz and others (1994) described the Travis interval sandstone beds as moderate- to low-density turbidite channel, debris flow, and gravity-flow deposits. We believe that tectonic activity resulted in development of a prominent east-to-west shelf break where thick cut-and-fill valley deposits accumulated during several lake level fall-and-rise cycles.

Two major clastic lithotypes are common to the Travis interval: (1) a chaotic, poorly sorted sandstone/siltstone deposit with erratically dispersed breccia clasts, probably derived from the sublacustrine channel walls, and (2) a rhythmically laminated very fine grained sandstone facies that occasionally exhibits classic grading that has better sorting. The latter facies appears to possess better reservoir quality as selective sorting allows for the development of void space, at least during the transportation phase (apart from the later possible effects of diagenesis). The chaotic deposit is so poorly sorted that indigenous void space is clearly less than is typically found in the laminated facies, and in fact, many framework grains remain coated by detrital mud. The chaotic deposit was also deposited more abruptly (reflected in the poor sorting), and dewatering and/or synsedimentary folding or faulting cause degradation in reservoir quality as well (figure 6).

Borehole imaging log data from the Travis interval indicate the presence of near-vertical fractures. The fractures are typically present in the comparatively brittle strata (sandstone) bounded by more ductile rocks (shale). Most fractures are cemented with calcite, but production can be enhanced if naturally occurring open fractures are encountered.

In the Desert Spring 11-20-10-17 well (appendix A), an example of open-lacustrine deposition is found at depths from 5,003 to 5,017

A

Figure 6. *Lacustrine turbidite facies in the Travis interval, Federal 2 – 33 well, section 33, T. 8 S., R. 16 E., SLBLM; see map number 3 on figure 1 and table 1. (A) Siltstone to very fine grained sandstone with brown, gray-green, and dark gray clasts, some clasts are deformed. Laminated lithotype is visible in second row from the bottom. Core is from 5,657 to 5,667 feet. (B) Chaotic debris flow with irregular breccia clasts and soft-sediment deformation. Core is from 5,667 to 5,677 feet (horizontal scale in centimeters).*

B

Figure 6. *Continued*

feet (1,524.9–1,529.2 m), where medium gray to medium-dark gray illitic mudstone is associated with remnants of pyritic, bioturbated, very fine grained sand and/or silt. The sandstone occasionally fines upward and appears locally graded. The mudstone overlies an oolitic limestone and represents a lake-level rise.

SANDSTONE PETROLOGY

Petrology of the sandstones in the Green River Formation is discussed by Pitman and others (1982) and Colburn and others (1985). Our study of the Green River core included megascopic examination, stained thin-section examination, scanning electron microscopy (appendix C), and analysis of x-ray diffraction (XRD) data provided by Sue Lutz, Energy and Geoscience Institute, University of Utah (appendix D). The reservoir quality of the Green River sandstones is controlled by one of several possible diagenetic pathways illustrated in figure 7. The diagenetic pathway may be controlled by local geochemical conditions present in isolated portions of any specific depositional system. As a result, correlative sandstone beds deposited in a similar environment may have differing reservoir quality due to separate diagenetic processes. The Green River contains four primary classes of

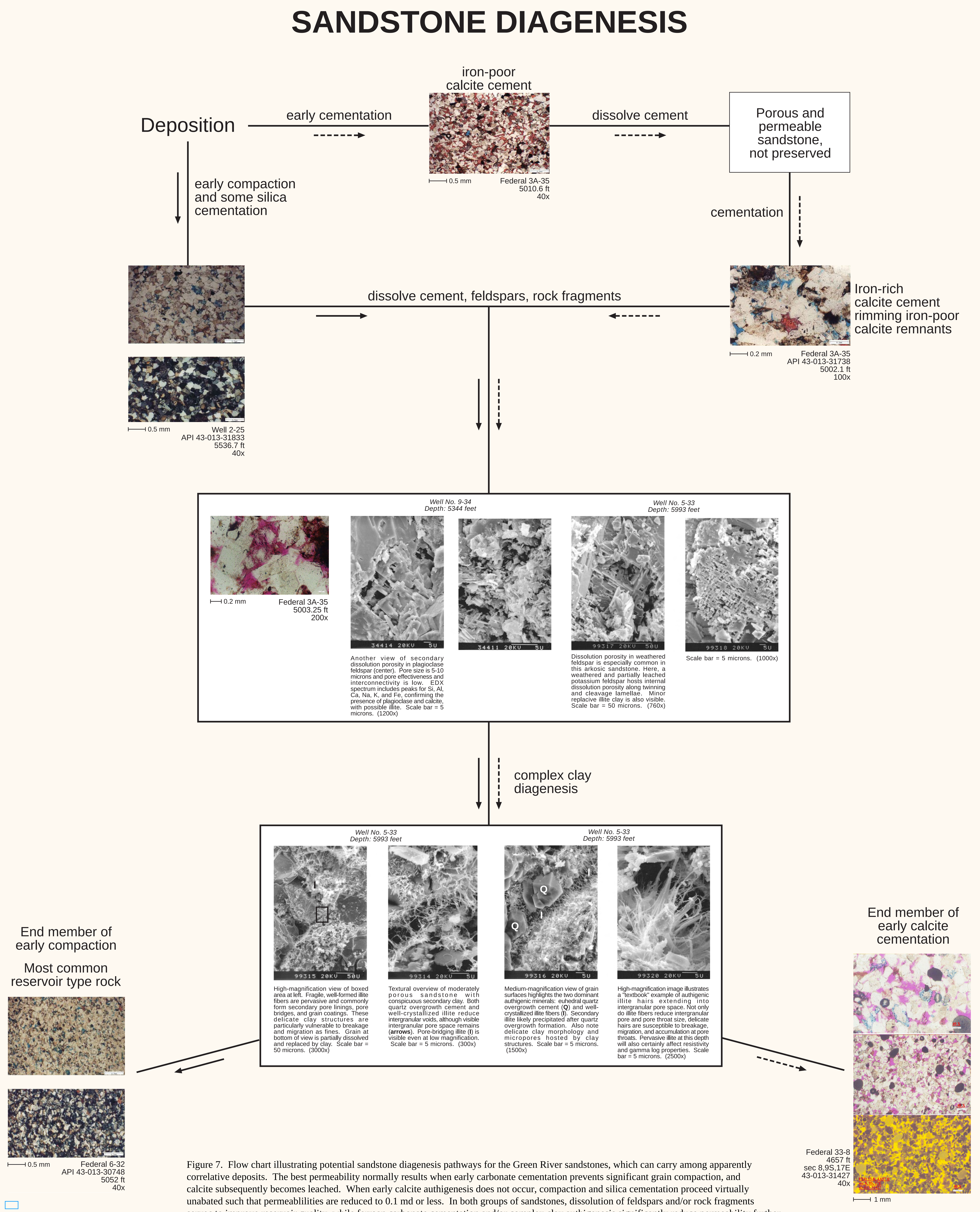

Figure 7. Flow chart illustrating potential sandstone diagenesis pathways for the Green River sandstones, which can carry among apparently correlative deposits. The best permeability normally results when early carbonate cementation prevents significant grain compaction, and calcite subsequently becomes leached. When early calcite authigenesis does not occur, compaction and silica cementation proceed virtually unabated such that permeablilities are reduced to 0.1 md or less. In both groups of sandstones, dissolution of feldspars and/or rock fragments serves to improve reservoir quality, while ferroan carbonate cementation and/or complex clay authigenesis significantly reduce permeability further.

sandstone: (1) medium-grained sandstone typically found only in the Castle Peak interval, (2) very fine to fine-grained sandstone which is the composition of most of the reservoir beds in the Monument Butte and Beluga intervals, (3) ripple-drift laminated sandstone which is a very fine grained sandstone with significant micaceous silt, and (4) very fine grained sandstone to coarse siltstone of the Travis unit.

Medium-Grained Sandstones

The medium-grained sandstones are almost exclusively seen in the Castle Peak interval of the lower member. The medium-sized grains may reflect a comparatively proximal position during Castle Peak time, or may be the result of a medium- to coarse-grain provenance that was not available during deposition of the middle member.

Provenance

The medium-grained sandstones (approximately 0.36-0.44 mm) are mostly lithic arkoses or feldspathic litharenites (figure 8). In the medium-grained deposits, framework elements include:

- abundant monocrystalline and polycrystalline quartz (some rutilated),
- potassium feldspar (orthoclase and microcline),
- plagioclase,
- chert (some of possible volcanic origin),
- sheared metaquartz, recrystallized metaquartz, hydrothermal quartz,
- intrusive rock fragments,
- very rare volcanic rock fragments,
- schist and questionable phyllitic metamorphic rock fragments,
- dolomitic siltstone and mudstone clasts (some clearly hematitic),
- carbonate ooids and/or intraclasts,
- reworked sandstone grains,
- isolated mica booklets (biotite, chlorite, and muscovite),
- occasional red-brown hematitic staining, and
- assorted heavy minerals including zircon, epidote, tourmaline, sphene and very rare amphibole.

The mixed assemblage of minerals and rock fragments indicates that sedimentary, metamorphic, and igneous sources provided material to the distributaries entering Lake Uinta's south shore. Based on the volume of metamorphic rock fragments, feldspars, and to a much lesser but important degree, the intrusive material, a basement complex such as the Uncompahgre uplift was likely a part of the source area. Case (1991) describes the Proterozoic rocks of the Uncompahgre region and lists approximately 10 lithologies present in the basement complex. The similarity between the Proterozoic of the Uncompahgre and the Eocene sandstones in the Green River Formation are:

- **quartz -** polycrystalline quartz common from plutons and metamorphic material, rutilated quartz from plutons,
- **sheared and recrystallized metaquartz -** from gneisses and metaquartzites,
- **hydrothermal quartz -** from pegmatitic material,
- **potassium feldspar -** including microcline from at least two pervasive Uncompahgre rock types,
- **biotite -** an extremely common ingredient in many of Case's observed basement lithologies,
- **plagioclase -** abundant with An30 approximate composition, and
- **heavy minerals -** as described including significant amounts of sphene.

Less stable amphiboles are about the only material abundant in the Proterozoic of the Uncompahgre that are not commonly found in the Green River Formation.

Textural Features

Most sandstones in the Green River Formation are poorly to moderately sorted, with angular to very well rounded grains, although rounding is occasionally masked by intense com-

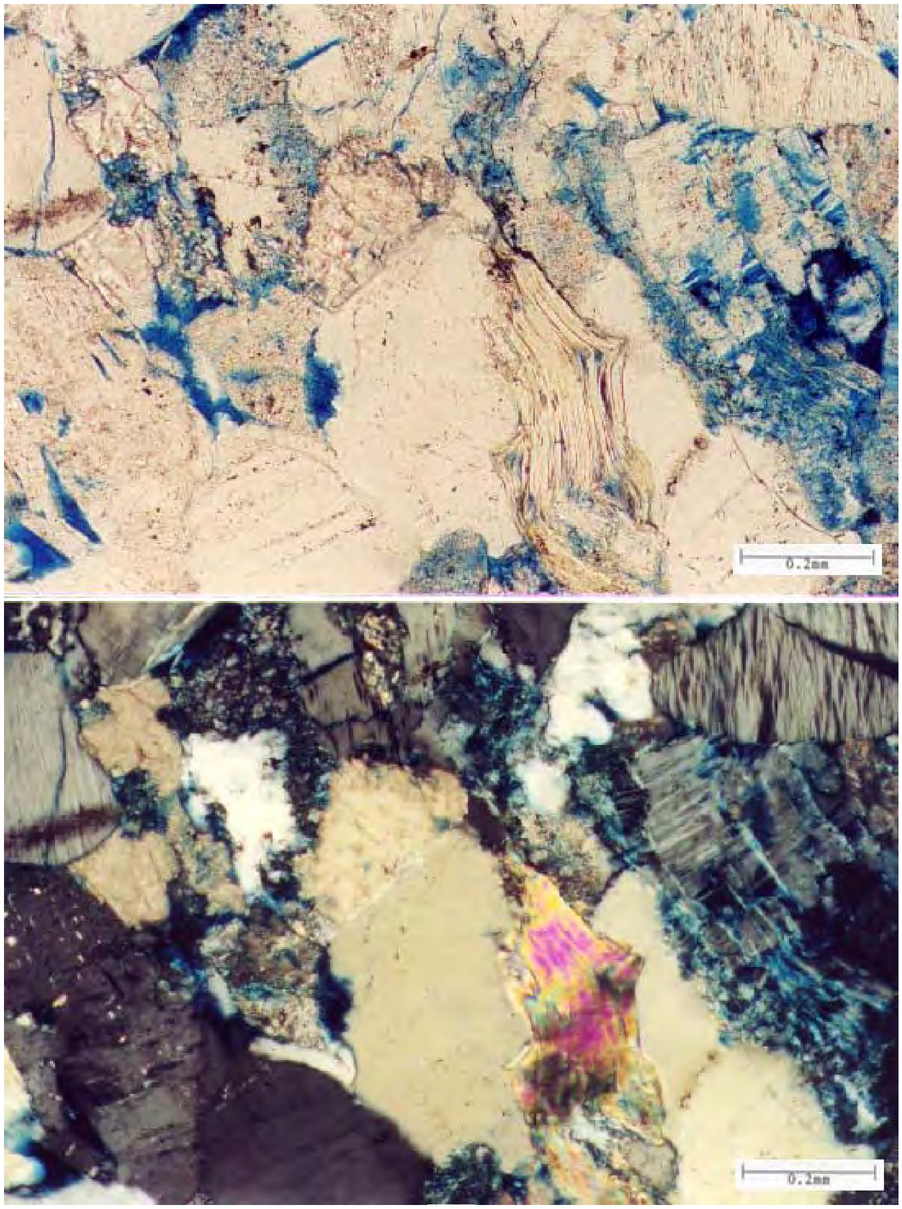

A

Figure 8. *Paired photomicrographs of medium-grained lithic arkose from the Castle Peak interval, Federal 10 – 34 well, section 34, T. 8 S., R. 16 E., SLBLM. (A) Example of a tightly packed sandstone, but some porosity is provided by the dissolution of feldspars and rock fragments. Note the highly birefringent muscovite flake (M) (upper view is plane-polarized light, lower is cross nicols, at 5,956 feet). (B) Same depth and magnification (cross nicols) showing partial leaching of large potassium feldspar (K) grains (stained yellow) and a smaller unstained plagioclase (P). Some infilling of the pore space by kaolinite. (C) At 5,961 feet, poorly sorted medium-grained sandstone is characterized by tight packing and compaction of grains, some selective leaching of feldspars, and quartz overgrowth cement (upper view is plane-polarized light and lower view is cross nicols). Lower view reveals sheared metamorphic quartz (MQ), chert (C), and many linear grain boundaries caused by compaction and by terminations of quartz overgrowth cement (quartz grains Q).*

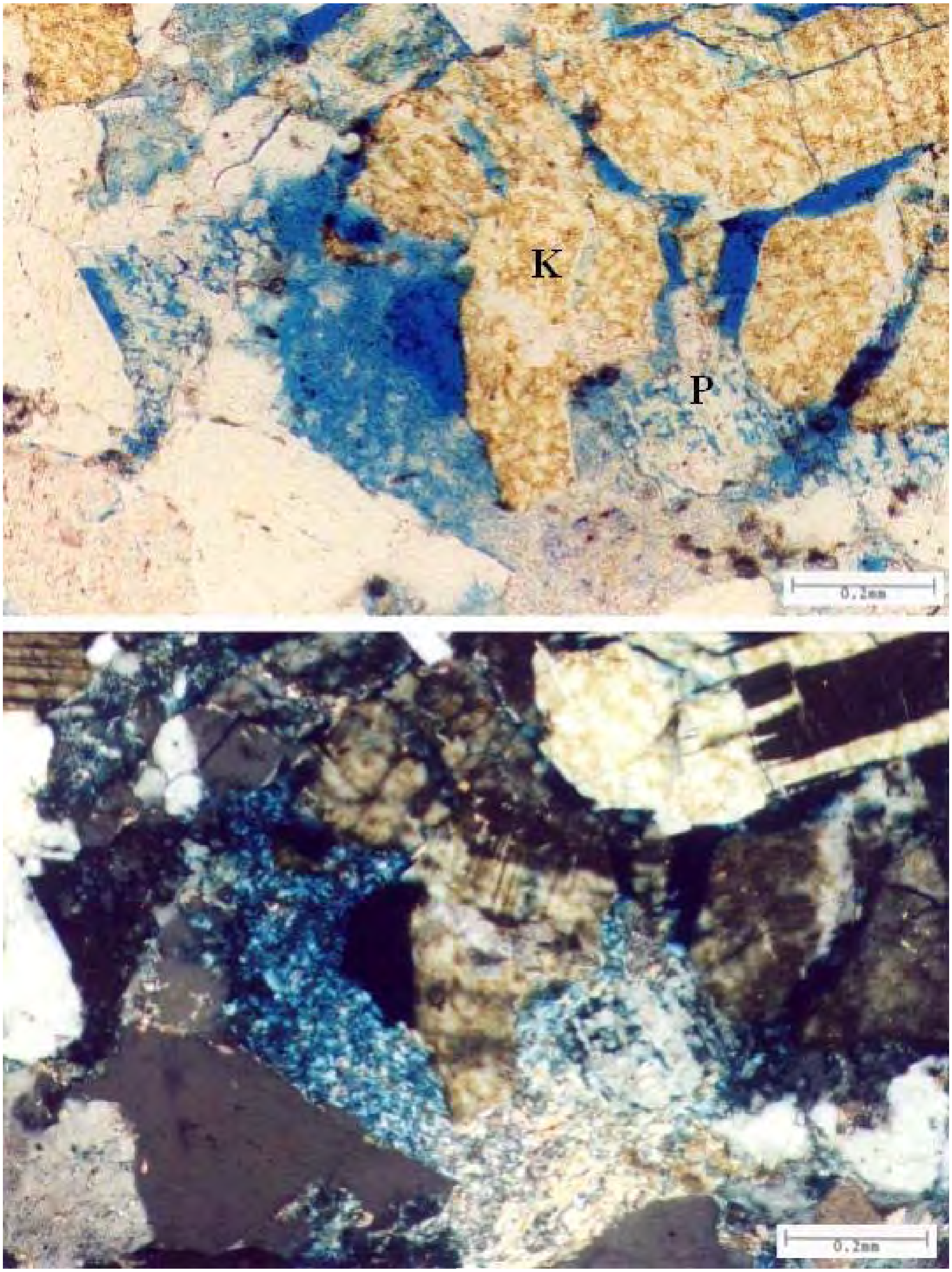

B

Figure 8. *Continued*

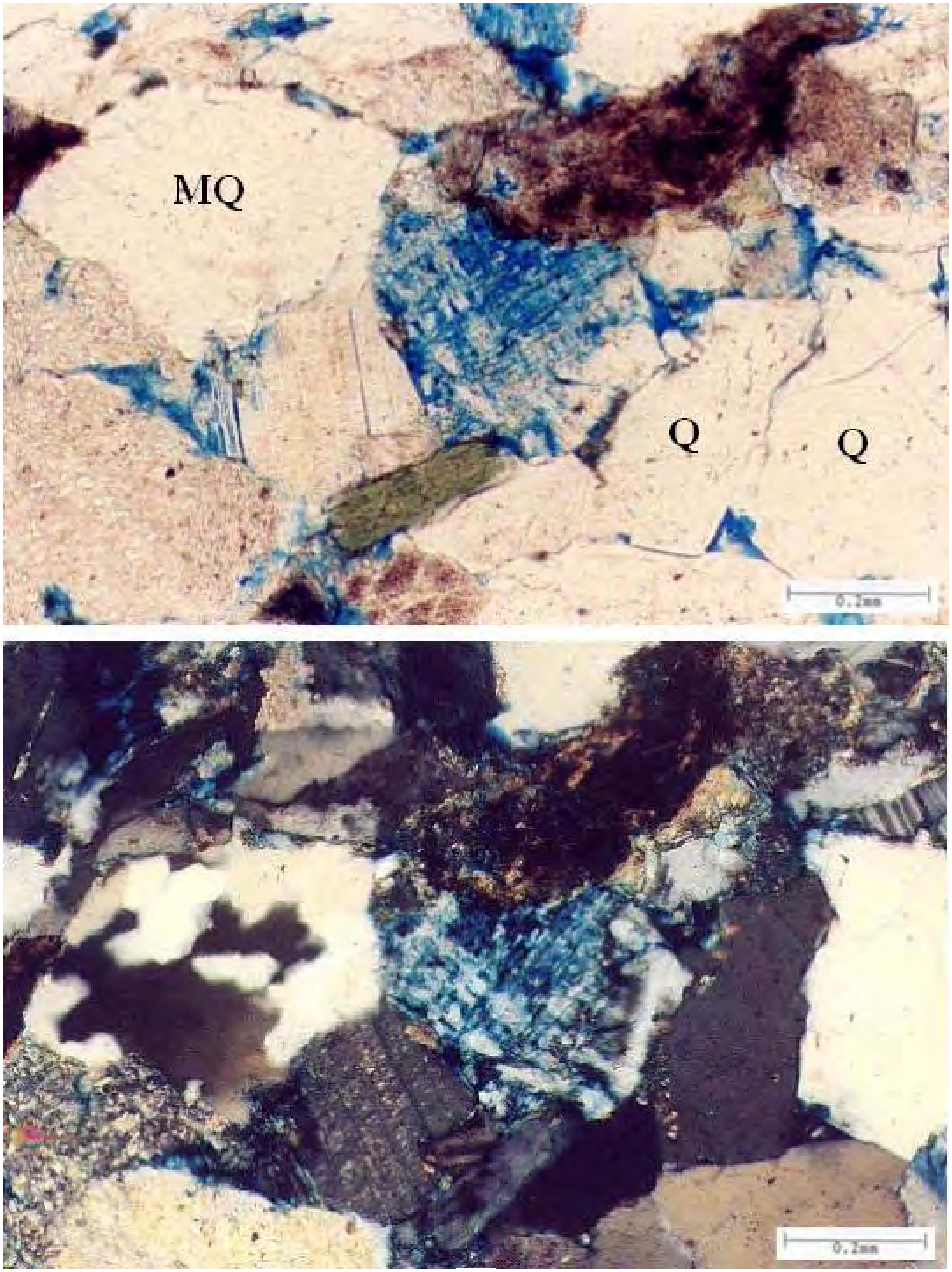

C

Figure 8. *Continued*

paction, cementation, and grain dissolution. The well-rounded grains and rounded overgrowth cements may be recycled from other sedimentary deposits. This medium-grained lithotype is consistently highly compacted, and grain contacts are commonly interpenetrative to the point of partially exhibiting crenulated grain boundaries (approaching metamorphic textures). The softer mudstone and phyllitic grains are deformed into pseudomatrix, and coupled with extensive quartz and feldspar cementation, would result in an extremely tight rock if it were not for the dissolution of some of the feldspars and rock fragments. Compositionally, the medium-grained sandstones are lithic arkoses (or feldspathic litharenites where there is abundant reworked mudstone).

Most medium-grained sandstones exhibit selective leaching, and potassium and plagioclase feldspar dissolution is the most common. Among the relatively abundant feldspars, dissolution can be especially pronounced for plagioclase, perthite, and microcline, while orthoclase dissolution is usually less pronounced. Selective rock fragments, micas, and modestly abundant low-magnesium calcite cements are also subject to dissolution. Because of this dissolution process, reservoir quality can be significantly enhanced, although the severity of leaching (permeability enhancement) varies from sample to sample, and even within feldspars from a single sample (figure 8).

Diagenesis

The complex and commonly intricate diagenetic processes impacting the medium-grained sandstones are similar to the diagenetic stages that modified most other Green River Formation sandstones. The major differences with these specific coarser grained deposits involve: (1) the intense degree of grain compaction and cementation, (2) the severity of feldspar dissolution, (3) the greater abundance of kaolin, ostensibly from feldspar dissolution, and (4) the comparative paucity of calcite diagenesis, both iron-poor calcite and iron-rich calcite.

The following paragenetic history is based on the use of cross-cutting textural relationships observed either in thin section, or through scanning electron microscopy (SEM) investigations.

1. Sediment deposited in distributary systems.
2. Intense compaction of grains followed soon after deposition and progressively developed until interpenetrative and/or crenulated grain contacts eventually resulted. Pseudomatrix formation when dolomitic or hematitic mudstone fragments are deformed into original pore space.
3. Formation of illitic and/or chlorite grain coatings around framework elements.
4. Formation of silica overgrowths developed alongside the compaction phase as grain-to-grain pressure solution products; many euhedral overgrowths are recognized both in thin section and in SEM investigations. Some overgrowth formation is incomplete in that some secondary intergranular pore space remains in the form of small triangular pores, expressed in two dimensions. Quartz overgrowth development may be part of a long-term authigenetic process.
5. Development of authigenic orthoclase and plagioclase as overgrowth cements. Minor amounts of early, low-magnesium, calcite cement invaded the already compacted (or reduced) primary intergranular pores. The amount of early calcite is rare compared to other Green River sandstones, perhaps indicating that compaction and silica cementation began almost immediately after deposition.
6. Dissolution mostly of feldspars, rock fragments, and rarely of calcite; kaolin infilling of isolated dissolution pores; dolomite infilling and replacement of leached pores. Pyrite formation as replacement crystals in the sandstone matrix, selective replacement of rock fragments, and as infilling of pores. Multiple stages of pyrite authigenesis are likely. Siderite ag-

gregates concentrated in isolated voids. Iron-rich calcite enveloping vestiges of partially dissolved iron-poor calcite and ankerite overgrowths or rims on precursor dolomite crystals. Illite and/or illite-smectite infilling of pores and as alteration/ replacement products on framework grains. Late-stage chlorite authigenesis is possible.

Pore Types

The major pore type for the medium-grained sandstones is the dissolution porosity produced through the complete to incomplete leaching of feldspars and rock fragments. Most examples involve partial leaching, as seen both in the thin section and SEM photomicrographs. As stated previously, the feldspars are so abundant that significant amounts of void space can be provided as simple dissolution pores, or as feldspar micropores associated with a partial leaching process. Micropores can also be produced as a result of authigenic clay infilling of original dissolution voids. The clays include most authigenic varieties; chlorite, kaolinite, illite, and illite-smectite. Reduced intergranular pores result when quartz overgrowth cement only partially occludes the original intergranular pore space. While this type of pore usually results in the most permeability, reduced intergranular voids are comparatively rare in these rocks. Fracture porosity is common in some of these rocks, and most fractures develop near the base of the sandstone where the carbonate content is commonly the highest, imparting a decided brittleness to the medium-grained sandstones. Because of the predominance of isolated dissolution voids and micropores, porosity in many examples exceeds 10 percent, but permeabilities seldom exceed single millidarcies, even with pronounced dissolution.

Very Fine to Fine-Grained Sandstones

Most sandstone beds in the middle member of the Green River Formation are very fine to fine grained. The sandstones, typically deposited in distributary channels, are the most abundant oil reservoirs in the Monument Butte area. The fine median grain size (0.11-0.17 mm) may be the result of a more distal deposition setting than the medium-grained sandstones, or erosion of source rocks having a smaller grain size.

Provenance

The grain composition of the very fine to fine-grained sandstones is very similar to the medium-grained sandstones, but with some differences. The very fine to fine-grained sandstones rarely contain red-brown, hematite-stained mudstones. In fact, most mudstone fragments in the finer grained deposits contain medium-gray dolomitic and/or ankeritic mudstones, and/or pronounced carbonate allochems, including ankeritic/dolomitic ooids, ankeritic/dolomitic rip-ups, ostracods, or intraclasts. The finer grained sandstones locally contain much less polycrystalline quartz and granitic rock fragments than the medium-grained sandstones. The near-complete lack of intrusive rock fragments and polycrystalline quartz is a function of finer grain size and the greater degree of transportation and abrasion. Biotite, chlorite, and muscovite are more abundant in the finer grained sandstones than in the medium-grained sandstones.

Textural Features

The very fine to fine-grained sandstones are lithic arkoses or feldspathic litharenites having a median grain size of 0.11-0.17 mm. Sorting ranges from moderately well sorted to well sorted, and most grains are subangular to subrounded, but are rarely angular or well rounded. Rounded overgrowth cements were observed in these deposits. Pseudomatrix is also a common textural feature formed when mudstone fragments were squeezed into pre-existing pore space. The mudstone fragments are smaller than the mudstone clasts commonly found in the medium-grained sandstones. This type of compaction may be the result of soft-sediment deformation.

Chemical compaction and cementation are highly variable within the finer grained sandstones, and the degree of such destructive processes may be controlled by early, iron-poor calcite cement. In some samples, chemical compaction effects are nonexistent when early, iron-poor calcite cementation occurred and preserved the original textures. In other samples, grain-to-grain contacts are linear, gently curved (consertal), or slightly interpenetrative. As a result, there is an extreme range of grain-to-grain contacts in the very fine to fine-grained sandstones. The crenulated contacts seen in the medium-grained sandstones are generally lacking in the finer grained sandstones.

Diagenesis

In the very fine to fine-grained sandstones, the precipitation of calcite can occur fairly early during diagenesis. If the process is especially early, just after deposition of the original materials, very little grain compaction occurs. In this case, the iron-poor calcite infills the near-original uncompacted pore space and produces a highly cemented rock (figure 9). If cementation occurs after significant burial, the grain-to-grain compaction, and possible silica overgrowth, will alter the original texture, reducing the original pore volume. In some samples, compaction and silica cementation have eliminated almost all the pore volume (figure 10). Early calcite cementation, when subsequently leached, can result in very porous (+20 percent) and permeable (tens of millidarcies) sandstone (figure 11).

Dolomite, ankerite, siderite, and iron-rich calcite cementation also affect the porosity of the very fine to fine-grained sandstones. In many samples, all four cements have been identified but some pore volume still remains (+10 percent). Pore volume is completely lost in some sandstones due to secondary, iron-rich carbonate cementation such as ankerite or iron-rich calcite.

Authigenic clay precipitation occurs in roughly the same order as in the medium-grained sandstones. Based on XRD data, the finer grained sandstones have chloritic clay coatings more commonly than illite, which is the opposite of the medium-grained sandstones (appendix D). Pore bridging illite-smectite is especially evident in sandstones where feldspar dissolution occurred. The paragenetic history of the very fine

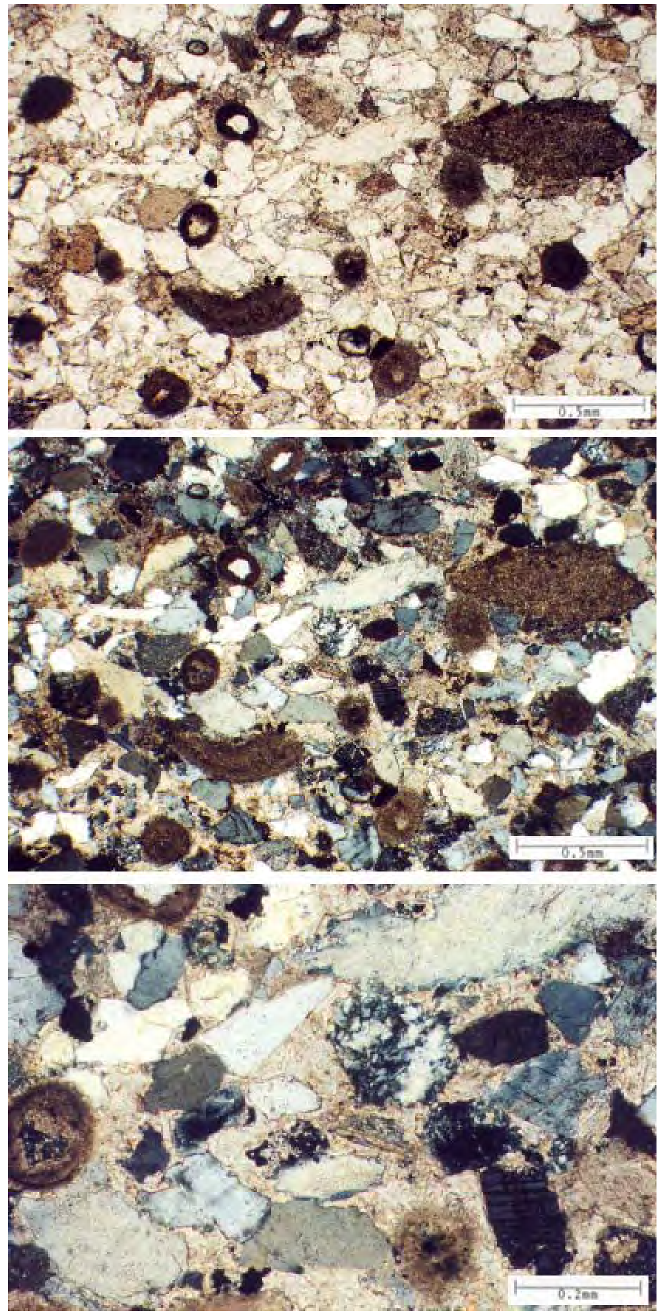

Figure 9. *Photomicrographs of very fine to fine-grained sandstone from the Federal 12 – 4 well, section 4, T. 9 S., R. 16 E., SLBLM, 4,894.1 feet depth. This sample is from the base of a distributary channel where mudstone lags and carbonate shoal material is often incorporated. The top and middle views (plane-polarized light and cross nicols, respectively) show the poor sorting that is typical in the channel base. The lower view (cross nicols) shows a sheared metamorphic quartz grain, variable rounding, and poorly sorted carbonate and siliceous material.*

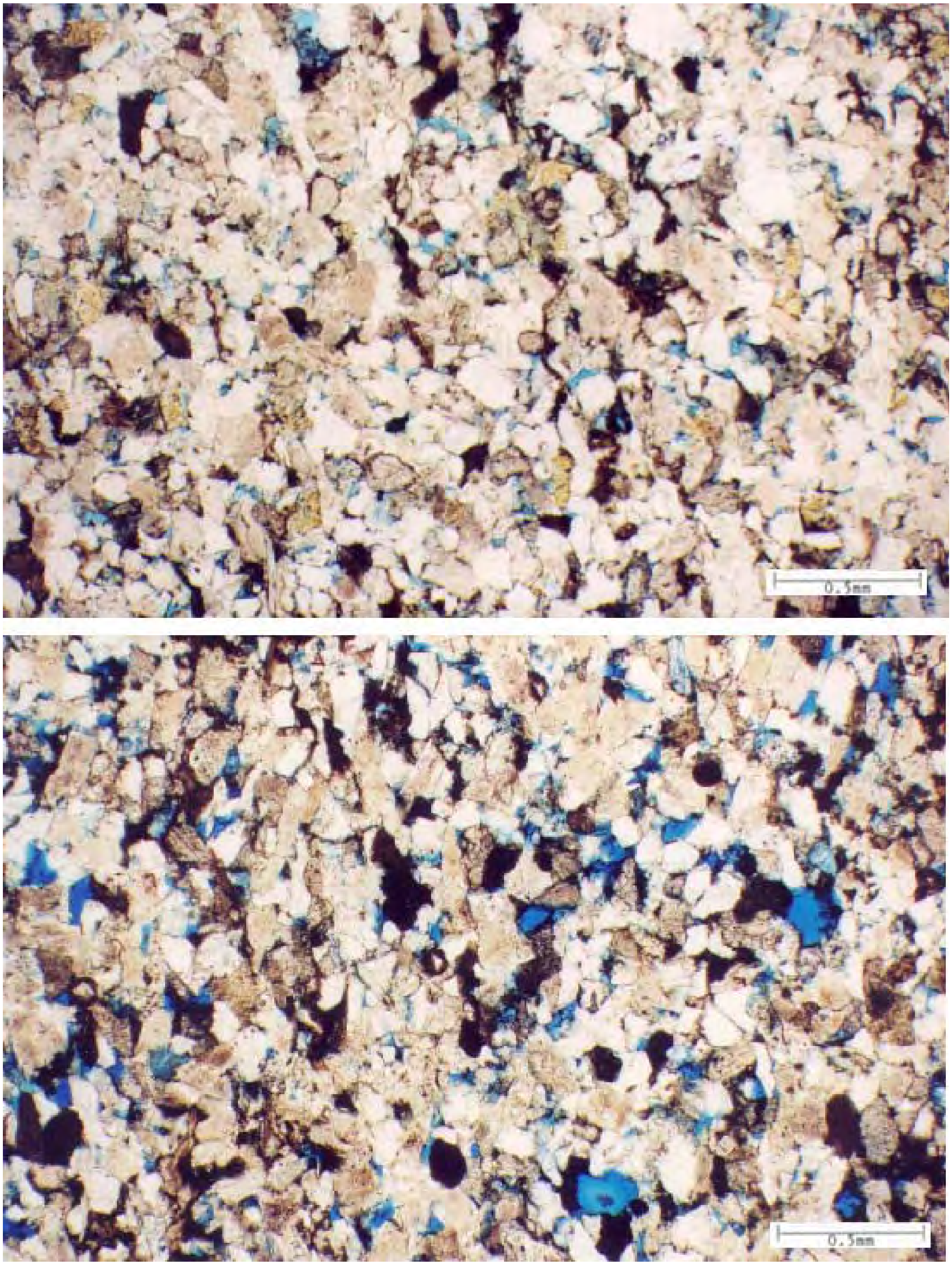

Figure 10. *Photomicrographs of very fine to fine-grained sandstone from the Federal 10 – 34 well, section 34, T. 8 S., R. 16 E., SLBLM, 5,006.0 feet, plane-polarized light. Upper view shows an example of a well compacted and quartz cemented sandstone. The lower view shows some selective dissolution of rock fragments.*

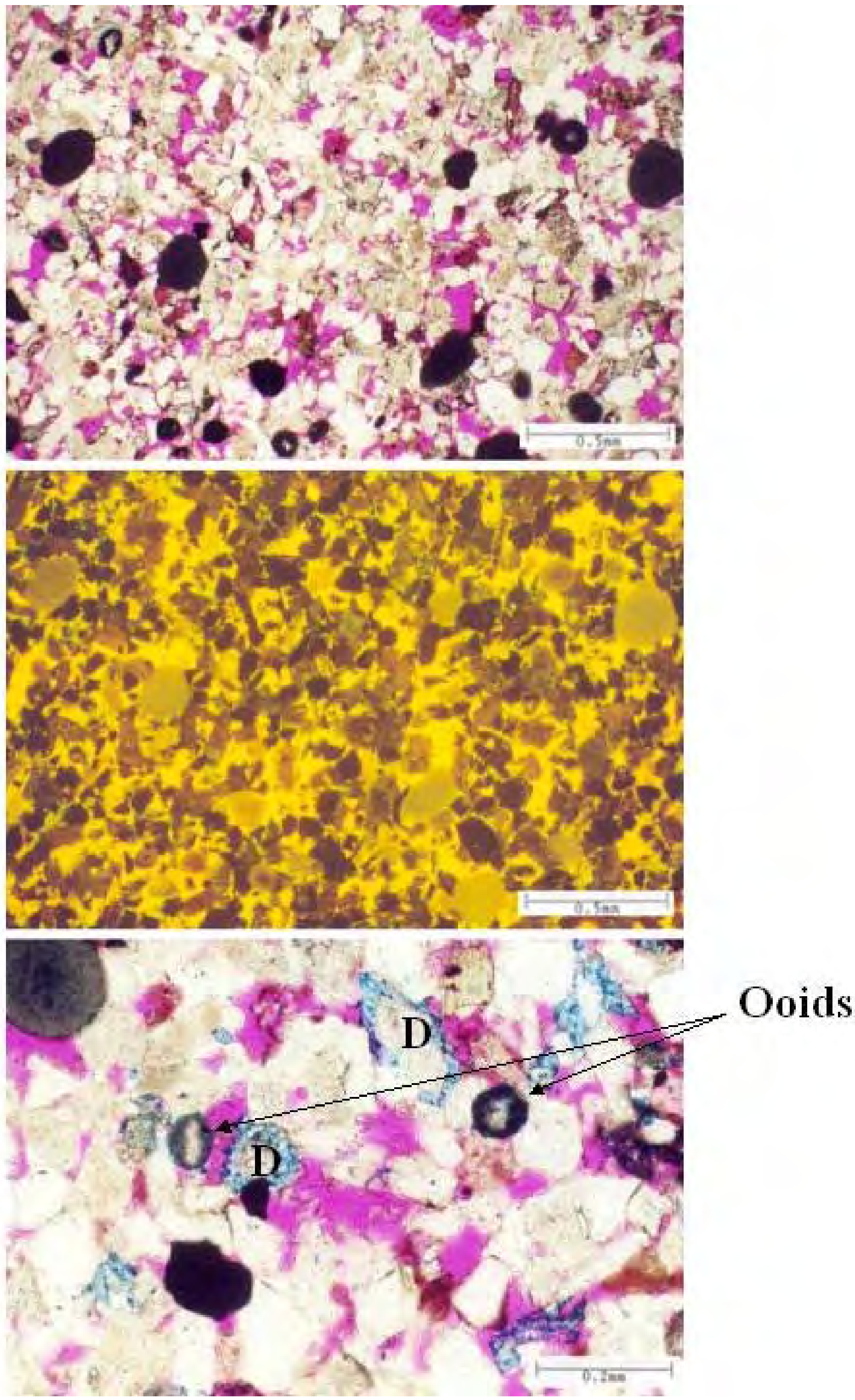

Figure 11. *Photomicrographs of very fine to fine-grained well-sorted feldspathic litharenite with very good porosity. The upper view is plane-polarized light and the middle view is reflected ultraviolet light in which the porosity appears light yellow-orange (secondary intergranular void space) or light yellow-green (carbonate microporosity associated with microcrystalline ankeritic ooids). The lower view is plane-polarized light and reveals late ankeritic (stained blue) infilling the secondary pore spaces. The ankerite commonly nucleated on iron-poor dolomite grains (D).*

to fine-grained sandstone is similar to the medium-grained sandstone, except that compaction/pressure solution is not as severe, and early and late carbonate cementation is more common.

Pore Types

Many pore types are present in the very fine to fine-grained sandstones, but the best reservoir quality is secondary intergranular voids, the majority of which are produced through early calcite cementation and dissolution processes. Secondary pores can be reduced by the incomplete precipitation of quartz overgrowth cements (figure 12). Silica is commonly produced when framework elements compact, releasing "free" silica at grain-to-grain contacts. These reduced intergranular voids are often triangular in two-dimensional cross section. Intergranular pore space can be further reduced by dolomite, ankerite, iron-rich calcite, feldspar, pyrite, and a variety of authigenic clays.

Other void types include dissolution pores, formed when feldspars and rock fragments are preferentially leached, or microporosity developed from partial dissolution. Other forms of microporosity are directly related to clay authigenesis, and include kaolinitic pore filling, illite-smectite pore bridging, and illite (or chlorite) pore lining and infilling. Both dissolution voids and microporosity can add significantly to the porosity volume, but the resulting permeability is usually poor, particularly if dissolution features are somewhat isolated from one another.

Ripple-Drift Laminated Sandstones

The ripple-drift laminated sandstone facies is a variation of the very fine to fine-grained sandstone. These sandstone beds are characterized by ripple-drift lamination and/or clear evidence of climbing ripples. These sedimentary structures are commonly related to transportation of a high sediment load, varying amounts of which are carried in suspension (Jopling and Walker, 1968). In this facies, both very fine grained sand and abundant coarse silt are distributed throughout, and grains commonly conform or are aligned with ripple morphology. Intricate

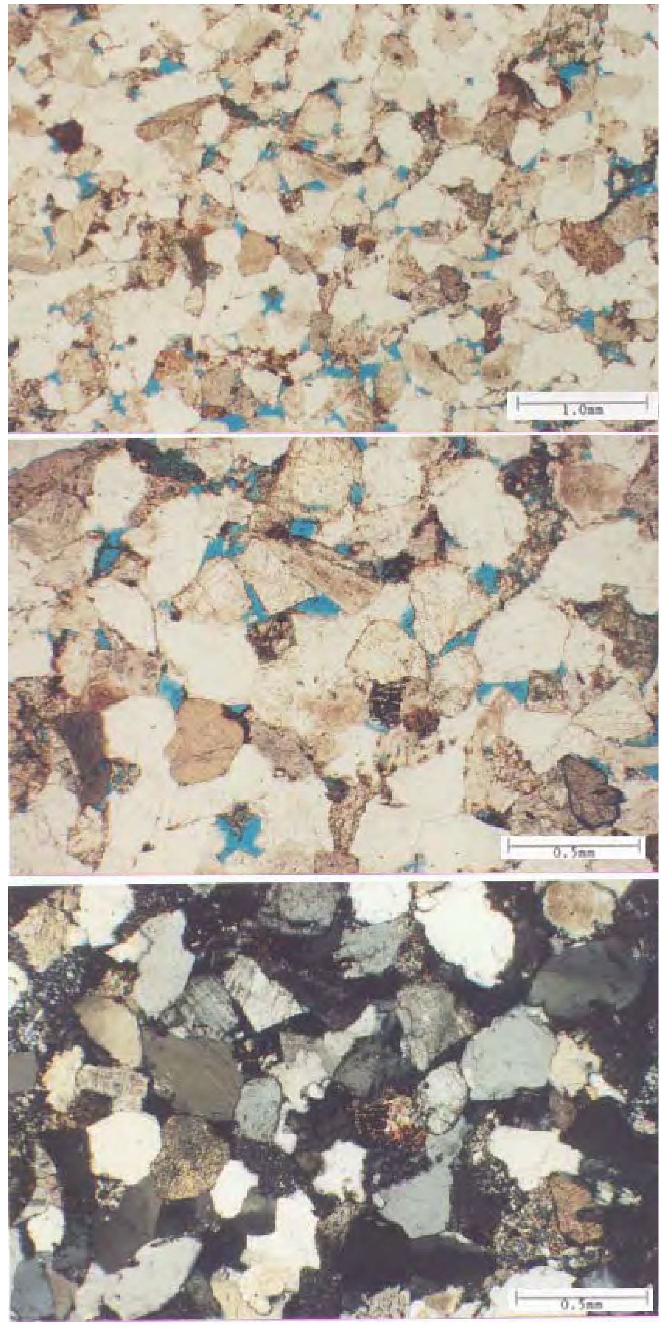

Figure 12. *Photomicrographs of very fine to fine-grained sandstone from the Federal 33 – 8 well, section 8, T. 9 S., R. 17 E., SLBLM, 5,442.6 feet. The upper view (plane-polarized light) shows compaction and quartz overgrowth due to pressure solution of the grains. The middle view (plane-polarized light) and lower view (cross nicols) illustrate reduced intergranular pores (stained blue) due to physical and chemical compaction.*

patterns of cross-lamination are usually evident. Furthermore, gamma-ray values are slightly higher compared to other sandstone facies because of increased mud content. This mud manifests itself in many ways, the two most common of which include abundant detrital clay coatings (mostly illite) of framework grains and increased mica content, especially muscovite. The muscovite is conspicuously aligned subparallel to existing bedding or ripple lamination.

Severe compaction is evident in this facies and must have occurred soon after or during sedimentation. Compaction is also manifested in the abundant microstylolites, which are discontinuously present subparallel to distinct trends in ripple lamination. Such stylolites are also made more visible by pyrite precipitated along the length of the stylolitic features.

Very few traces of early calcite cement are detectable in the ripple drift facies. Porosity and permeability values are very low due to the tightly packed grains with gently curved to distinct interpenetrative contacts. Some porosity is developed by feldspar leaching and clay microporosity. The mineralogy and rock fragment content of the ripple-drift laminated sandstones is similar to that of the very fine to fine-grained sandstones. Sorting is poor, and most grains are angular to subangular.

Very Fine Grained Sandstone and Coarse Siltstone of the Travis Interval

The very fine grained sandstones to coarse siltstones of the Travis interval are cut-and-fill valley deposits that can attain a thickness of over 200 feet (60 m) but are somewhat laterally discontinuous. Two major rock types have been identified in this interval: lithotype T-1, a very poorly sorted combination of siltstone and very fine grained sandstone that commonly contains detrital clay coatings around many of the grains, as well as large clasts of highly compacted dolomitic and illitic mudstones; and lithotype T-2, a distinctly laminated assemblage of very fine to fine-grained sandstone that is characteristically folded and faulted by soft sediment deformation.

Rock Type T-1

The poorly sorted siltstone and very fine grained sandstone lithotype megascopically resembles a chaotic breccia, characterized by haphazardly distributed carbonate mudstone clasts in very poorly sorted silt to very fine grained sandy matrix. The rock is profoundly affected by soft-sediment dewatering, is microscopically very poorly sorted, and has very tightly packed grains. Grain-to-grain contacts are mostly point to linear contacts reflecting a lack of intense pressure solution. Most grains are coated by detrital and authigenic illitic clay. Mineral composition of these rocks is similar to the ripple-drift laminated sandstones, but feldspathic litharenites are more common due to the significant mudstone content. Some clasts appear as distinct, slightly compacted breccia fragments, and other clasts are flattened to the point of developing clear stylolitic seams of modest lateral extent.

Porosity and permeability values are poor due to the detrital/authigenic clay coatings, tight packing, and overall lack of secondary intergranular pores. The most commonly developed void spaces are clay microporosity and fairly isolated dissolution voids. Fractures are rare because the rock is not brittle enough due to the cushioning effect of the detrital clays.

Rock Type T-2

In the laminated sandstone lithotype (T-2), composition and textural relationships are similar to the very fine to fine-grained sandstone. Compacted mudstone clasts are more common at the top of the lamination, resulting in lower porosity. Grain-to-grain compaction is not severe, point and linear contacts are most common, but in poorly sorted portions of the sandstone, extremely tight packing of grains has produced a tight fabric, especially when detrital clay remnants seal some of the interparticle pore space. While the detrital coatings are not present everywhere in the laminated lithotype, they still adversely affect reservoir quality of the microscopic scale (figure 13).

The individual laminations are not strikingly graded, although some grading has been

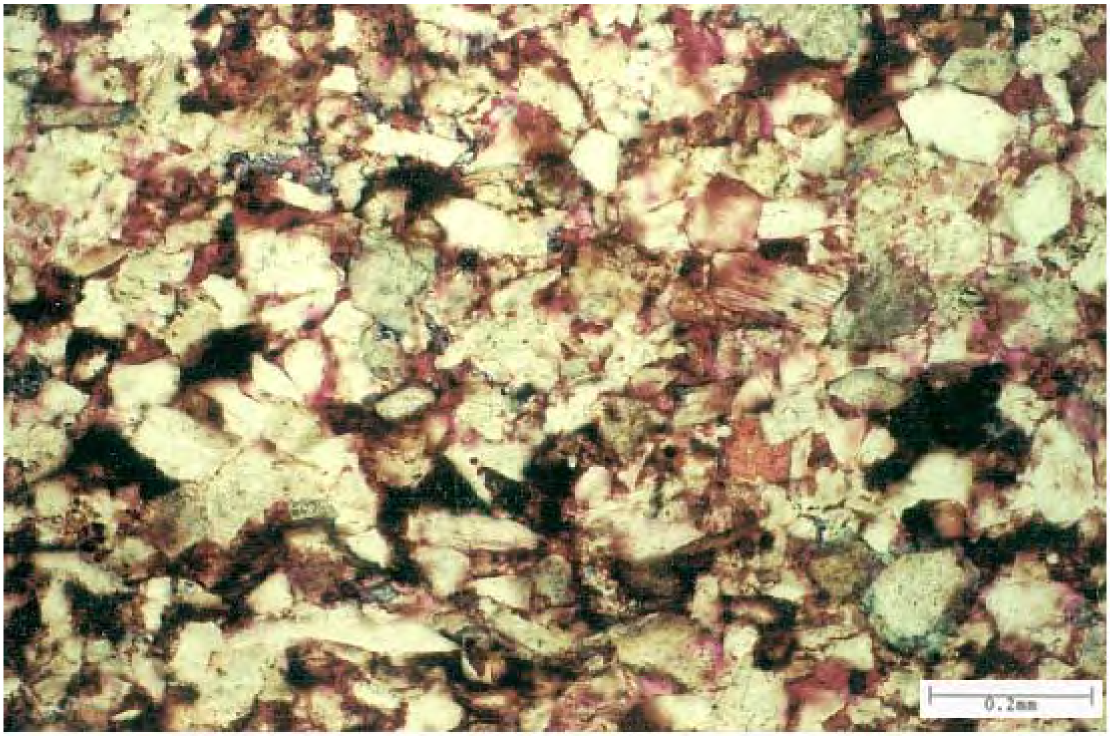

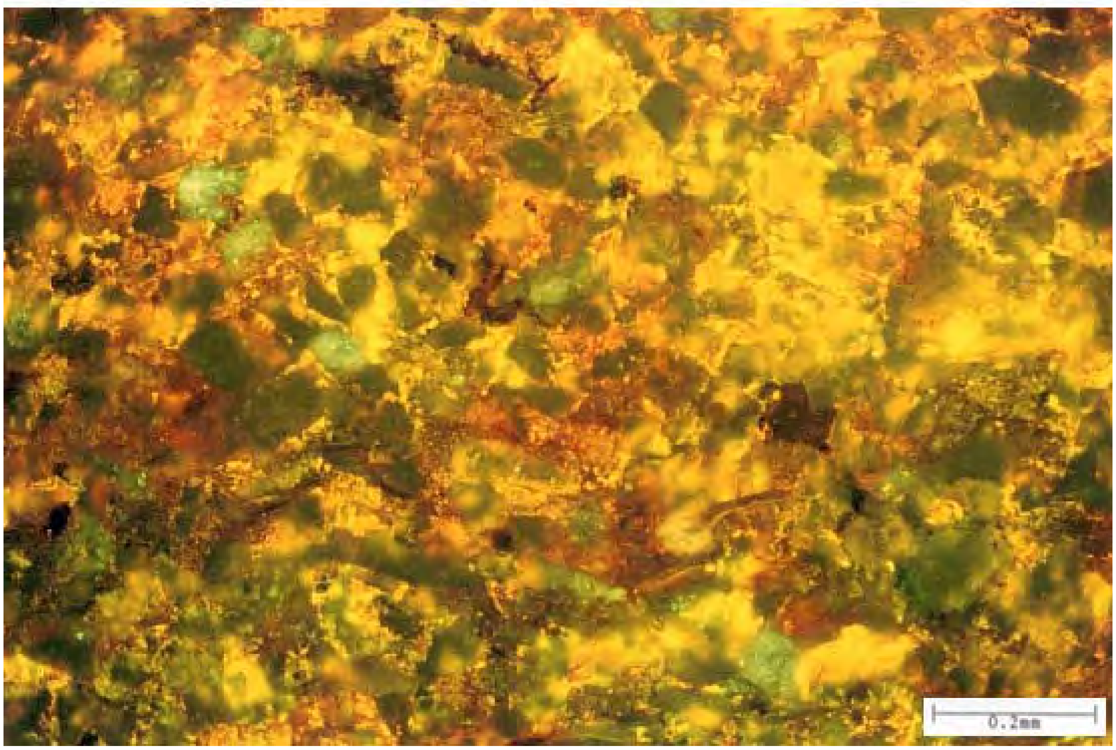

Figure 13. *Paired photomicrographs of the laminated sandstone lithotype of the turbidite facies in the Travis interval from the Federal 13 – 32 well, section 32, T. 8 S., R. 16 E., SLBLM, 5,397 feet. Both views show very poor sorting, variable rounding, localized compaction, and detrital and authigenic clays. Upper view under plane-polarized light reveals porosity through red-dyed epoxy. Dark grains are mudstone fragments which have been physically compacted. Lower view under reflected ultraviolet light, illustrates the varying pore sizes as light yellow-orange (large pores) and reddish hues (small pores).*

observed (figure 14). In the graded intervals, the basal portion of the lamination is loaded or scoured into the underlying layer, fine sand passes upward to very fine grained sand and/or coarse silt, and the uppermost portion is characterized by the highly compacted and elongate carbonate mudstone clasts. These clasts are so elongate and compacted, one can almost recognize the incipient development of stylolites or microstylolitic swarms. Numerous vertical permeability barriers are present on a laminar scale mostly due to mudstone concentration, compaction, and near-stylolitization, although hydraulic fracturing should break these millimeter-scaled barriers.

Porosity is locally variable in these rocks,

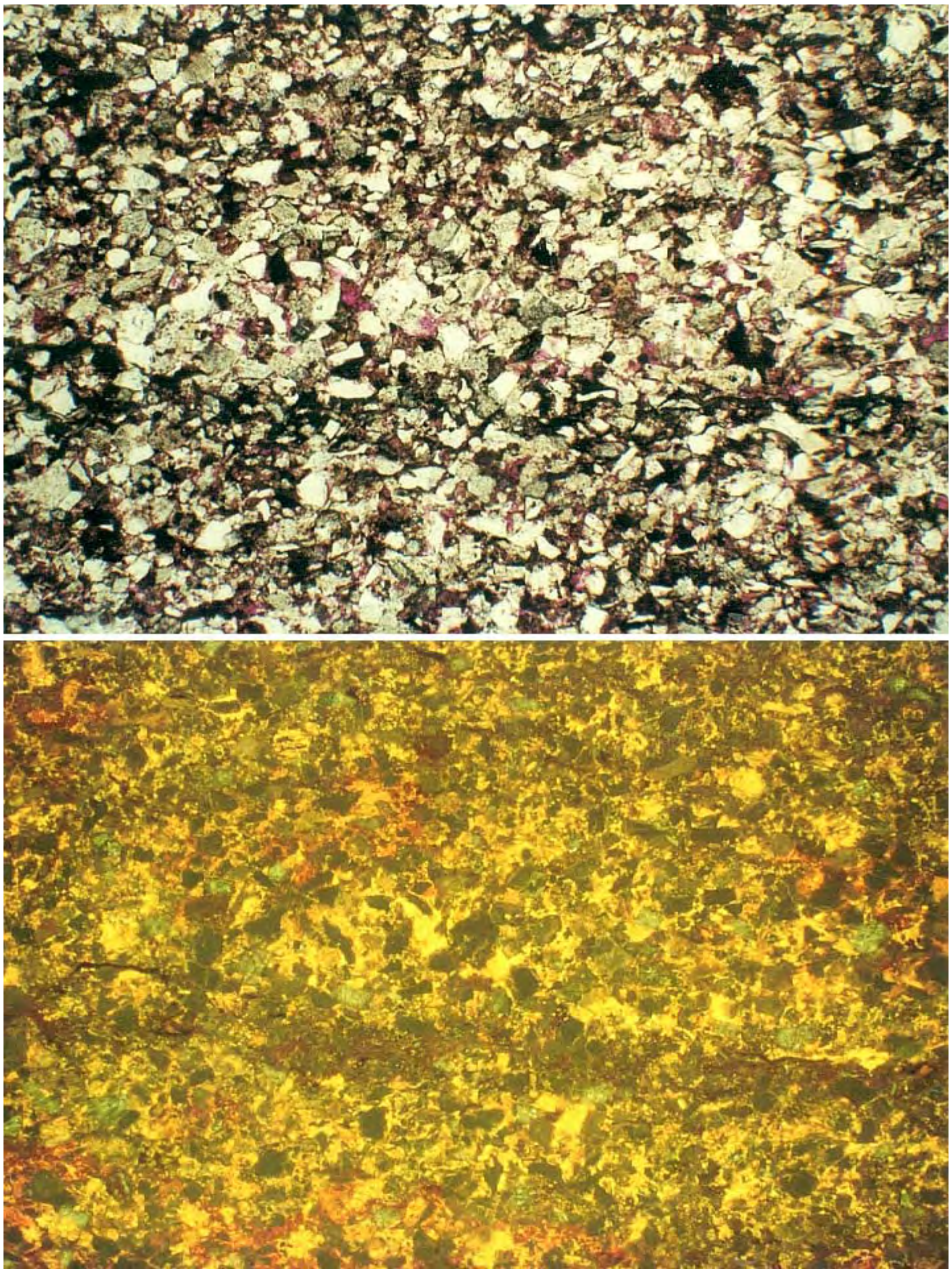

Figure 14. *Photomicrographs of laminated sandstone lithotype of the turbidite facies in the Travis interval from the Federal 13 – 32 well, section 32, T. 8 S., R. 16 E., SLBLM, 5,397 feet. The upper view (plane-polarized light) shows laminated mudstone partings and tightly packed silt-sized material that can impair vertical permeability. The lower view (reflected ultraviolet light) shows varying pore size throughout the sample. Many of the grains are coated by detrital mud, greatly reducing the permeability.*

but some secondary, reduced intergranular porosity exists, especially where early calcite cement was subsequently dissolved. Other voids include partial dissolution pores and clay microporosity. Porosity and permeability values are typically low due to grain packing, sporadic detritial clay coatings, pseudomatrix formation of mudstone clasts, and cementation.

CARBONATE ROCKS

Carbonate beds throughout the lower and middle members of the Green River Formation are usually thin (less than 10 feet [3 m]) but often laterally extensive. The Uteland Butte interval contains the highest percentage of carbonate rock in the lower and middle members. The Uteland Butte interval ranges in thickness from 125 to 250 feet (38-76 m) (Little, 1988). The Uteland Butte interval in the Monument Butte area consists mostly of light brown to medium dark gray limestone and dolomitic shale.

Uteland Butte Carbonates

The Uteland Butte interval consists of limestones and dolostones, calcareous mudstones, siltstones, sandstones, and mixed rocks (containing both carbonate allochems and siliciclastics) (figure 15). Potential reservoir rocks in the Uteland Butte are thin sandstones and dolomitic limestones that are commonly porous and sporadically permeable.

The grain-supported limestones are fairly similar to one another in that ostracod carapaces and/or ooids comprise many of the recognized allochems. The ostracods are: (1) broken or whole, (2) disarticulated or articulated, (3) compacted or noncompacted, or (4) a single carapace or as concentric instars. Other allochems include: (1) fresh-water mollusks including disarticulated pelecypods or turriform gastropods, (2) ooids or superficial ooids, (3) algae, (4) fish fragments, (5) intraclasts, (6) peloids of indeterminate origin, and (7) varying amounts of sand or silt-sized siliciclastics.

Ostracods are common to both mud-supported and grain-supported limestones (wackestones, packstones, and grainstones) (figure 16). When not totally surrounded by nonporous lime mud or spar cement, the ostracodal carbonates contain one or more of the following void types: (1) intraskeletal porosity, (2) shelter porosity (immediately beneath a disarticulated carapace), (3) moldic porosity due to partial dissolution of allochems or matrix, and (4) microporosity or microintercrystalline porosity (dolomitized). Permeability is partially controlled by compaction and/or dolomitization. Compaction allows the ostracod to pass from a closed oblate spheroid (football-shape) to a more open and communicative entity, in which ostracod terminations are not morphologically closed. Porosity can be developed in a grain-supported limestone or dolomite in which the individual carapaces have “open” terminations due to significant compaction.

Locally, the top of the Uteland Butte interval contains a high-porosity (+20 percent) dolomitic bed. The bed is a compacted wackestone/packstone comprised of ostracods associated with lime mud. Compaction has significantly deformed many ostracod carapaces, and the wackestone/packstone lithology was sufficiently compacted and grain supported to permit dolomitizing fluids to pass among the many allochems and muddy elements. The porous cryptocrystalline dolomite is so finely crystalline that permeability values are very low (single millidarcies).

Sedimentary structures are rare, or difficult to identify, in the grain-supported limestones. Rip-ups, lag deposits, and modest channeling are observed, usually near the base, and lamination or very low angle cross-lamination, perhaps reflective of small ripple features on the bedding plane surfaces, can be observed in both hand specimen and thin section.

Carbonate Marker Bed

The carbonate marker bed (figure 3), also known as the Castle Peak limestone, is the top of the lower member of the Green River Formation. The carbonate marker bed is laterally extensive and is easily identified on most well logs throughout the south-central Uinta Basin. The

A

Figure 15. *Core from the Uteland Butte interval from the Desert Springs 11 – 20 – 10 – 17 well, section 20 T. 10 S., R. 17 E., SLBLM, (A) 4,981 to 4,991 feet and (B) 4,991 to 5,001 feet. Dark organic mudstones are interbedded with light brown (oil stained) carbonate ostracodal and oolitic packstones and grainstones (top row of A and most of B).*

bed is typically about 10 feet (3 m) thick, but locally thickens and can be a petroleum reservoir. The best example is at the West Willow Creek field [T. 9 S., R. 19 E., Salt Lake Base Line and Meridian (SLBLM)] where the bed is an algal bioherm or stromatolite mound (Osmond, 2000) up to 100 feet (30 m) thick containing abundant algal material (figure 17). The bioherm contains both limestone and finely to microcrystalline dolomite, the latter commonly present as an admixture (dolomitic limestone). Because of the finely crystalline nature of the dominantly subhedral dolomite, most intercrystalline pores are relatively small, and resulting permeabilities within this bioherm fall within the single millidarcy range. The buildup of the bioherm ended when the lake deepened as evidenced by the overlying black shale at 4,768 feet (1,453.3 m) in the PG & E 15-24B well (appendix A).

B

Figure 15. *Continued*

Figure 16. *Photomicrographs of mud-suported and grain-supported ostracodal limestones from the Uteland Butte interval from the Desert Creek 16 – 17 – 10 – 17 well, section 17, T. 10 S., R. 17 E., SLBLM. (A) From 5,152.0 feet, the upper view (plane-polarized light) shows detrital quartz mixed with broken and whole ostracode debris dominating the lower lamination. The lower view (plane-polarized light) consists of a laminated fabric where a partially consolidated silty mud-rich lamina is deformed by ostracodal grainstone. (B) From 5,154.0 feet, the upper view (plane-polarized light) illustrates presence of abundant articulated ostracodal carapaces and very little apparent porosity (mauve color). The lower view (reflected ultraviolet light) demonstrates abundant porosity (light yellow to yellow-orange), but most voids lie within individual carapaces and are probably not well connected (poor permeability). (C) From 5,094.0 feet, the upper view (plane-polarized light with a dual-carbonate stain) was originally an ostracodal packstone which was compacted and subsequently dolomitized. Compaction of ostracods causes the carapace to gape at the shell termination rather than producing a normally closed termination. This type of compaction provides porosity and permeability, and may have allowed flow of dolomitizing fluids. Lower view (reflected ultraviolet light) in yellow-orange fluorescence light shows the well-developed porosity with varying pore size as seen by variations in the yellow-orange intensity.*

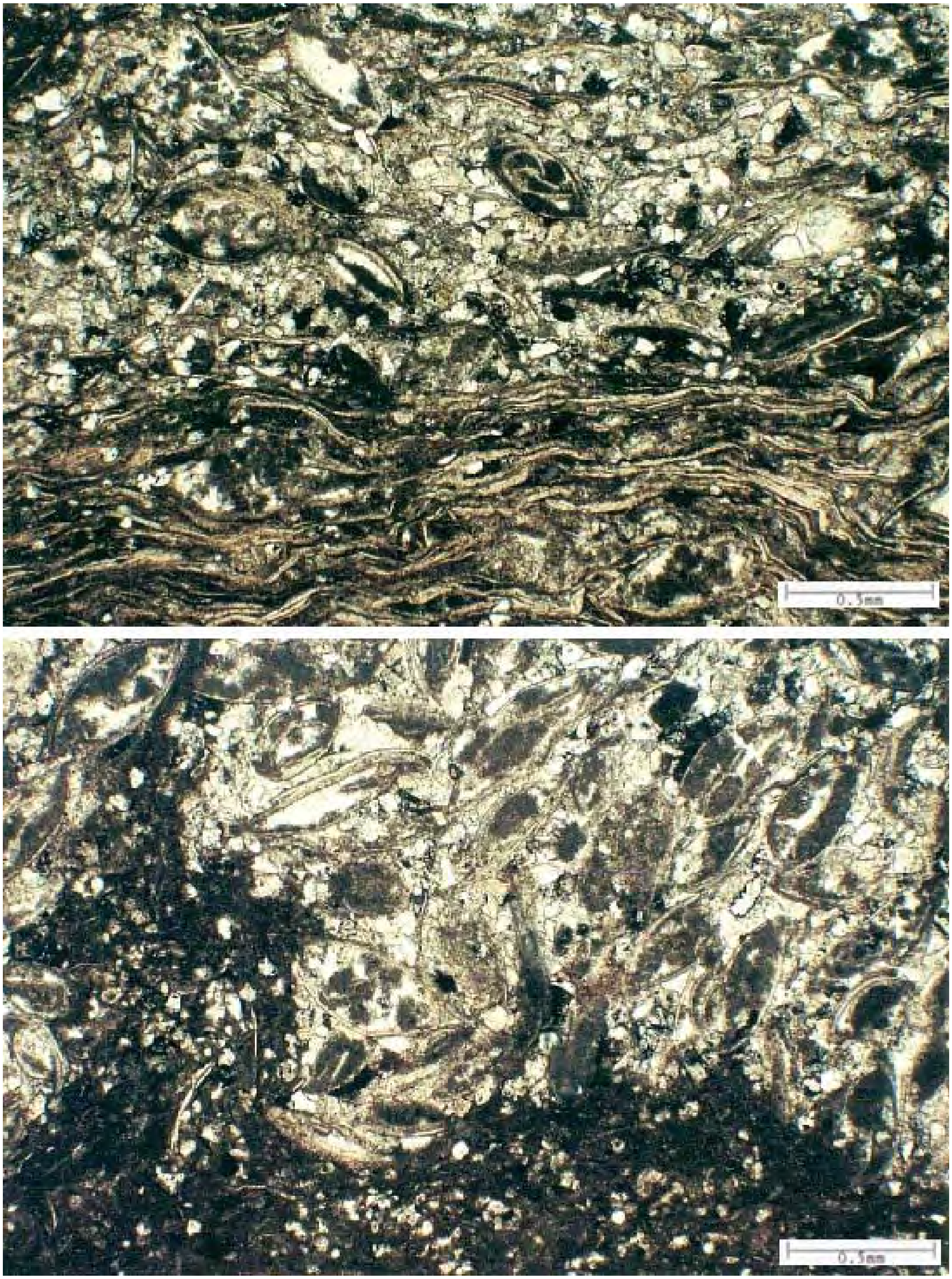

A

Figure 16. *Continued*

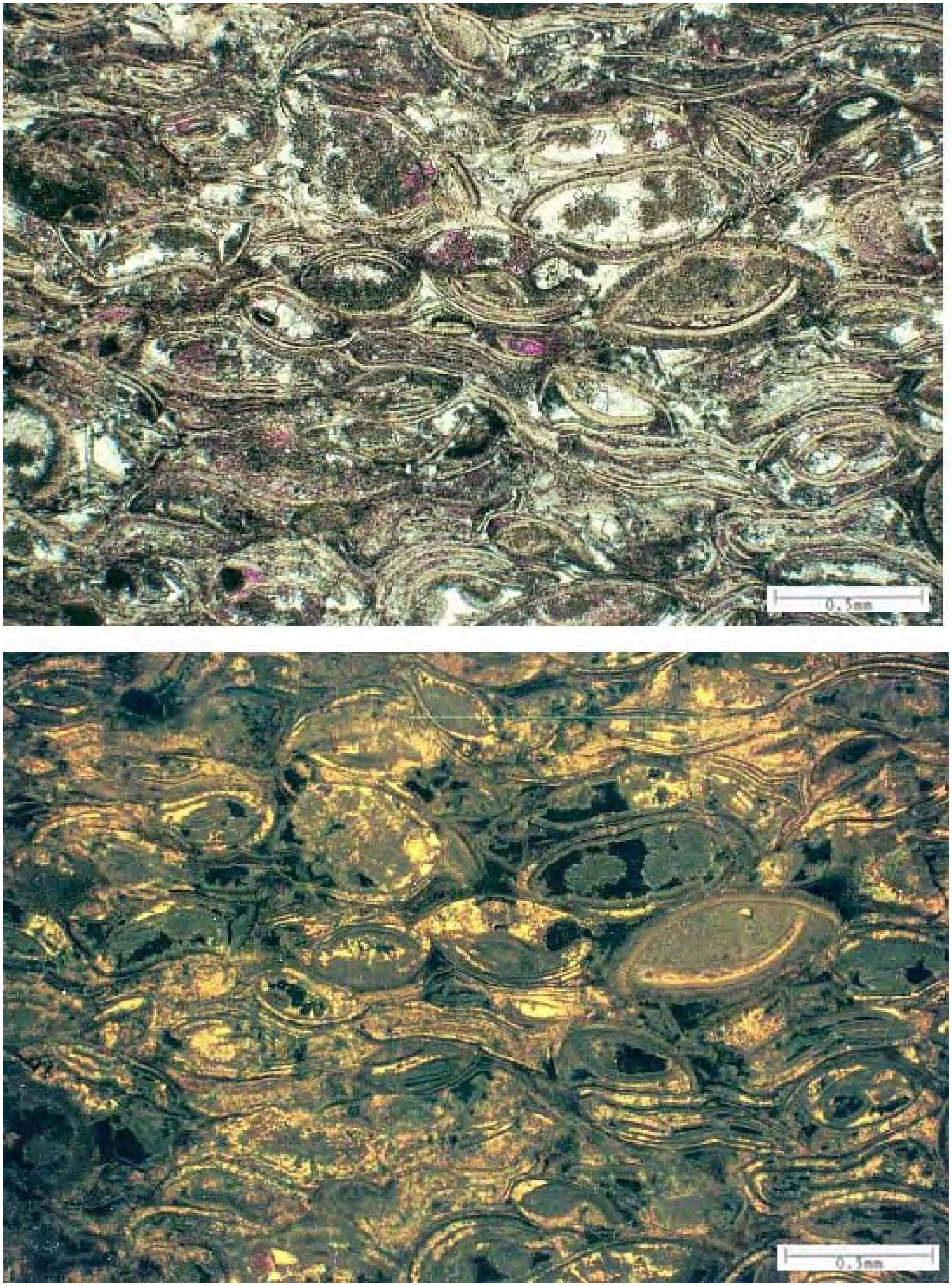

B

Figure 16. *Continued*

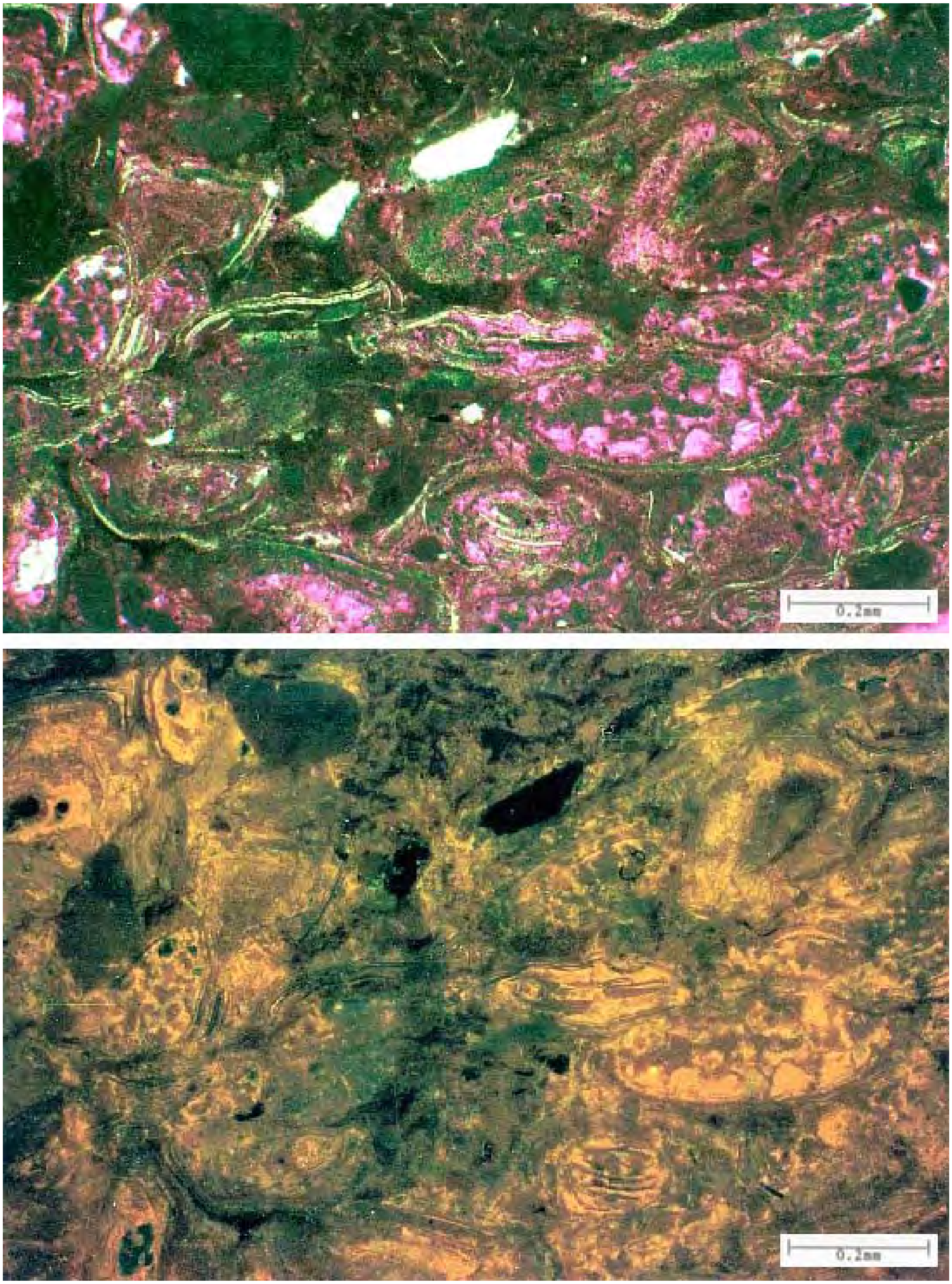

C

Figure 16. *Continued*

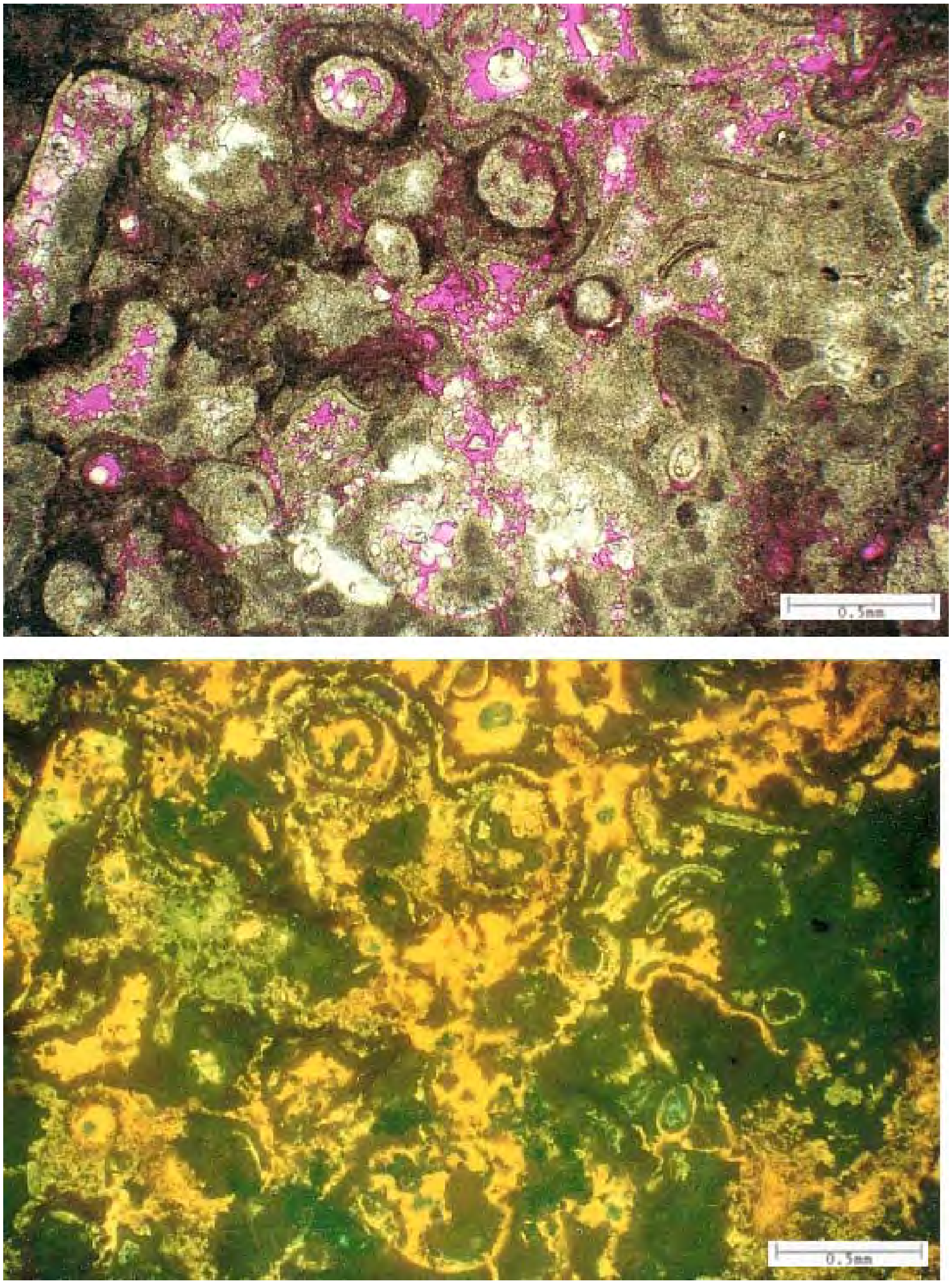

A

Figure 17. *Photomicrographs of algal material from a bioherm buildup in the carbonate marker bed in the Federal 15 – 24B well, section 24, T. 9 S., R. 19 E., SLBLM. (A) From 4,733.1 feet, showing presence of dolomitized algae with fairly good porosity as evidenced by the yellow-orange in the lower view (both views, upper view is plane-polarized light and the lower view is reflected ultraviolet light). (B) From 4,799.0 feet, illustrating a carbonate interbed constructed from abundant algal material (plane-polarized light). (C) From 4,784.2 feet, the upper view (plane-polarized light) shows a pisoid clearly constructed by algal material and the lower view (plane-polarized light) shows a close-up of algal microstructural detail.*

B

Figure 17. *Continued*

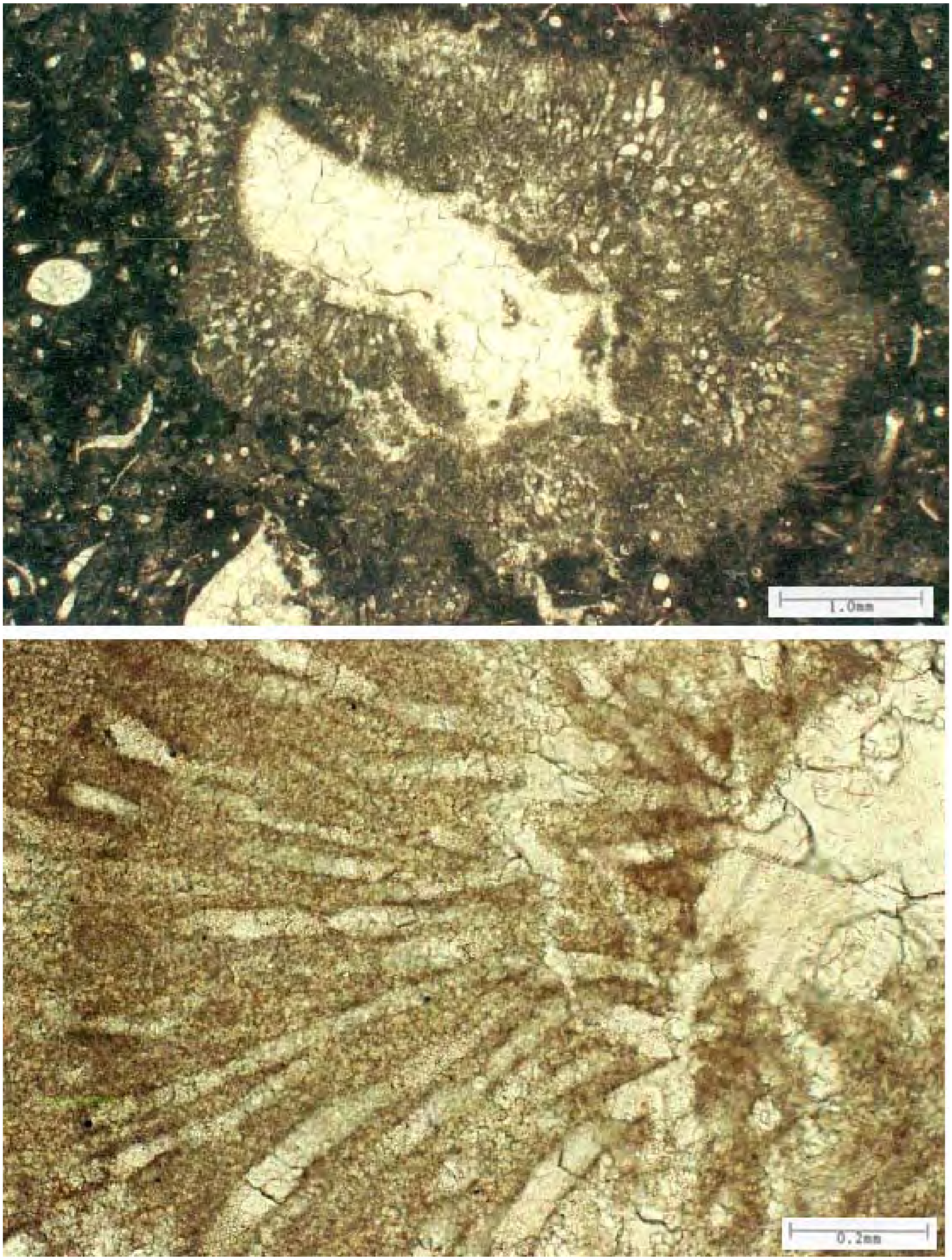

C

Figure 17. *Continued*

SUMMARY

- Most Green River sandstones are either feldspathic litharenites or lithic arkoses derived from sedimentary and basement source terrains to the south. Aside from the medium-grained sandstones in the Castle Peak interval, the dominant grain size is very fine to fine grained.

- Evidence for an igneous/metamorphic source is provided by abundant feldspars, metamorphic and granitic rock fragments, composition of heavy minerals (including sphene), rutilated quartz, and significant amounts of biotite (partially altered to chlorite in some instances), common to many of the basement rocks of the Uncompaghre uplift

- Sandstone deposition in the south-central Uinta Basin mostly occurred in moderate- to low-gradient distributary channels. These channels were part of an anastomosing system that migrated laterally over time. In some cases, distributary sands appear subaqueous with abundant dewatering phenomena; in other areas, root casts, associated coal seams, mud-cracked horizons, and penecontemporaneous dolomites indicate proximity to subaerial conditions.

- Reservoir quality (porosity and permeability) in the sandstones is largely determined by the diagenesis. The best reservoir quality usually results from early iron-poor calcite cementation and subsequent dissolution. The poorest quality is caused by extensive packing of poorly sorted materials and grain-to-grain compaction, along with quartz and/or iron-rich carbonate cementation.

- Clay diagenesis involves many authigenic episodes that can partition existing pores into tortuous micropores. Authigenic clay includes chlorite, kaolinite, illite, and illite-smectite.

- Open-lacustrine materials dominantly consist of light gray-green or dark gray to black mudstones, and the more distal, dark gray argillaceous carbonates.

- Lacustrine turbidites in the Travis interval contain a debris-flow facies with chaotic poorly sorted materials including deformed breccia clasts, and a rhythmically laminated, partially graded, siltstone to very fine grained sandstone facies. Slumping, cut-and-fill features, and soft-sediment folding and faulting are very common.

- Carbonates are present as intermittent stratigraphic markers among the more prevalent siliciclastic sandstones, siltstones, and mudstones except for the Uteland Butte interval which is dominantely carbonate. These thin carbonates typically have very low porosity.

- Most carbonate reservoir rocks consist of grain-supported oolitic and/or ostracodal packstones or grainstones, with varying permeabilities. Low permeabilities (~0.1 md) exist where intraorganic and moldic void space remains isolated within articulated and calcite-cemented ostracod carapaces and selectively leached concentric ooid laminae. Better permeabilities exist where ostracod carapaces are compacted but not flattened. Open, rather than closed terminations of biconvex shells allow the connectivity of dominant intraorganic void space. Good permeabilities also result when some limestones are dolomitized.

- Algal bioherms have been recognized in the Castle Peak limestone. A combination of intraorganic void space and dolomitization provides reasonably good reservoir quality.

CONCLUSIONS

- Typically, the best reservoir-quality rocks are the distributary-channel sandstones found mostly in the Monument Butte interval and to a lesser extent the Beluga interval.

- The ripple-drift laminated sandstone facies and the very poorly sorted combination of siltstone and very fine-grained sandstone lithotype in the lacustrine turbidite facies are often poor exploration targets.

- The diagenesis of a sandstone bed may vary significantly when compared to correlative beds. The isolated channels within the anastomosing system may possess individually isolated diagenetic histories.

- The naturally fractured Castle Peak sandstones and the lacustrine turbidite facies with complex internal heterogeneity in the Travis interval are good targets for horizontal drilling.

- Algal bioherms, particularly in the carbonate marker bed, may be a good exploration target throughout many parts of the Uinta Basin.

ACKNOWLEDGMENTS

These cores were described and photographed as part of a UGS project titled *Reservoir Characterization of the Lower Green River Formation, Southwest Uinta Basin, Utah* funded, in part, under the Fundamental Geoscience for Reservoir Characterization Program of the U.S. Department of Energy (DOE), National Petroleum Technology Office, Tulsa, Oklahoma, contract number DE-AC26-98BC15103. The DOE Contracting Officer's Representative was Virginia Weyland.

Thin sections and SEM samples were prepared by TerraTek, Salt Lake City. UGS staff members Carolyn Olsen and Thomas Dempster photographed much of the core. Nan Glen (formerly Oleson) provided thin sections from her masters thesis (Nan E. Oleson, 1986). Sue Lutz made available the core and photomicrographs from the Travis 14A-28 well and XRD data from several wells.

REFERENCES

Bradley, W.H., 1931, Origin and microfossils of the oil shale of the Green River Formation of Colorado and Utah: U.S. Geological Survey Professional Paper 168, 56 p.

Case, J.E., 1991, Geologic map of the northwestern part of the Uncompahgre uplift, Grand County, Utah and Mesa County, Colorado, with emphasis on Proterozoic rocks: U.S. Geological Survey Miscellaneous Investigations Series Map I-2088, 2 sheets, 1:24,000.

Chidsey, T.C., Jr., and Laine, M.D., 1992, The fractured Green River and Wasatch Formations of the Uinta Basin, Utah - targets for horizontal drilling, *in* Fouch, T.D., Nuccio, V.F., and Chidsey, T.C., Jr., editors, Hydrocarbon and mineral resources of the Uinta Basin, Utah and Colorado: Utah Geological Association Guidebook 20, p. 123-134.

Colburn, J.A., Bereskin, S.R., McGinley, D.C., and Schiller, D.M., 1985, Lower Green River Formation in the Pleasant Valley producing area, Duchesne and Uintah Counties, Utah, *in* Picard, M.D., editor, Geology and energy resources, Uinta Basin, Utah: Utah Geological Association Publication 12, p. 177-186.

Fouch, T.D., 1975, Lithofacies and related hydrocarbon accumulations in Tertiary strata of the western and central Uinta Basin, Utah, *in* Bolyard, D.W., editor, Symposium on deep drilling frontiers in the central Rocky Mountains: Rocky Mountain Association of Geologists, p. 163-173.

Fouch, T.D., and Dean, W.E., 1982, Lacustrine and associated clastic depositional environments, *in* Scholle, P.A., and Spearing, Darwin, editors, Sandstone depositional environments: American Association of Petroleum Geologists Memoir 31, p. 87-114.

Fouch, T.D., Nuccio, V.F., and Chidsey, T.C., Jr., editors, 1992, Hydrocarbon and mineral resources of the Uinta Basin, Utah and Colorado: Utah Geological Association Guidebook 20, 366 p.

Jacob, A.F., 1969, Delta facies of the Green River Formation (Eocene), Carbon and Duchesne Counties, Utah: Boulder, University of Colorado, Ph.D. dissertation, 97 p.

Jopling, A.V., and Walker, R.G., 1968, Morphology and origin of ripple-drift cross-lamination, with examples from the Pleistocene of Massachusetts: Journal of Sedimentary Petrology, v. 38, p. 971-984.

Keighley, D., Flint, S., Howell, J., Anderson, D., Collins, S., Moscariello, A., and Stone, G., 2002, Surface and subsurface correlation of the Green River Formation in central Nine Mile Canyon, SW Uinta Basin, Carbon and Duchesne Counties, east-central Utah: Utah Geological Survey Miscellaneous Publication 02-1, CD-ROM, 29 p., 4 appendices.

Little, T.M., 1988, Depositional environments, petrology, and diagenesis of the basal limestone facies, Green River Formation (Eocene), Uinta Basin, Utah: Salt Lake City, University of Utah, M.S. thesis, 154 p.

Lutz, S.J., Nielson, D.L., and Lomax, J.D., 1994, Lacustrine turbidite deposits in the lower portion of the Green River Formation, Monument Butte field, Uinta Basin, Utah [abs.]: American Association of Petroleum Geologists Annual Meeting Program with Abstracts, v. 3, p. 203.

McDonald, R.E., 1972, Eocene and Paleocene rocks of the southern and central basins, *in* W.W. Mallory, editor, Geologic atlas of the Rocky Mountain region: Rocky Mountain Association of Geologists, p. 243-256.

Morgan, C.D., McClure, K.P., Bereskin, S.R., Deo, M.D., and Weller, Kevin, 2000, Reservoir characterization of the lower Green River Formation, southwest Uinta Basin, Utah: Unpublished biannual technical progress report to the U.S. Department of Energy for the period 10/1/99 through 3/31/00, 56 p.

Morgan, C.D., Chidsey, T.C., Jr., Hanson, J.A., McClure, K.P., Weller, Kevin, Bereskin, S.R., Deo, M.D., and Yeager, Randy, 1999, Reservoir characterization of the lower Green River Formation, southwest Uinta Basin, Utah: Unpublished biannual technical progress report to the U.S. Department of Energy for the period 10/1/98 through 3/31/99, 11 p.

Morgan, C.D. and Bereskin, S.R., 2003, Characterization of petroleum reservoirs in the Eocene Green River Formation, central Uinta Basin, Utah: The Mountain Geologist, v. 40, no. 4, p. 111-127.

Morgan, C.D., Chidsey, T.C., Jr., McClure, K.P., Bereskin, S.R., and Deo, M.D., 2003, Reservoir characterization of the lower Green River Formation, southwest Uinta Basin, Utah: Utah Geological Survey Open-File Report 411, CD-ROM, 140 p.

Oleson, N.E., 1986, Petroleum geology of the Eocene lower Green River Formation, Duchesne and Uintah Counties, Utah: Waco, Baylor University, M.S. thesis, 173 p.

Osmond, J.C., 2000, West Willow Creek - first productive lacustrine stromatolite mound in the Eocene Green River Formation, Uinta Basin, Utah: Rocky Mountain Association of Geologists, The Mountain Geologist, v. 37, no. 3, p. 157-170.

Picard, M.D., 1955, Subsurface stratigraphy and lithology of the Green River Formation in Uinta Basin, Utah: American Association of Petroleum Geologists Bulletin, v. 39, no. 1, p. 75-102.

---1957a, Criteria used for distinguishing lacustrine and fluvial sediments in Tertiary beds of Uinta Basin, Utah: Journal of Sedimentary Petrology, v. 27, no. 4, p. 75-102.

---1957b, Green shale facies, lower Green River Formation, Utah: American Association of Petroleum Geologists Bulletin, v. 41, p. 2373-2376.

Pitman, J.K., Fouch, T.D., and Goldaber, M.B., 1982, Depositional setting and diagenetic evolution of some Tertiary unconventional reservoir rocks, Uinta Basin, Utah: American Association of Petroleum Geologists Bulletin, v. 66, no. 10, p. 1581-1596.

Remy, R.R., 1992, Stratigraphy of the Eocene part of the Green River Formation in the south-central part of the Uinta Basin, Utah: U.S. Geological Survey Bulletin 1787-BB, 79 p.

Ryder, R.T., Fouch, T.D., and Elison, J.H., 1976, Early Tertiary sedimentation in the western Uinta Basin, Utah: Geological Society of America Bulletin, v. 87, p. 496-512.

Weiss, M.P., Witkind, I.J., and Cashion, W.B., 1990, Geologic map of the Price 30'X60' quadrangle, Carbon, Duchesne, Uintah, Utah, and Wasatch Counties, Utah: U.S. Geological Survey Miscellaneous Investigations Series Map I-1981, 1 sheet, 1:100,000.

APPENDICES

APPENDIX A: Core description sheets with log curves, porosity and permeability curves, core photographs and photomicrographs.

APPENDIX B: Routine core analysis data.

APPENDIX C: Scanning electron microscopy report prepared by TerraTek, Salt Lake City, Utah.

APPENDIX D: X-ray diffraction data.

APPENDIX A
CORE DESCRIPTIONS AND GRAPHICAL REPRESENTATIONS OF WELL LOG AND ROUTINE CORE ANALYSIS DATA

Location and cored interval data of the well core examined for this study.

MAP NUMBER[1] (figure 1)	WELL NUMBER	API NUMBER[2]	LOCATION Sec., T., R.[3]	CORED INTERVAL (feet)	CORRELATION INTERVAL[4] (figure 2)
1	Ute Tribal 2-25	43-013-31833	25, T5S, R5W Uinta Base Line and Meridian	5527-5596	Castle Peak
2	Travis 14A-28	43-013-30792	28, T8S, R16E	5550-5646	Travis
3	Travis 10-28	43-013-30856	28, T8S, R16E	5586-5603	Travis
4	Federal 2-33	43-013-30749	33, T8S, R16E	5647-5676	Travis
5	Federal 6-33	43-013-30747	33, T8S, R16E	5596-5616	Monument Butte
6	Federal 6-35	43-013-30752	35, T8S, R16E	5026-5048	Monument Butte
7	Monument Federal 3A-35	43-013-31738	35, T8S, R16E	4993-5022	Monument Butte
8	Federal 23-24	43-047-32710	24, T8S, R17E	5325-5363	Monument Butte
9	Federal 23-25	43-047-32529	25, T8S, R17E	5145-5185	Monument Butte
10	State 6-32	43-013-30748	32, T8S, R17E	5042-5053	Monument Butte
11	Federal 33-11J	43-013-31451	11, T9S, R16E	4840-4870 5158-5207 5370-5424	Monument Butte Travis Travis
12	Allen 34-5	43-013-30721	5, T9S, R17E	4995-5045	Travis
13	Federal 33-8	43-013-31427	8, T9S, R17E	4632-4660 5440-5470	Monument Butte Castle Peak
14	Paiute 34-8	43-013-30778	8, T9S, R17E	4050-4129	Beluga
15	Pariette 5	43-047-10298	9, T9S, R18E	5407-5457	Castle Peak
16	Pariette 6	43-047-10873	5, T9S, R19E	4454-4487 4867-4894 5046-5080	Beluga Travis Travis
17	State 13-16J	43-047-31128	16, T9S, R19E	4238-4328 5350-5385	Monument Butte Uteland Butte
18	Federal 15-17	43-047-31002	17, T9S, R19E	4255-4306	Monument Butte
19	Federal 15-24B	43-047-32420	24, T9S, R19E	4738-4817	Castle Peak
20	Island 16	43-047-31505	11, T10S, R18E	4690-4812	Uteland Butte
21	Desert Springs 11-20-10-17	43-013-32088	20, T10S, R17E	4970-5030 5100-5150	Uteland Butte Uteland Butte

[1] Map number refers to numbers found on figure 1.
[2] API number is the American Petroleum Institute numbering system.
[3] Location: Sec. = section, T. = township, R. = range; all are SLBLM unless noted otherwise.
[4] Correlation interval: nomenclature from figure 3.

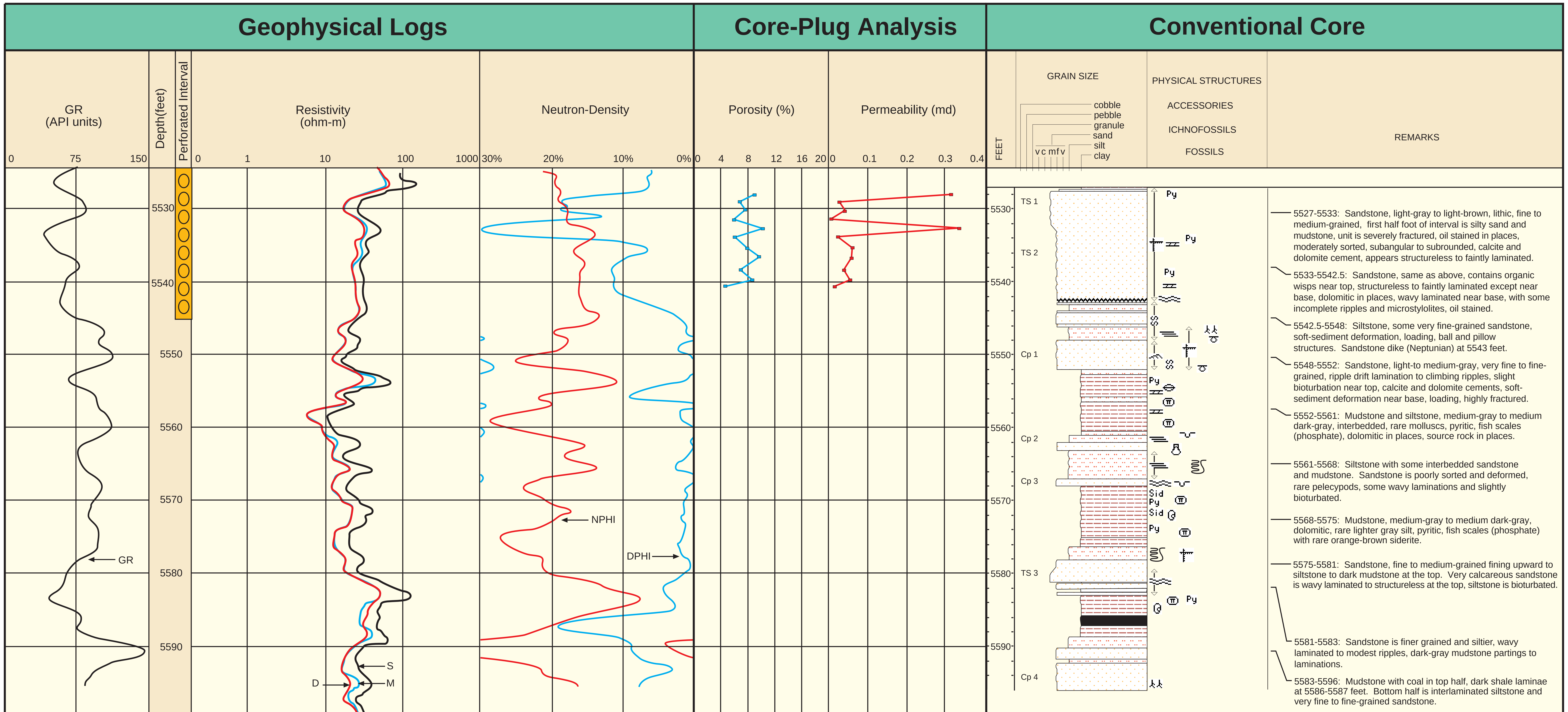

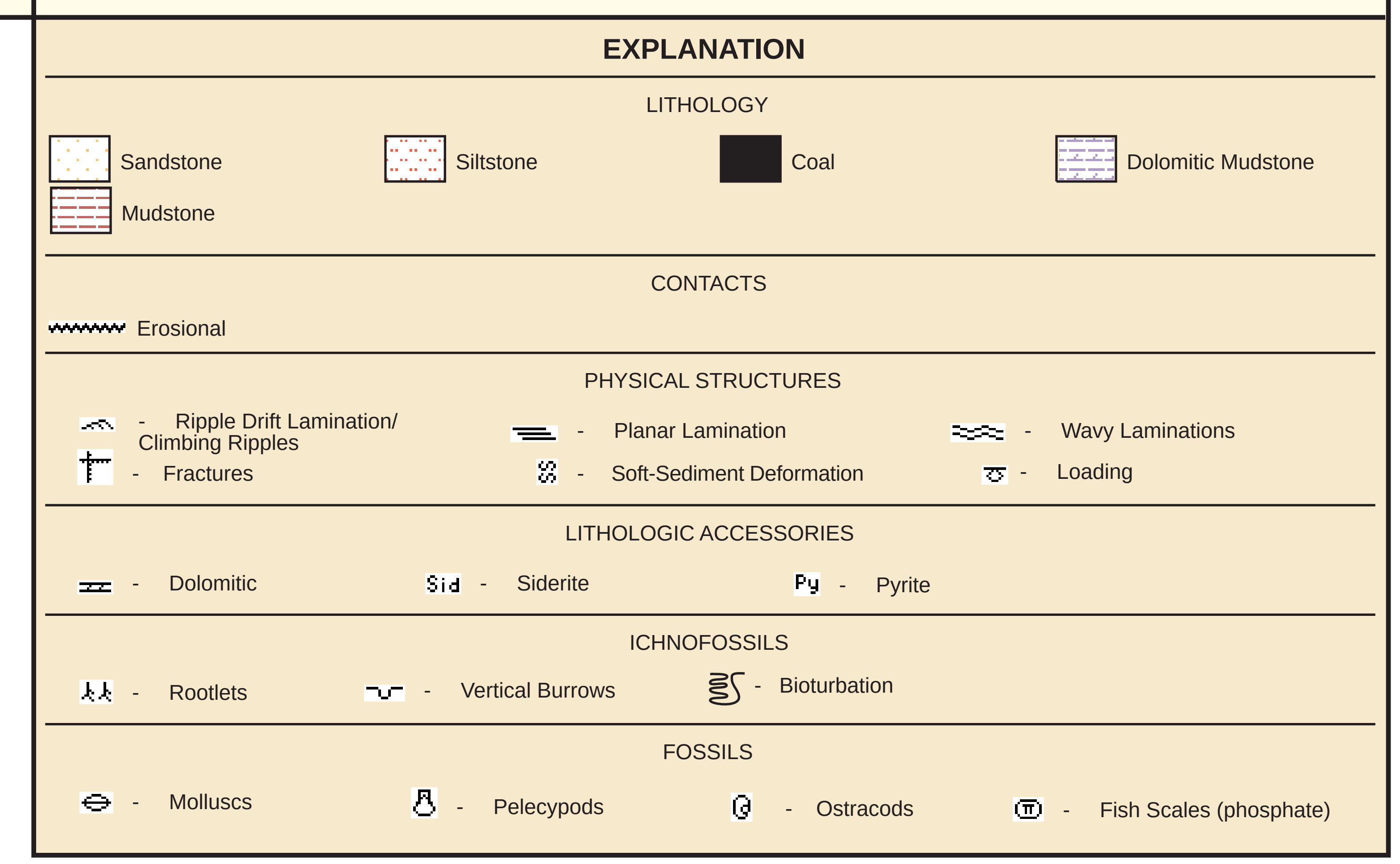

Ute Tribal 2-25

NW1/4NE1/4 section 25,
T. 5 S., R. 5 W., UBL

Brundage Canyon Field
API: 43-013-31833
Depth: 5,527 - 5,596 feet
Interval: Carbonate marker unit (Castle Peak reservoir)
Core Description by: S. Robert Bereskin

Abbreviations

GR - Gamma Ray
S - Resistivity Shallow
M - Resistivity Medium
D - Resistivity Deep
NPHI - Neutron Porosity
DPHI - Density Porosity
md - Millidarcies
TS - Thin Section Photo
Cp - Core Photo
UBL - Uinta Base Line
API - American Petroleum Institute well number

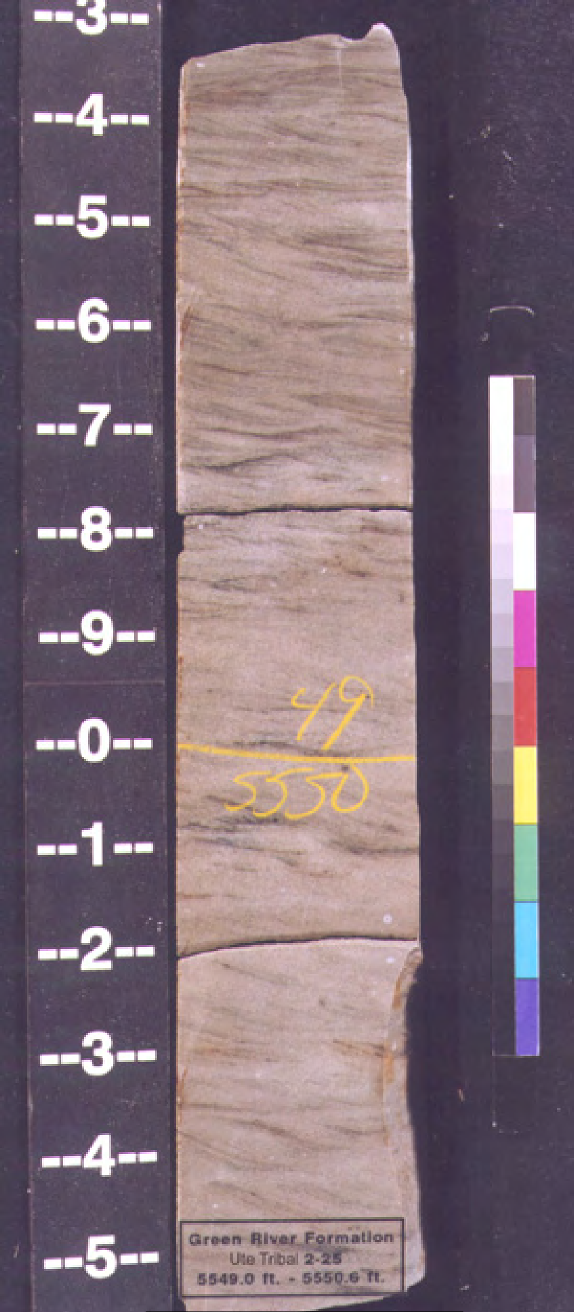

Back to Core Description

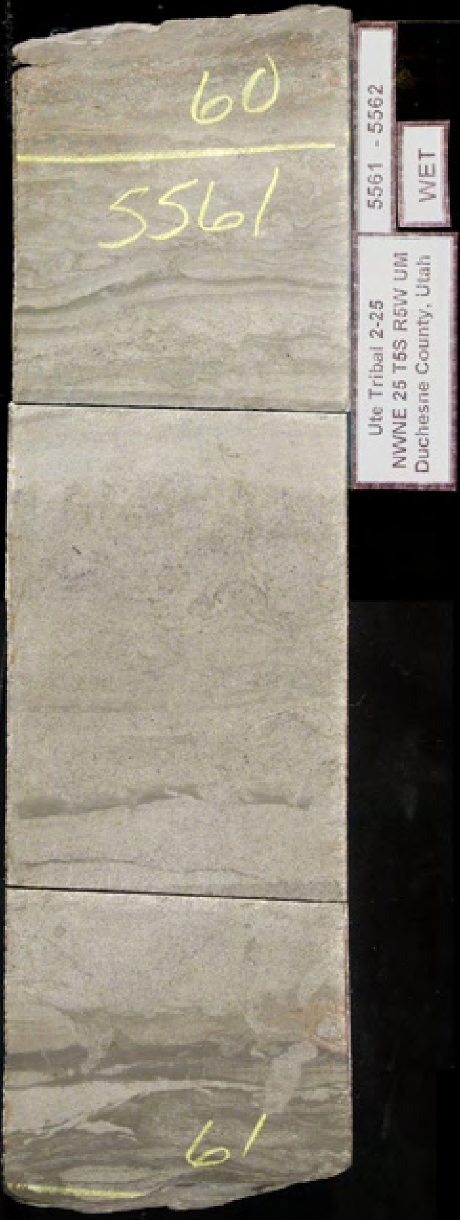

Back to Core Description

Back to Core Description

Back to Core Description

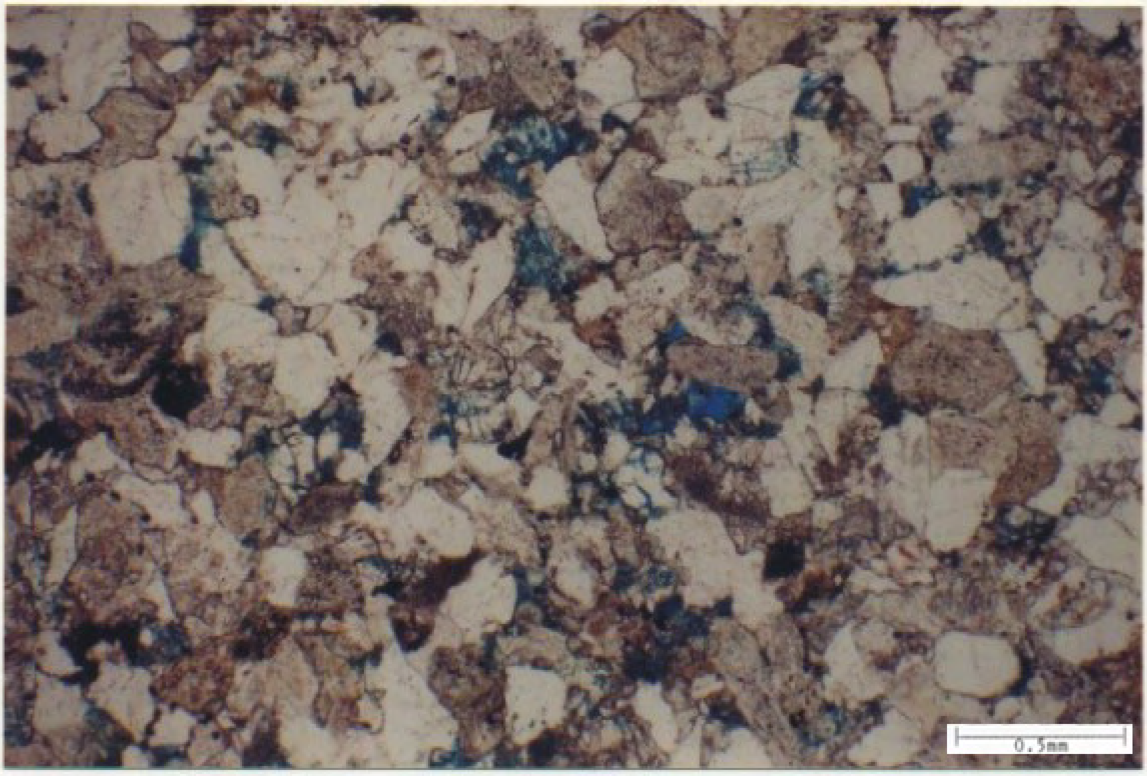

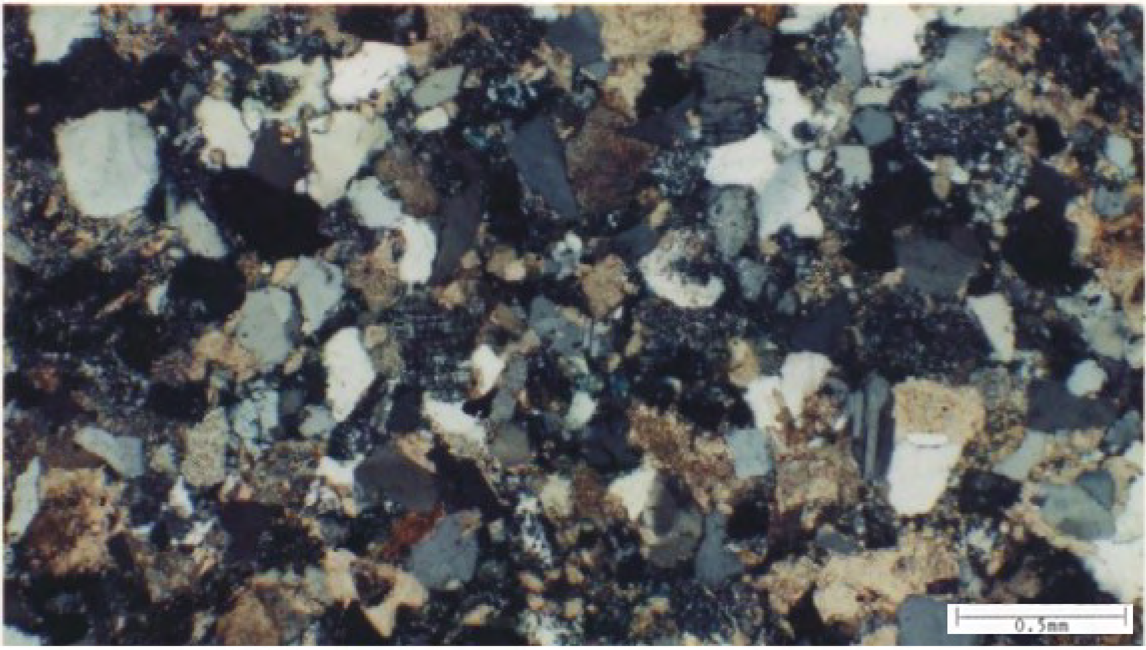

Well 2-25
API 43-013-31833
5529.6 ft
40x

Back to Core Description

Go to TS 2 40x

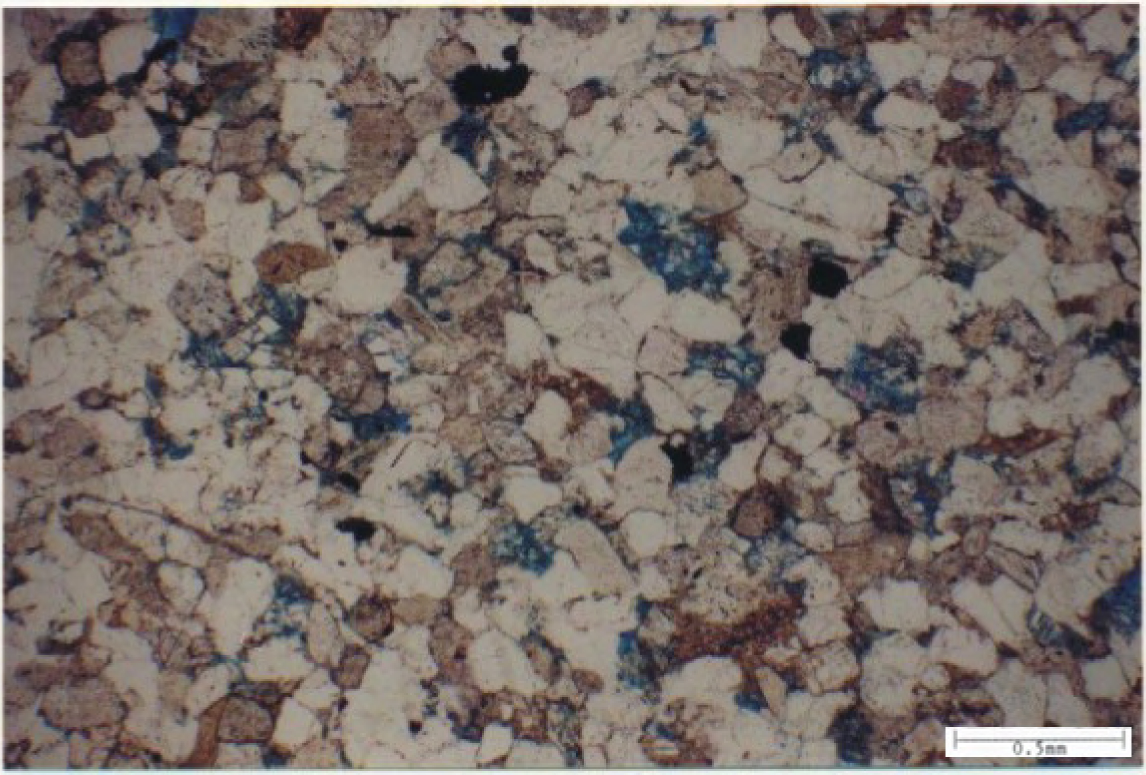

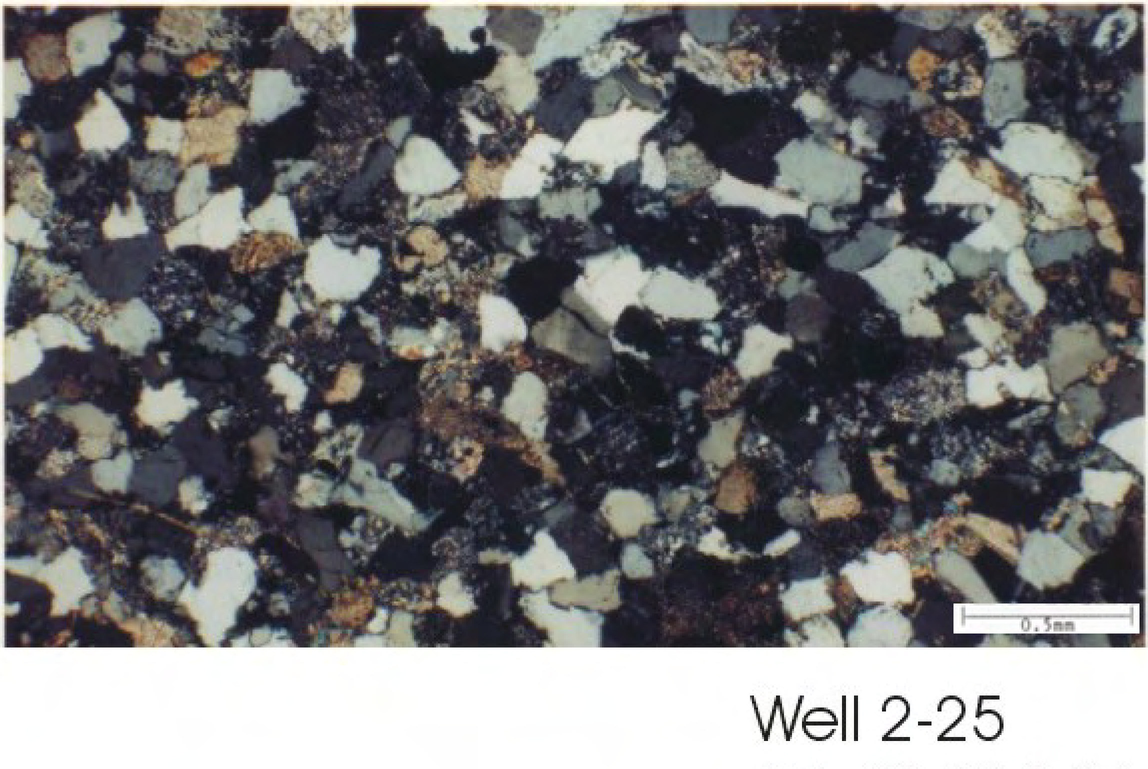

Well 2-25
API 43-013-31833
5536.7 ft
40x

Back to Core Description

Go to TS 3 40x

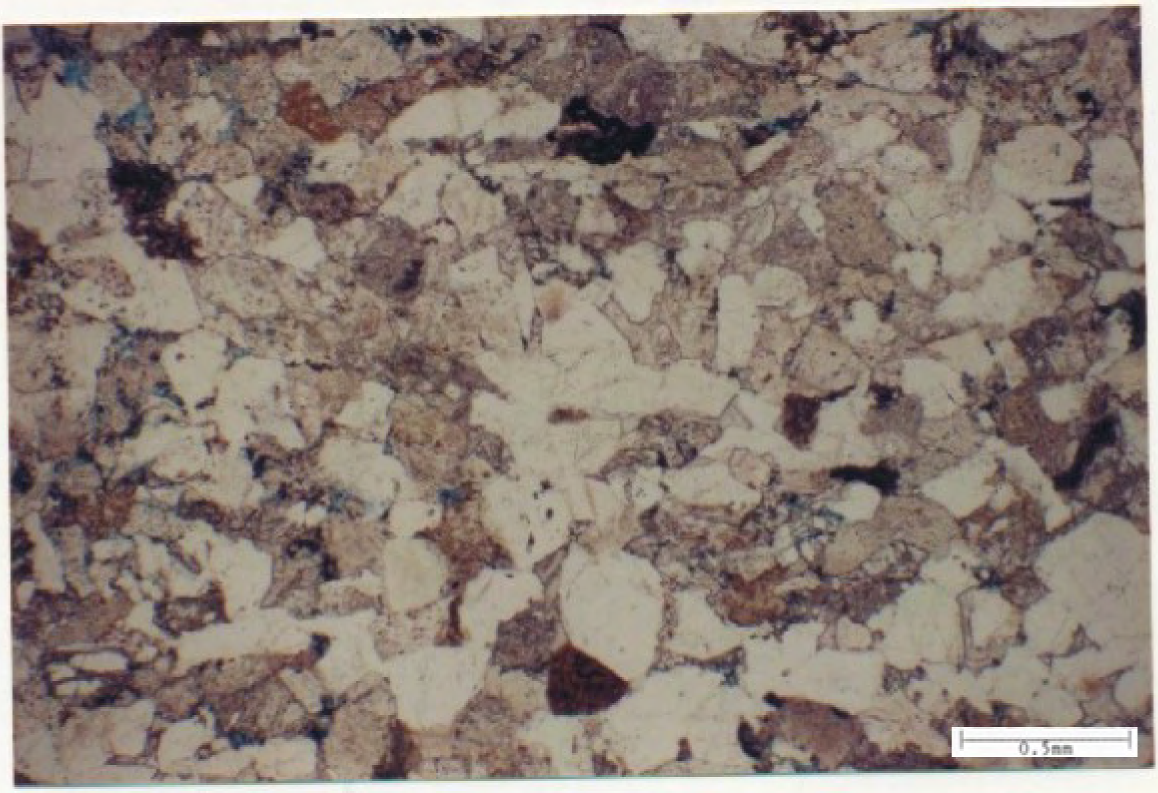

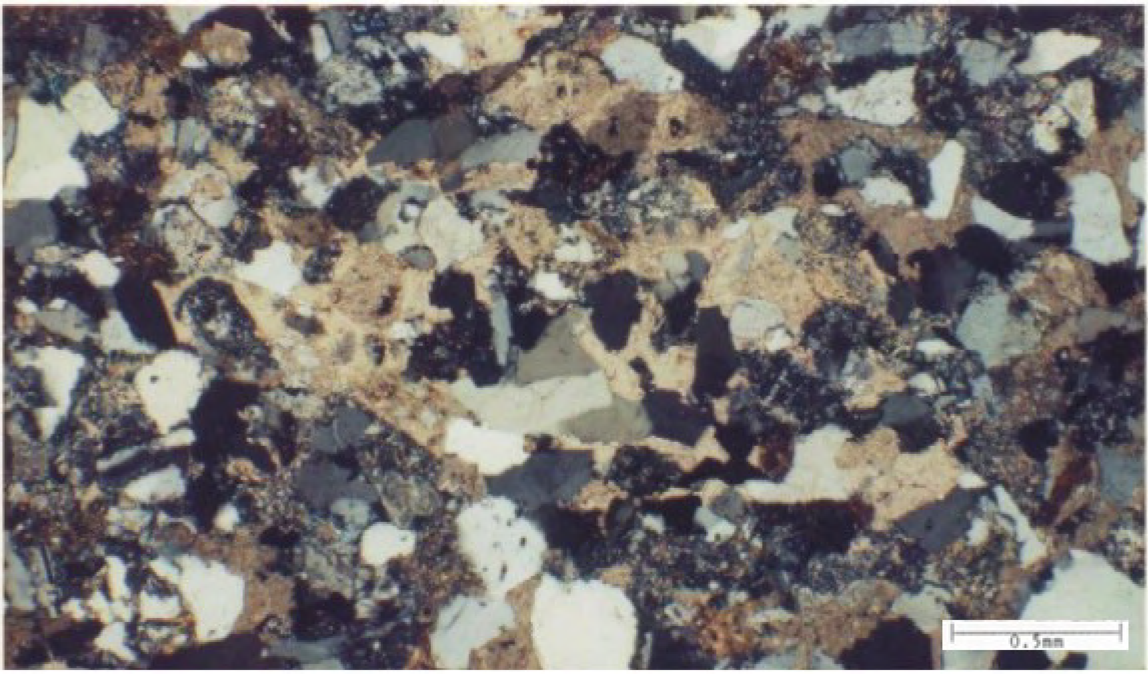

Well 2-25
API 43-013-31833
5580.23 ft
40x

Back to Core Description

Go to TS 3 100x

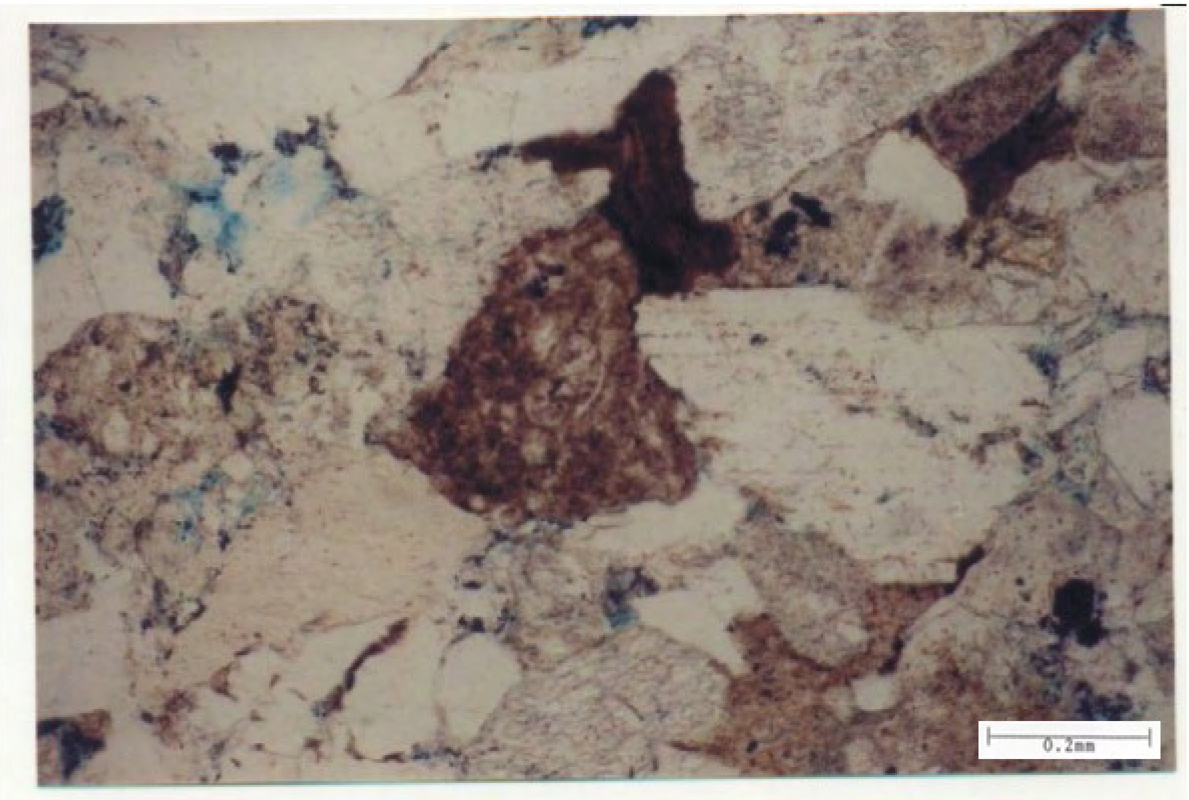

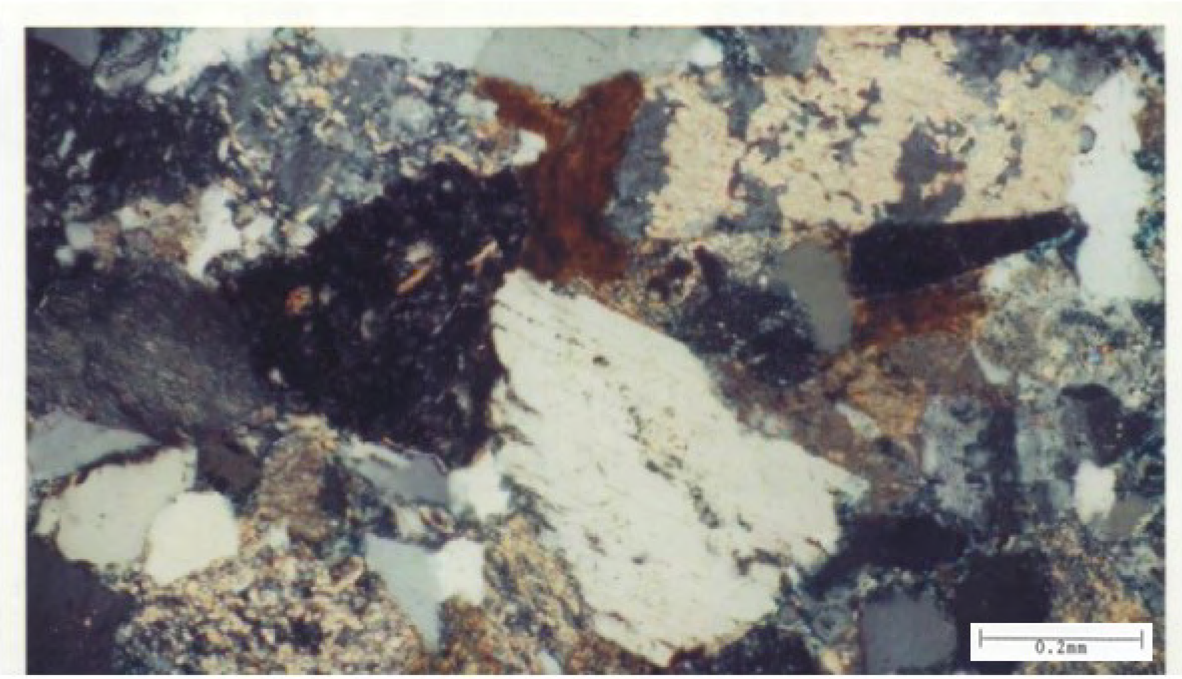

Well 2-25
API 43-0013-31833
5580.2 ft
100x

Back

Go to TS 3 200x

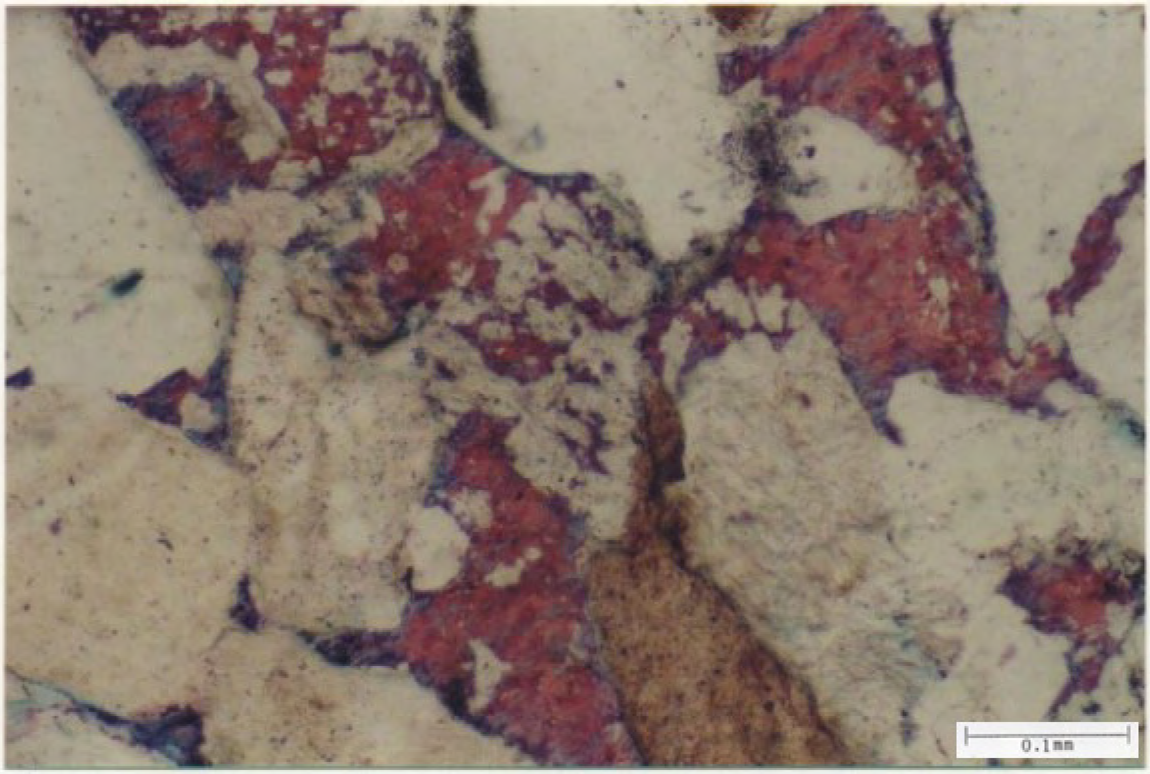

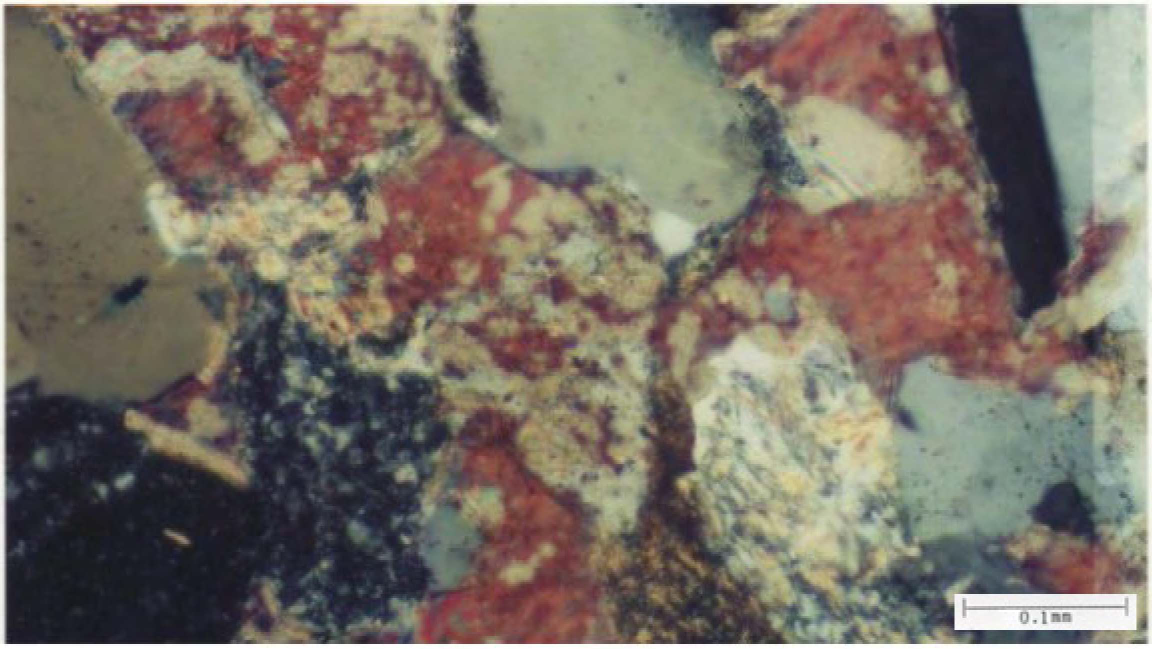

Well 2-25
API 43-013-31833
5580.2 ft
200x

Back to Core Description

Back

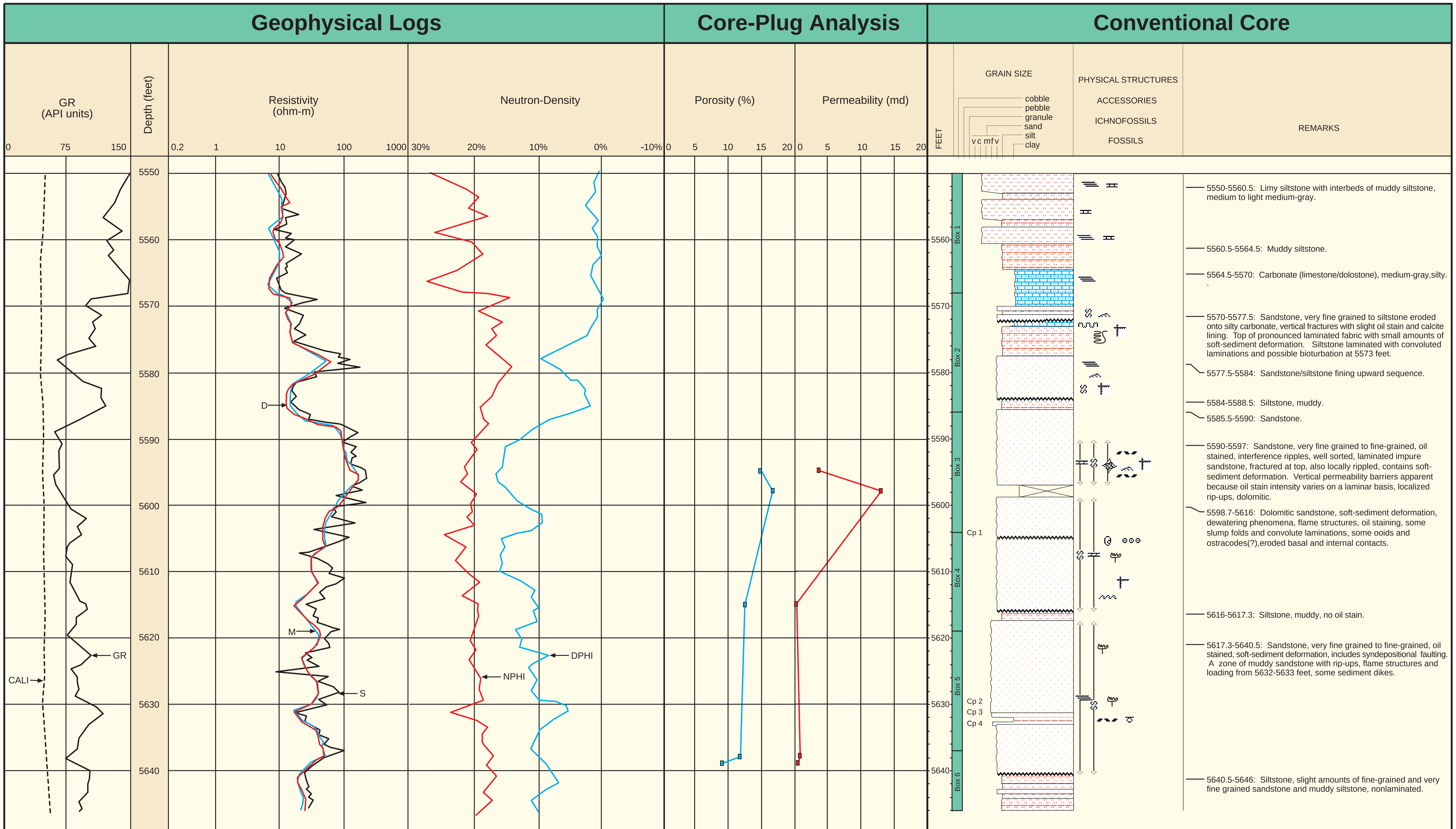

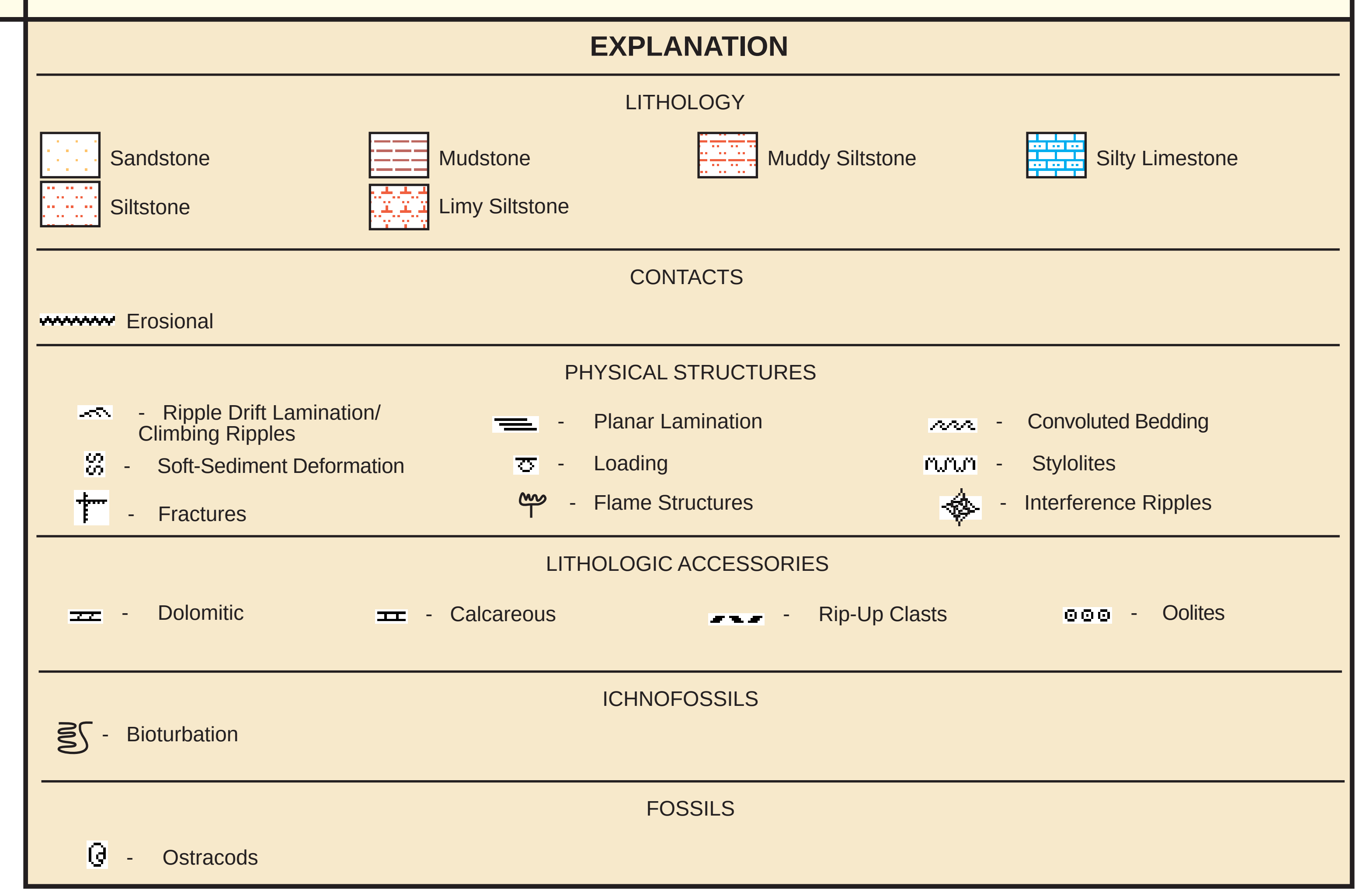

Travis 14A-28

SE1/4SW1/4 section 28, T. 8 S., R.16 E., SLBL

Monument Butte Field
Travis water-flood unit
API: 43-013-30792
Depth: 5,550 - 5,646 feet
Interval: MGR 3-MGR 2 (Travis reservoir)
Core Description by: S. Robert Bereskin

Abbreviations

GR - Gamma Ray
CALI - Caliper
S - Resistivity Shallow
M - Resistivity Medium
D - Resistivity Deep
NPHI - Neutron Porosity
DPHI - Density Porosity
md - Millidarcies
Box - Core Box Photo
Cp - Core Photo
SLBL - Salt Lake Base Line
API - American Petroleum Institute well number

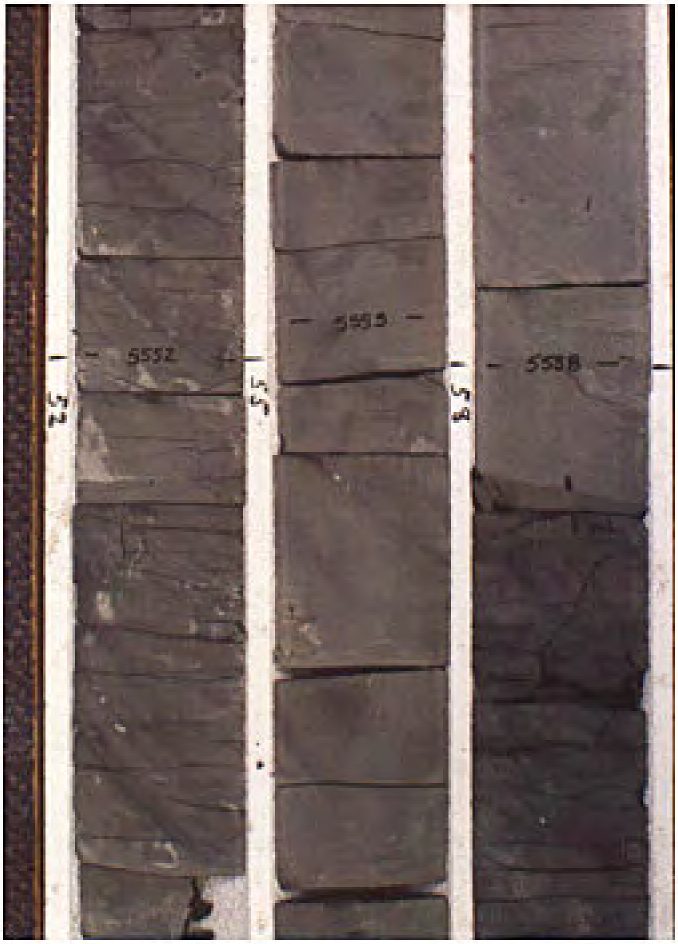

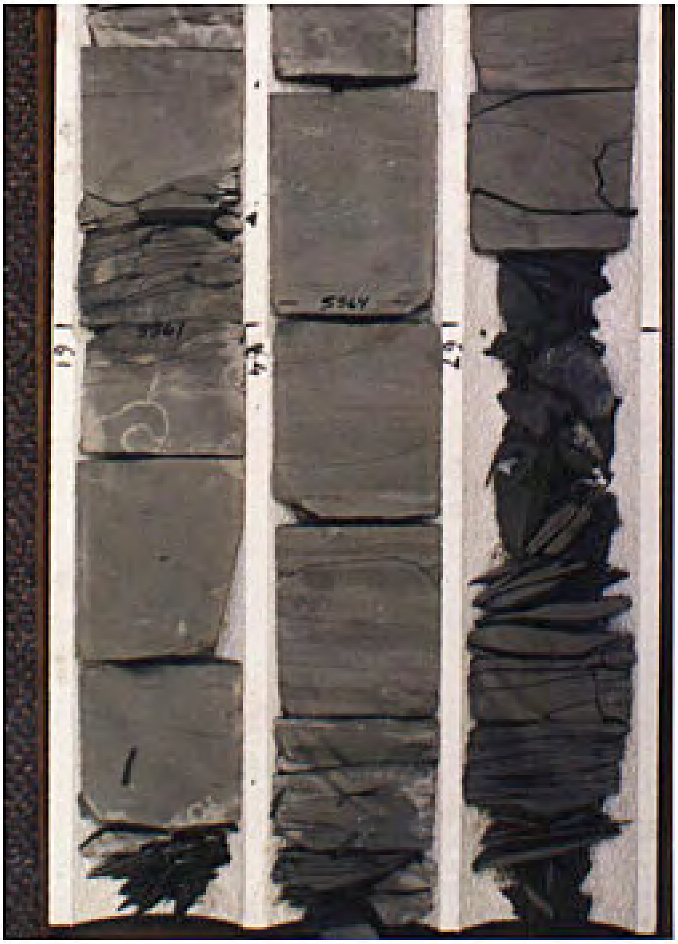

Back to Core Description

Travis 14A-28
43-013-30792
Sue Lutz, EGI

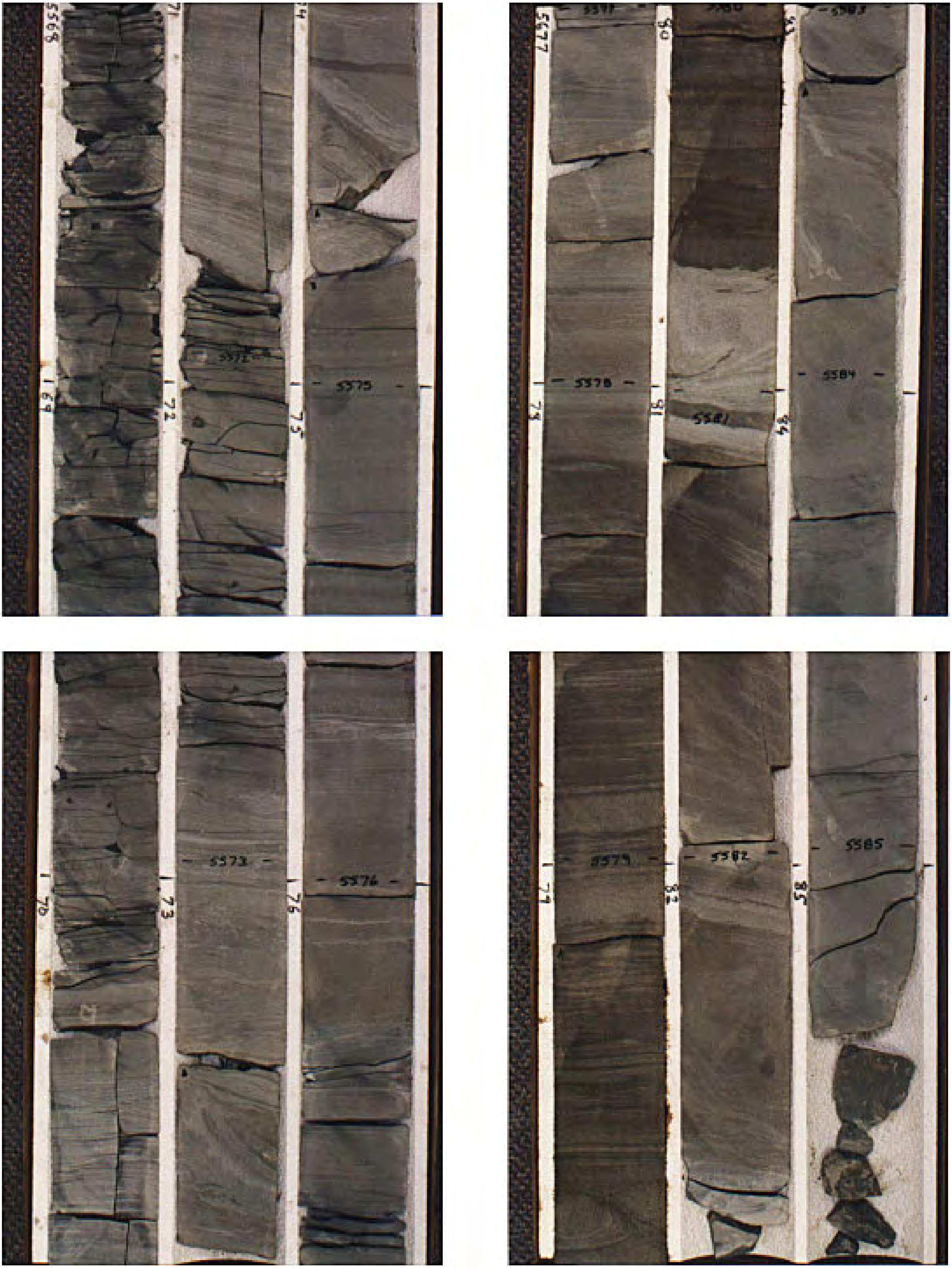

Back to Core Description

Travis 14A-28
43-013-30792
Sue Lutz, EGI

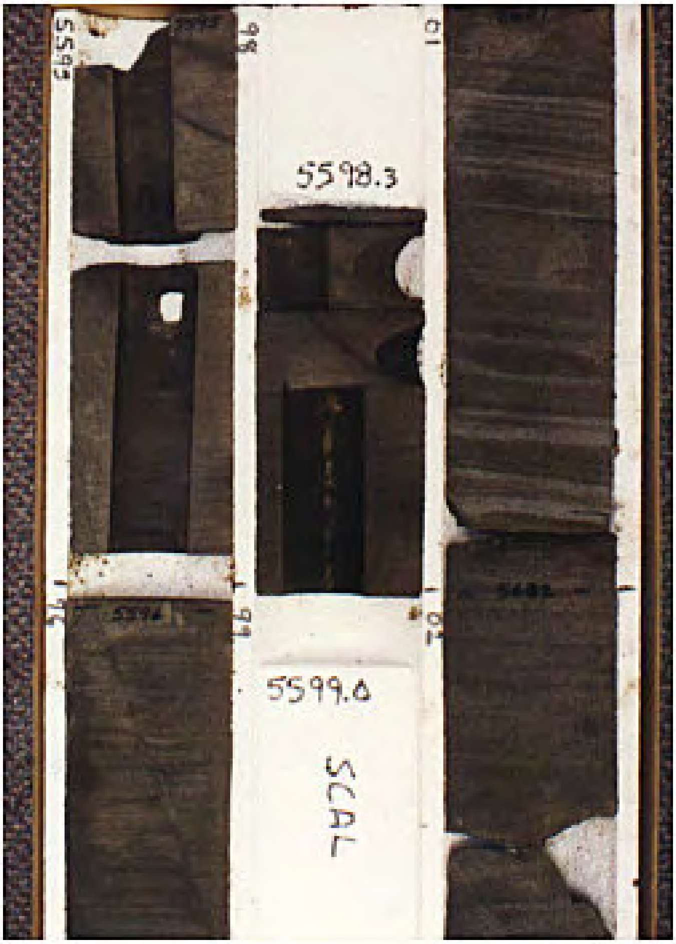

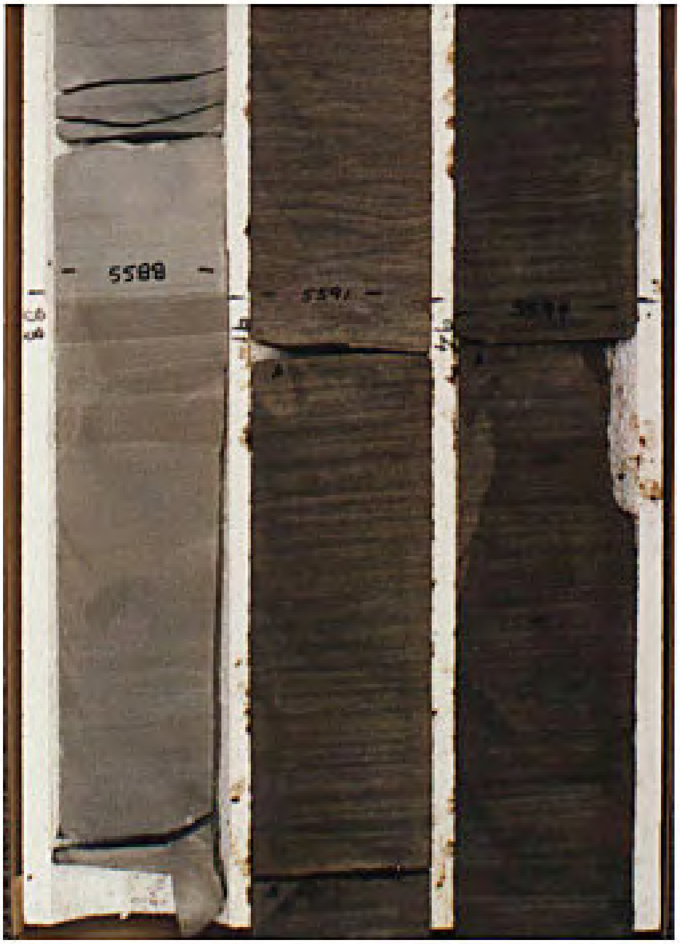

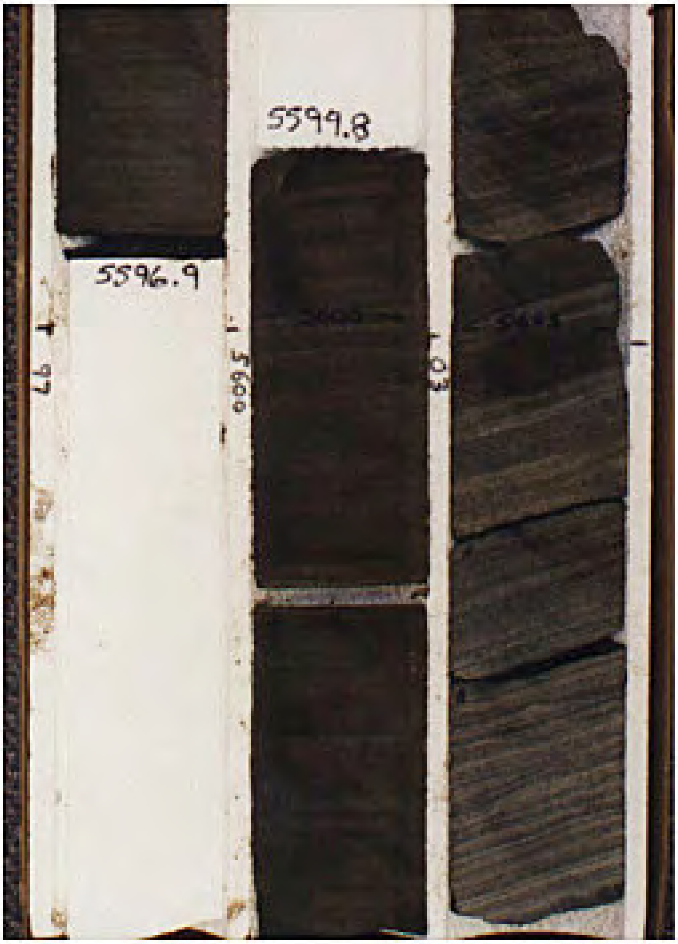

Back to Core Description

Travis 14A-28
43-013-30792
Sue Lutz, EGI

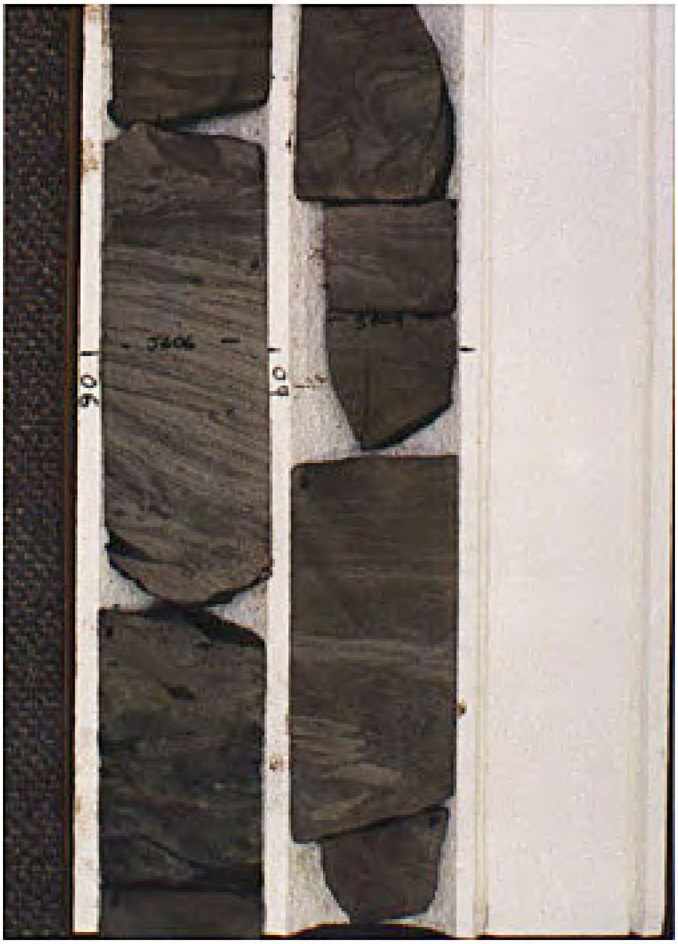

Back to Core Description

Travis 14A-28
43-013-30792
Sue Lutz, EGI

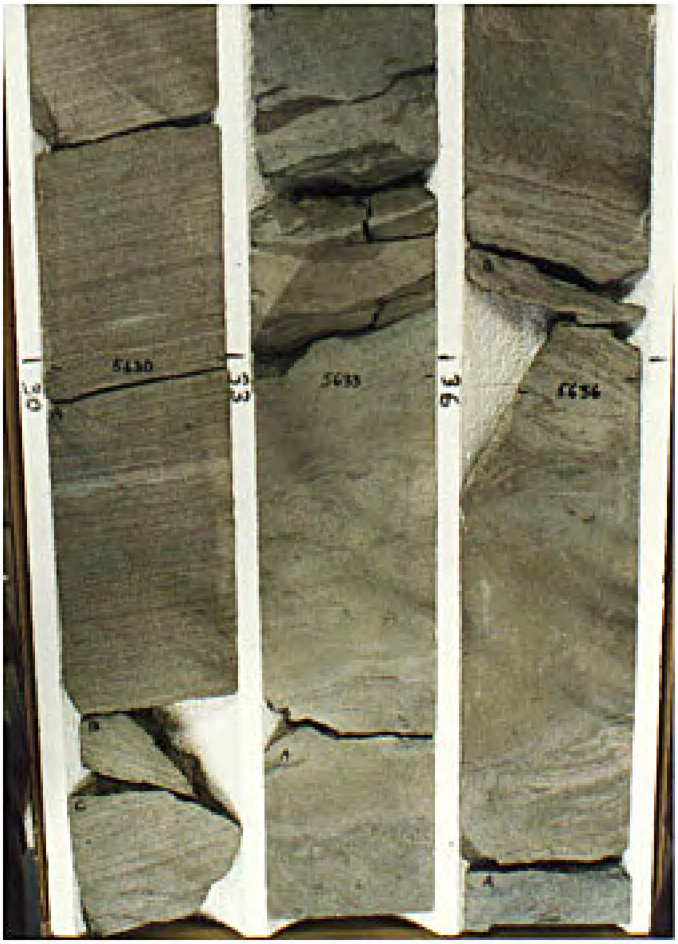

Back to Core Description

Travis 14A-28
43-013-30792
Sue Lutz, EGI

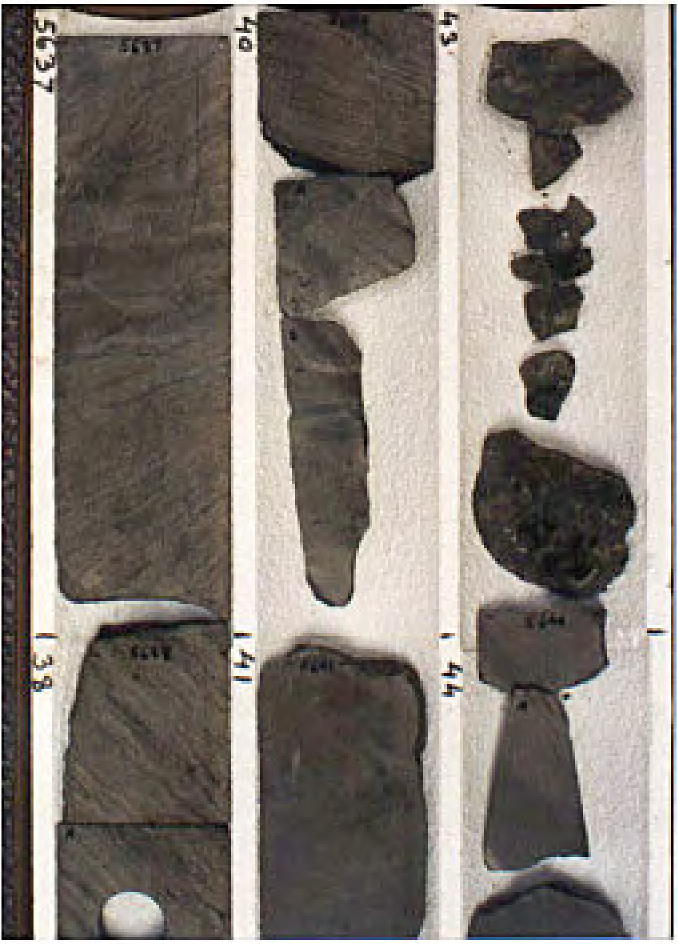

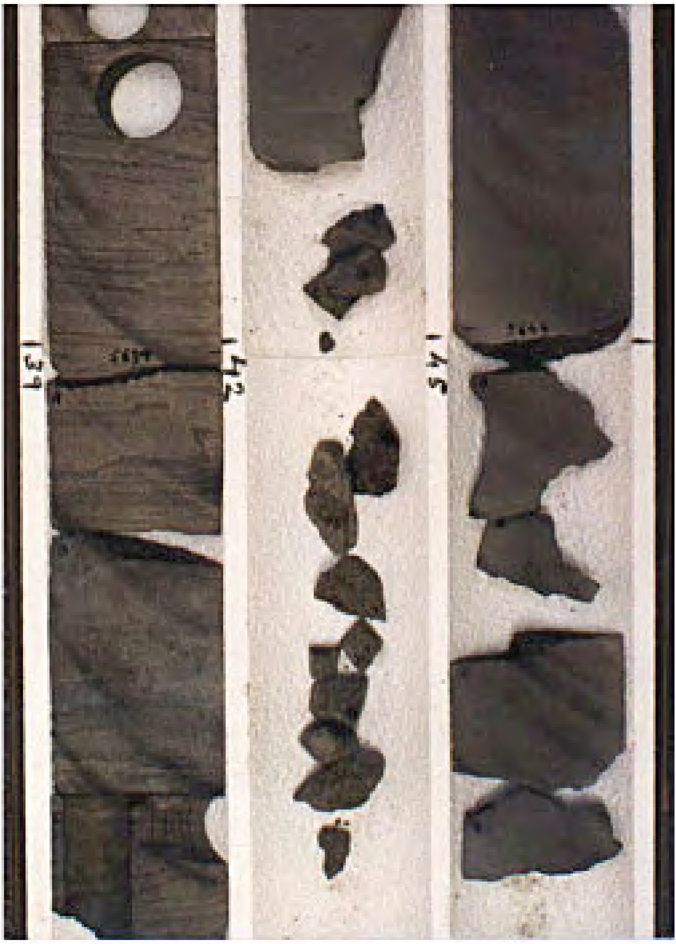

[Back to Core Description]

Travis 14A-28
43-013-30792
Sue Lutz, EGI

Back to Core Description

Back to Core Description

Back to Core Description

Back to Core Description

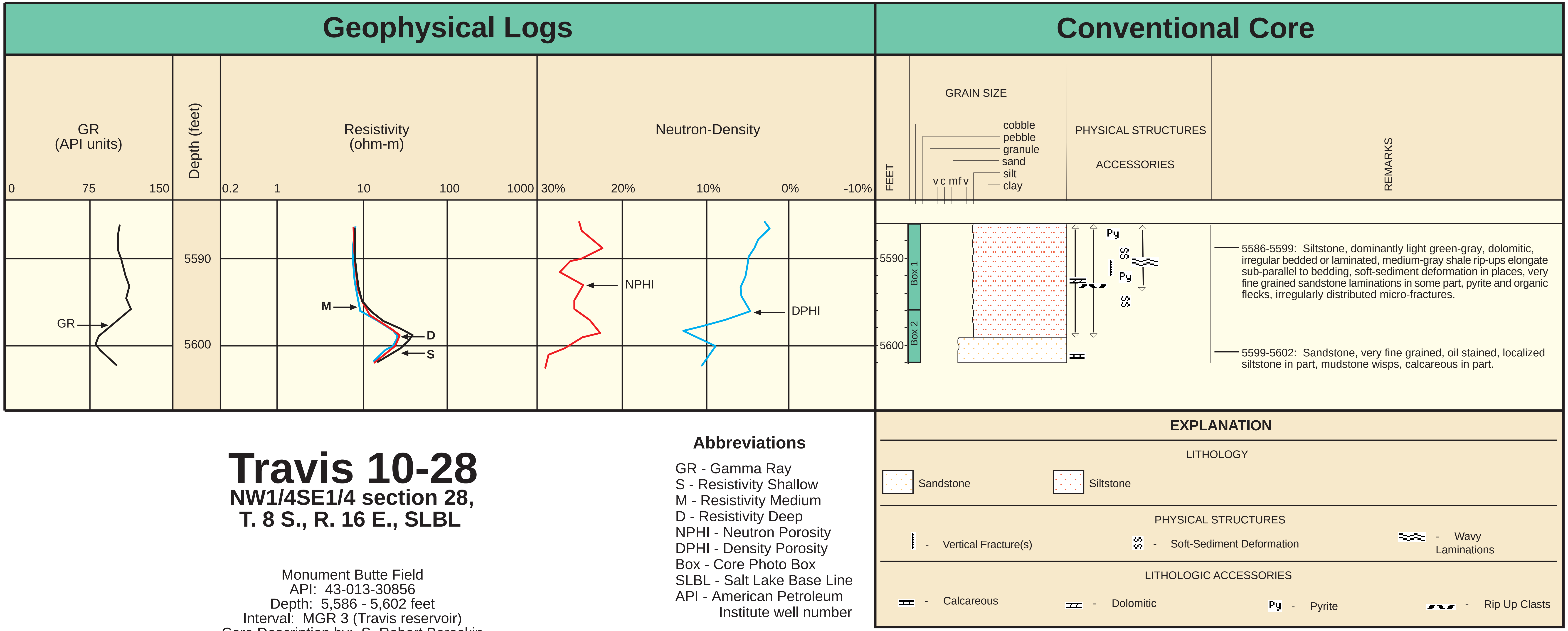

Travis 10-28

NW1/4SE1/4 section 28, T. 8 S., R. 16 E., SLBL

Monument Butte Field
API: 43-013-30856
Depth: 5,586 - 5,602 feet
Interval: MGR 3 (Travis reservoir)
Core Description by: S. Robert Bereskin

Abbreviations

GR - Gamma Ray
S - Resistivity Shallow
M - Resistivity Medium
D - Resistivity Deep
NPHI - Neutron Porosity
DPHI - Density Porosity
Box - Core Photo Box
SLBL - Salt Lake Base Line
API - American Petroleum Institute well number

Back to Core Description

Back to Core Description

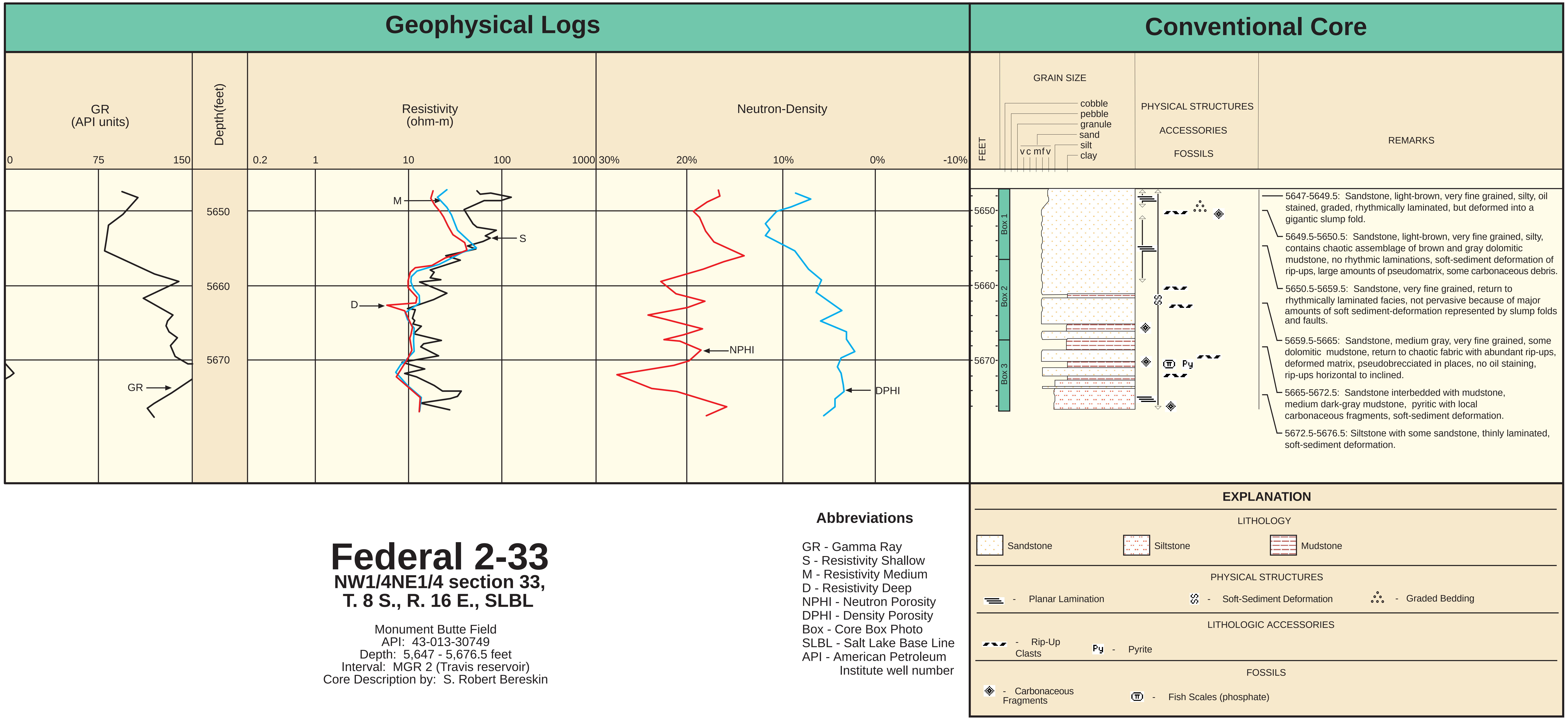

Federal 2-33

NW1/4NE1/4 section 33, T. 8 S., R. 16 E., SLBL

Monument Butte Field
API: 43-013-30749
Depth: 5,647 - 5,676.5 feet
Interval: MGR 2 (Travis reservoir)
Core Description by: S. Robert Bereskin

Abbreviations

GR - Gamma Ray
S - Resistivity Shallow
M - Resistivity Medium
D - Resistivity Deep
NPHI - Neutron Porosity
DPHI - Density Porosity
Box - Core Box Photo
SLBL - Salt Lake Base Line
API - American Petroleum Institute well number

Back to Core Description

Back to Core Description

Back to Core Description

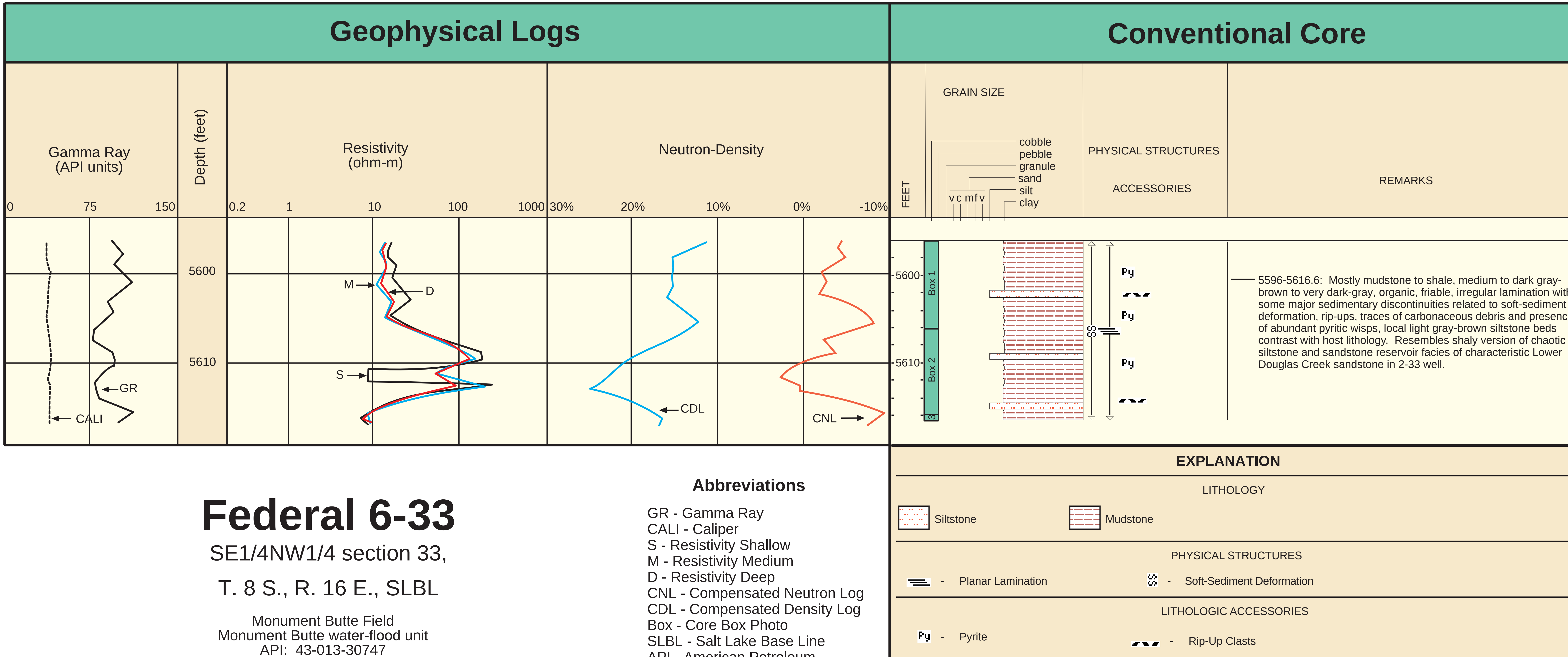

Federal 6-33

SE1/4NW1/4 section 33,

T. 8 S., R. 16 E., SLBL

Monument Butte Field
Monument Butte water-flood unit
API: 43-013-30747
Depth: 5,596 - 5,616.6 feet
Interval: MGR 7 (Monument Butte reservoir, D sandstone)
Core Description by: S. Robert Bereskin

Abbreviations

GR - Gamma Ray
CALI - Caliper
S - Resistivity Shallow
M - Resistivity Medium
D - Resistivity Deep
CNL - Compensated Neutron Log
CDL - Compensated Density Log
Box - Core Box Photo
SLBL - Salt Lake Base Line
API - American Petroleum Institute well number

Back to Core Description

WELL NAME:	Federal #6-33
OPERATOR:	Lomax Exploration Company
LOCATION:	SENW 33, T8S R16E Duchesne County

Blue Cyan Green Yellow Red Magenta White 3/Color Black

5606 TO 5616 FEET

BOX 2 OF 3

Back to Core Description

Go to Core Box Photo 3

Back to Core Description

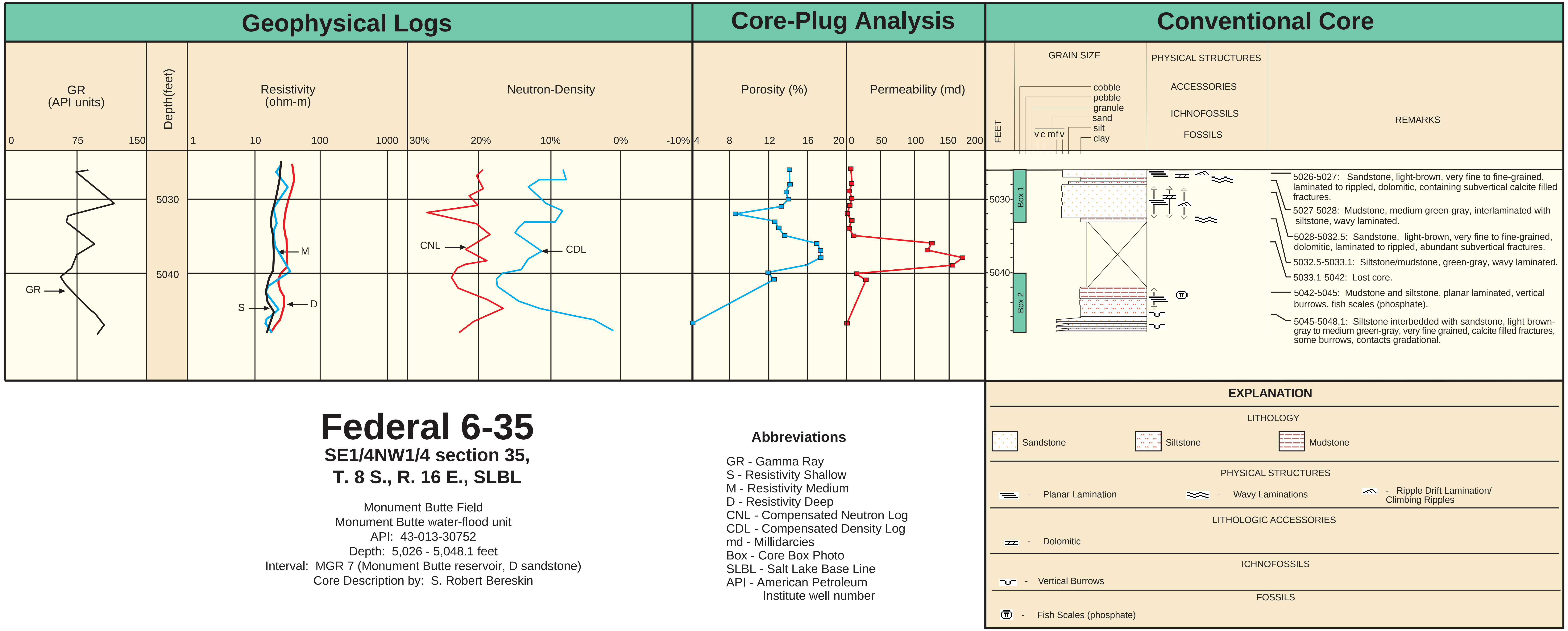

Federal 6-35

SE1/4NW1/4 section 35, T. 8 S., R. 16 E., SLBL

Monument Butte Field
Monument Butte water-flood unit
API: 43-013-30752
Depth: 5,026 - 5,048.1 feet
Interval: MGR 7 (Monument Butte reservoir, D sandstone)
Core Description by: S. Robert Bereskin

Abbreviations

GR - Gamma Ray
S - Resistivity Shallow
M - Resistivity Medium
D - Resistivity Deep
CNL - Compensated Neutron Log
CDL - Compensated Density Log
md - Millidarcies
Box - Core Box Photo
SLBL - Salt Lake Base Line
API - American Petroleum Institute well number

Back to Core Description

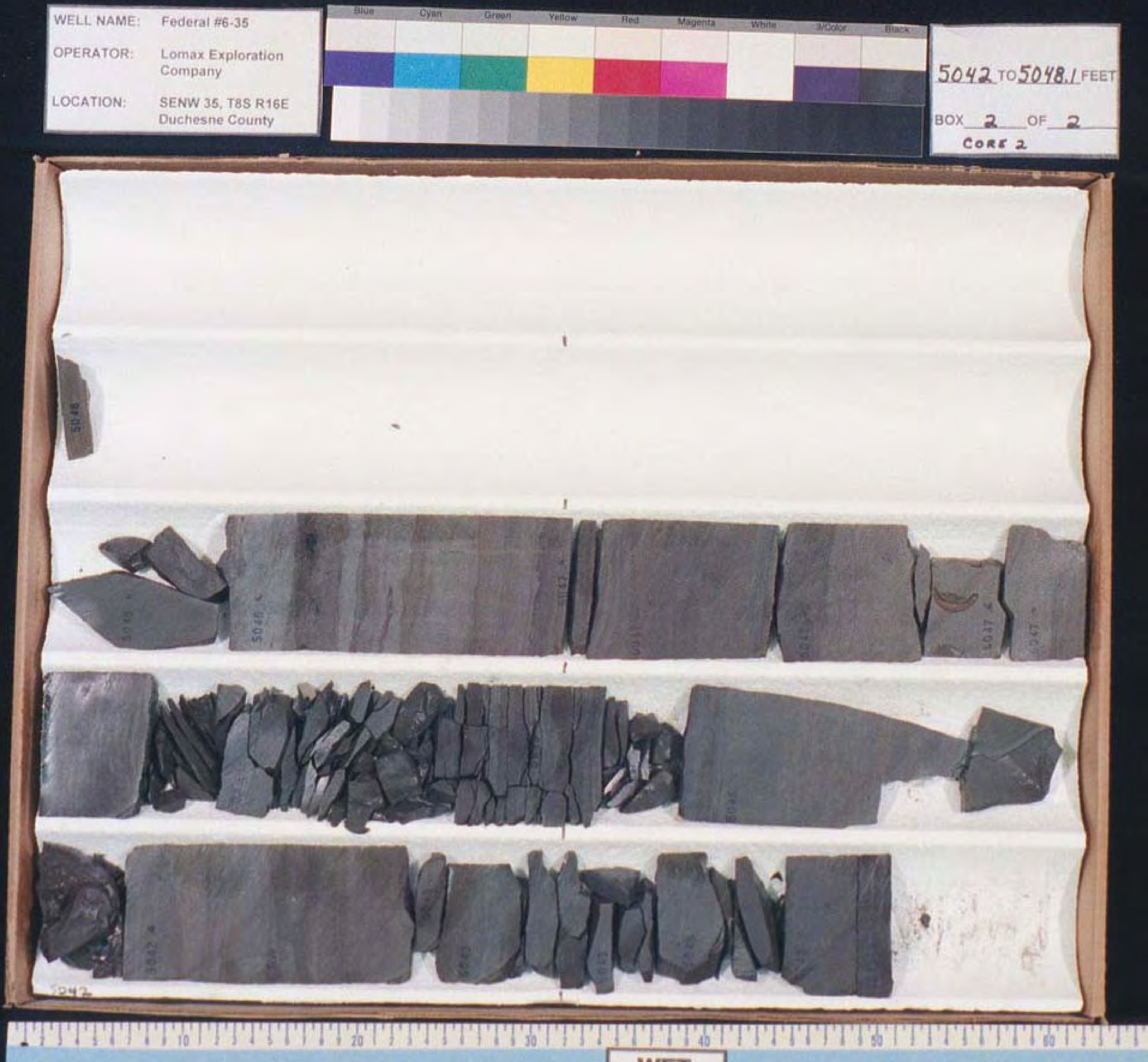

Back to Core Description

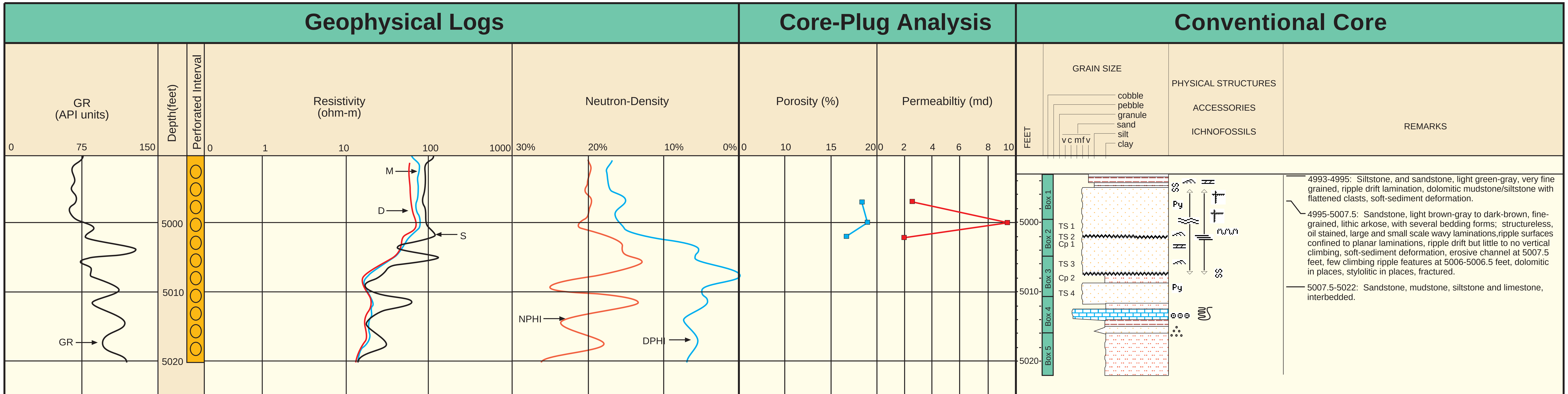

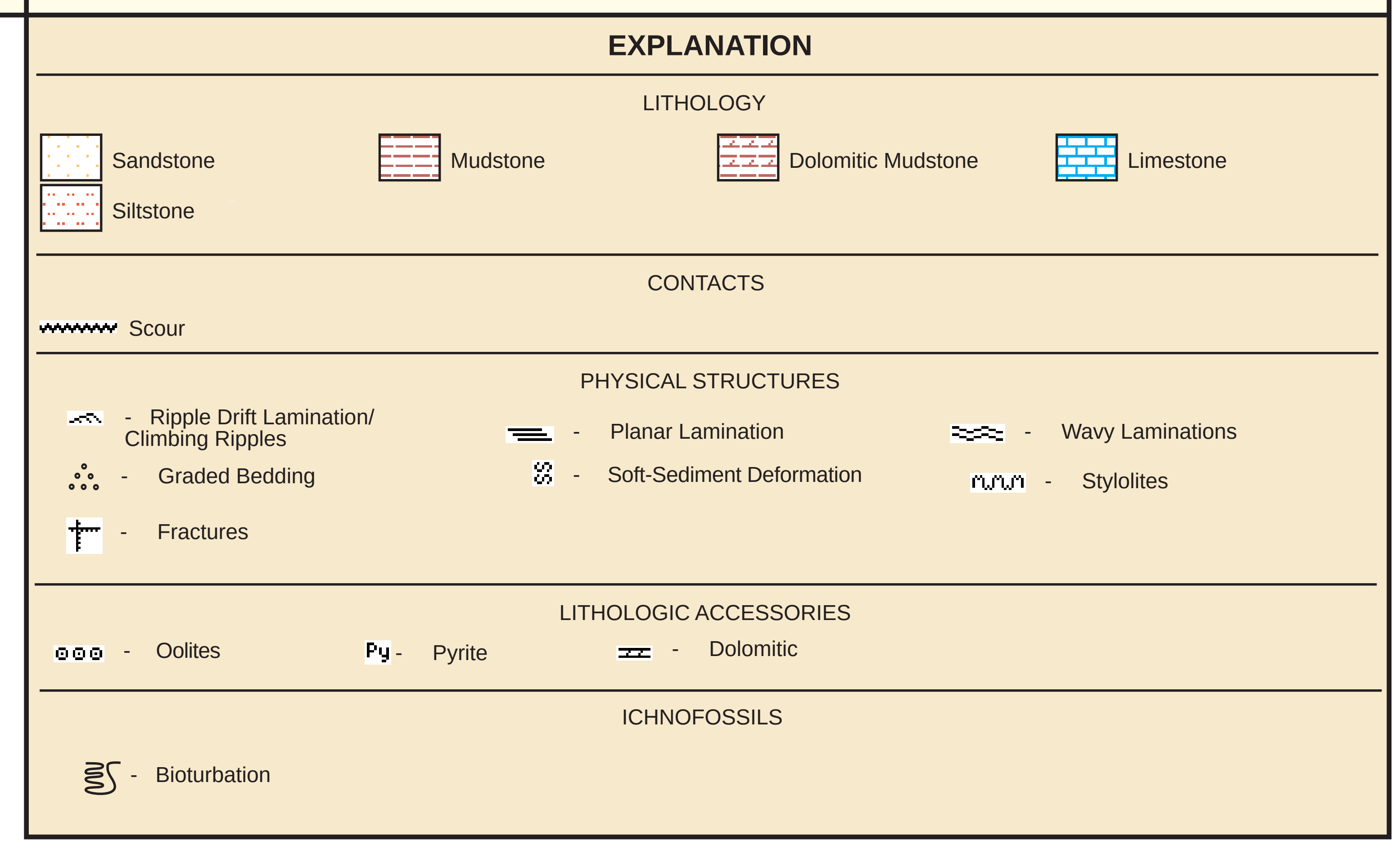

Monument Federal 3A-35

SW1/4NE1/4 section 35, T. 8 S., R. 16 E., SLBL

Monument Butte Field
Monument Butte water-flood unit
API: 43-013-31738
Depth: 4,993 - 5,022 feet.
Interval: MGR 7 (Monument Butte reservoir, D sandstone)
Core Description by: S. Robert Bereskin

Abbreviations

GR - Gamma Ray
S - Resistivity Shallow
M - Resistivity Medium
D - Resistivity Deep
NPHI - Neutron Porosity
DPHI - Density Porosity
md - Millidarcies
TS - Thin Section Photo
Box - Core Box Photo
Cp - Core Photo
SLBL - Salt Lake Base Line
API - American Petroleum Institute well number

Back to Core Description

Back to Core Description

Back to Core Description

Back to Core Description

Back to Core Description

Monument Fed 3A-5
NENW 35 T8S R16E
Duchesne County, Utah

5002.6 - 5003 ft.

WET

Back to Core Description

Monument Fed 3A-35
NENW 35 T8S R16E
Duchesne County, Utah

5007.2 - 5008.5 ft.

WET

Back to Core Description

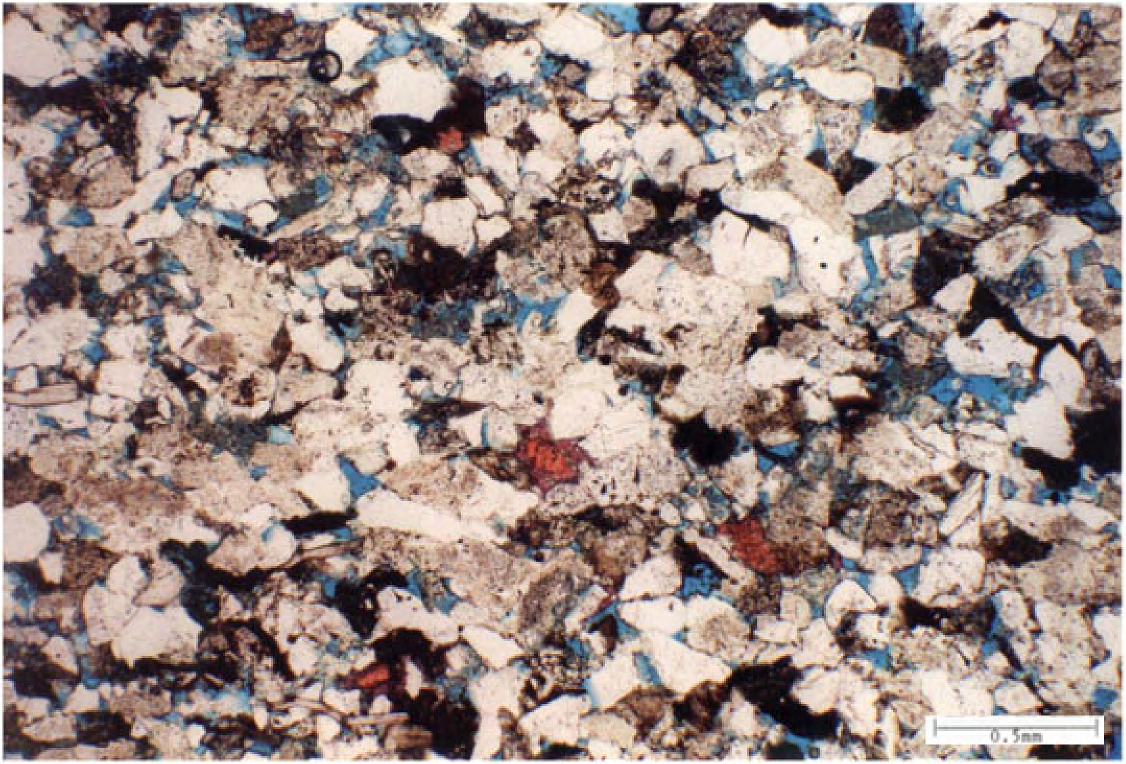

Well 3A-35
API 43-013-31738
5002.1 ft
40x

Back to Core Description

Go to TS 1 100x a

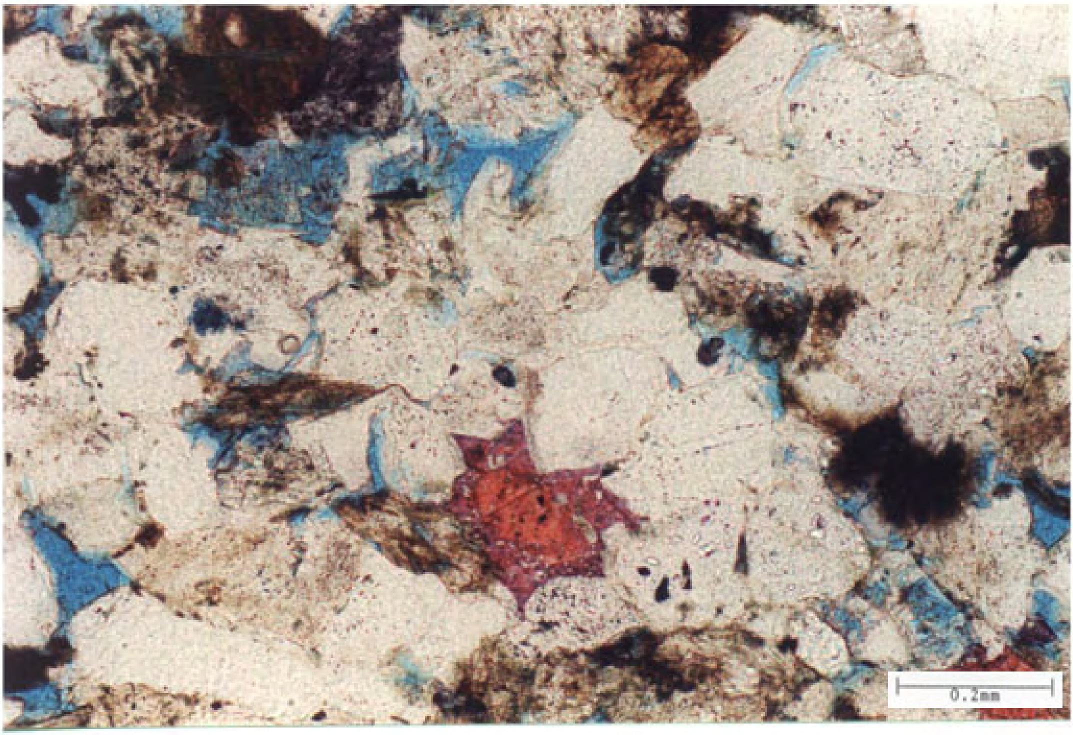

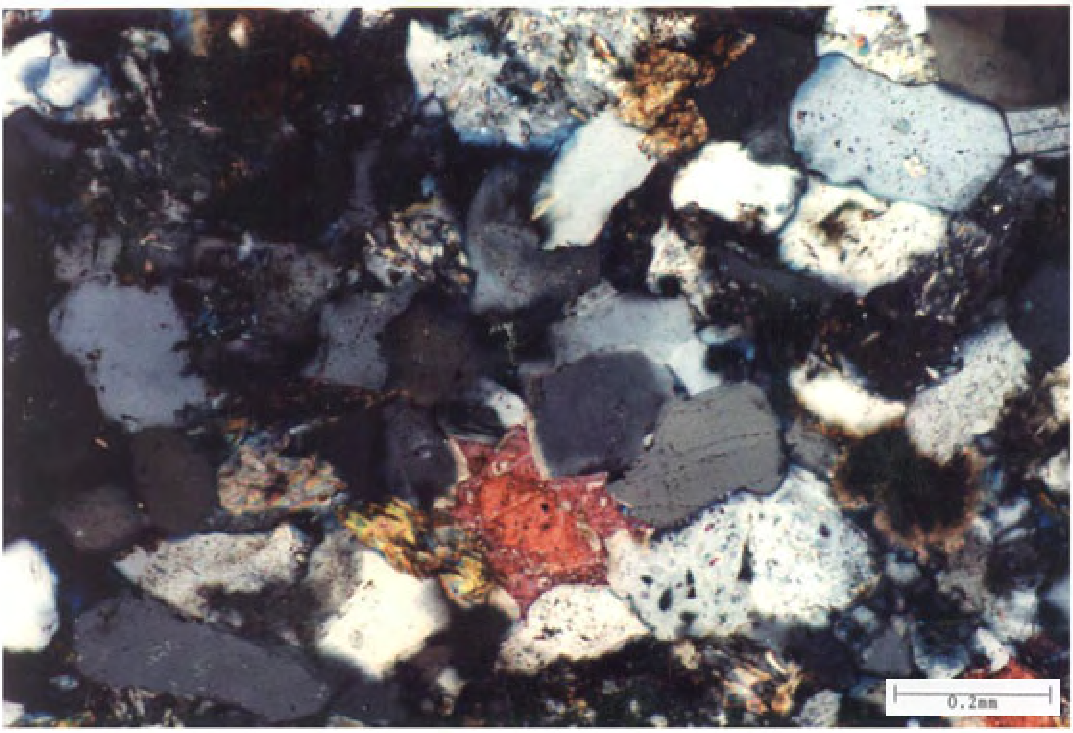

Well 3A-35
API 43-013-31738
5002.1 ft
100x

Back Go to TS 1 100x b

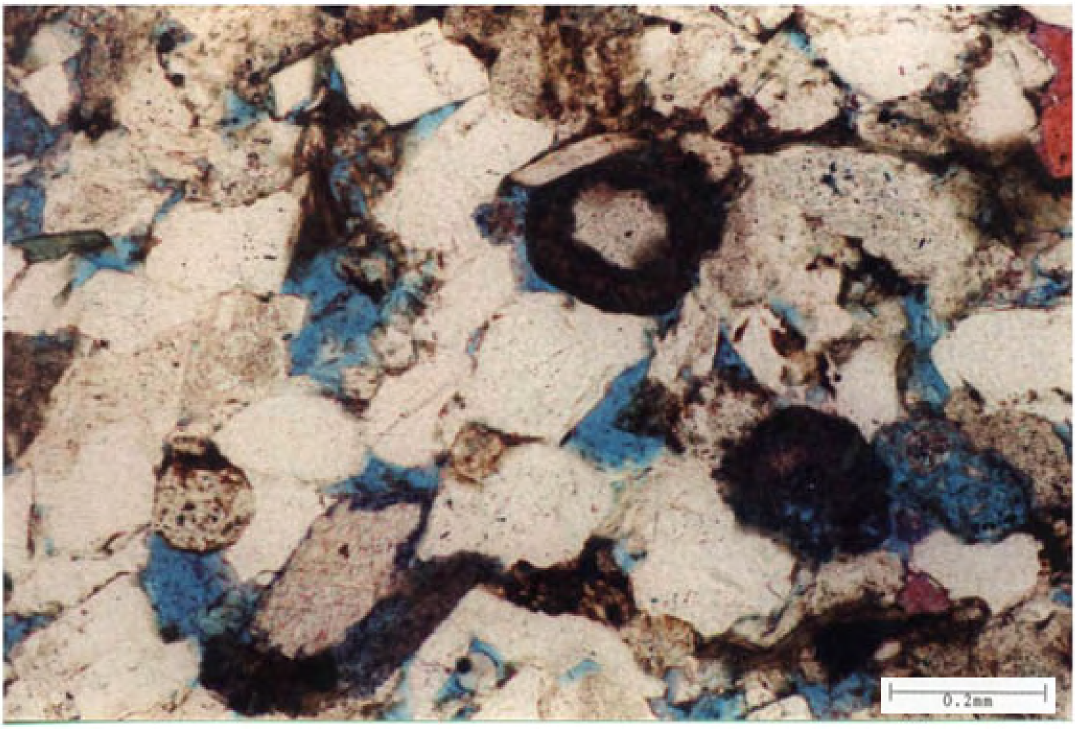

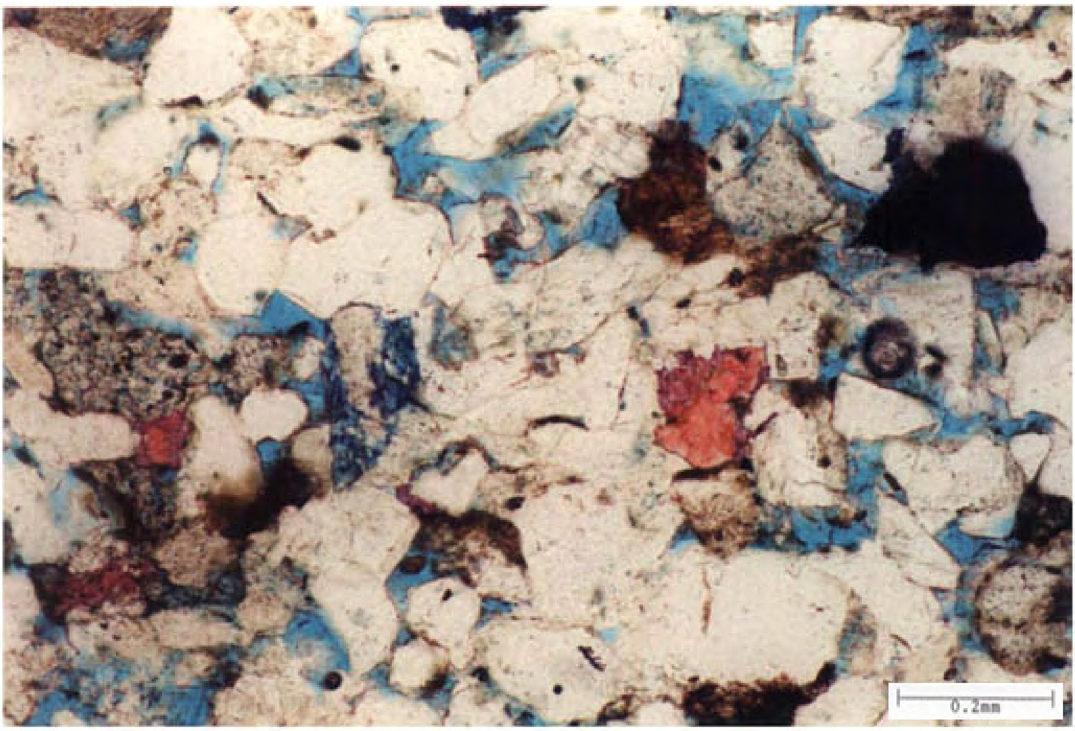

Well 3A-35
API 43-013-31738
5002.1 ft
100x

Back
Go to TS 2 40x a

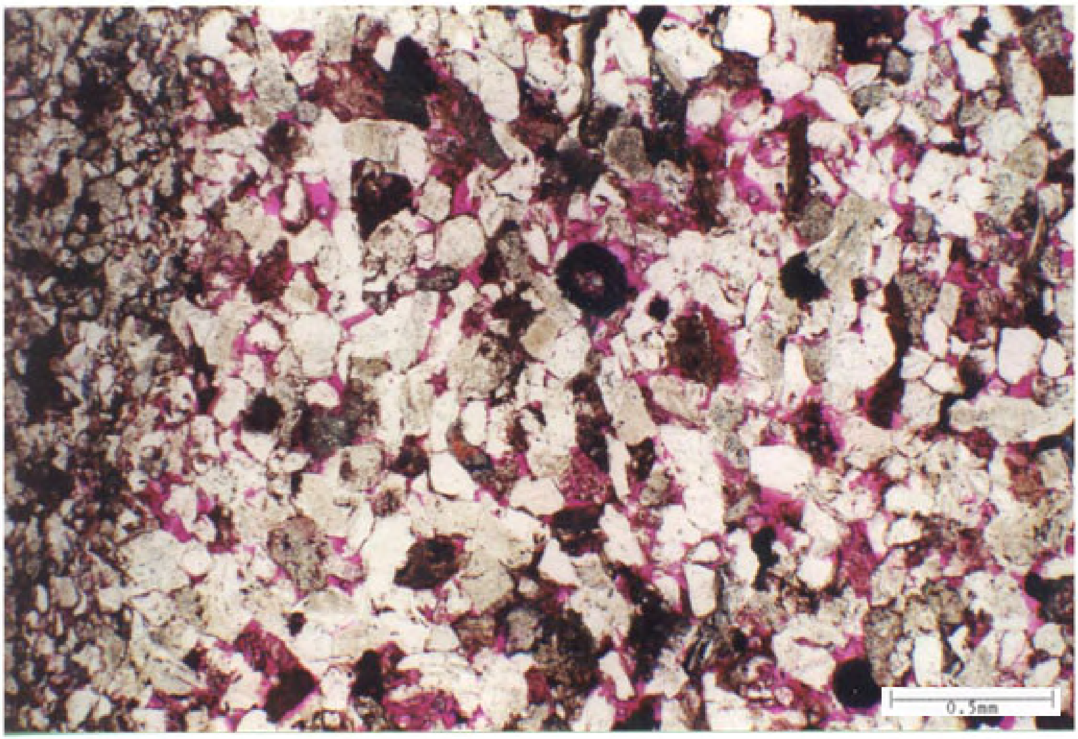

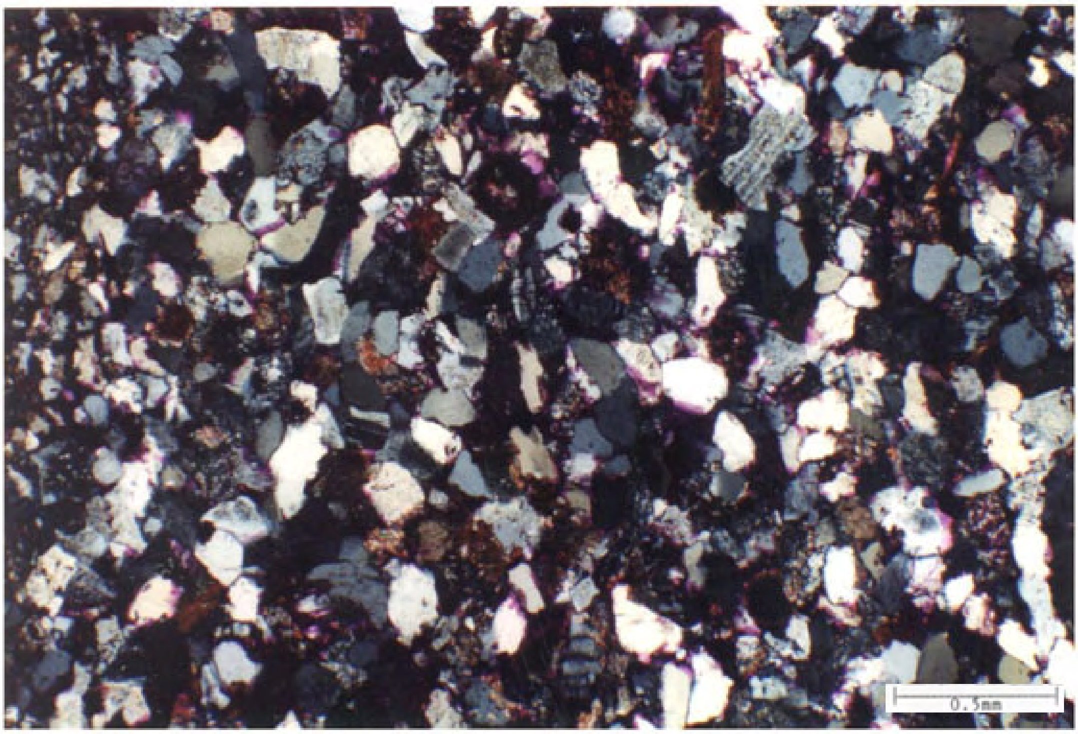

Well 3A-35
API 43-013-31738
5003.25 ft
40x

Back to Core Description

Go to TS 2 40x b

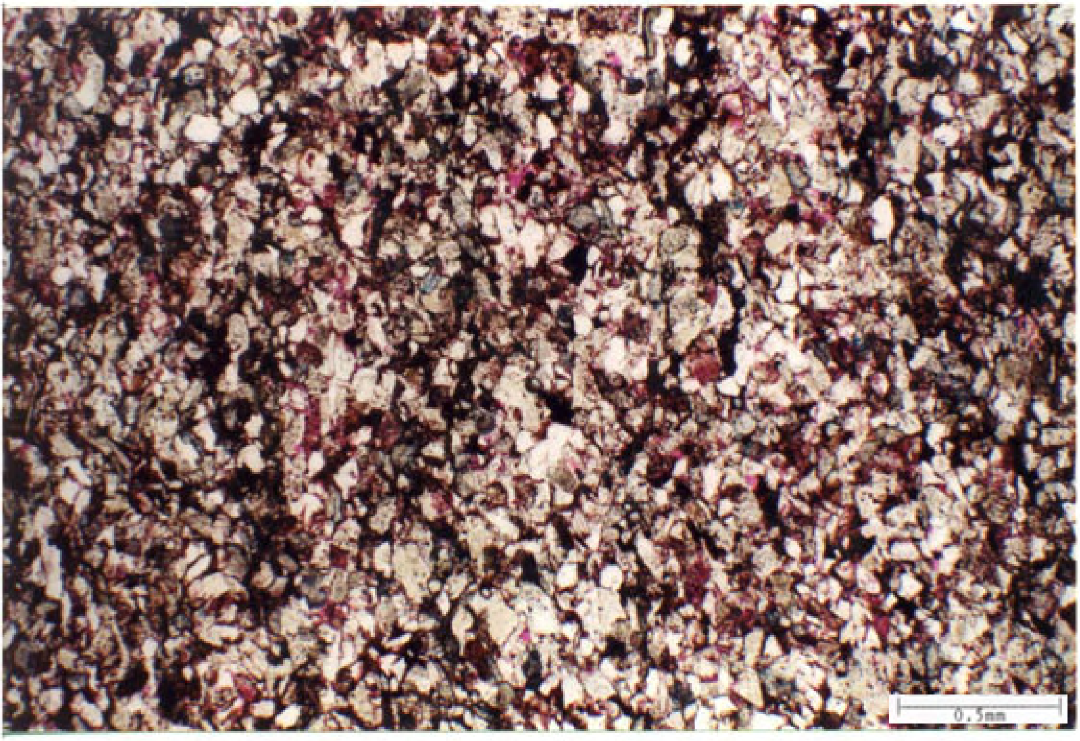

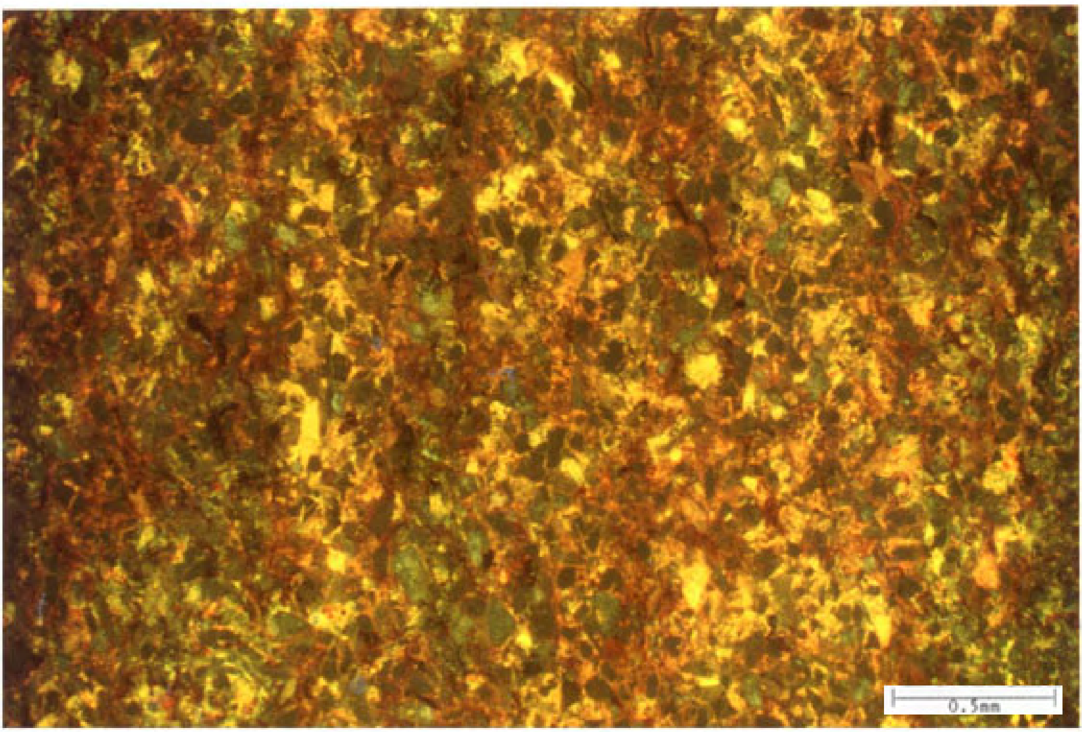

Well 3A-35
API 43-013-31738
5003.25 ft
40x

Back

Go to TS 2 100x

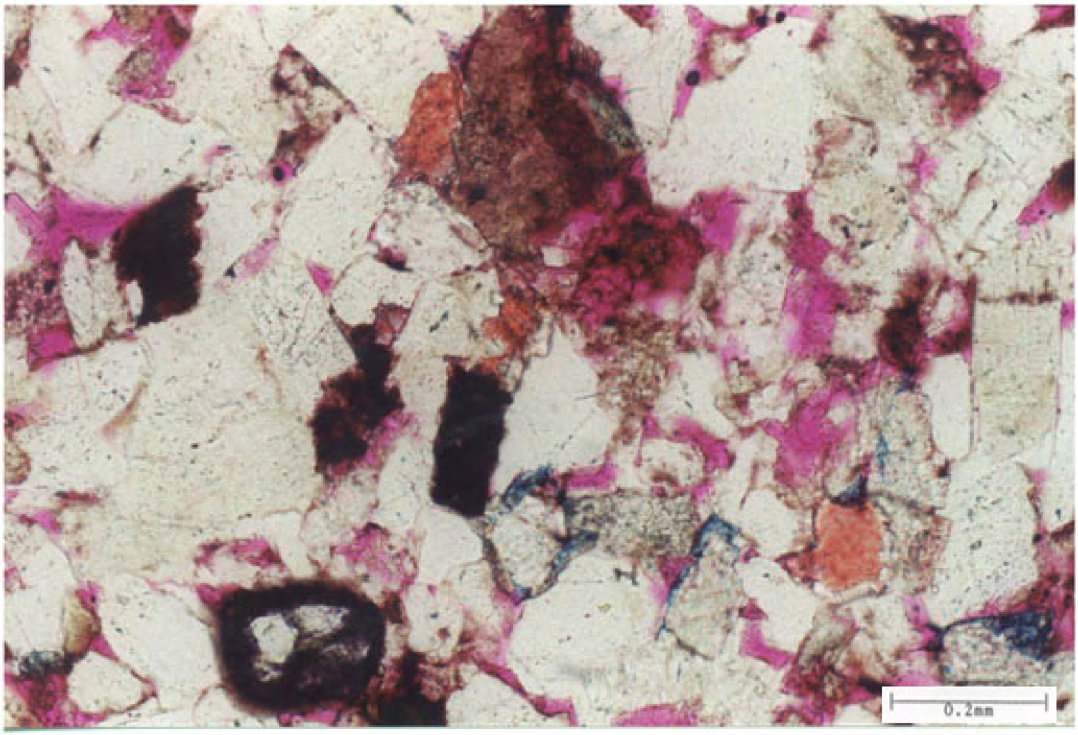

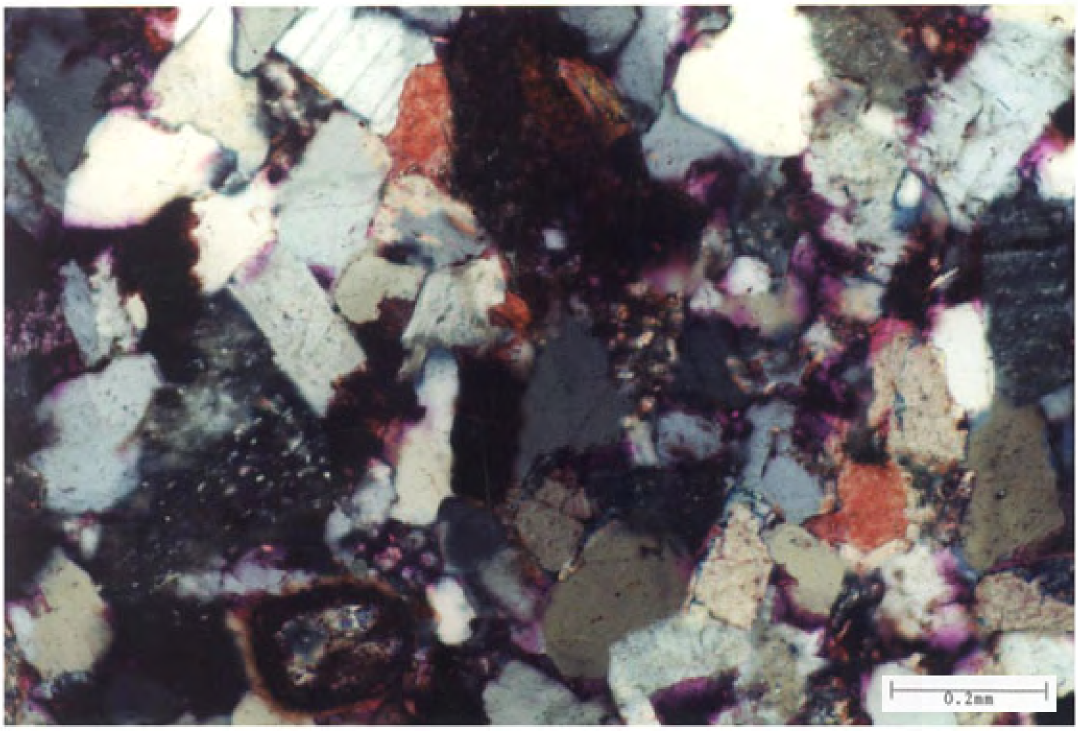

Well 3A-35
API 43-013-31738
5003.25 ft
100x

Back

Go to TS 3 100x

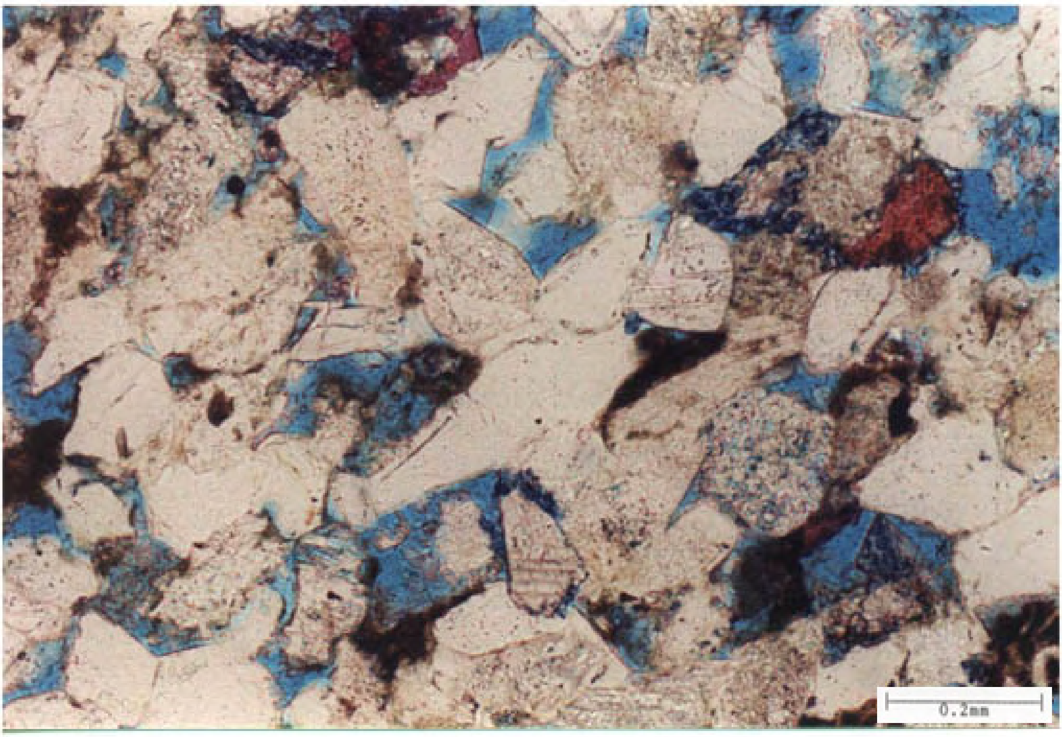

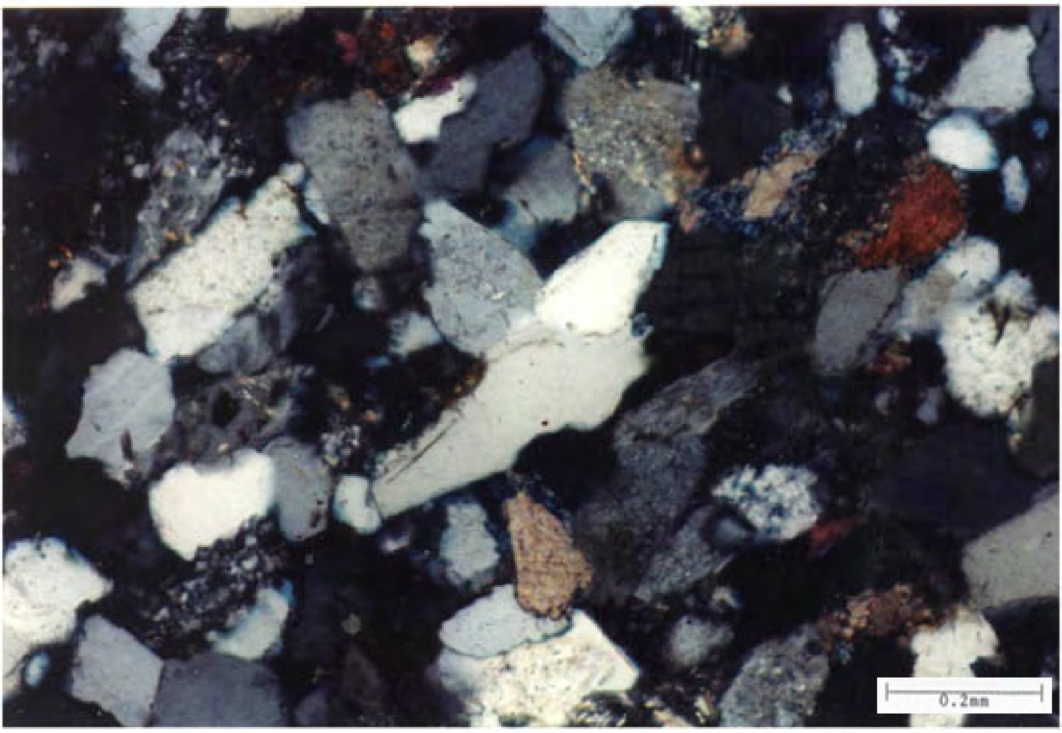

Well 3A-35
API 43-013-31738
5006.4 ft
100x

Back to Core Description

Go to TS 4 40x

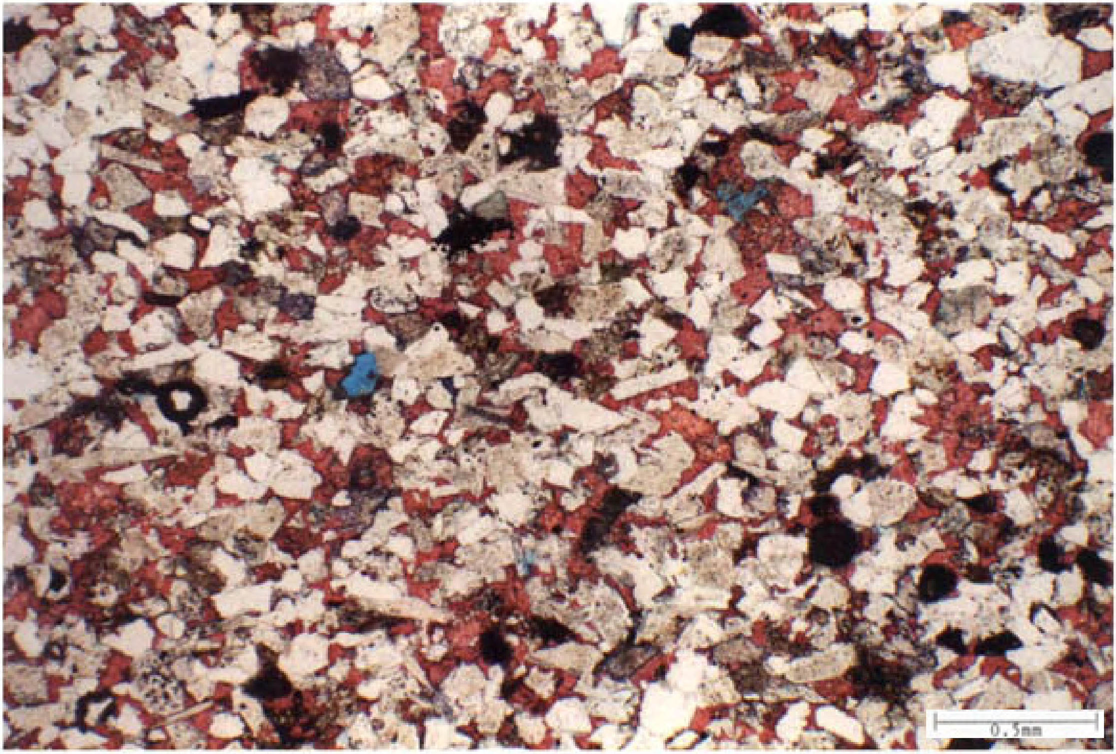

Well 3A-35
API 43-013-31738
5010.6 ft
40x

Back to Core Description

Go to TS 4 100x a

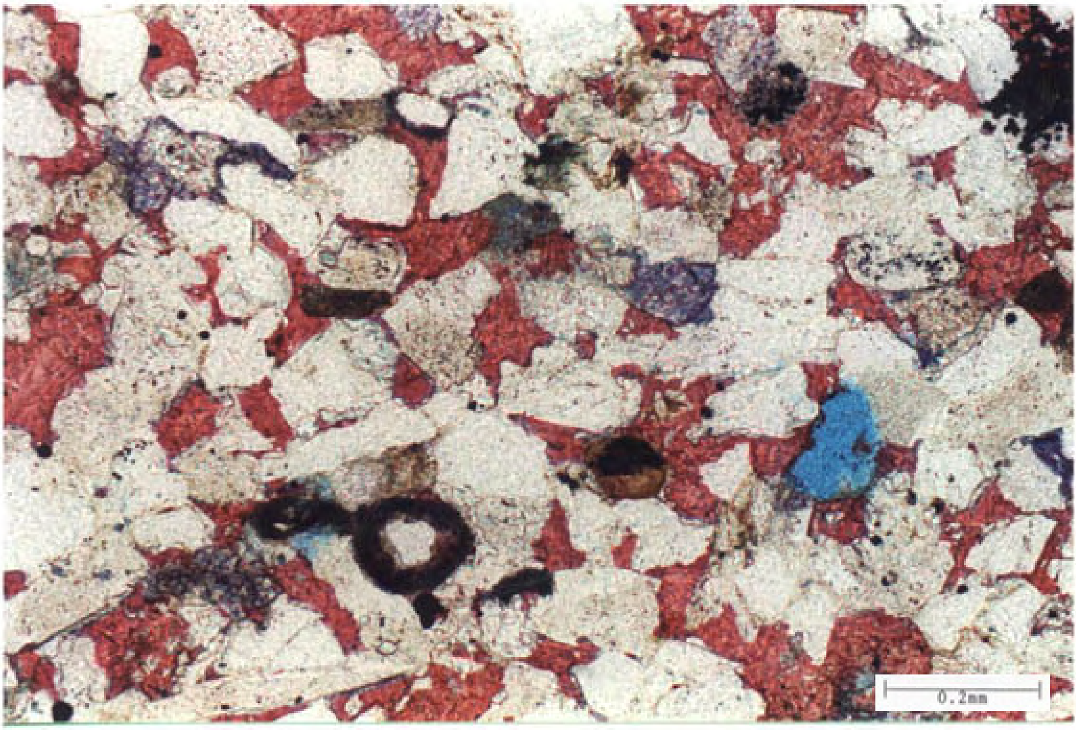

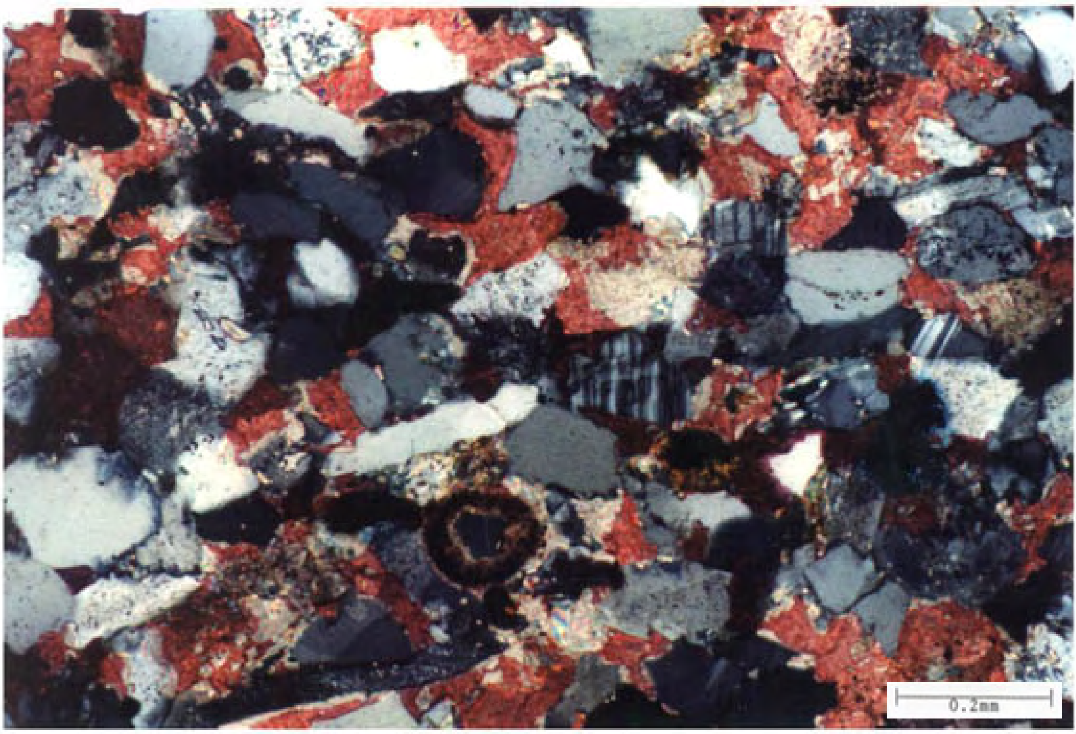

Well 3A-35
API 43-013-31738
5010.6 ft
100x

Back

Go to TS 4 100x b

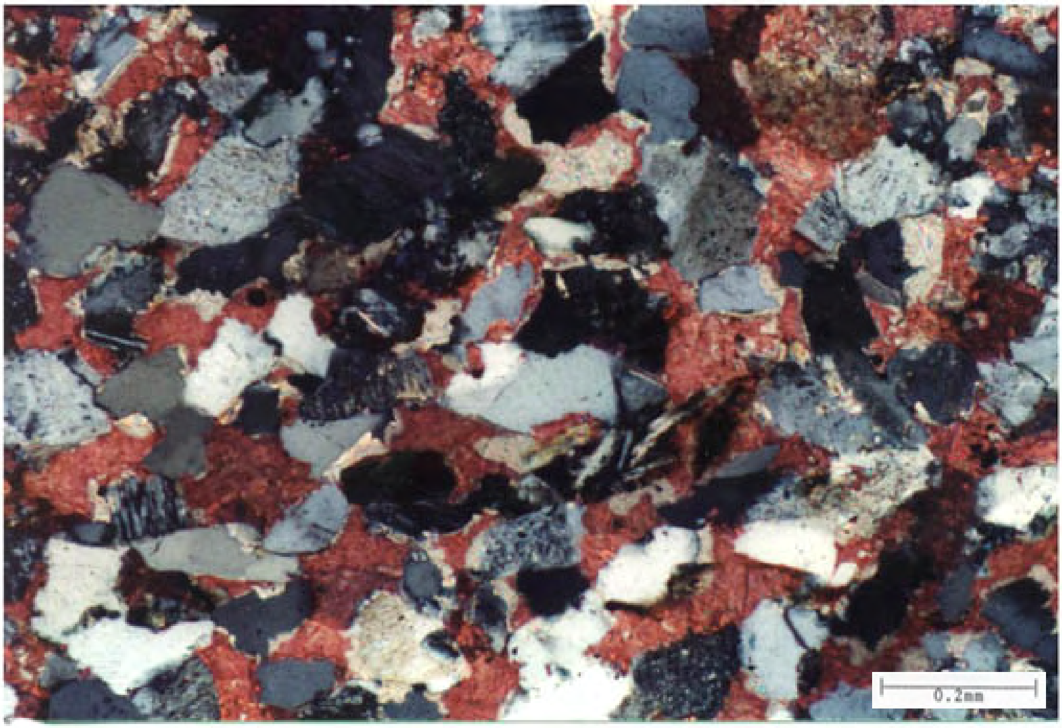

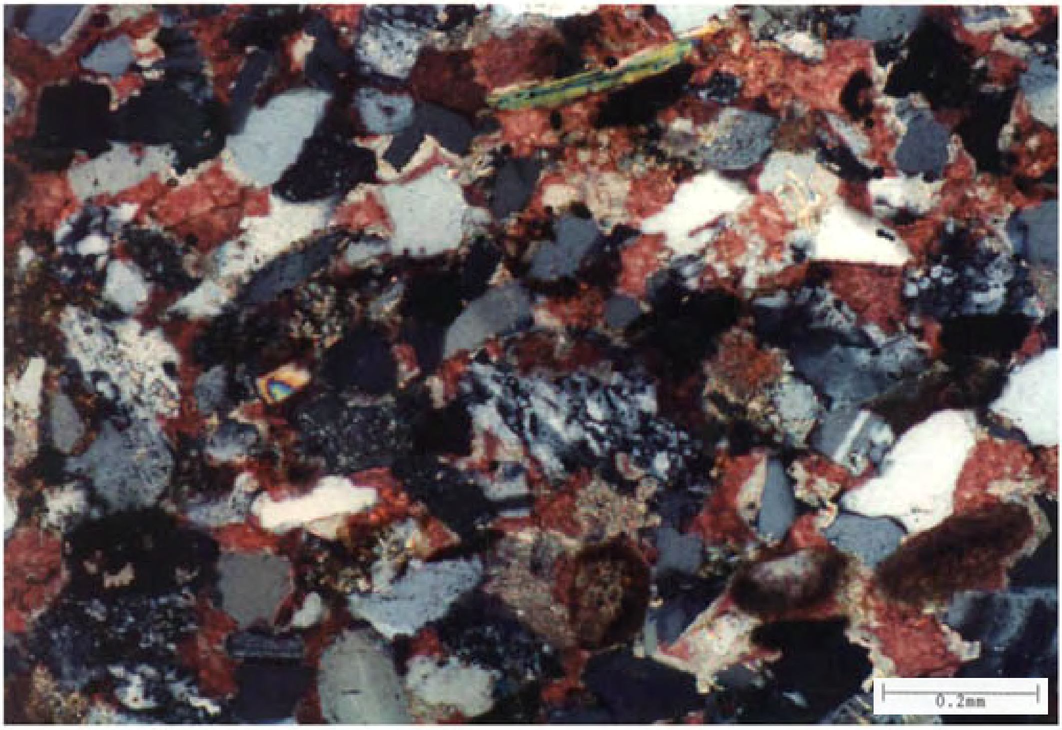

Well 3A-35
API 43-013-31738
5010.6 ft
100x

Back to Core Description

Back

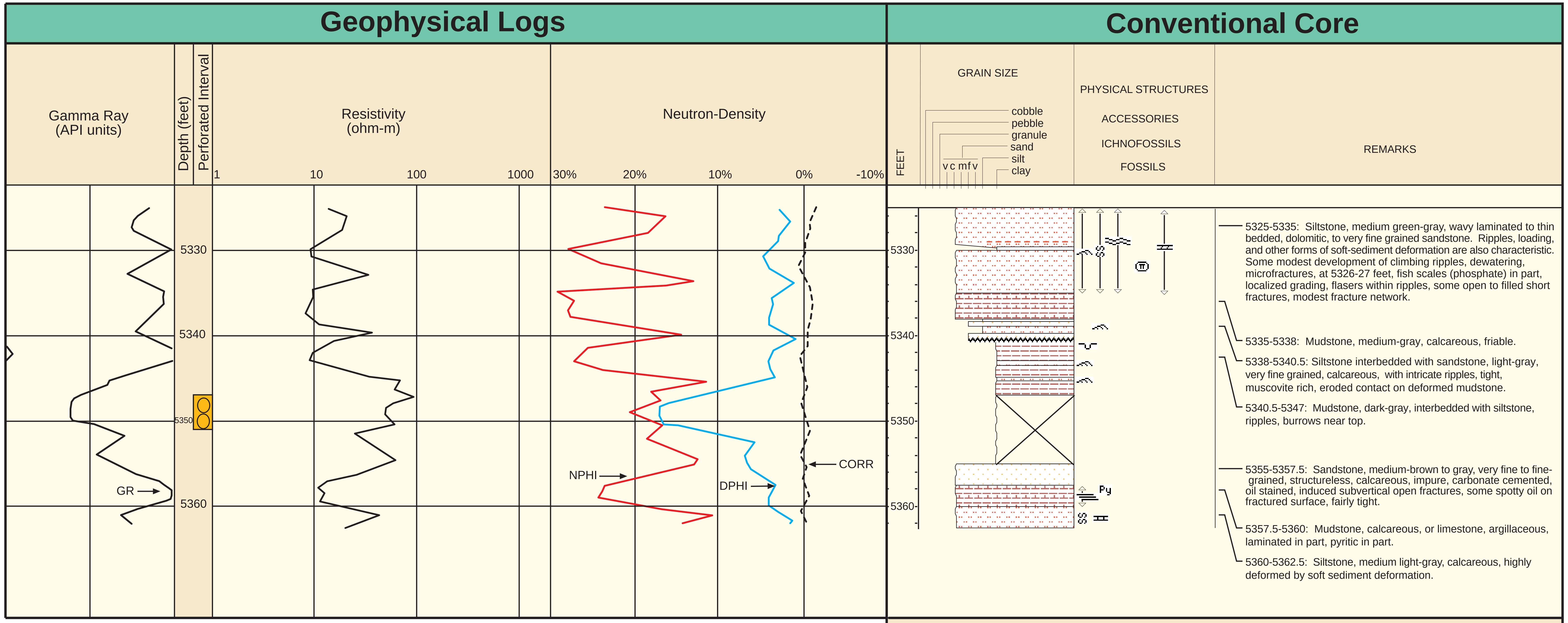

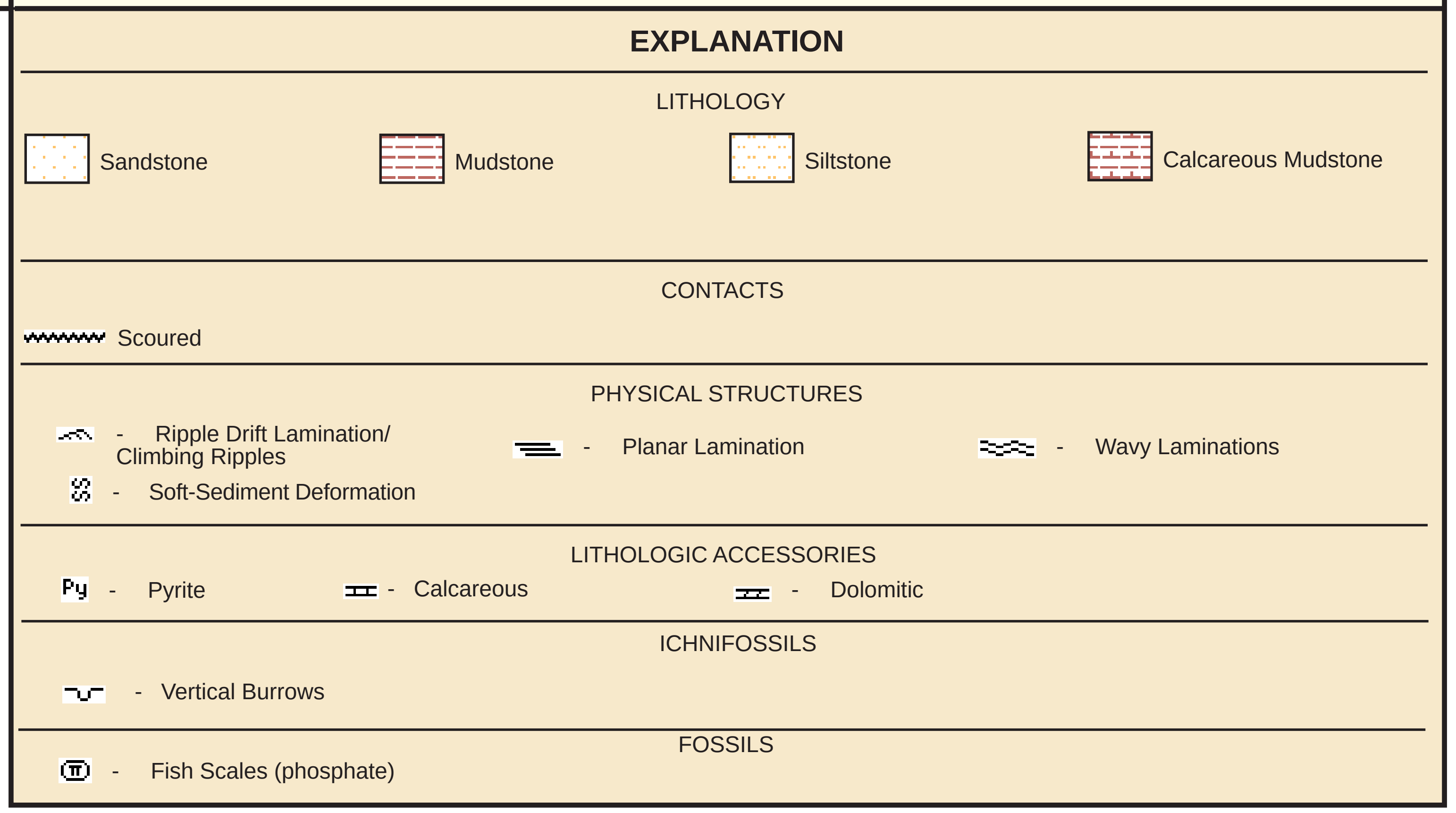

Federal 23-24

NE1/4SW1/4 section 24,
T. 8 S., R. 17 E., SLBL

Pariette Draw Field
API: 43-047-32710
Depth: 5325-5362.5 feet
Interval: MGR 5 and MGR 6 (Monument Butte reservoir, C sandstone)
Core Description by: S. Robert Bereskin

Abbreviations

GR - Gamma Ray
NPHI - Neutron Porosity
DPHI - Density Porosity
CORR - Density Correction
SLBL - Salt Lake Base Line
API - American Petroleum Institute well number

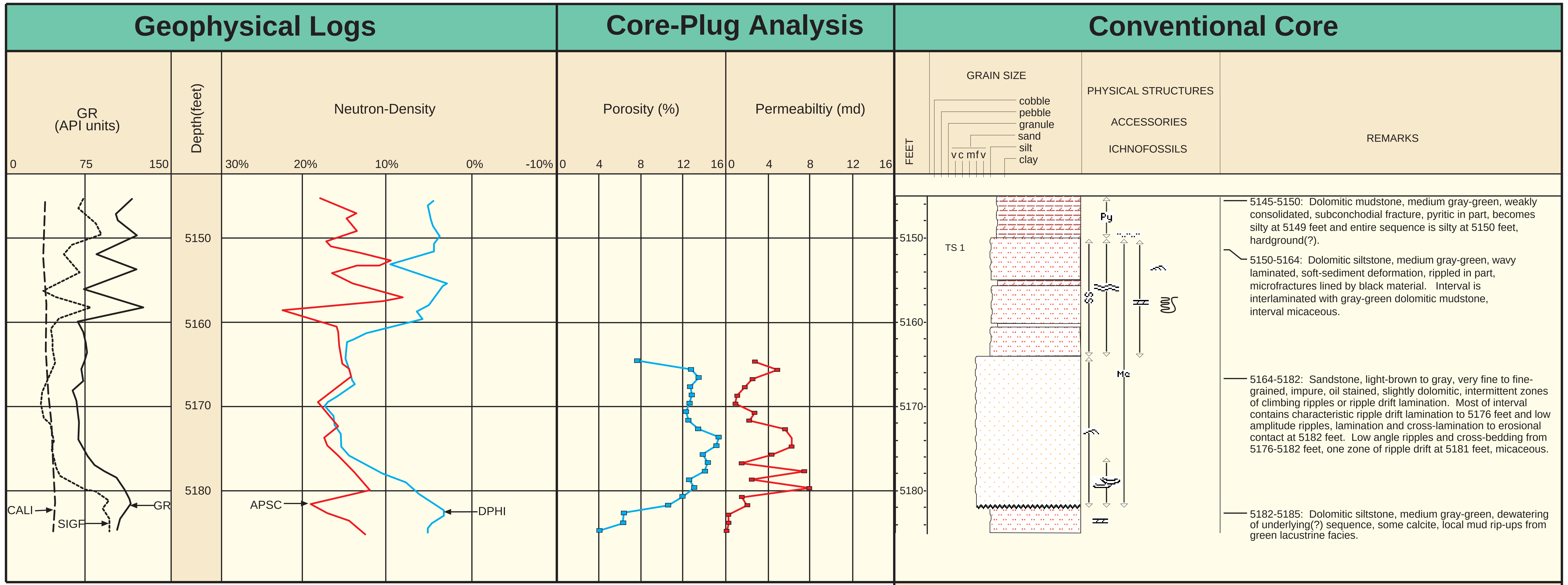

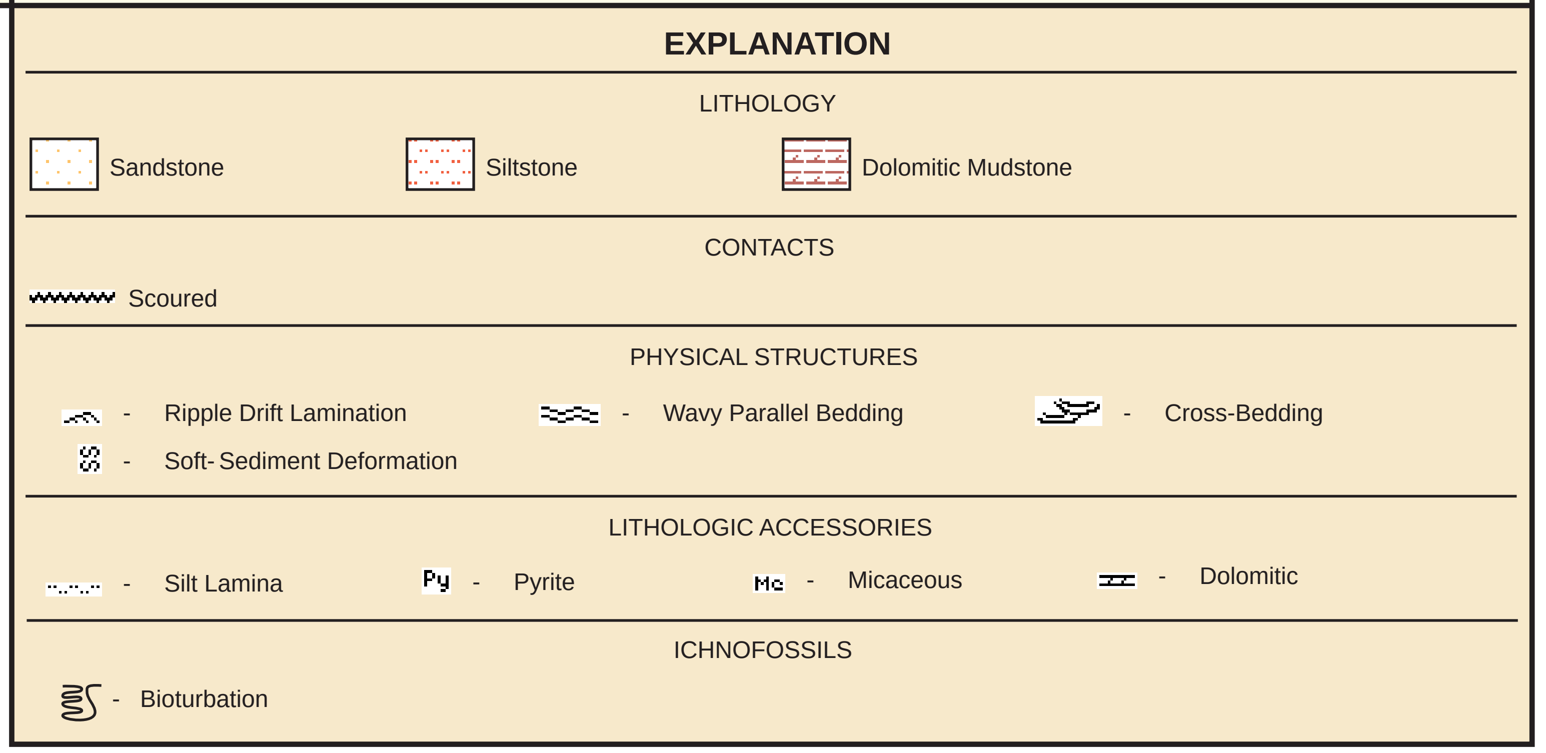

Federal 23-25

NE1/4SW1/4 section 25,
R. 8 S., T. 17 E., SLBL

Eight Mile Flat North Field
Humpback water-flood unit
API: 43-047-32529
Depth: 5,145-5,185 feet
Interval: MGR 5 (Monument Butte reservoir, C sandstone)
Core Description by: S. Robert Bereskin

Abbreviations

GR - Gamma Ray
SIGF - Sigma Formation
CALI - Caliper
APSC - Epithermal Array Porosity sandstone corrected
DPHI - Density Porosity
md - Millidarcies
TS - Thin Section Photo
SLBL - Salt Lake Base Line
API - American Petroleum Institute well number

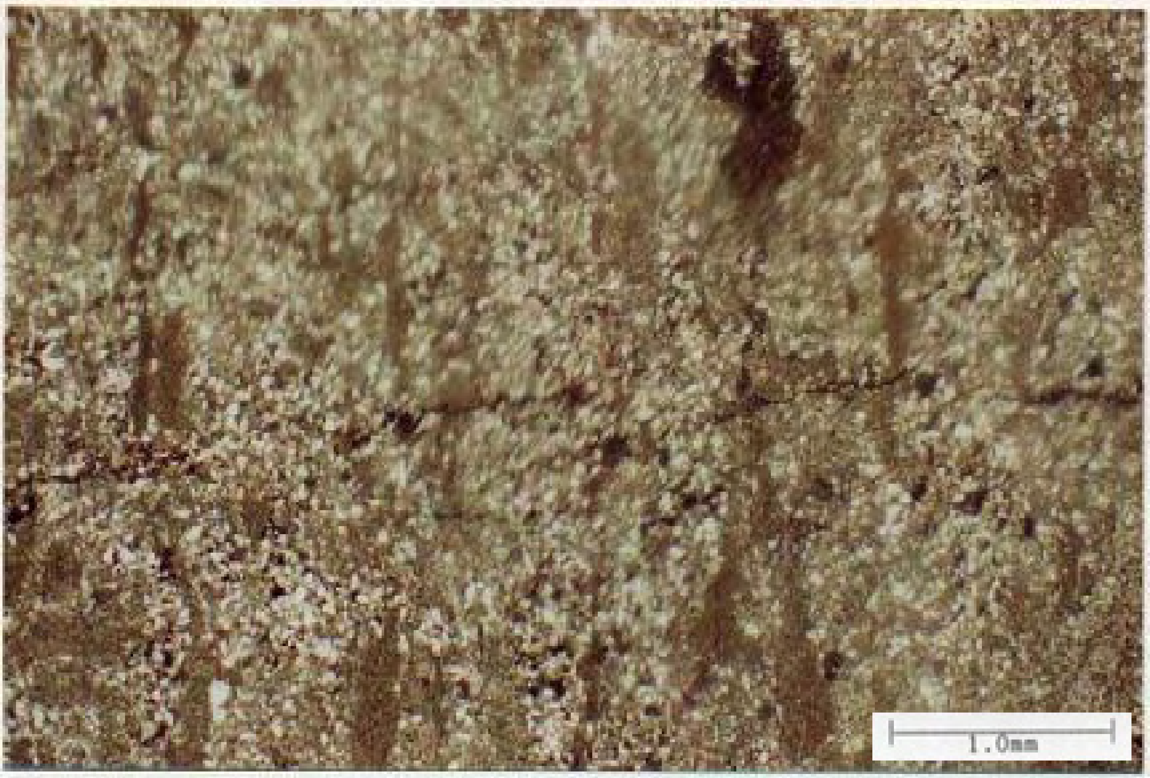

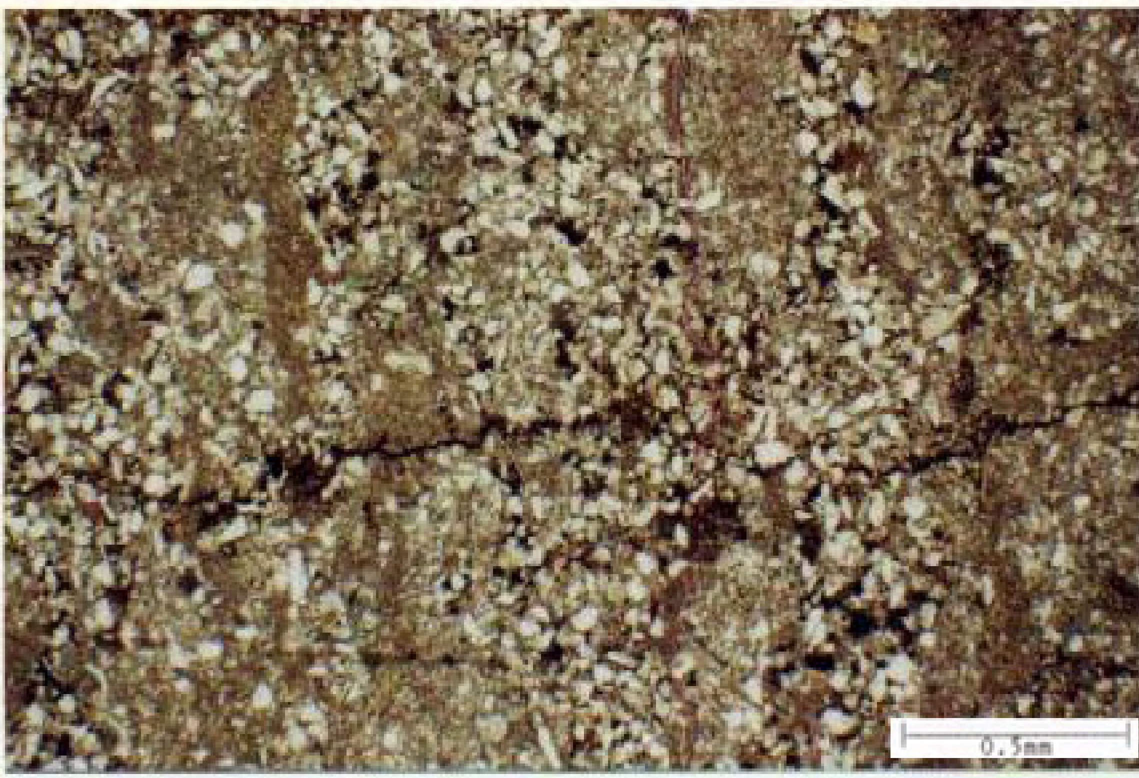

Federal 23-25
43-047-325229
5151 ft
20x and 40x

Back to Core Description

Go to TS 1 40x

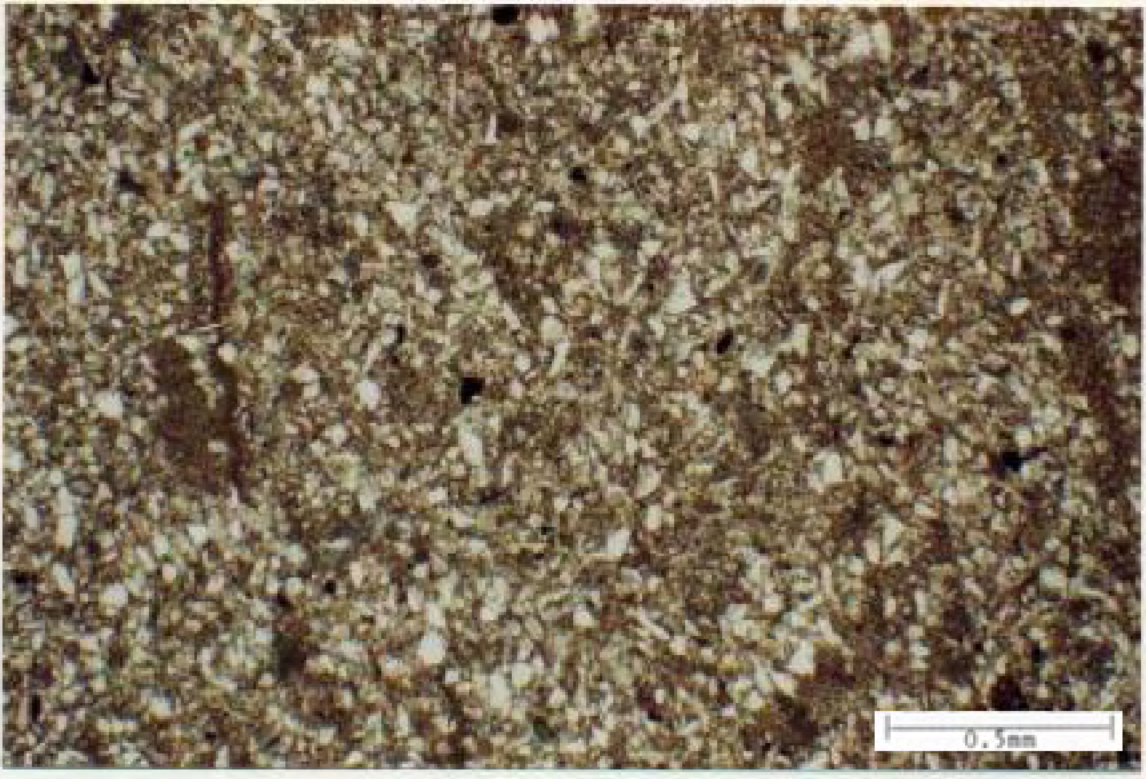

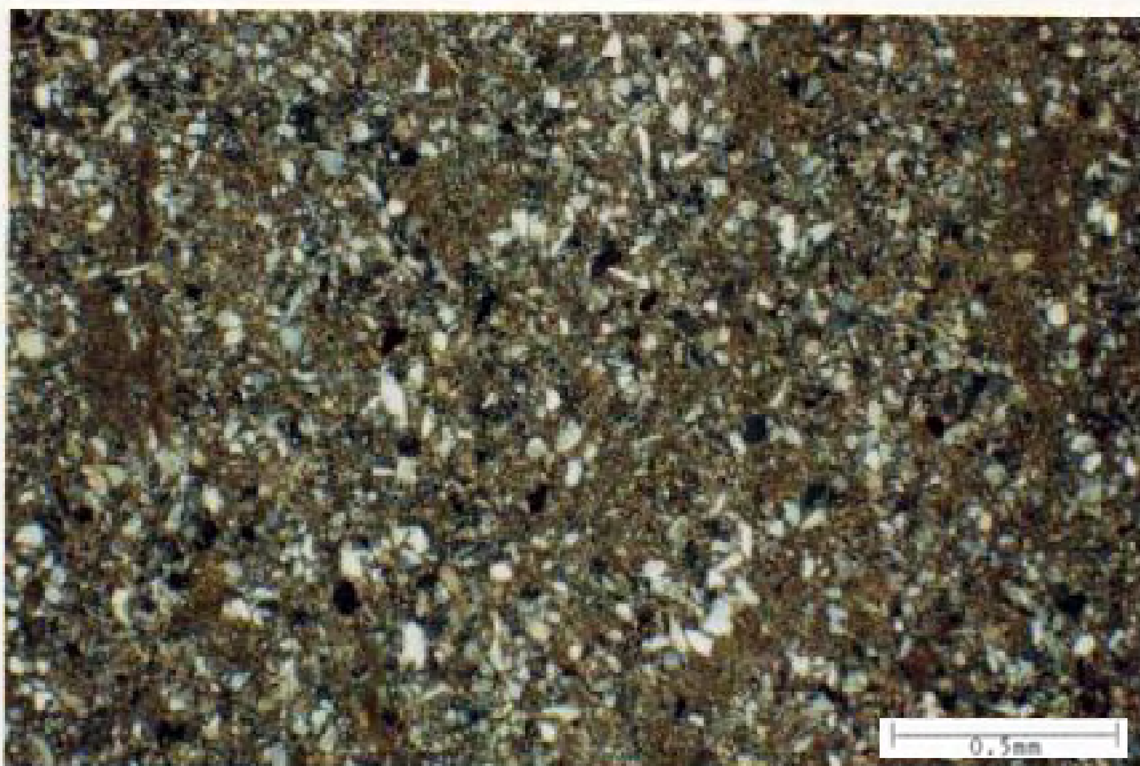

Federal 23-25
43-047-325229
5151 ft
40x

Back

Go to TS 1 100x

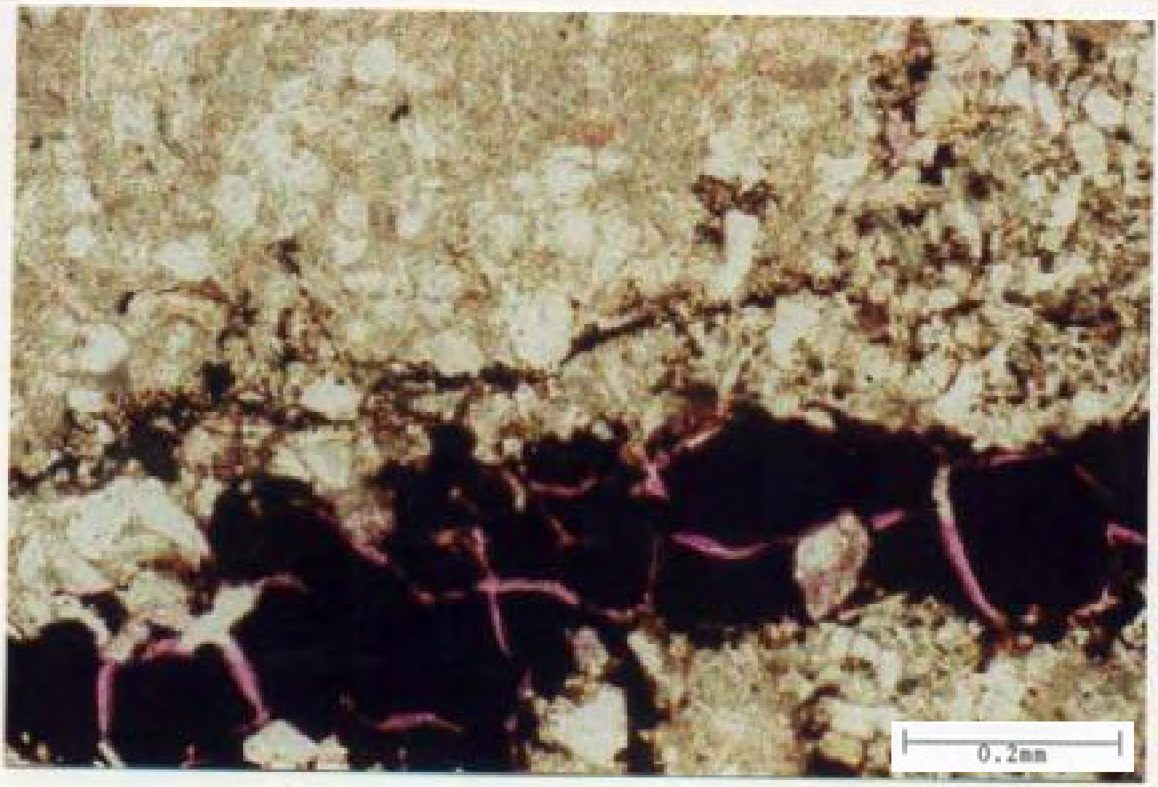

Federal 23-25
43-047-325229
5151 ft
100x

Back to Core Description

Back

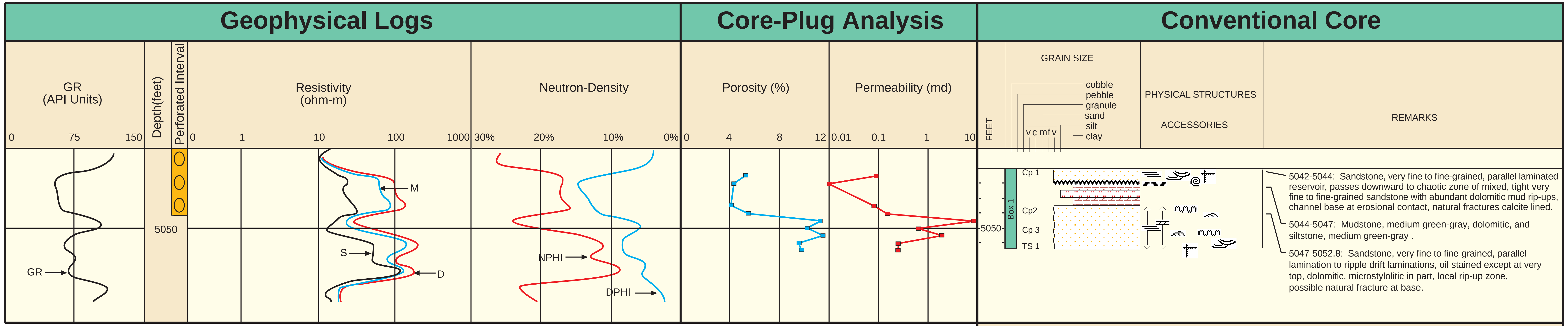

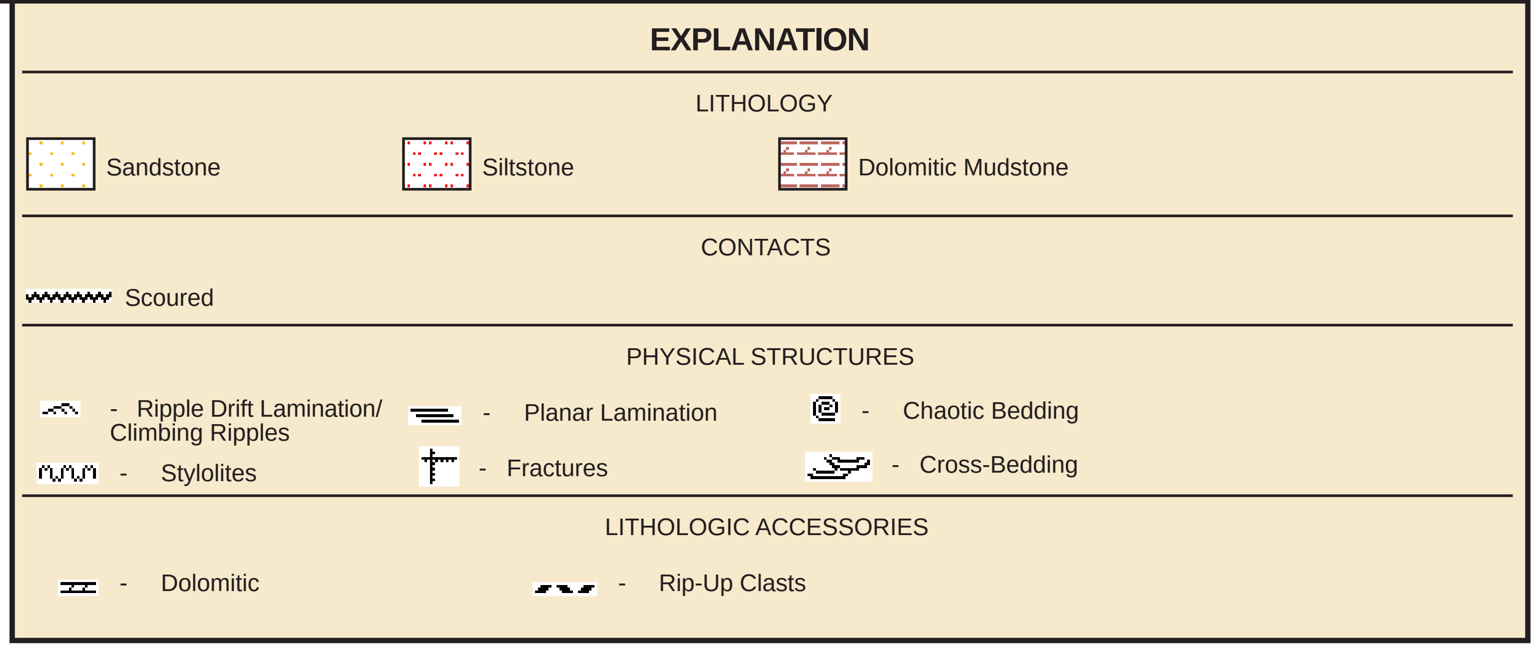

State 6-32

SE1/4NW1/4 section 32, T. 8 S., R. 17 E., SLBL

Monument Butte Field
Gilsonite water-flood unit
API: 43-013-30748
Depth: 5,042 - 5,052.8 feet
Interval: MGR 5 (Monument Butte reservoir, C sandstone)
Core Description by: S. Robert Bereskin

Abbreviations

GR - Gamma Ray
S - Resistivity Shallow
M - Resistivity Medium
D - Resistivity Deep
NPHI - Neutron Porosity
DPHI - Density Porosity
md - Millidarcies
TS - Thin Section Photo
Box - Core Box Photo
Cp - Core Photo
SLBL - Salt Lake Base Line
API - American Petroleum Institute well number

Back to Core Description

Go to Core Box Photo 2

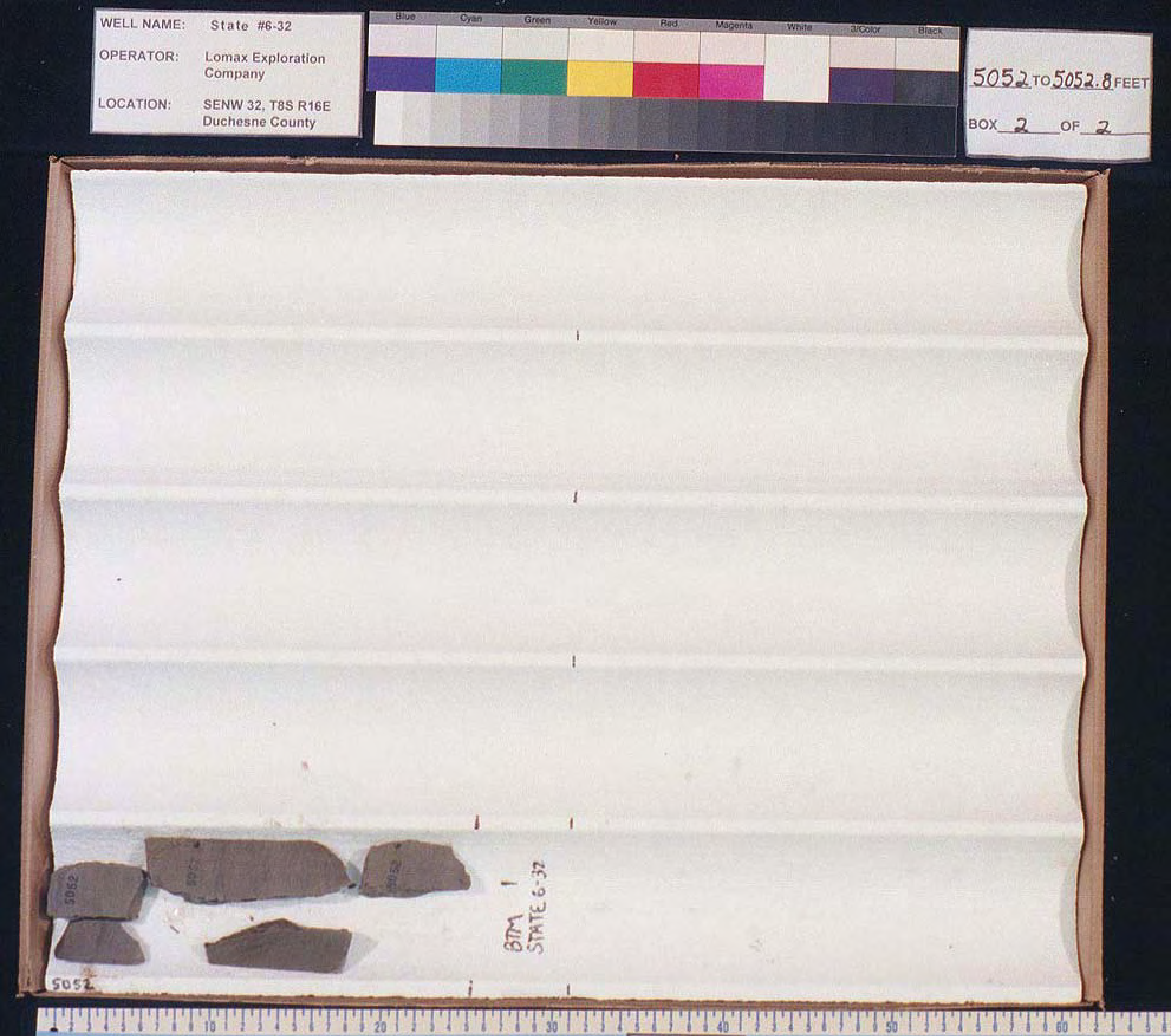

Back to Core Description

Back to Core Description

Back to Core Description

Back to Core Description

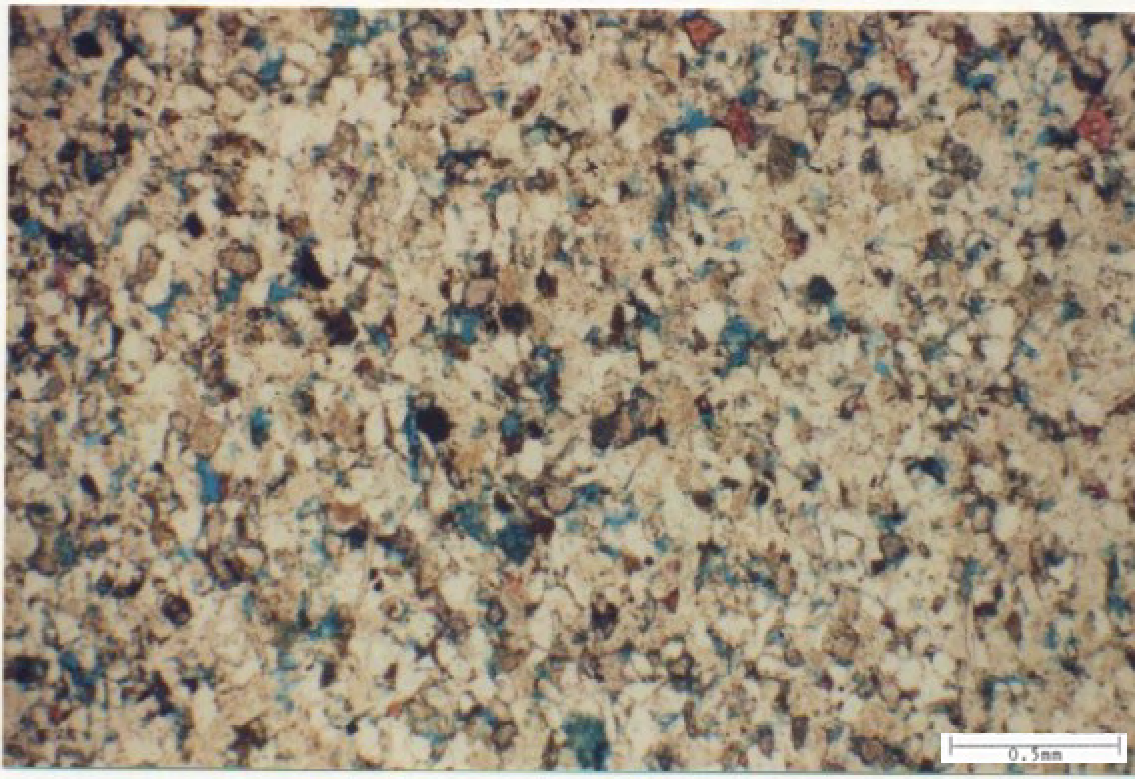

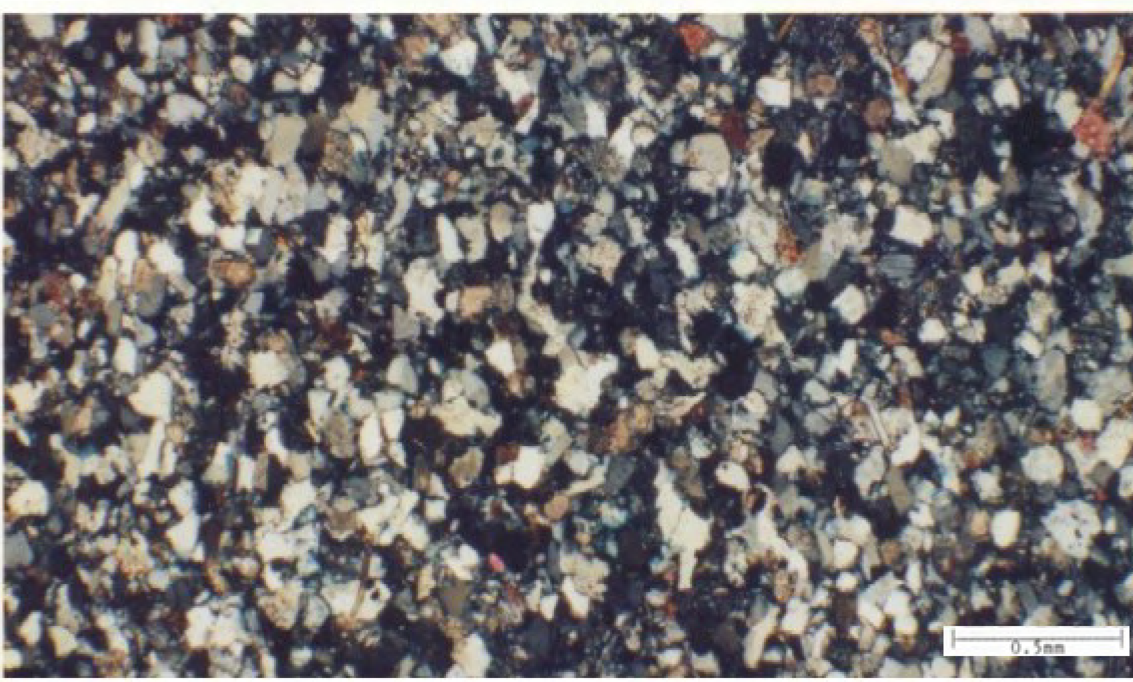

Well 6-32
API 43-013-30748
5052 ft
40x

Back to Core Description

Go to TS 1 100x a

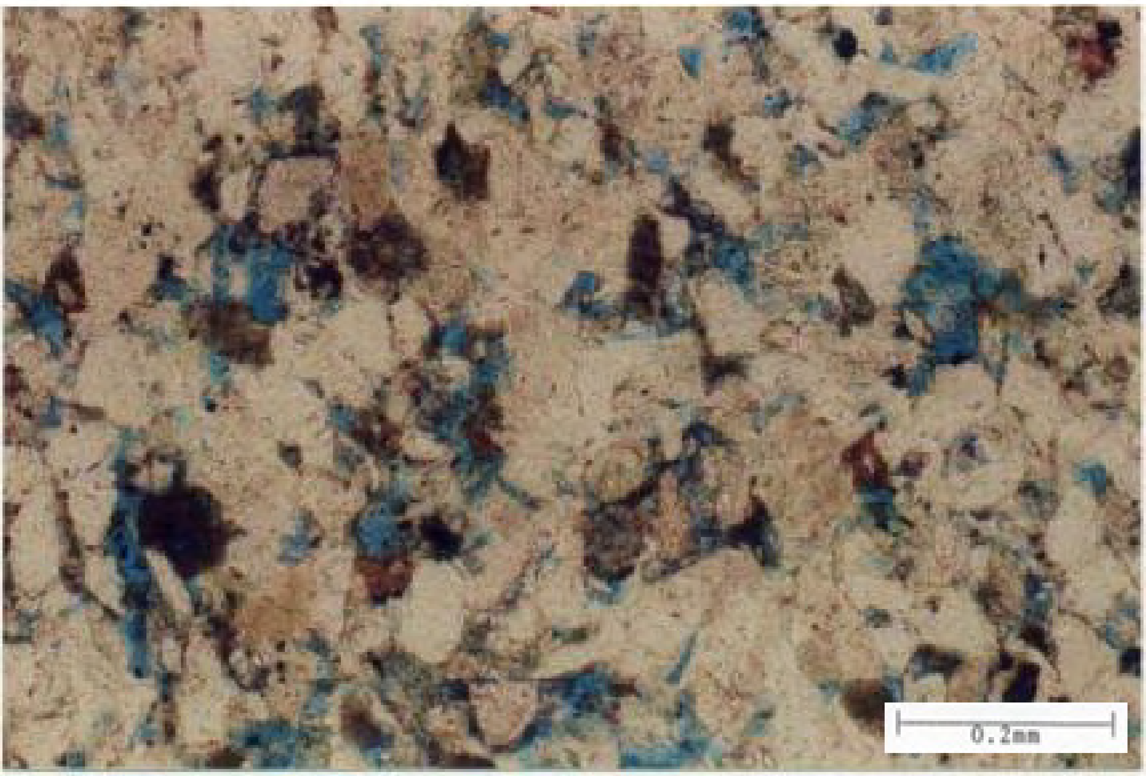

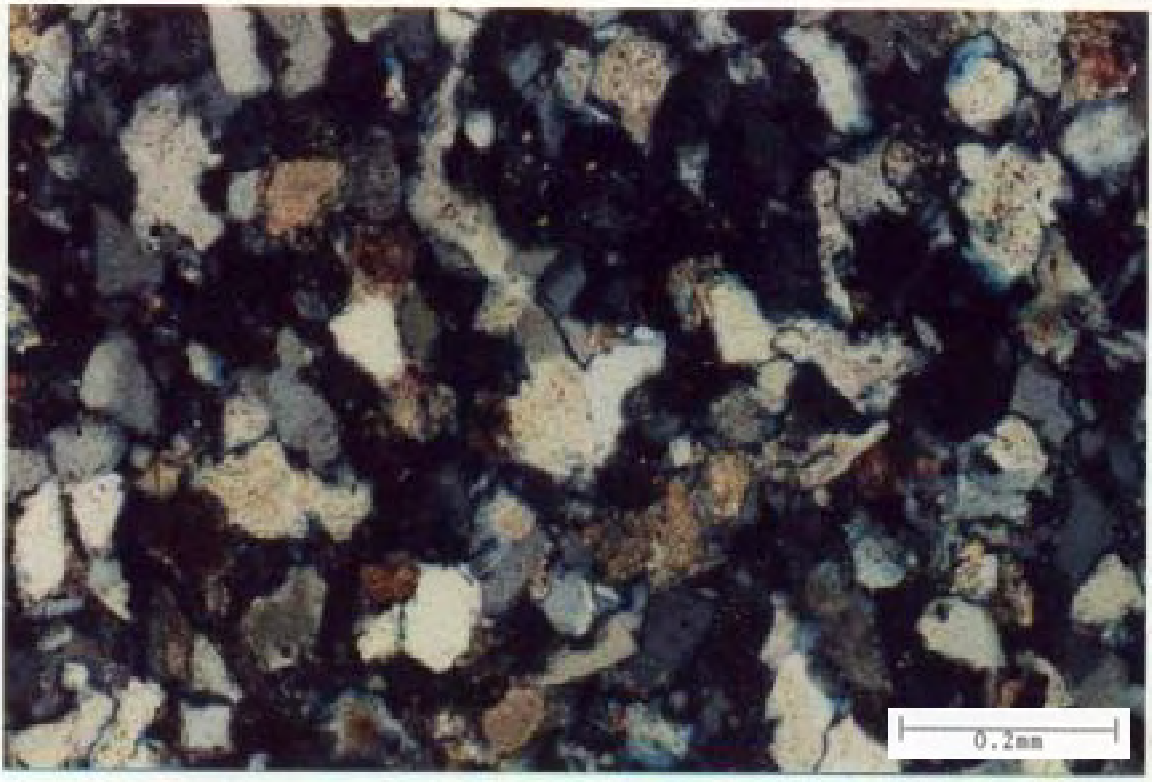

Federal 6-32
43-013-30748
5052 ft
100x

Back

Go to TS 1 100x b

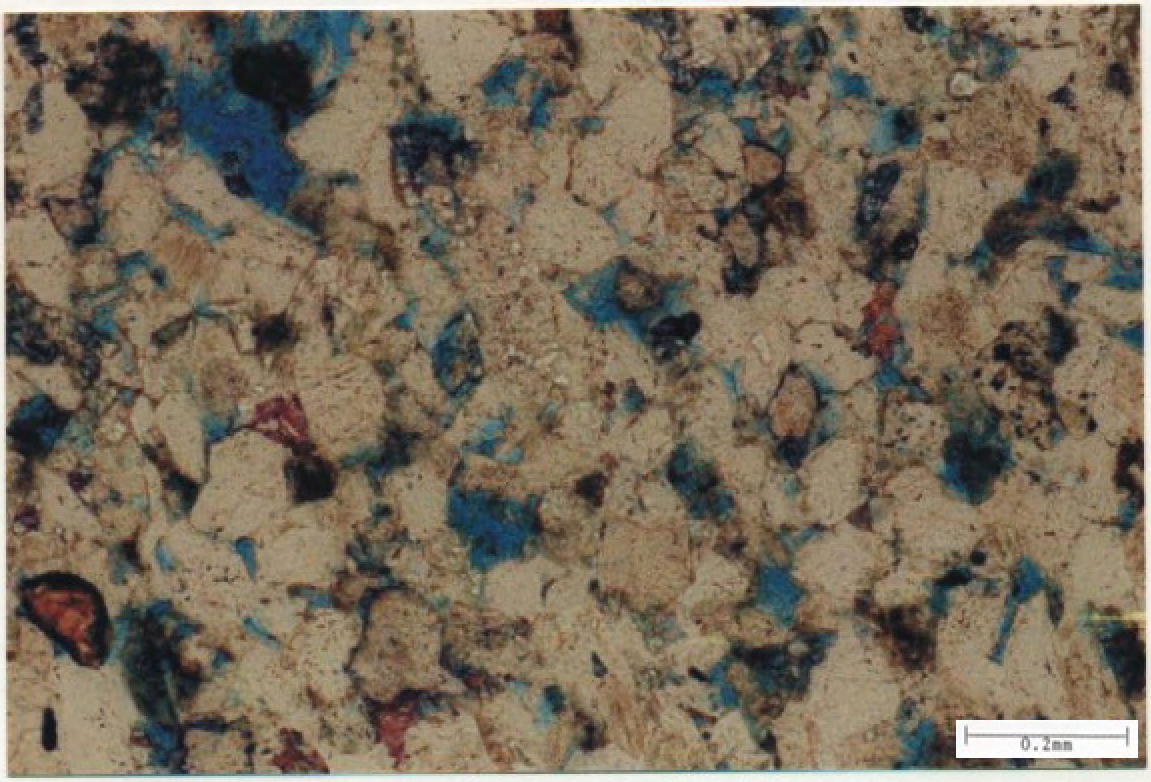

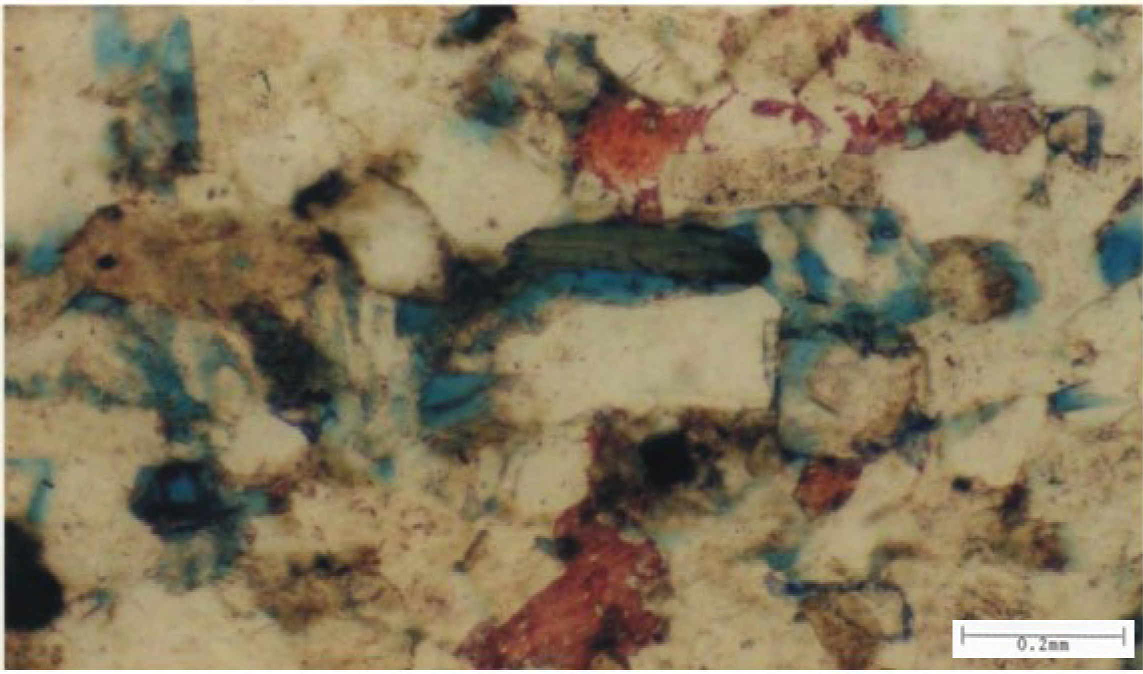

Well 6-32
API 43-013-30748
5052 ft
100x

Back

Go to TS 1 200x a

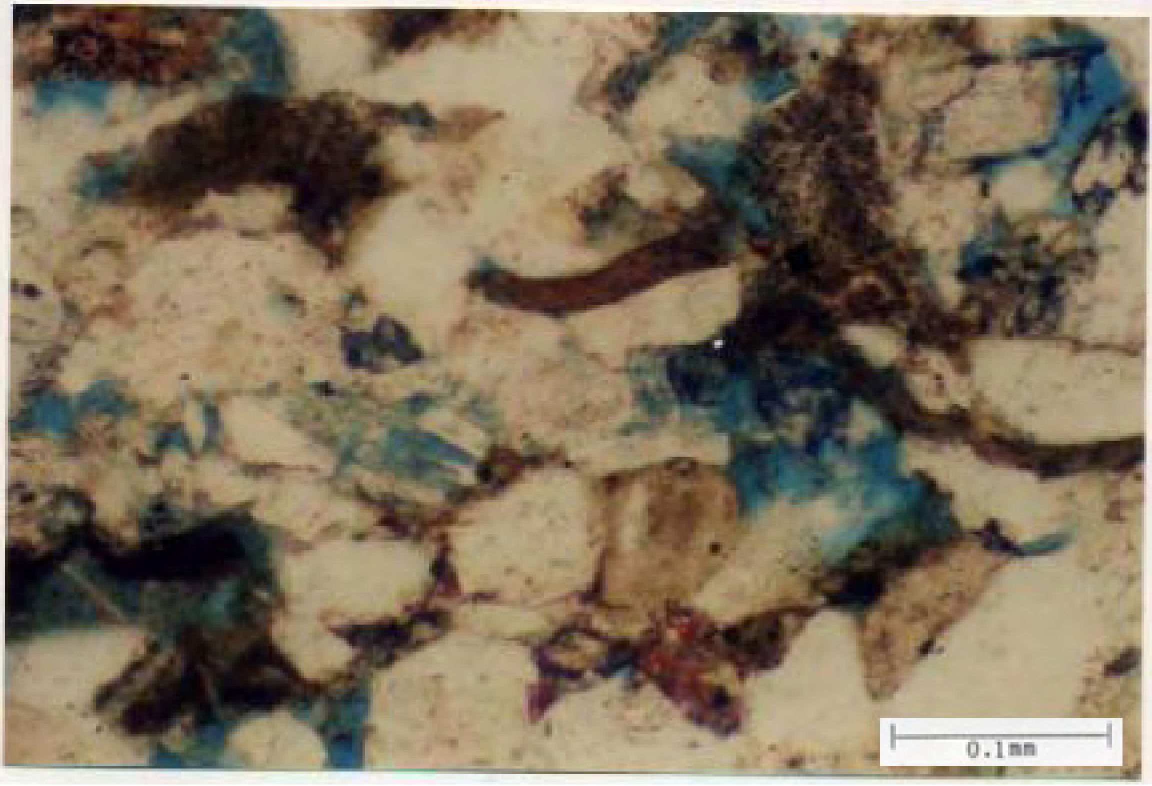

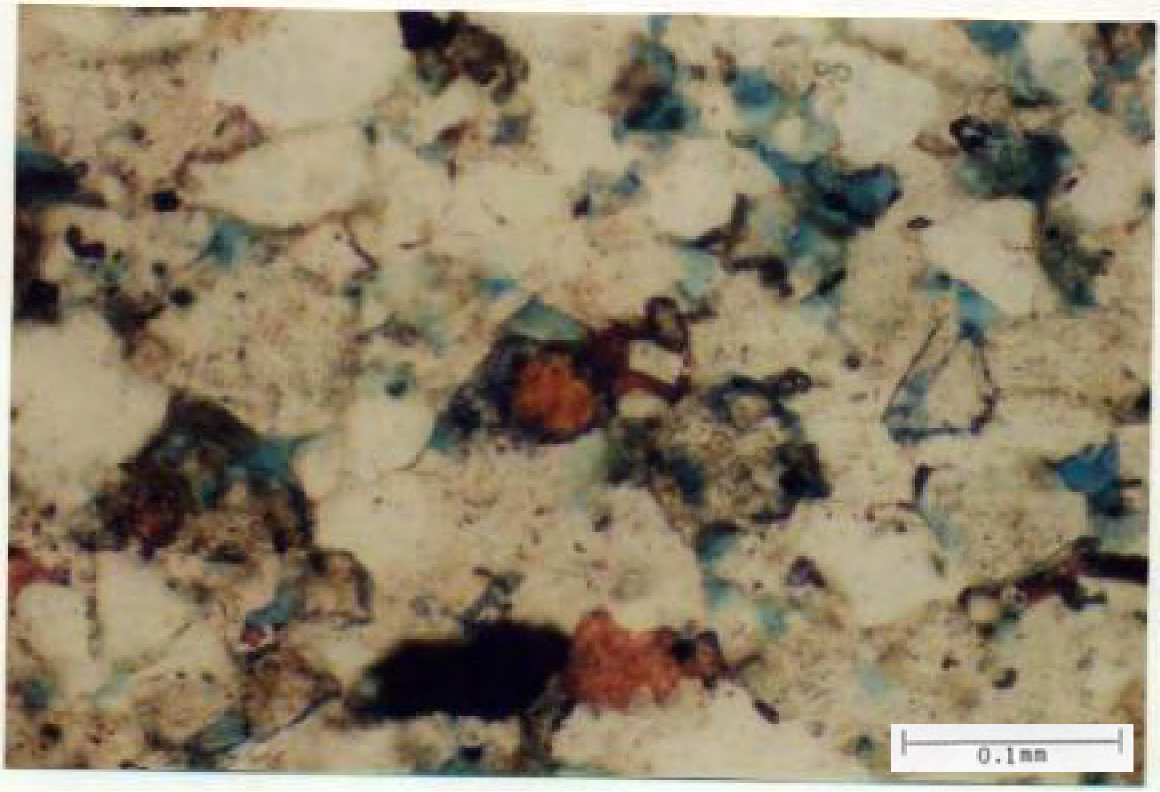

Federal 6-32
43-013-30748
5052 ft
200x

Back to Core Description

Back

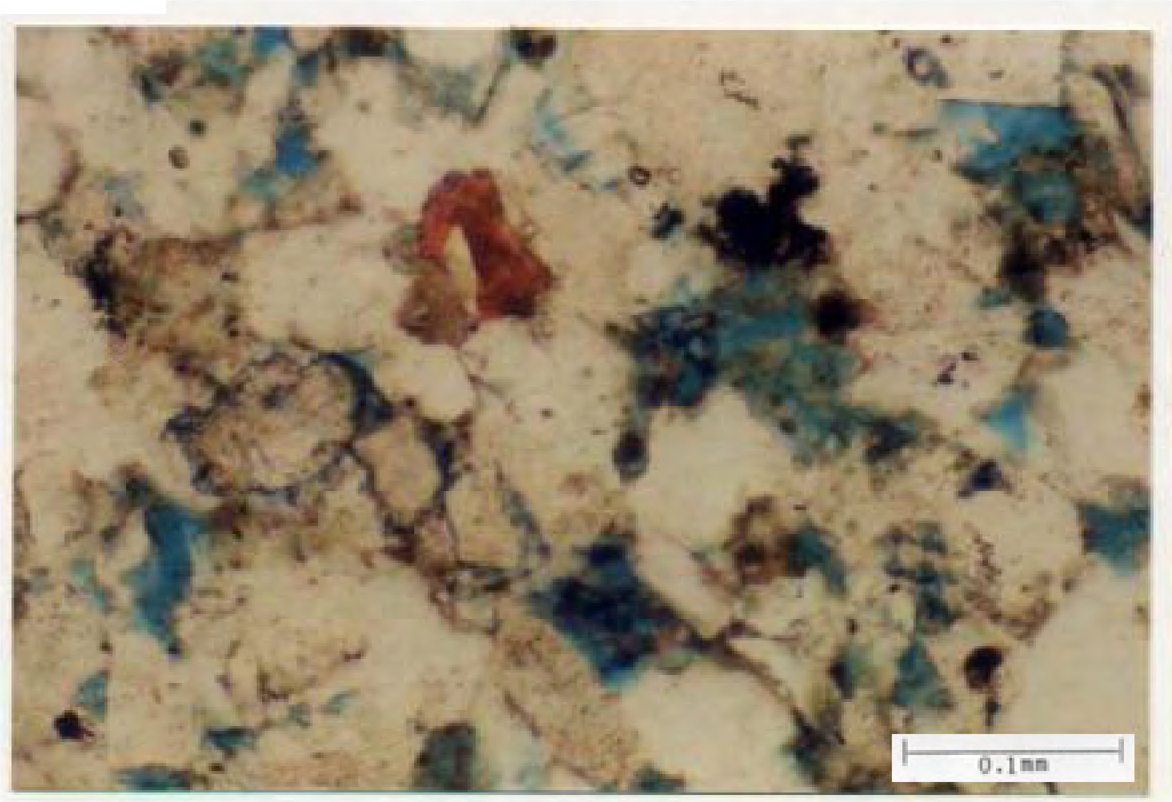

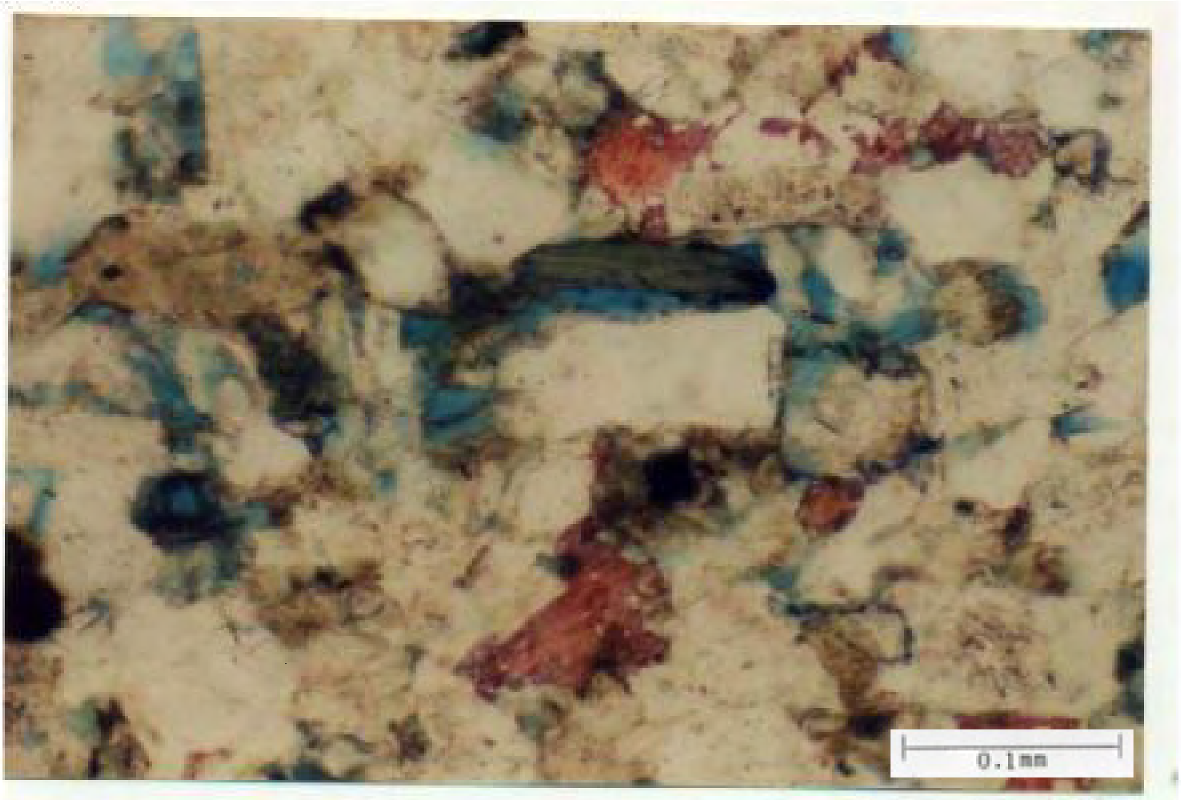

Federal 6-32
43-013-30748
5052 ft
200x

Back

Go to TS 1 200x b

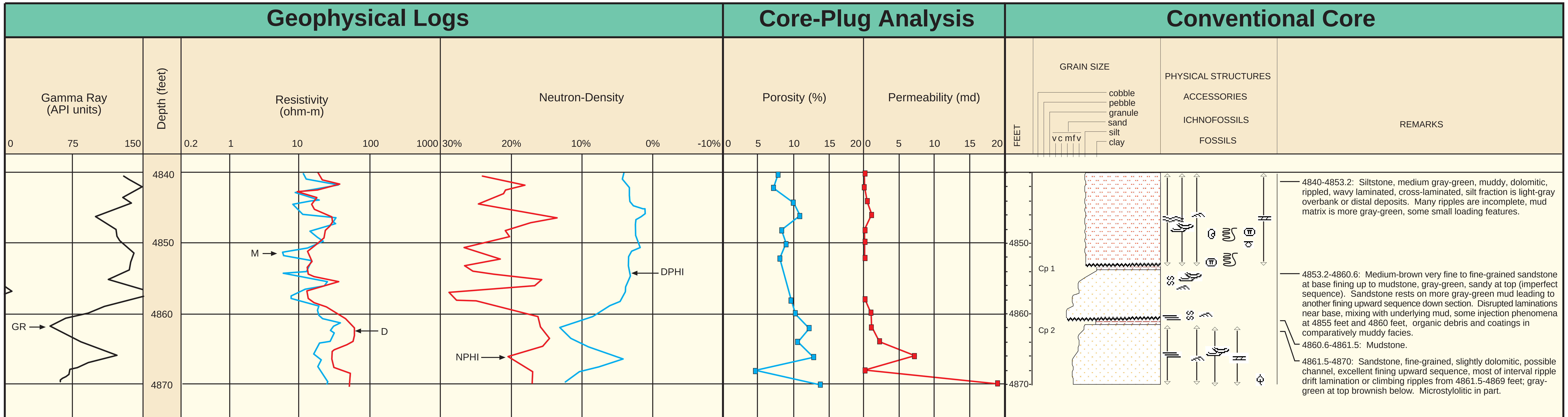

Federal 33-11J (core 1)

NW1/4SE1/4 section 11,
T. 9 S., R. 16 E., SLBL

Monument Butte Field
Jonah water-flood unit
API: 43-013-31451
Depth: 4,840-4,870 feet
Interval: MGR 5 (Monument Butte Reservoir, C sandstone)
Core Description by: S. Robert Bereskin

Abbreviations

GR - Gamma Ray
M - Resitivity Medium
D - Resistivity Deep
NPHI - Neutron Porosity
DPHI - Density Porosity
md - Millidarcies
Cp - Core Photo
SLBL - Salt Lake Base Line
API - American Petroleum Institute well number

EXPLANATION

LITHOLOGY

Sandstone
Dolomitic Mudstone
Siltstone

CONTACTS

Erosional

PHYSICAL STRUCTURES

- Ripple Drift Lamination/ Climbing Ripples
- Soft-Sediment Deformation
- Planar Lamination
- Wavy Parallel Bedding
- Cross-Bedding
- Loading

LITHOLOGIC ACCESSORIES

- Dolomitic

ICHNOFOSSILS

- Bioturbation

FOSSILS

- Carbonaceous Plant Remains
- Ostracods
- Fish Scales (phosphate)

Back to Core Description

Back to Core Description

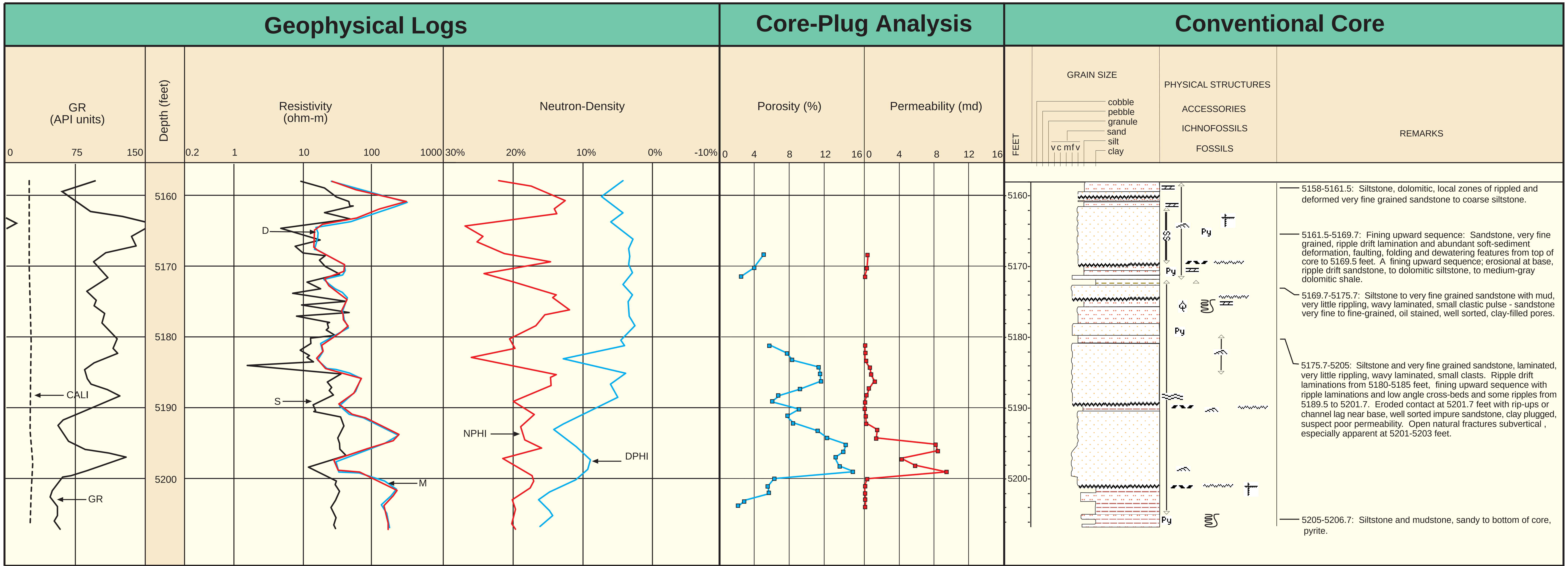

Federal 33-11J (core 2)

NW1/4SE1/4 section 11, T. 9 S., R. 16 E., SLBL

Monument Butte Field
Jonah water-flood unit
API: 43-013-31451
Depth: 5,158 - 5,207 feet
Interval: MGR 3 (Travis reservoir)
Core Description by: S. Robert Bereskin

Abbreviations

GR - Gamma Ray
CALI - Caliper
S - Resistivity Shallow
M - Resistivity Medium
D - Resistivity Deep
NPHI - Neutron Porosity
DPHI - Density Porosity
md - Millidarcies
SLBL - Salt Lake Base Line
API - American Petroleum Institute well number

EXPLANATION

LITHOLOGY

Sandstone; Mudstone; Dolomitic Siltstone; Dolomitic Shale; Siltstone

CONTACTS

Erosional

PHYSICAL STRUCTURES

- Ripple Drift Lamination/ Climbing Ripples
- Wavy Parallel Bedding
- Scour
- Cross-Bedding
- Soft-Sediment Deformation
- Open Oil Stained Fractures

LITHOLOGIC ACCESSORIES

Py - Pyrite
- Rip-Up Clasts
- Dolomitic

ICHNOFOSSILS

- Bioturbation

FOSSILS

- Carbonaceous Plant Remains

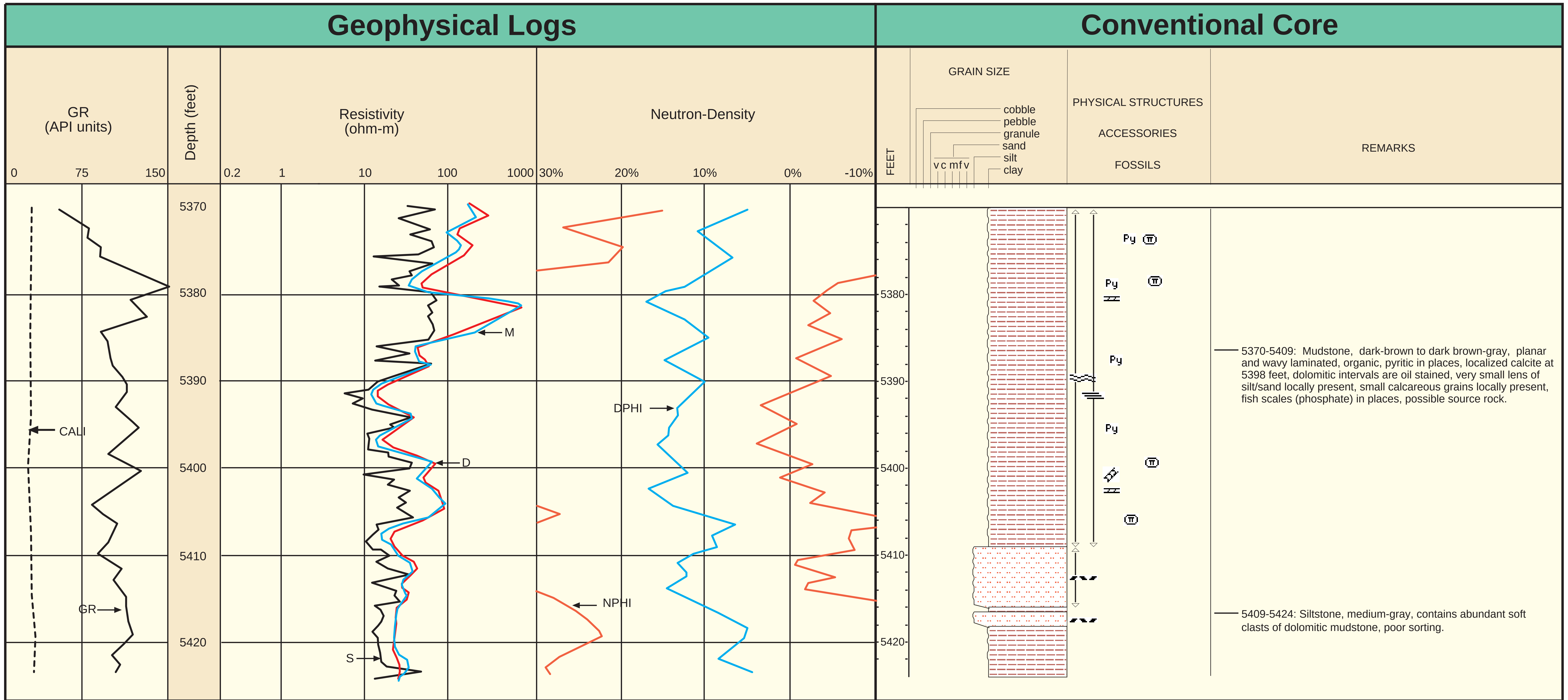

EXPLANATION

LITHOLOGY

Siltstone   Mudstone

PHYSICAL STRUCTURES

- Planar Lamination   - Wavy Laminations

LITHOLOGIC ACCESSORIES

- Dolomitic   Py - Pyrite   - Rip-Up Clasts

FOSSILS

- Algae   - Fish Scales (phosphate)

Federal 33-11J (core 3)

NW1/4SE1/4 section 11, T. 9 S., R. 16 E., SLBL

Monument Butte Field
API: 43-013-31451
Depth: 5,370 - 5,424 feet
Interval: MGR 1 (Travis reservoir)
Core Description by: S. Robert Bereskin

Abbreviations

GR - Gamma Ray
CALI - Caliper
S - Resistivity Shallow
M - Resistivity Medium
D - Resistivity Deep
NPHI - Neutron Porosity
DPHI - Density Porosity
SLBL - Salt Lake Base Line
API - American Petroleum Institute well number

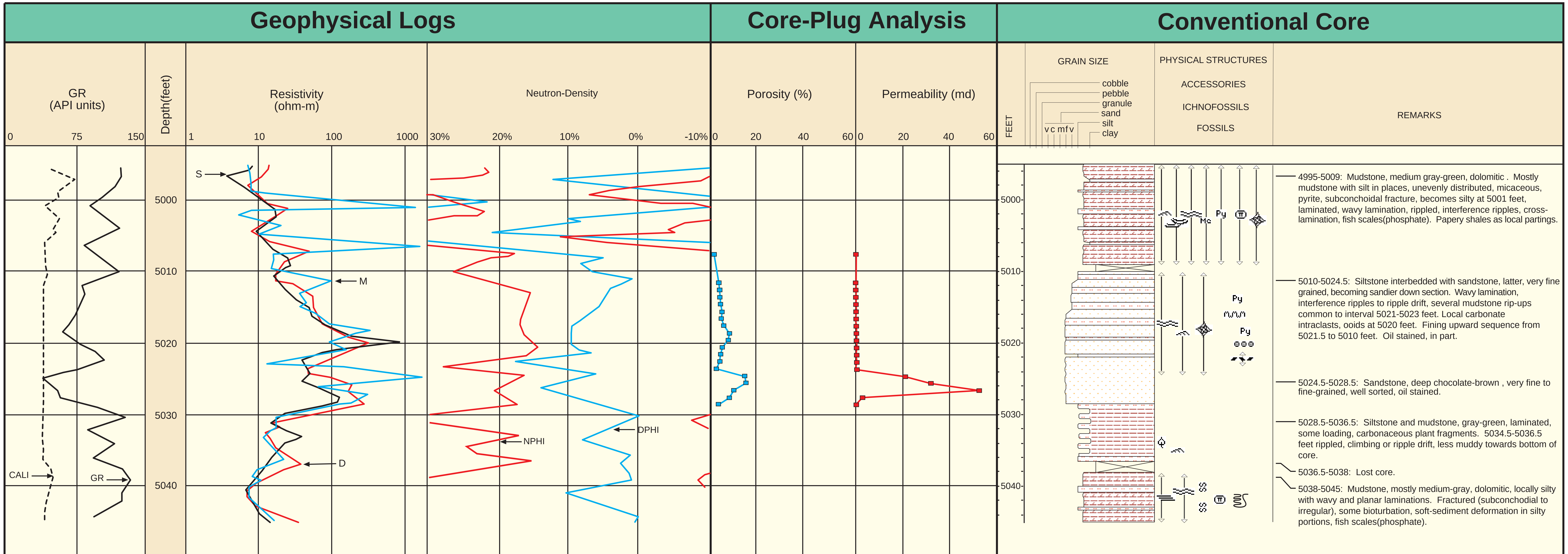

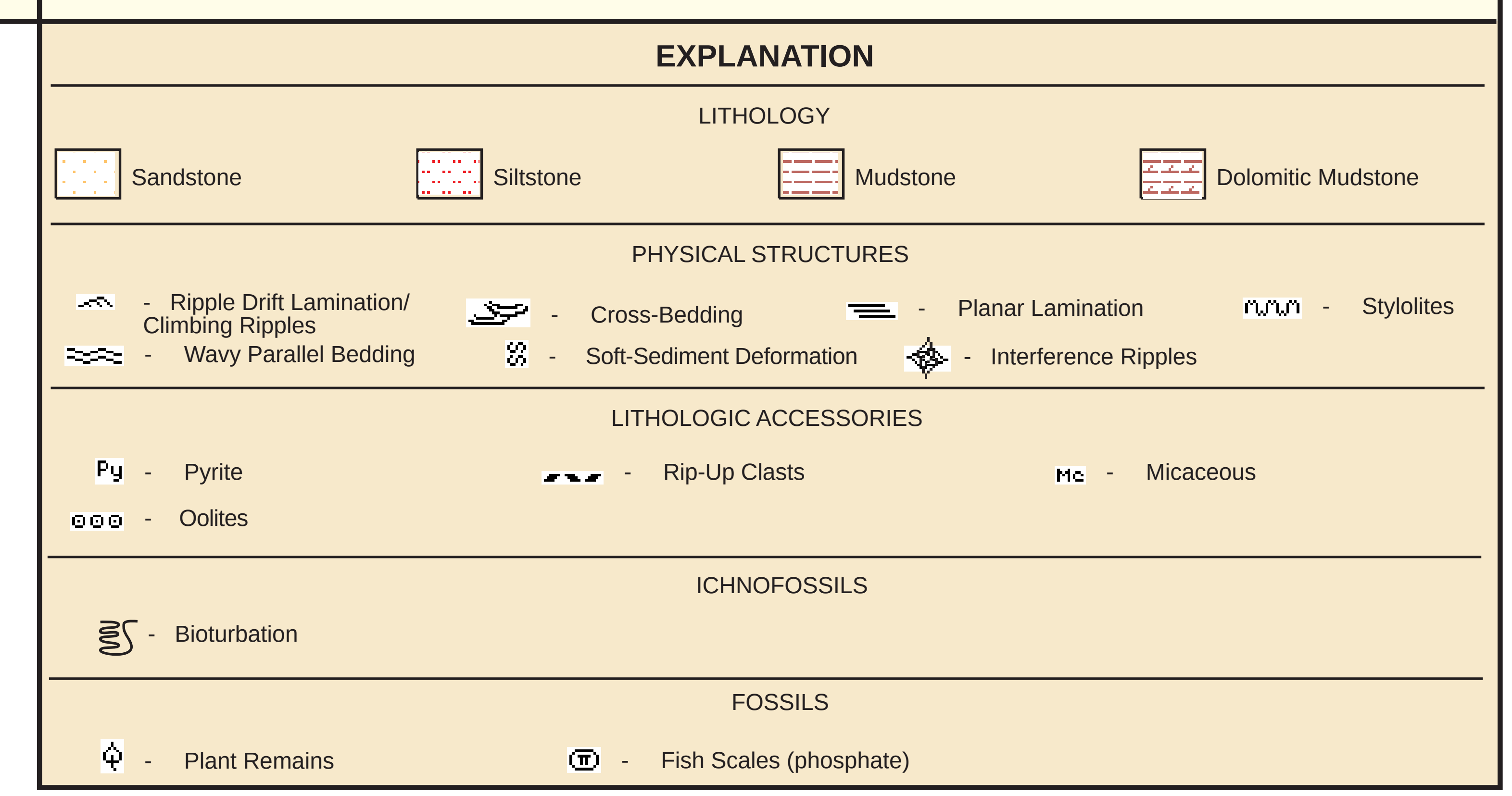

Allen 34-5

SW1/4SE1/4 section 5, T. 9 S., R. 17 E., SLBL

Monument Butte Field
Pleasant Valley water-flood unit
API: 43-013-30721
Depth: 4,995 - 5,045 feet
Interval: MGR 3 (Travis reservoir)
Core Description by: S. Robert Bereskin

Abbreviations

GR - Gamma Ray
CALI - Caliper
S - Resistivity Shallow
M - Resistivity Medium
D - Resistivity Deep
NPHI - Neutron Porosity
DPHI - Density Porosity
md - Millidarcies
SLBL - Salt Lake Base Line
API - American Petroleum Institute well number

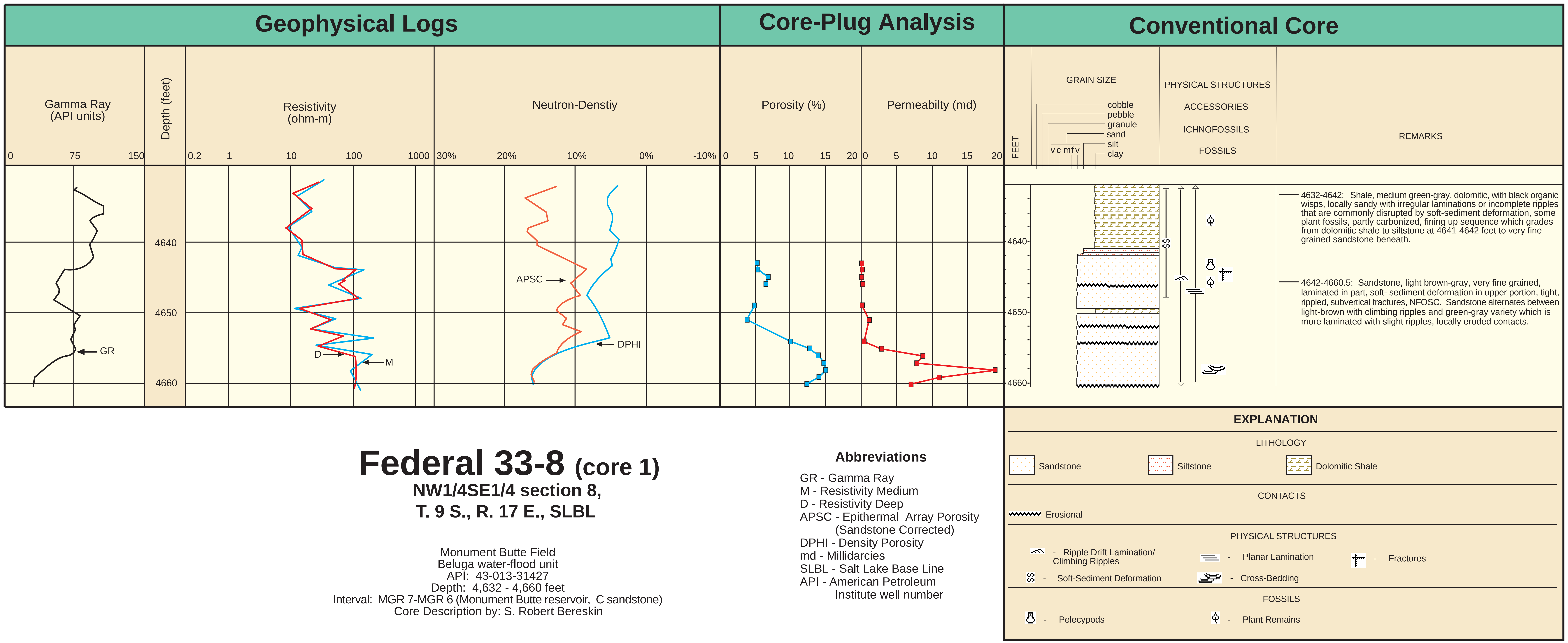

Federal 33-8 (core 1)

NW1/4SE1/4 section 8,
T. 9 S., R. 17 E., SLBL

Monument Butte Field
Beluga water-flood unit
API: 43-013-31427
Depth: 4,632 - 4,660 feet
Interval: MGR 7-MGR 6 (Monument Butte reservoir, C sandstone)
Core Description by: S. Robert Bereskin

Abbreviations

GR - Gamma Ray
M - Resistivity Medium
D - Resistivity Deep
APSC - Epithermal Array Porosity (Sandstone Corrected)
DPHI - Density Porosity
md - Millidarcies
SLBL - Salt Lake Base Line
API - American Petroleum Institute well number

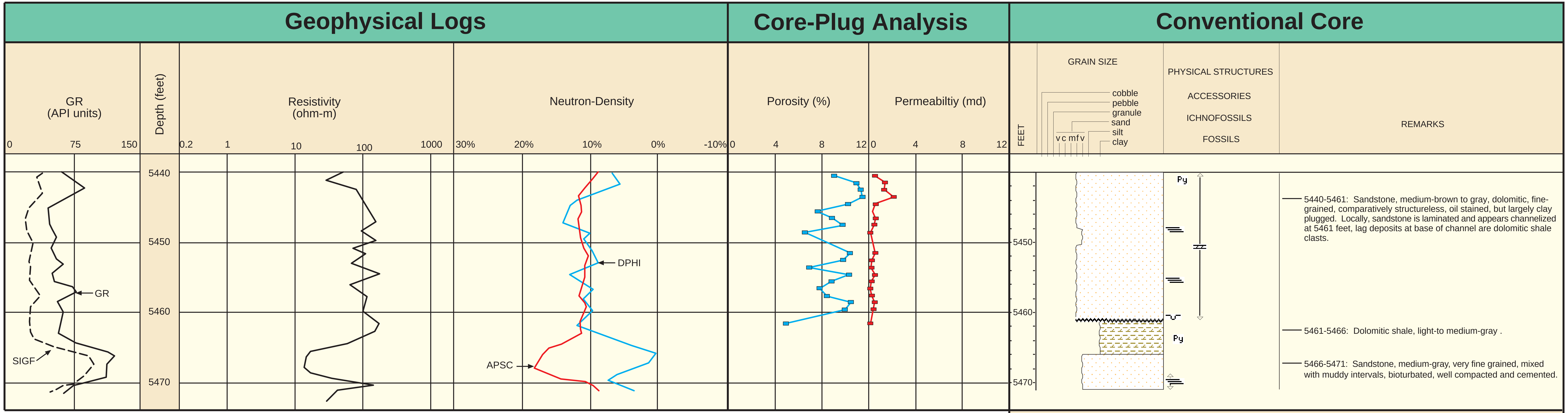

EXPLANATION

LITHOLOGY

Sandstone — Dolomitic Shale

CONTACTS

Scour

PHYSICAL STRUCTURES

Planar Lamination

LITHOLOGIC ACCESSORIES

Py - Pyrite — Dolomitic

ICHNOFOSSILS

Vertical Burrows

Federal 33-8 (core 2)

NW1/4SE1/4 section 8, T. 9 S., R. 17 E., SLBL

Monument Butte Field
Beluga water-flood unit
API: 43-013-31427
Depth: 5,440 - 5,470 feet
Interval: Carbonate marker unit (Castle Peak reservoir)
Core Description by: S. Robert Bereskin

Abbreviations

GR - Gamma Ray
SIGF - Sigma Formation
APSC - Epithermal Array Porosity Sandstone Corrected
DPHI - Density Porosity
md - Millidarcies
TS - Thin Section Photo
SLBL - Salt Lake Base Line
API - American Petroleum Institute well number

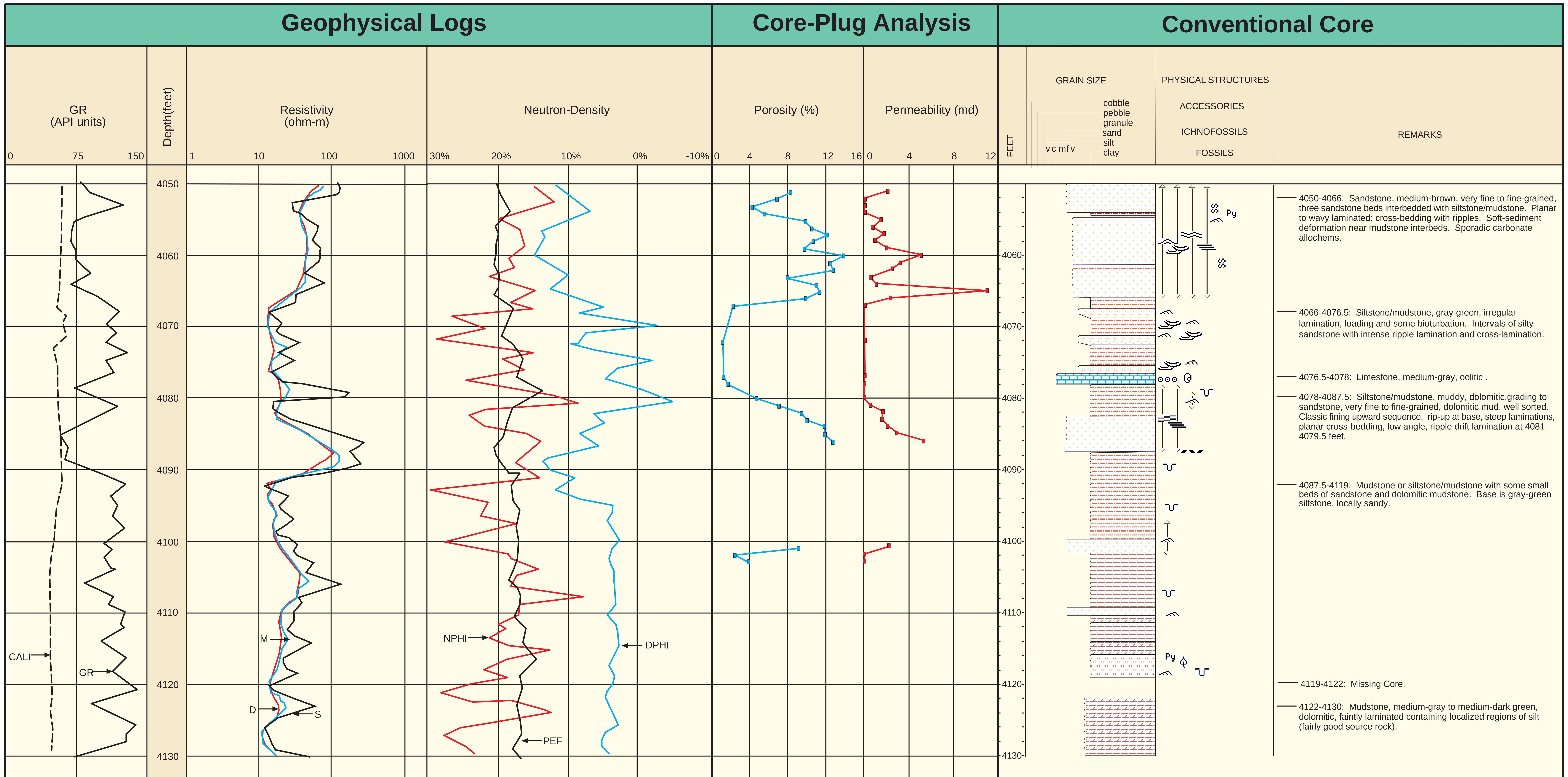

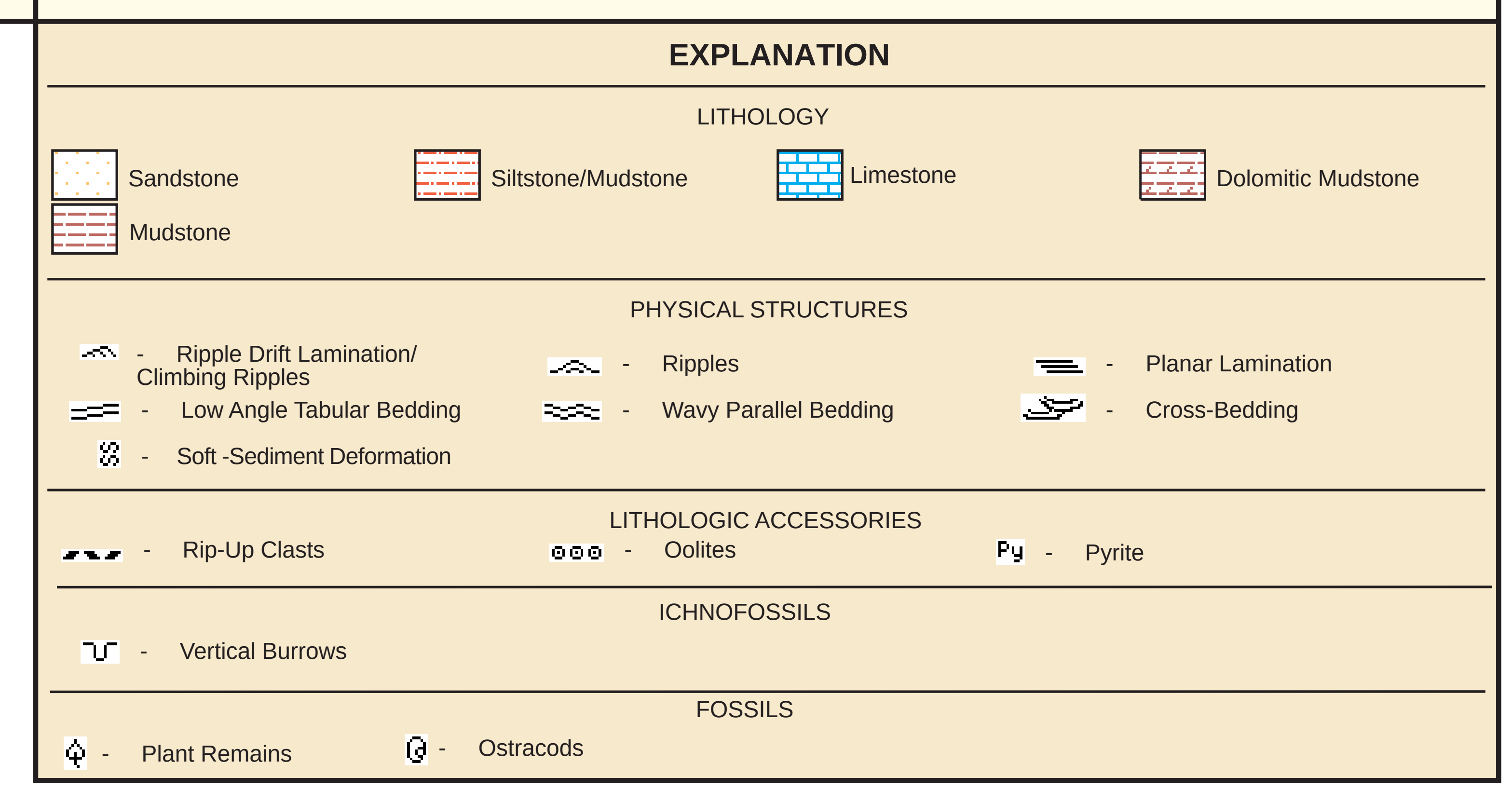

Paiute 34-8

SW1/4SE1/4 section 8, T.9 S., R. 17 E., SLBL

Monument Butte Field
Beluga water-flood unit
API: 43-013-30778
Depth: 4,050 - 4,129 feet
Interval: MGR 13 (Beluga reservoir)
Core Description by: S. Robert Bereskin

Abbreviations

GR - Gamma Ray
CALI - Caliper
S - Resistivity Shallow
M - Resistivity Medium
D - Resistivity Deep
NPHI - Neutron Porosity
DPHI - Density Porosity
PEF - Photoelectric Factor
md - Millidarcies
SLBL - Salt Lake Base Line
API - American Petroleum Institute well number

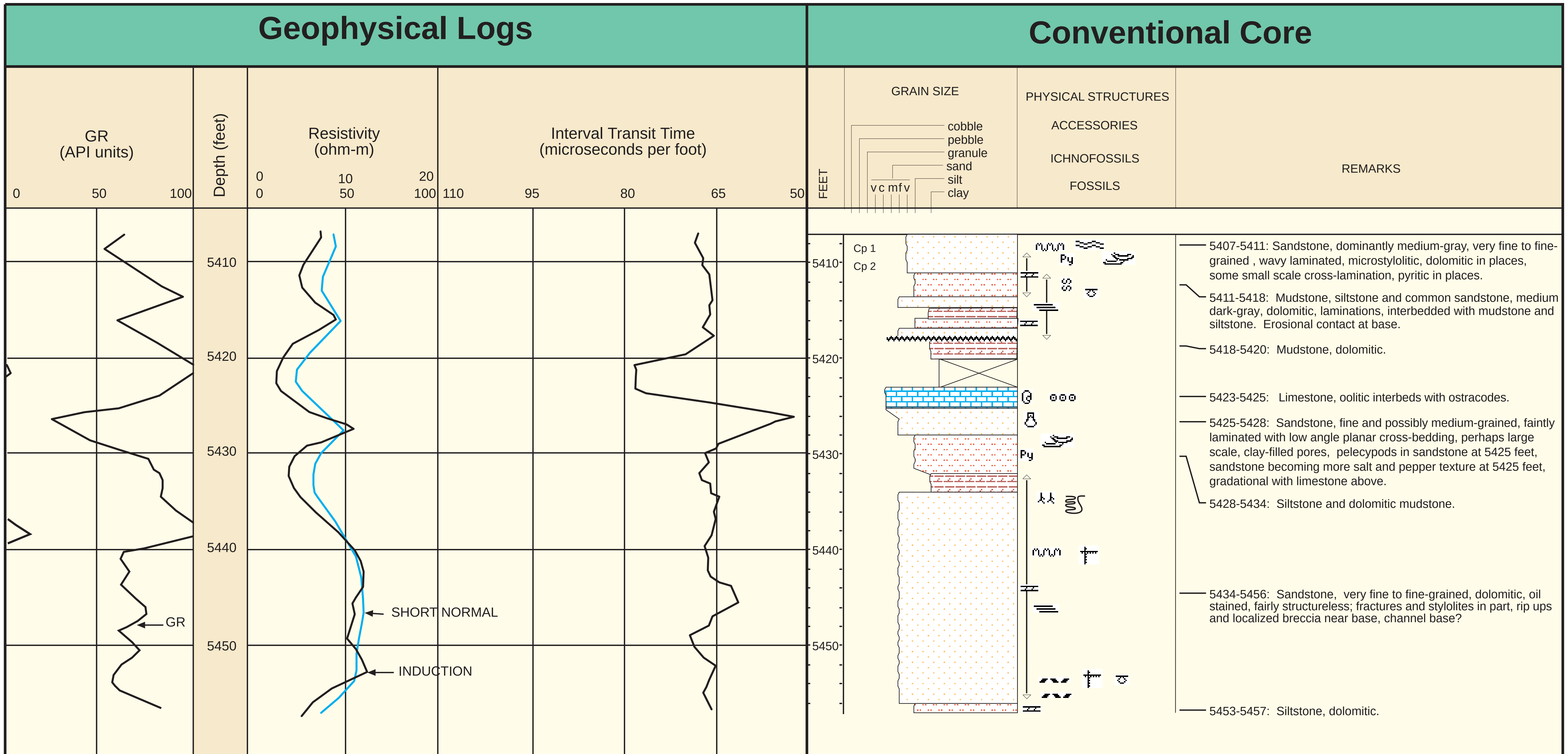

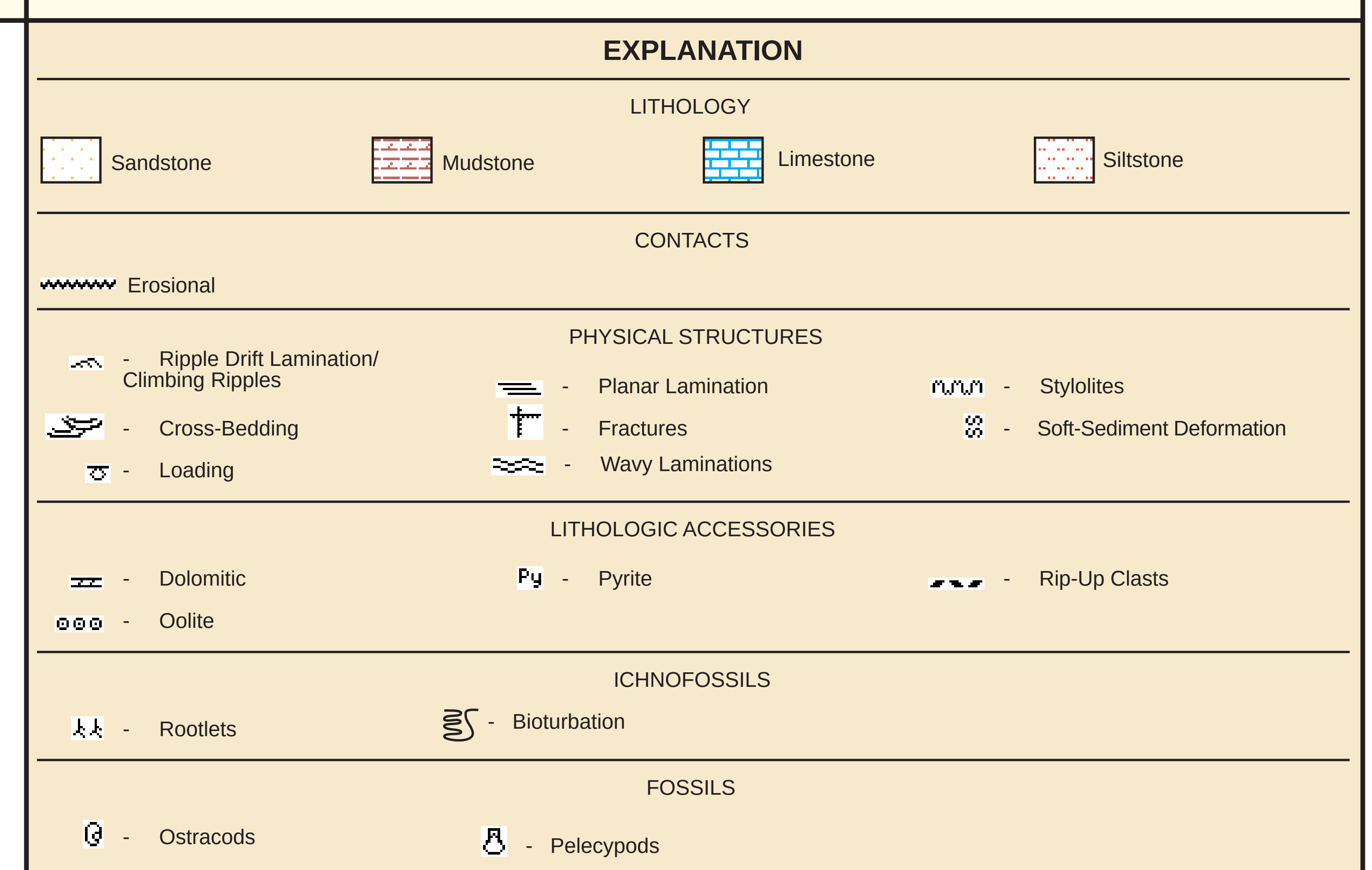

Pariette 5

SE1/4SE1/4 section 9, T. 9 S., R. 18 E., SLBL

Eight Mile Flat North Field
API: 43-047-10298
Depth: 5,407-5,457 feet
Interval: Carbonate marker unit (Castle Peak reservoir)
Core Description by: S. Robert Bereskin

Abbreviations

GR - Gamma Ray
Cp - Core Photo
SLBL - Salt Lake Base Line
API - American Petroleum Institute well number

Back to Core Description

Back to Core Description

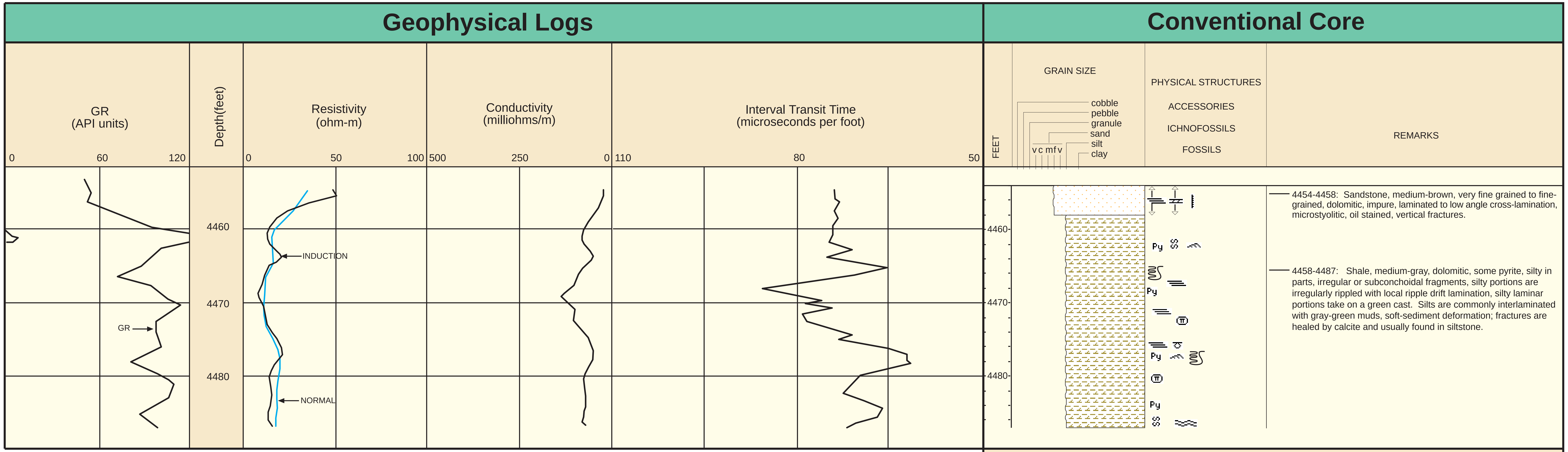

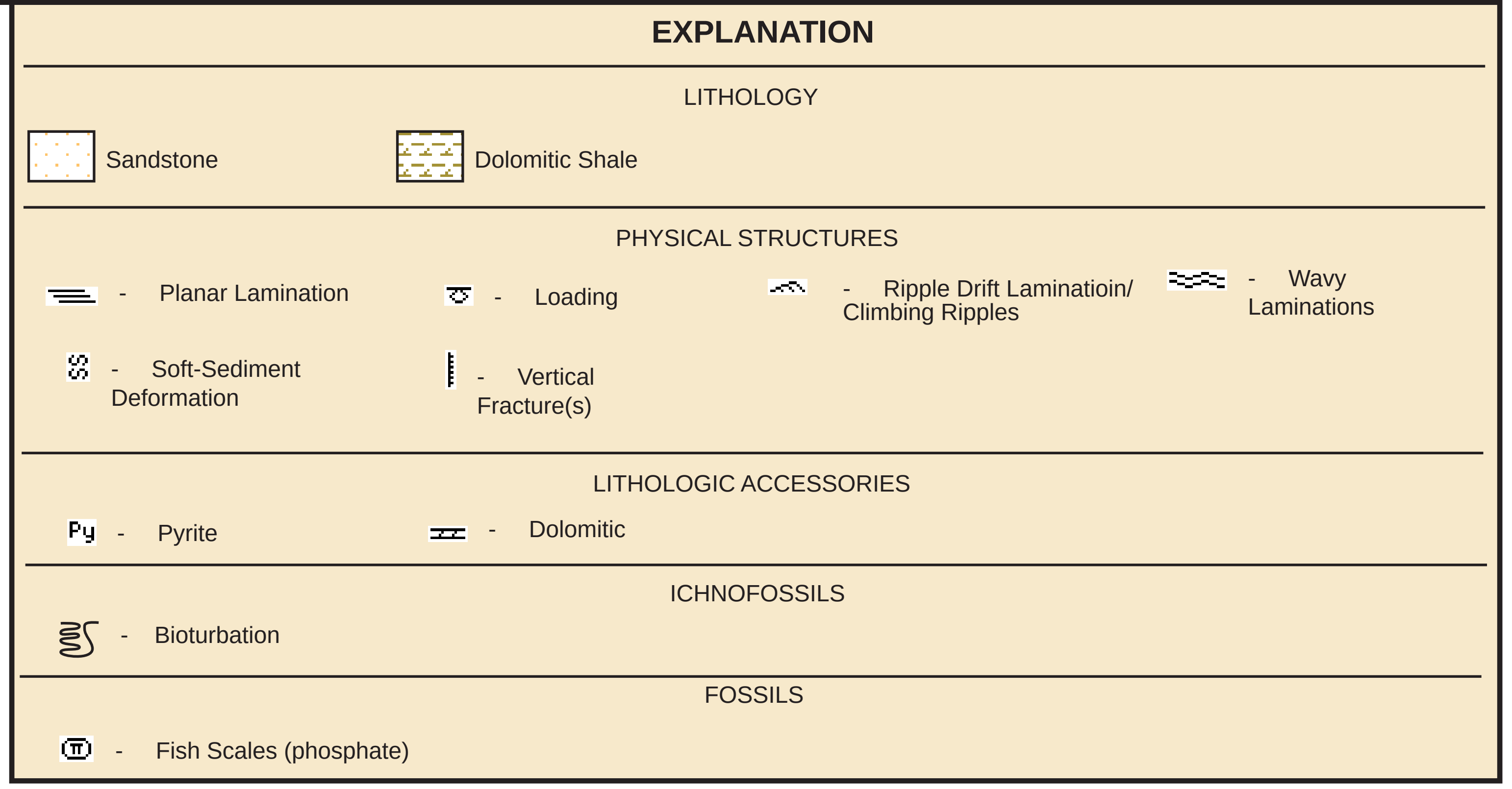

Pariette 6 (core 1)

SW1/4SW1/4 section 5, T. 9 S., R. 19 E., SLBL

Pariette Bench Field
API: 43-047-10873
Depth: 4,454 - 4,487 feet
Interval: MGR 8 (Beluga reservoir)
Core Description by: S. Robert Bereskin

Abbreviations

GR - Gamma Ray
SLBL - Salt Lake Base Line
API - American Petroleum Institute well number

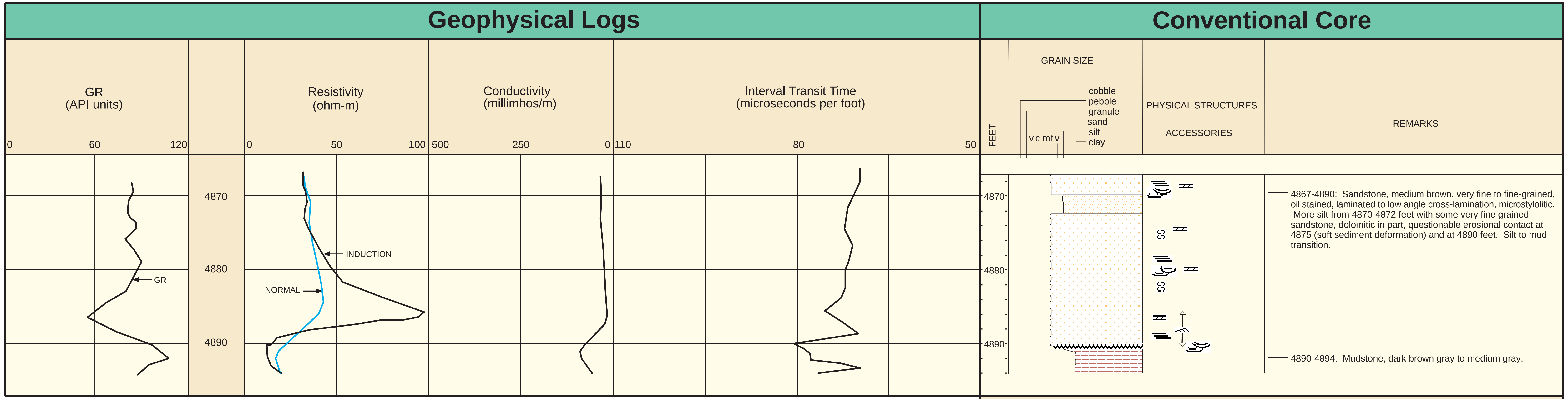

Pariette 6 (core 2)

SW1/4SW1/4 section 5, T. 9 S., R. 19 E., SLBL

Pariette Bench Field
API: 43-047-10873
Depth: 4,867-4,894 feet
Interval: MGR 3 (Travis reservoir)
Core Description by: S. Robert Bereskin

Abbreviations

GR - Gamma Ray
SLBL - Salt Lake Base Line
API - American Petroleum Institute well number

EXPLANATION

LITHOLOGY

Sandstone   Silty Sandstone   Mudstone

CONTACTS

Scoured

PHYSICAL STRUCTURES

- Planar Lamination
- Soft-Sediment Deformation
- Cross-Bedding
- Ripple Drift Lamination/Climbing Ripples

LITHOLOGIC ACCESSORIES

- Dolomitic

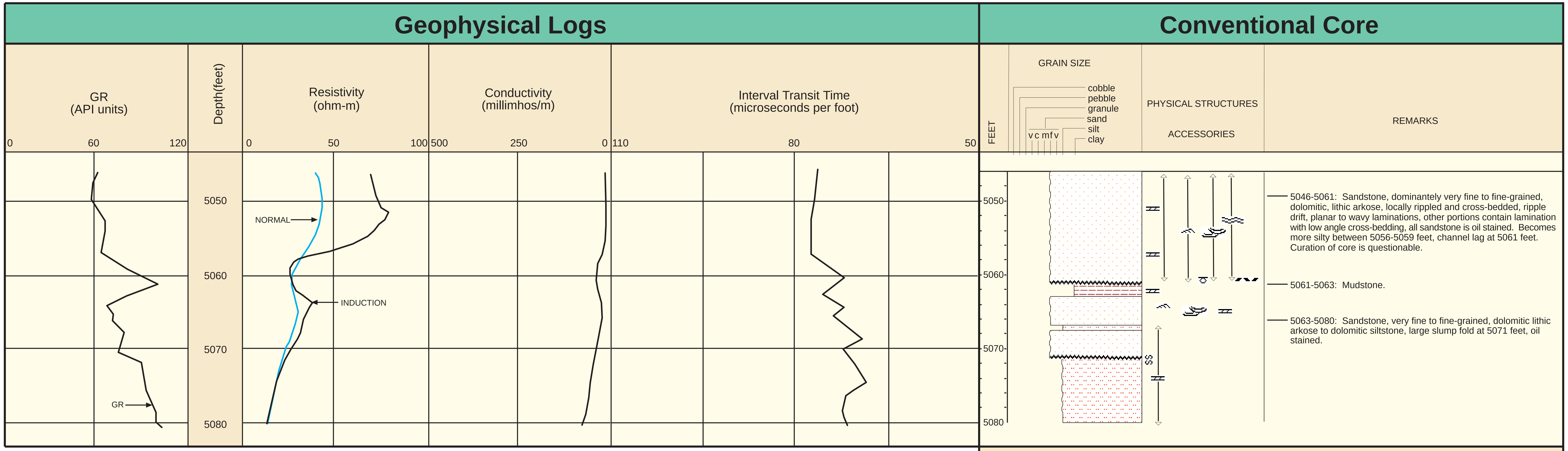

EXPLANATION

LITHOLOGY

Sandstone
Siltstone
Mudstone

CONTACTS

Scoured

PHYSICAL STRUCTURES

- Cross-Bedding
- Ripple Drift Lamination/ Climbing Ripples
- Wavy Laminations
- Loading
- Soft-Sediment Deformation

LITHOLOGIC ACCESSORIES

- Rip-Up Clasts
- Dolomitic

Pariette 6 (core 3)

SW1/4SW1/4 section 5, T. 9 S., R. 19 E., SLBL

Pariette Bench Field
API: 43-047-10873
Depth: 5,046 - 5,080 feet
Interval: MGR 3 (Travis reservoir)
Core Description by: S. Robert Bereskin

Abbreviations

GR - Gamma Ray
SLBL - Salt Lake Base Line
API - American Petroleum Institute well number

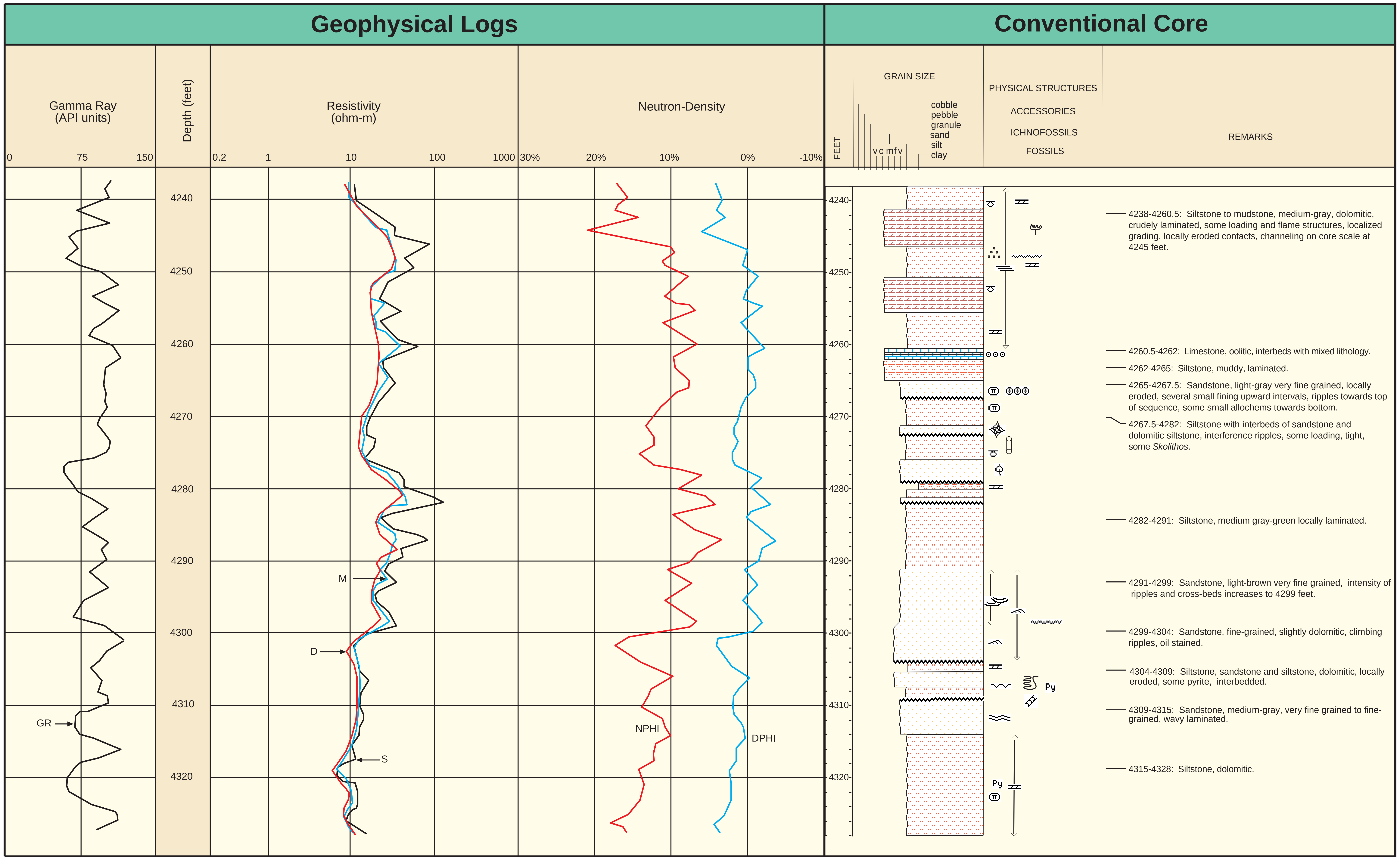

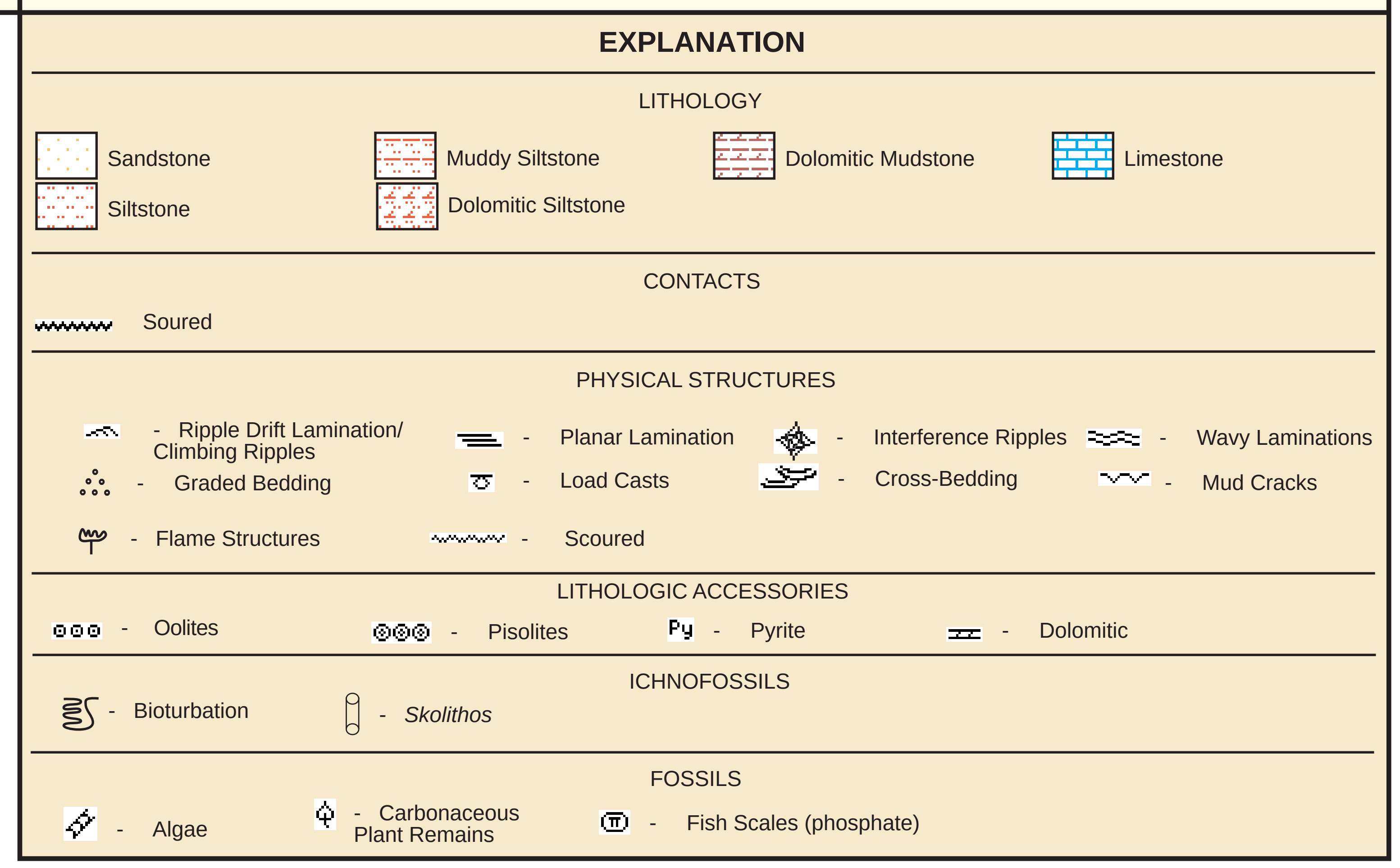

State 13-16J (core 1)

NW1/4SW1/4 section 16,
T. 9 S., R. 19 E., SLBL

Pariette Bench Field
API: 43-047-31128
Depth: 4,238 - 4,328 feet
Interval: MGR 7 (Monument Butte, D Sandstone)
Core Description by: S. Robert Bereskin

Abbreviations

GR - Gamma Ray
S - Resistivity Shallow
M - Resistivity Medium
D - Resistivity Deep
NPHI - Neutron Porosity
DPHI - Density Porosity
SLBL - Salt Lake Base Line
API - American Petroleum Institute well number

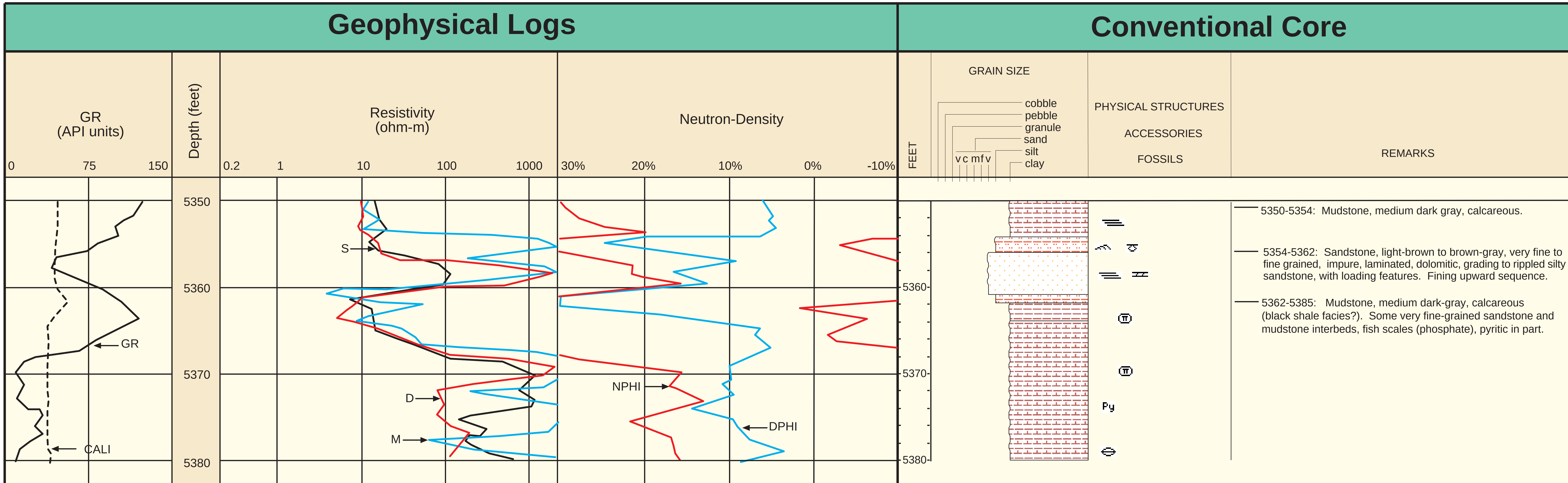

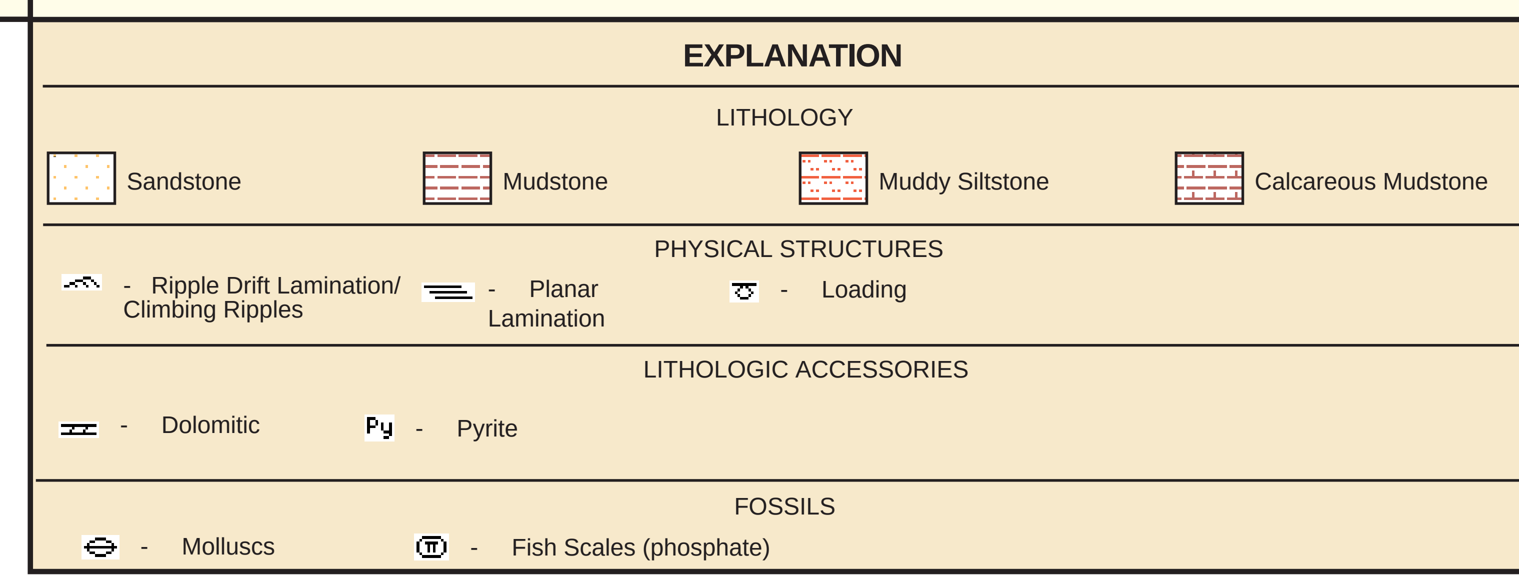

State 13-16J (core 2)

NW1/4SW1/4 section 16, T. 9 S., R. 19 E., SLBL

Pariette Bench Field
API: 43-047-31128
Depth: 5,350 - 5,385 feet
Interval: LGR 3 (Uteland Butte reservoir)
Core Description by: S. Robert Bereskin

Abbreviations

GR - Gamma Ray
CALI - Caliper
S - Resistivity Shallow
M - Resistivity Medium
D - Resistivity Deep
NPHI - Neutron Porosity
DPHI - Density Porosity
SLBL - Salt Lake Base Line
API - American Petroleum Institute well number

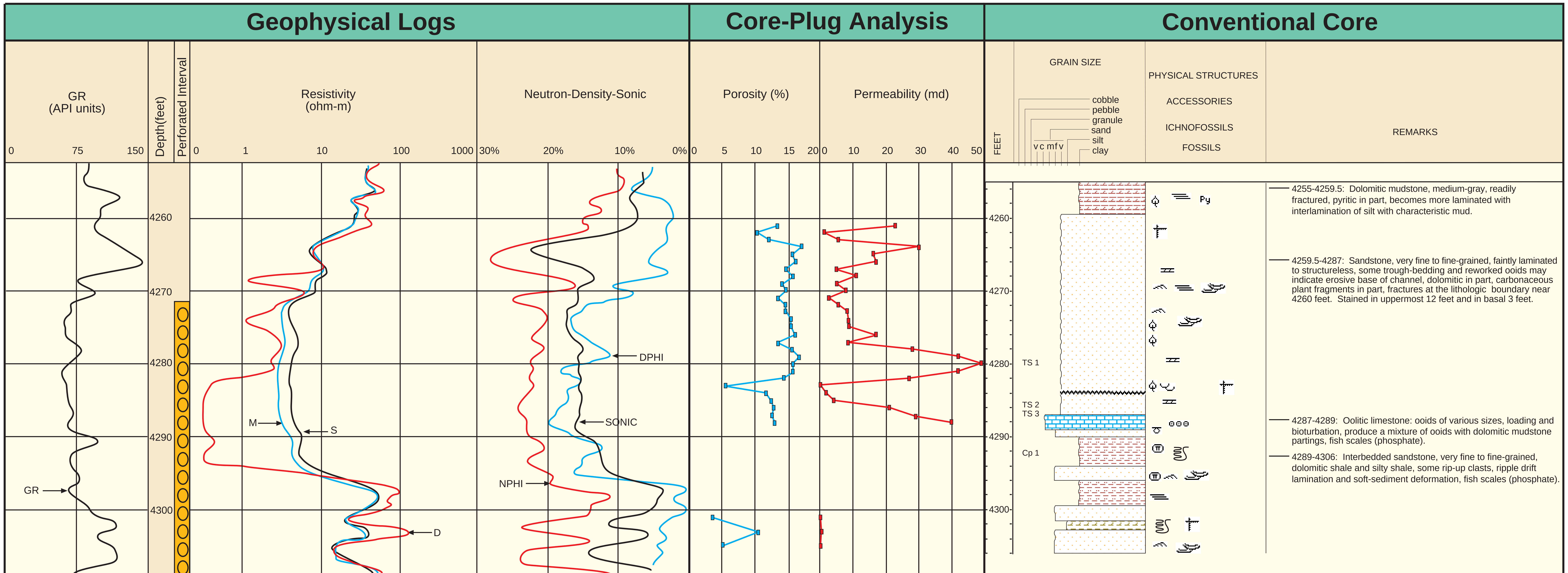

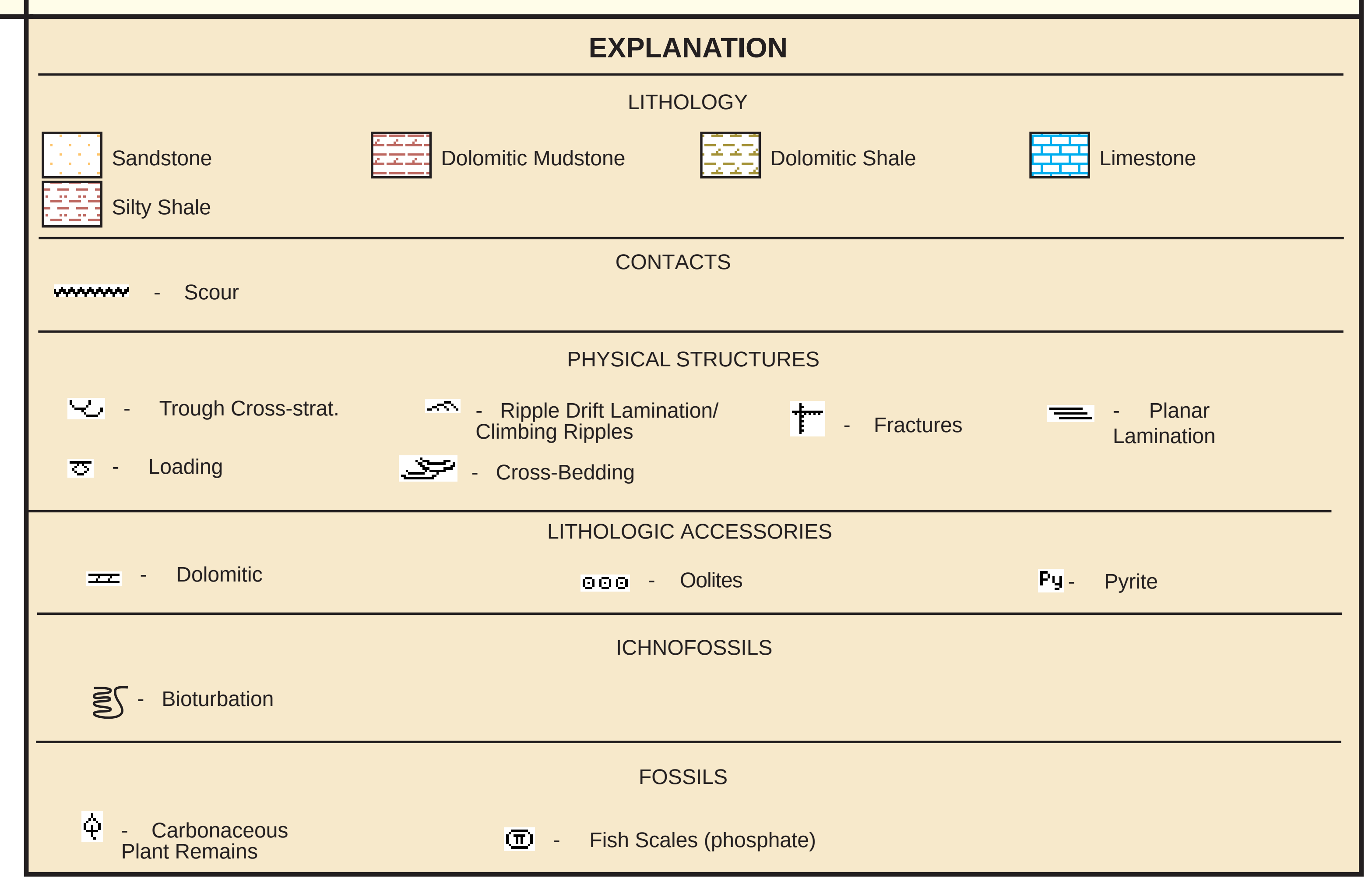

Federal 15-17

SW1/4SE1/4 section 17, T. 9 S., R. 19 E., SLBL

Pariette Bench Field
API: 43-047-31002
Depth: 4,255 - 4,306 feet
Interval: MGR 6 (Monument Butte reservoir, C sandstone)
Core Description by: S. Robert Bereskin

Abbreviations

GR - Gamma Ray
S - Resistivity Shallow
M - Resistivity Medium
D - Resistivity Deep
NPHI - Neutron Porosity
DPHI - Density Porosity
md - Millidarcies
TS - Thin Section Photo
Cp - Core Photo
SLBL - Salt Lake Base Line
API - American Petroleum Institute well number

Back to Core Description

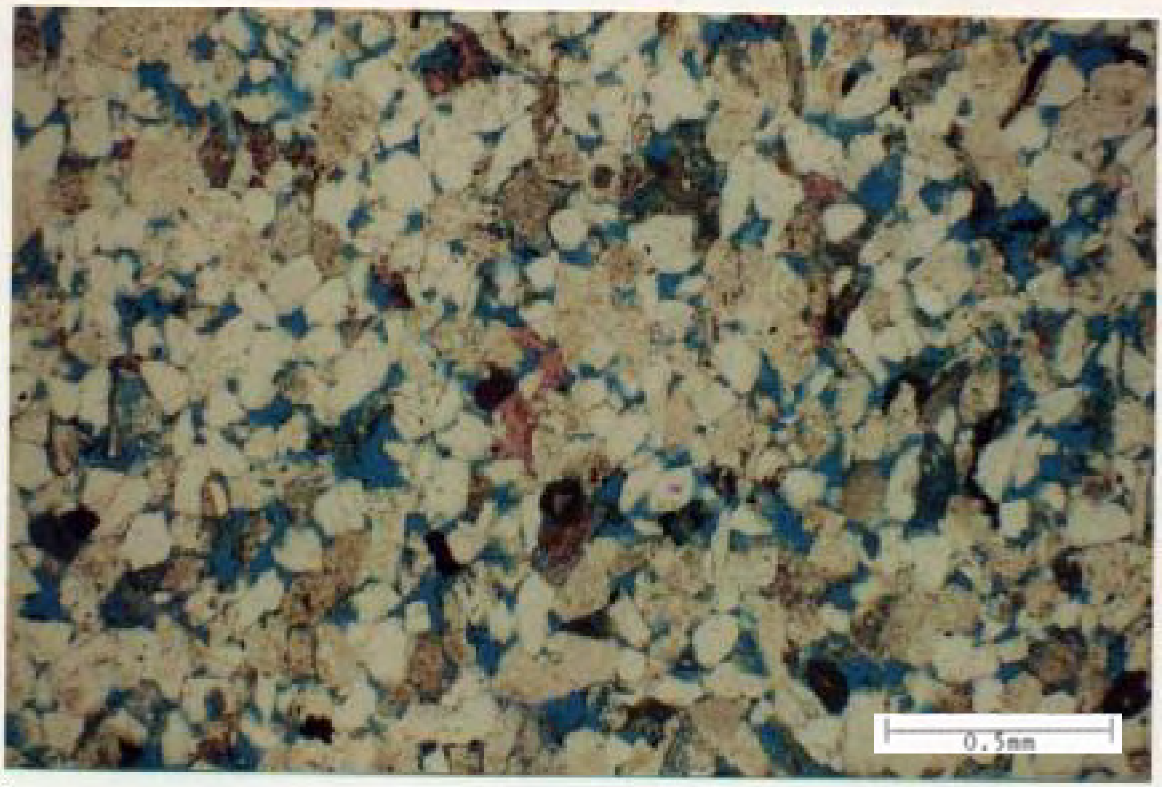

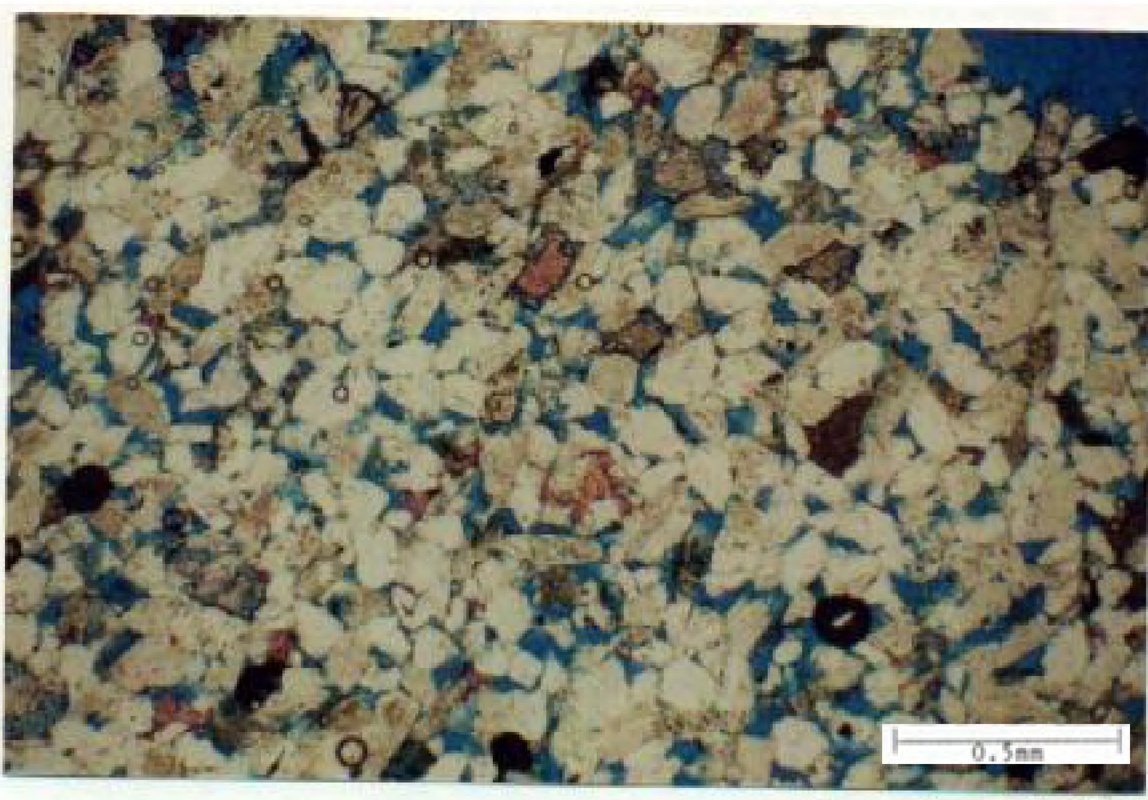

Federal 15-17
43-047-31002
4279.6 ft
40x

Back to Core Description

Go to TS 1 40x b

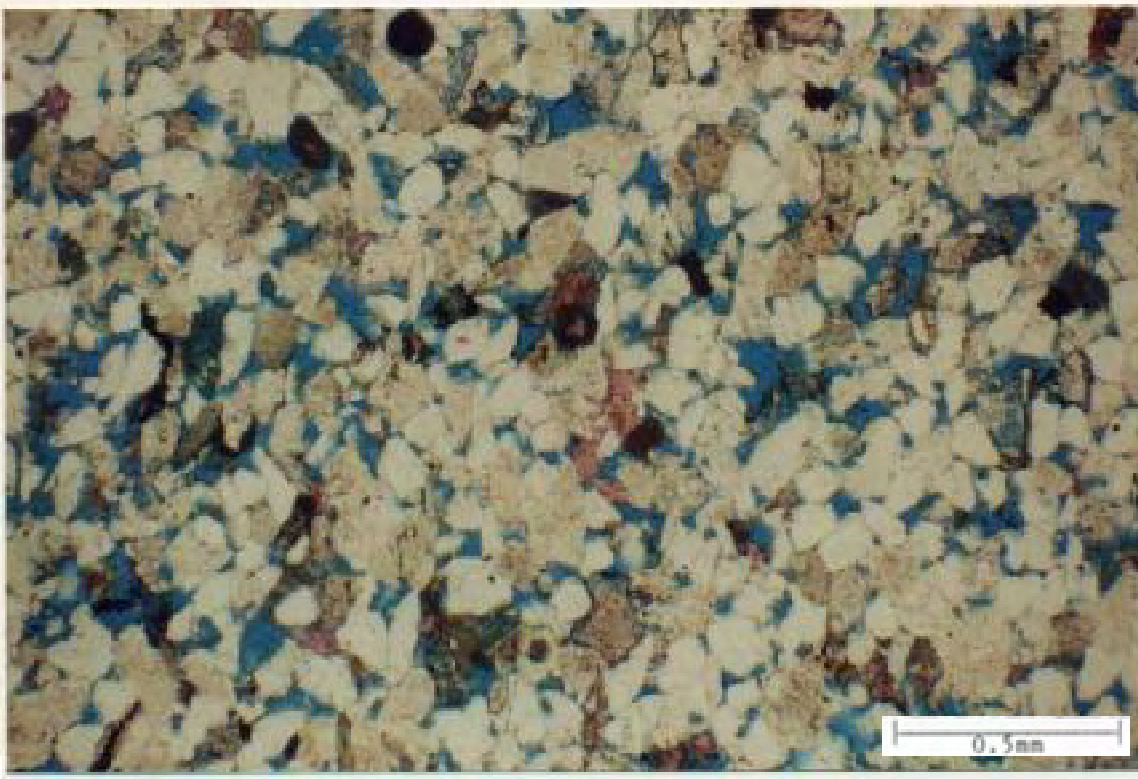

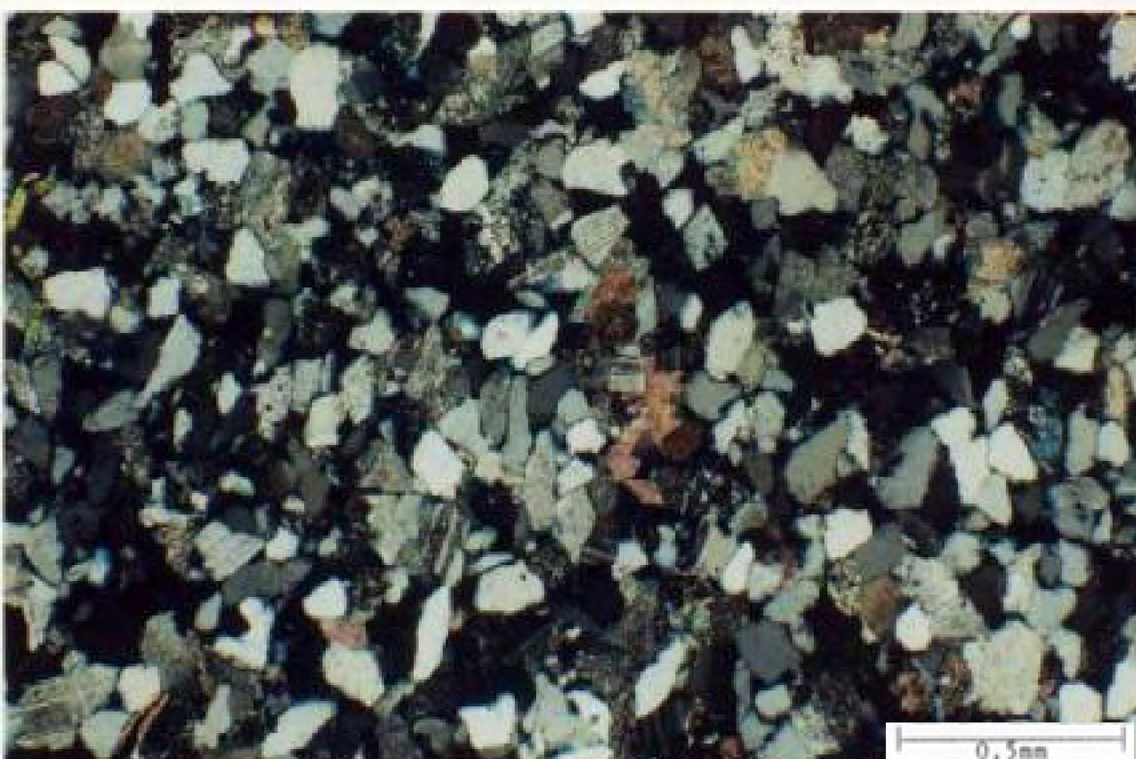

Federal 15-17
43-047-31002
4279.6 ft
40x

Back

Go to TS 1 40x c

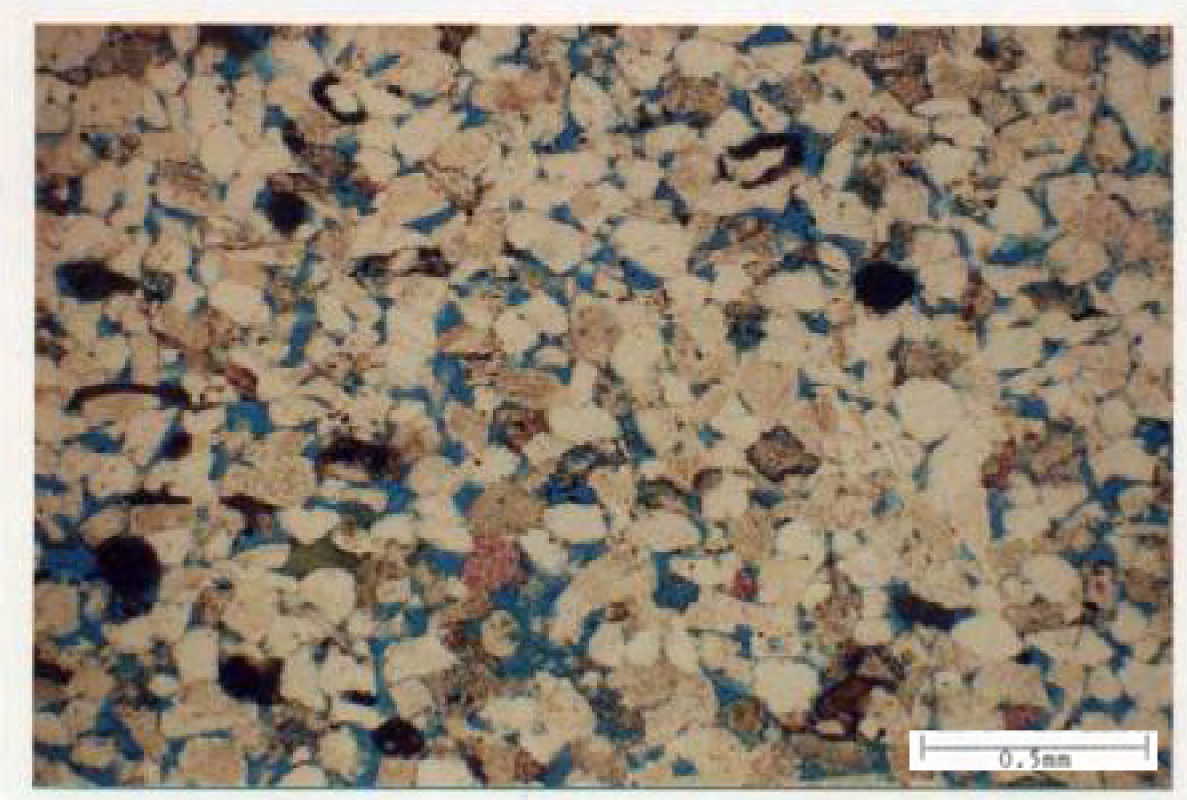

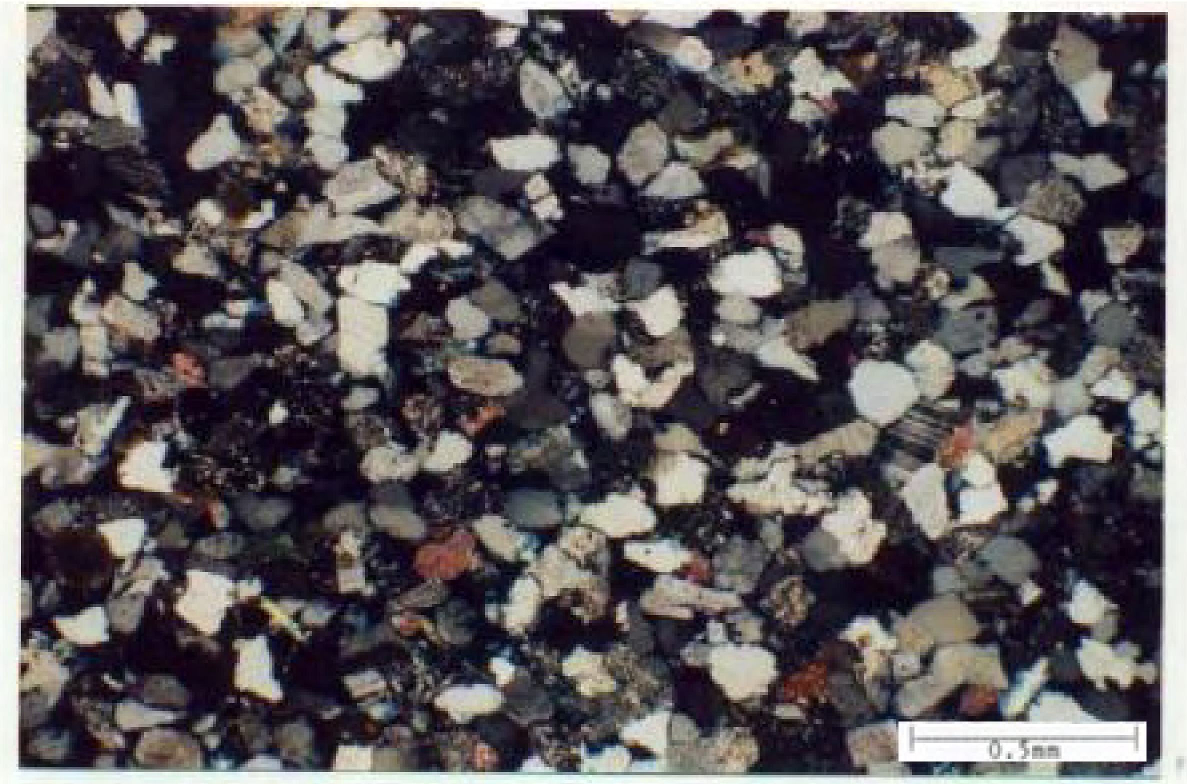

Federal 15-17
43-047-31002
4279.6 ft
40x

Back

Go to TS 1 100x a

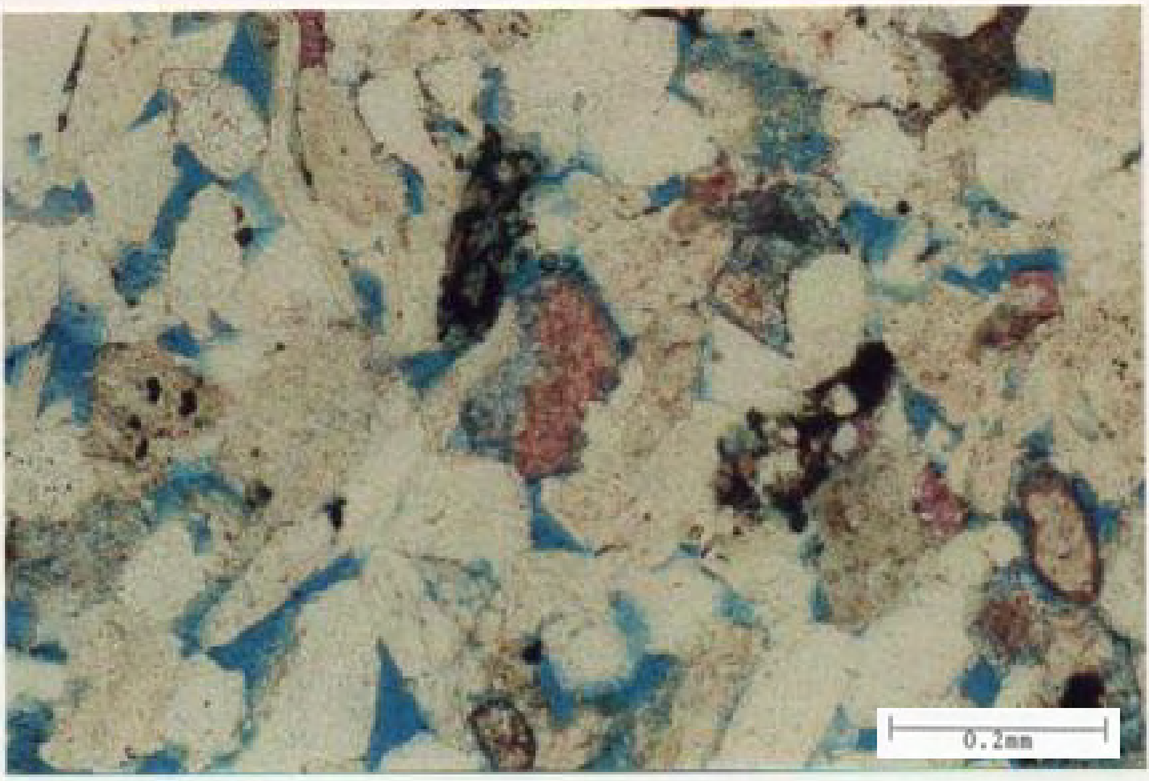

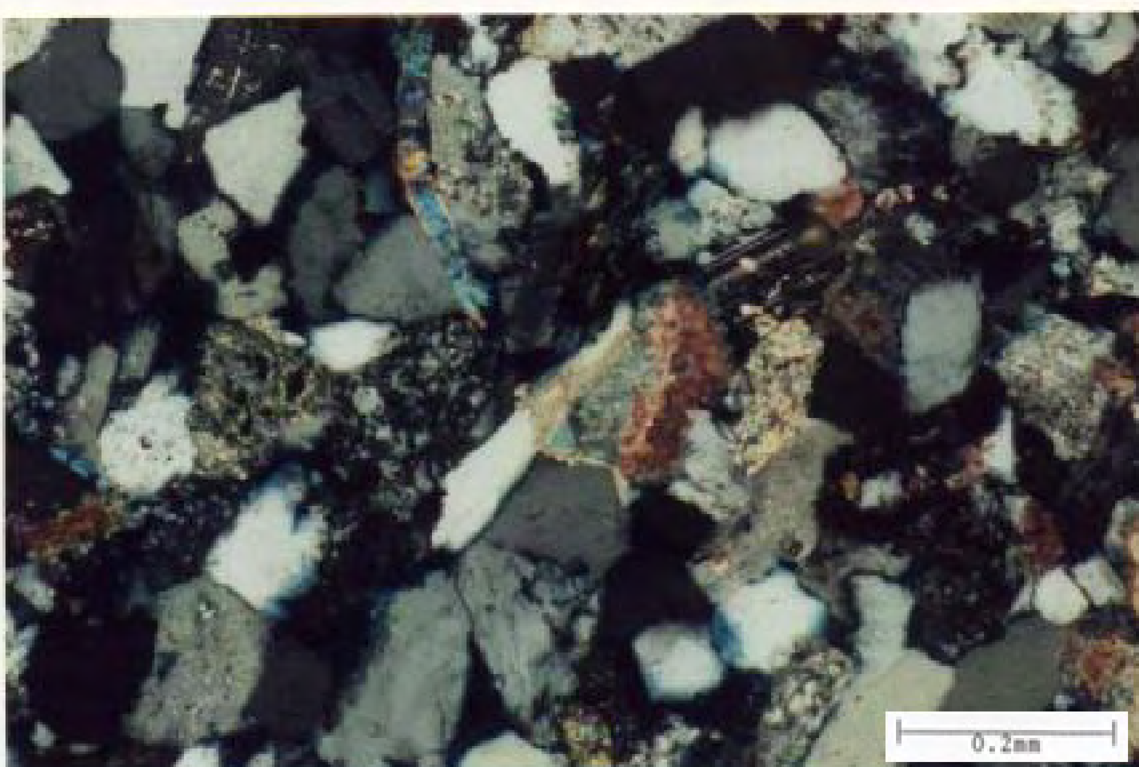

Federal 15-17
43-047-31002
4279.6 ft
100x

Back to Core Description

Go to TS 1 40x b

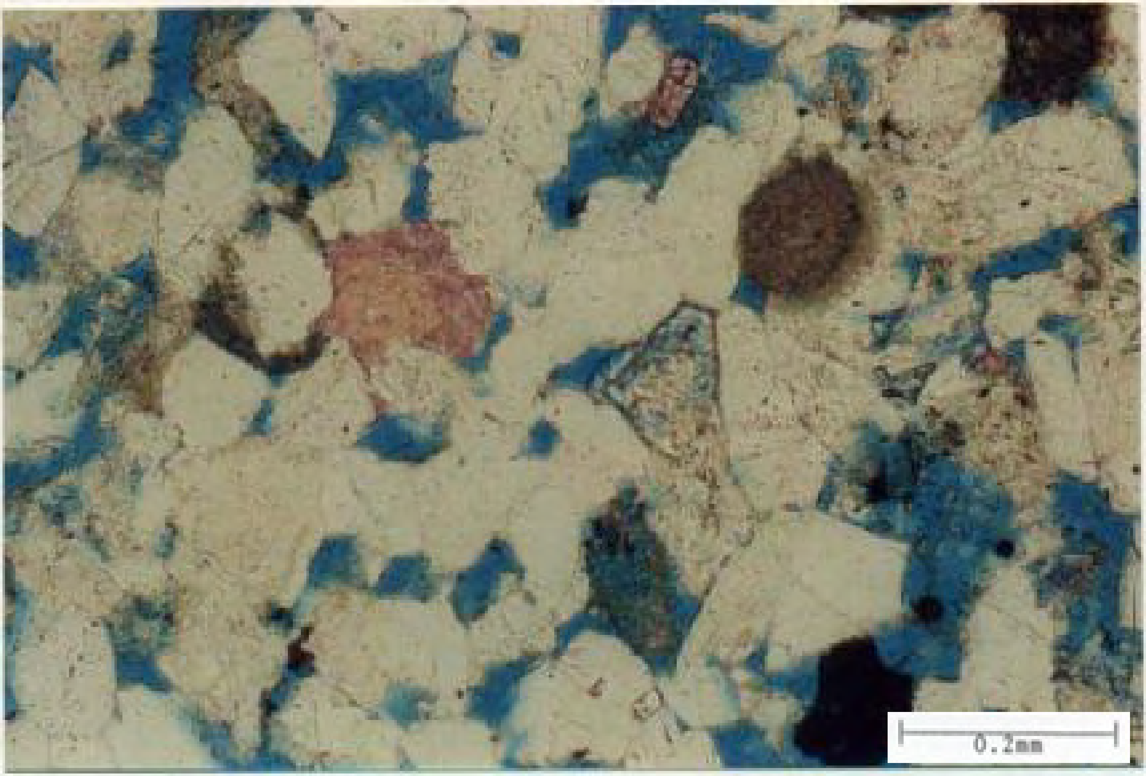

Federal 15-17
43-047-31002
4279.6 ft
100x

Back

Go to TS 1 100x c

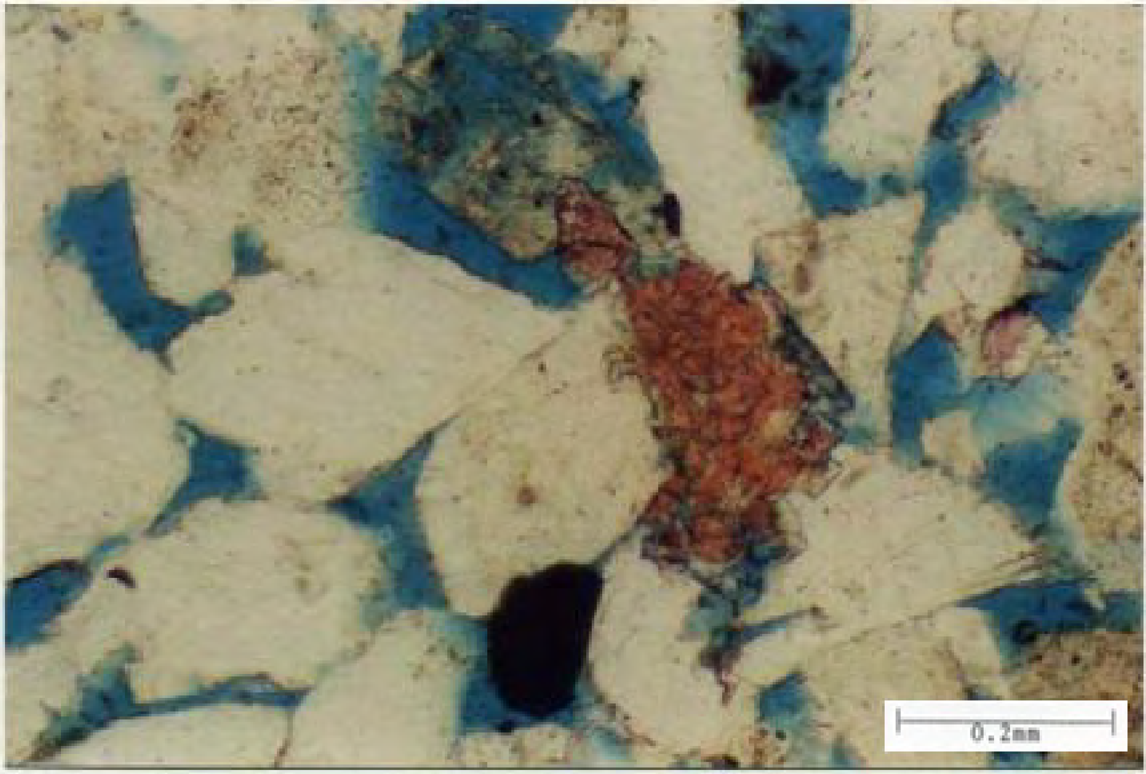

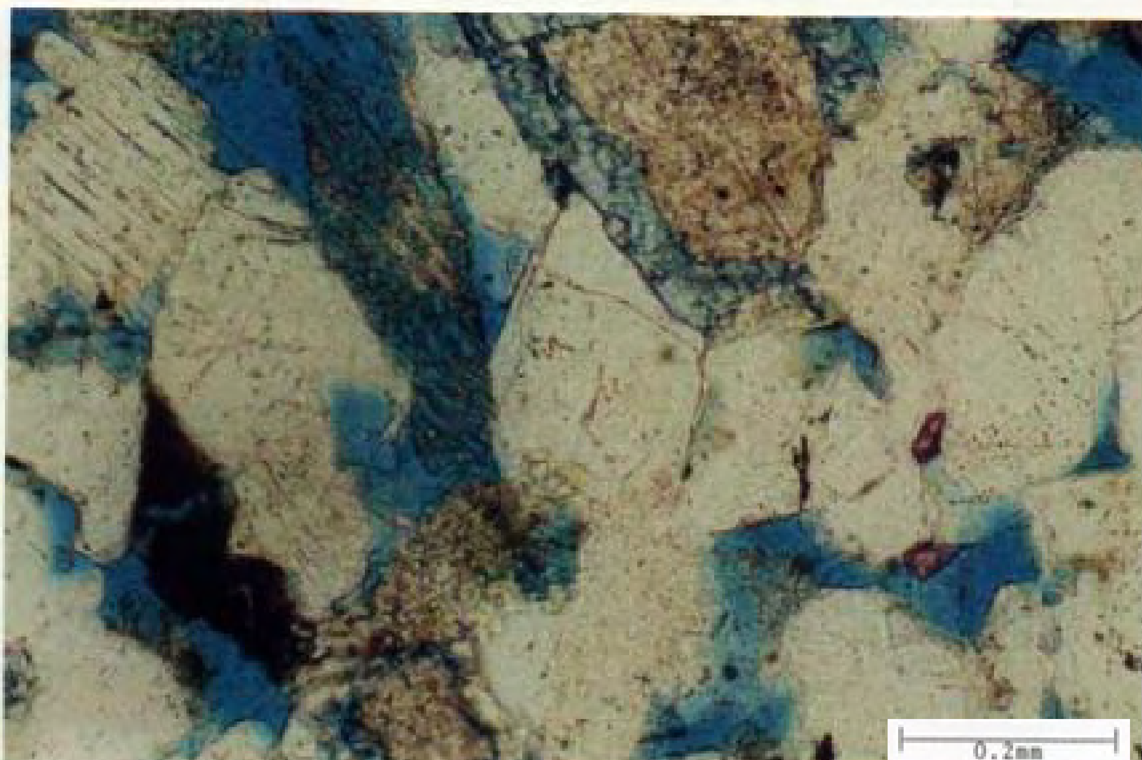

Federal 15-17
43-047-31002
4279.6 ft
100x

Back

Go to TS 1 100x d

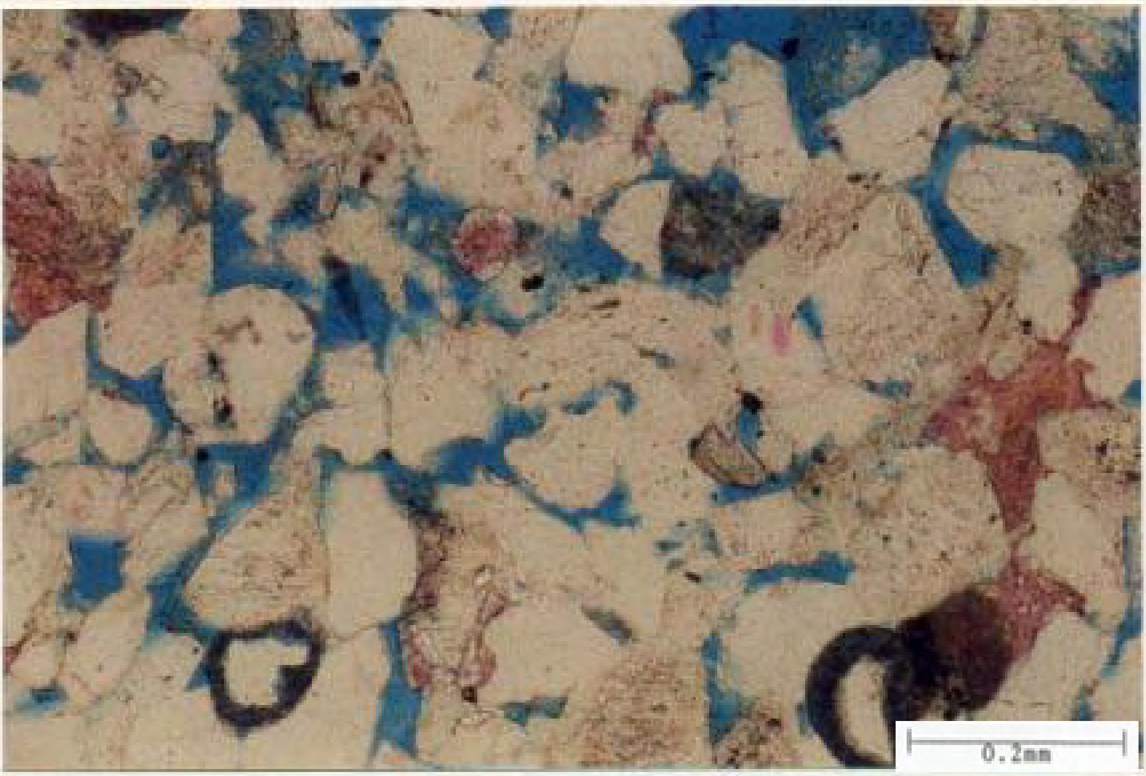

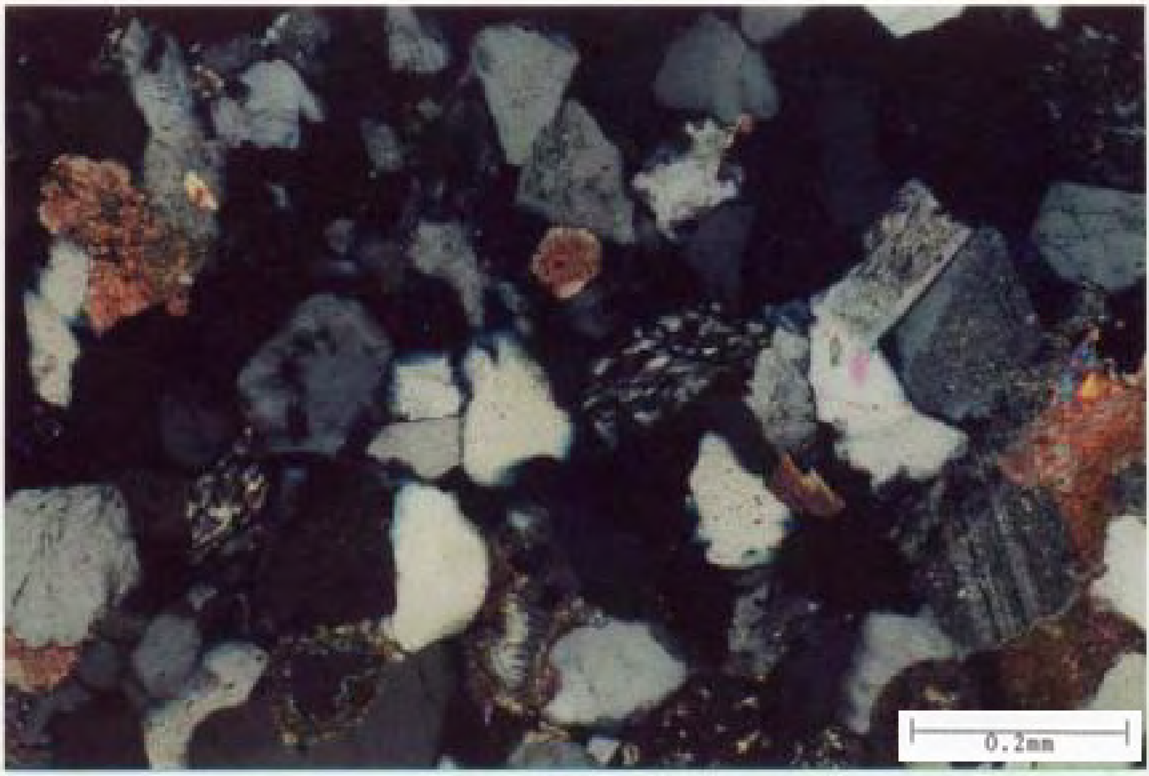

Federal 15-17
43-047-31002
4279.6 ft
100x

Back

Go to TS 1 100x e

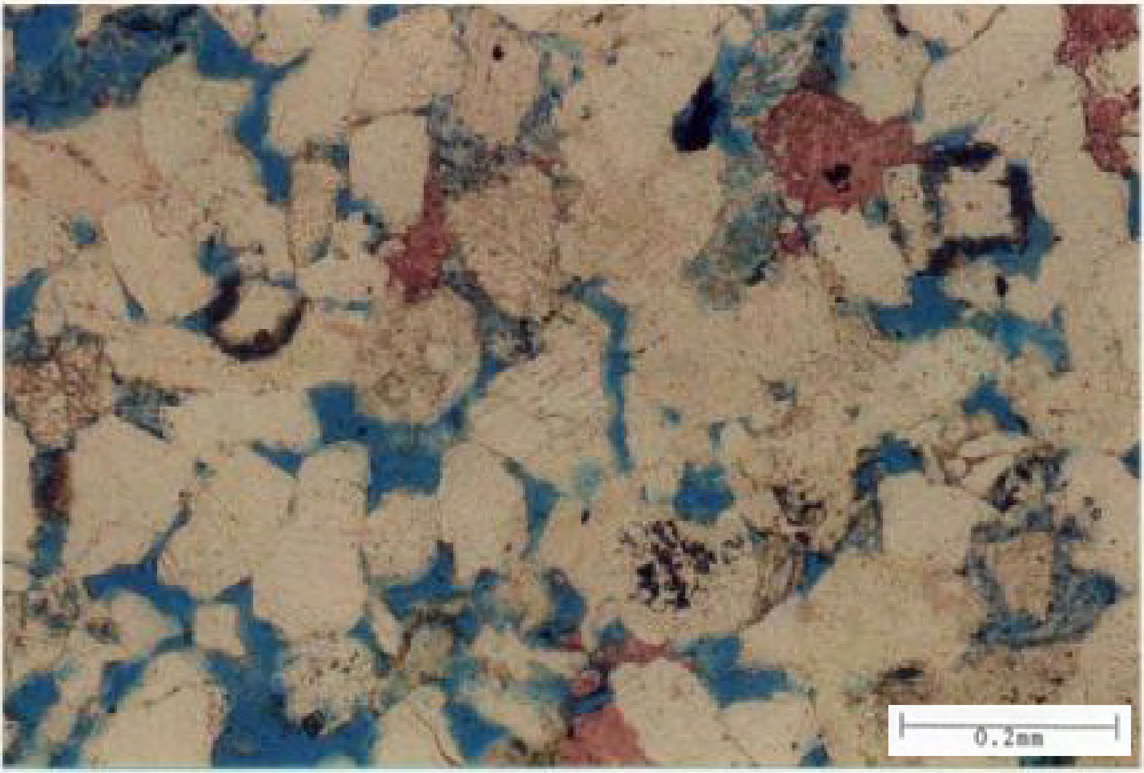

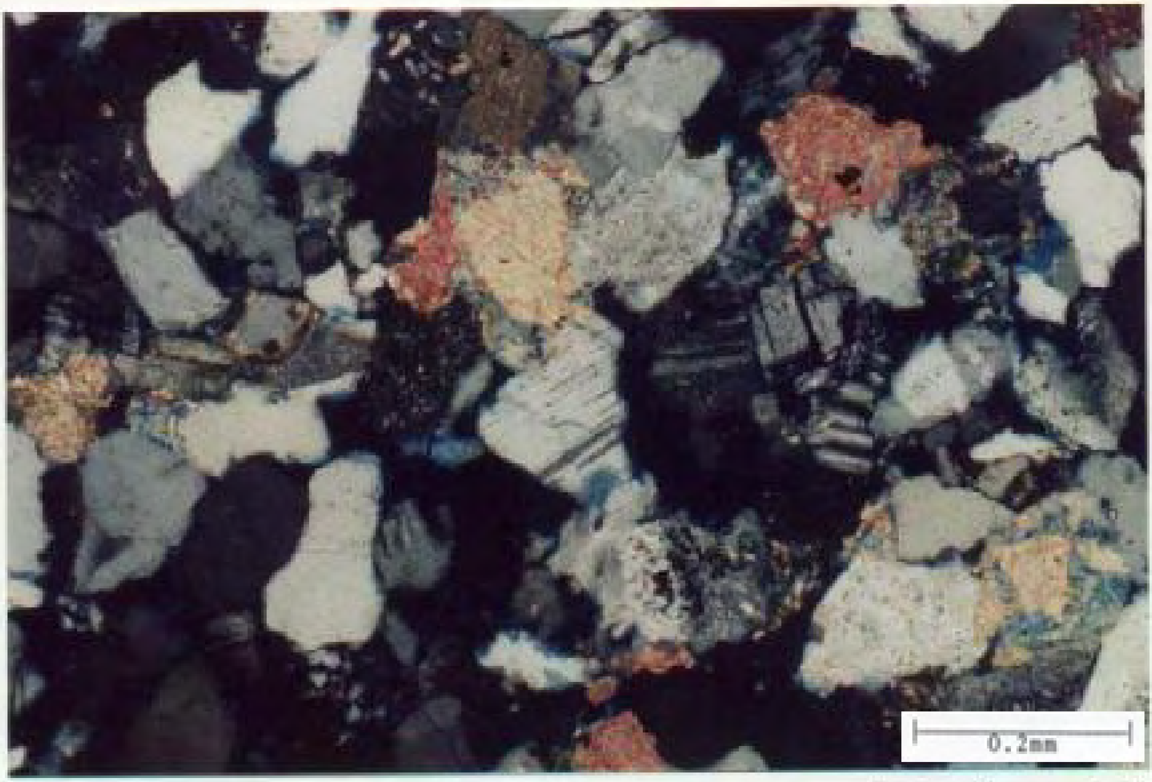

Federal 15-17
43-047-31002
4279.6 ft
100x

Back

Go to TS 1 100x f

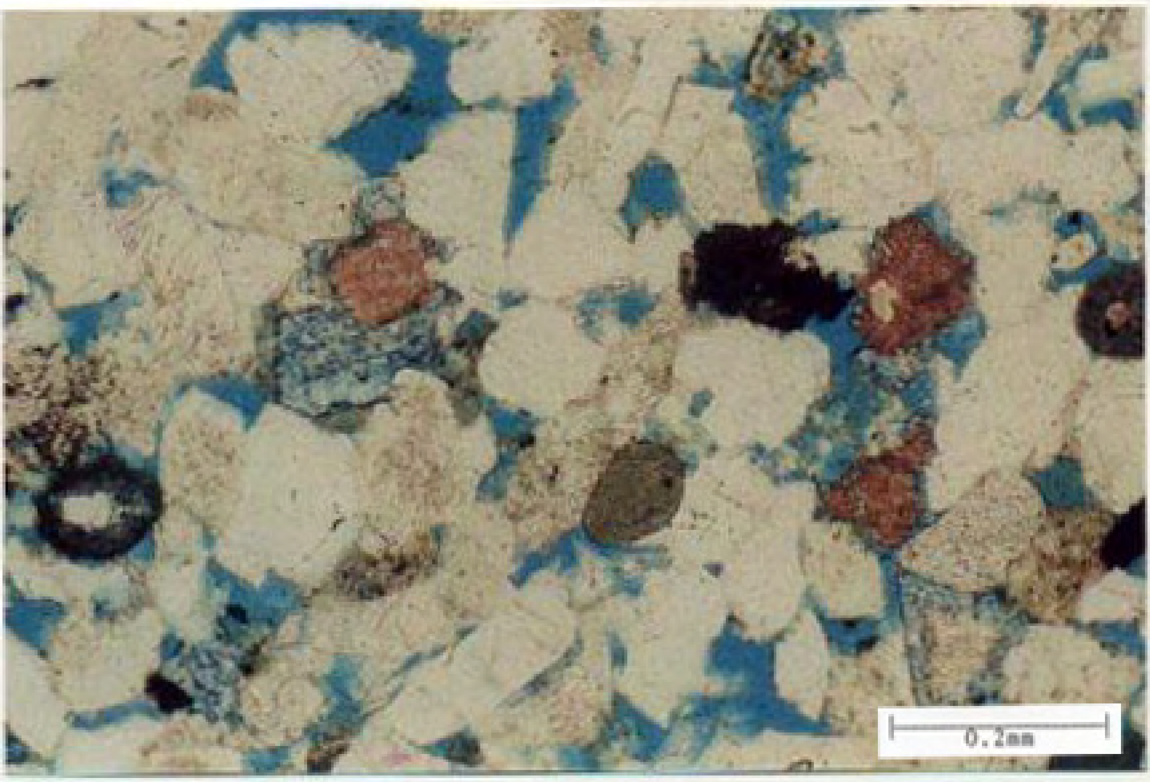

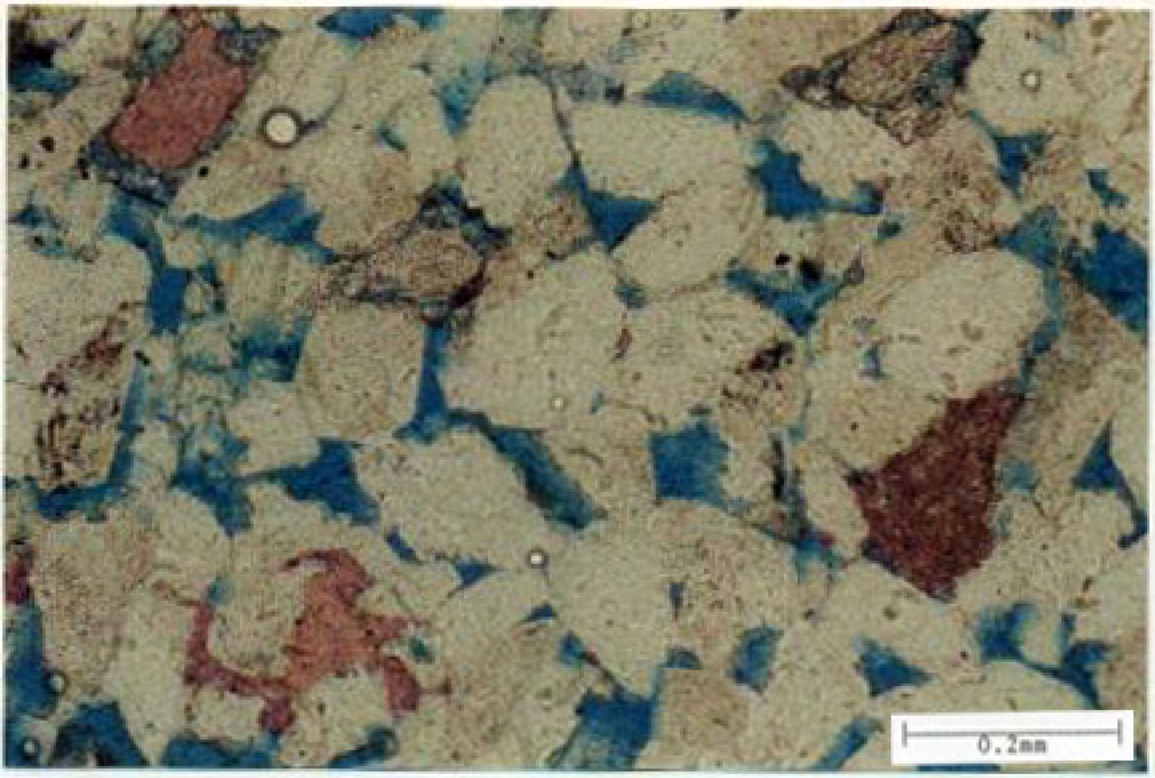

Federal 15-17
43-047-31002
4279.6 ft
100x

Back

Go to TS 1 200x

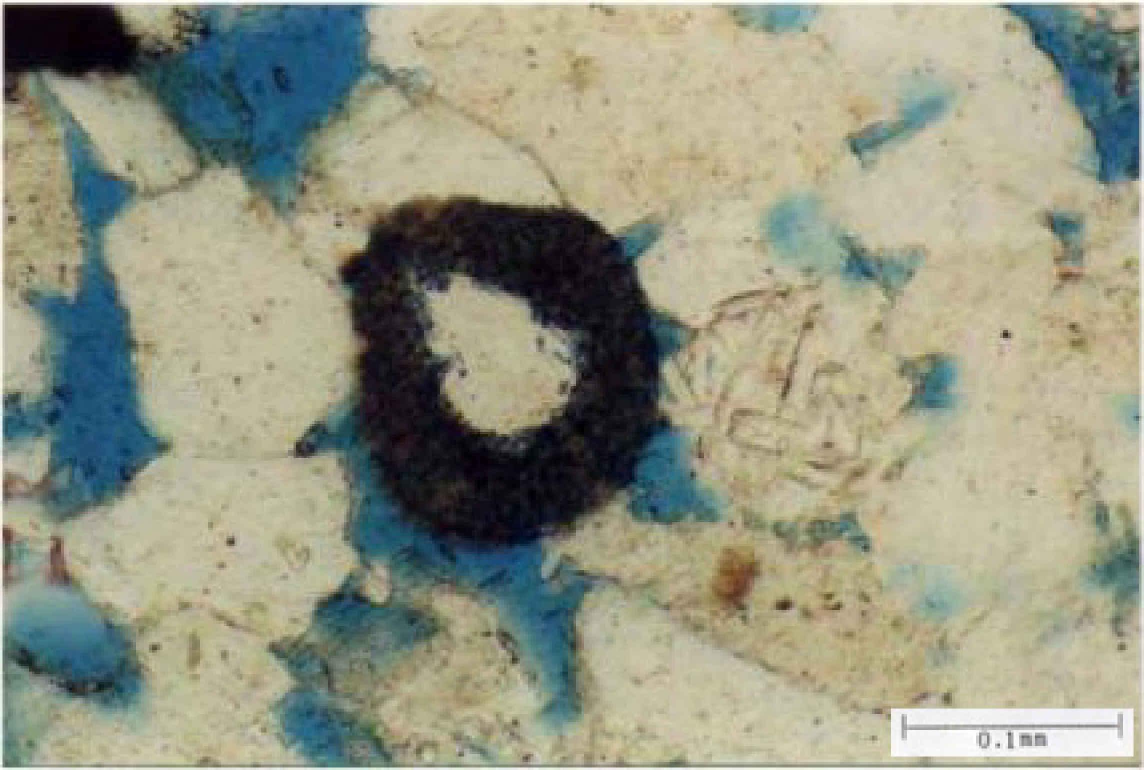

Federal 15-17
43-047-31002
4279.6 ft
200x

Back to Core Description

Go to TS 2 40x a

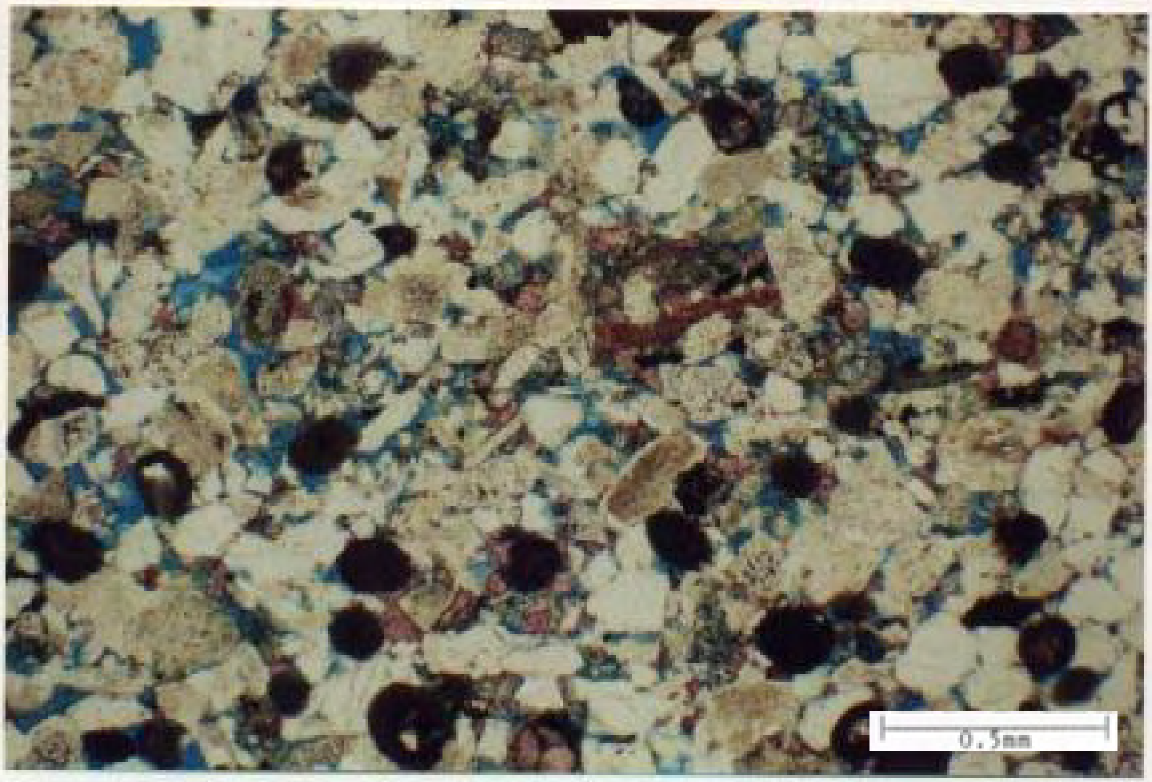

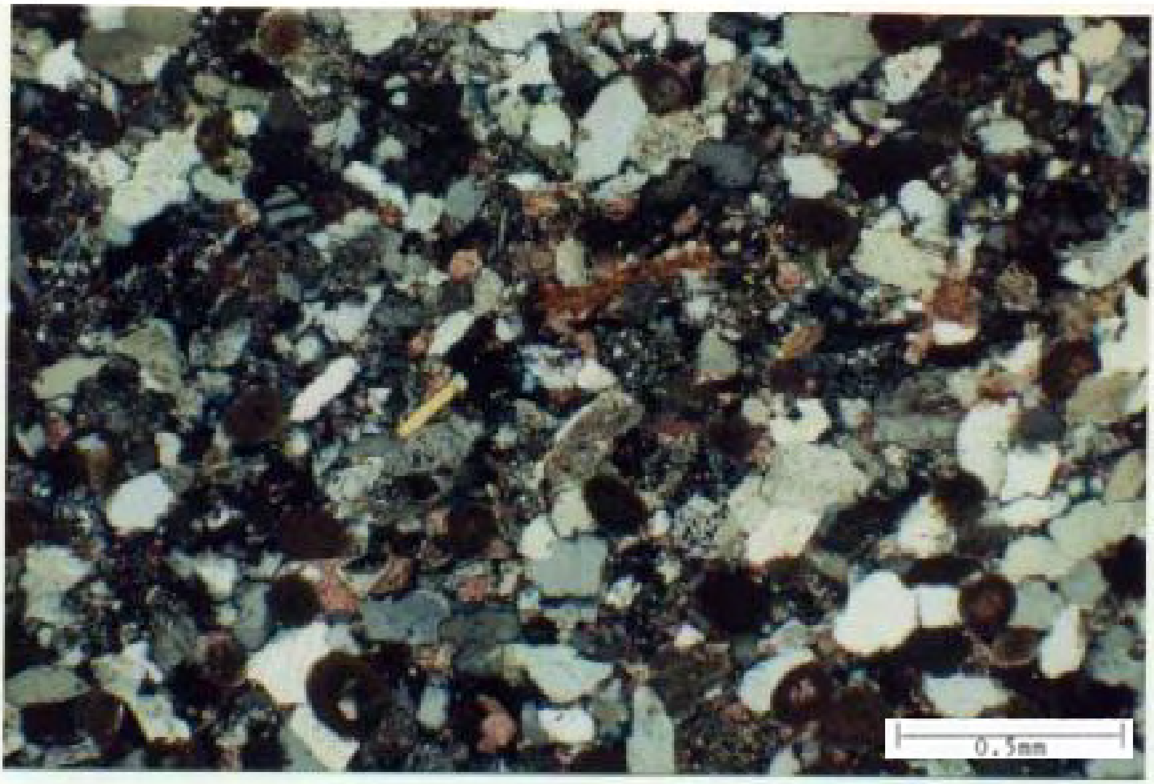

Federal 15-17
43-047-31002
4286 ft
40x

Back to Core Description

Go to TS 2 40x b

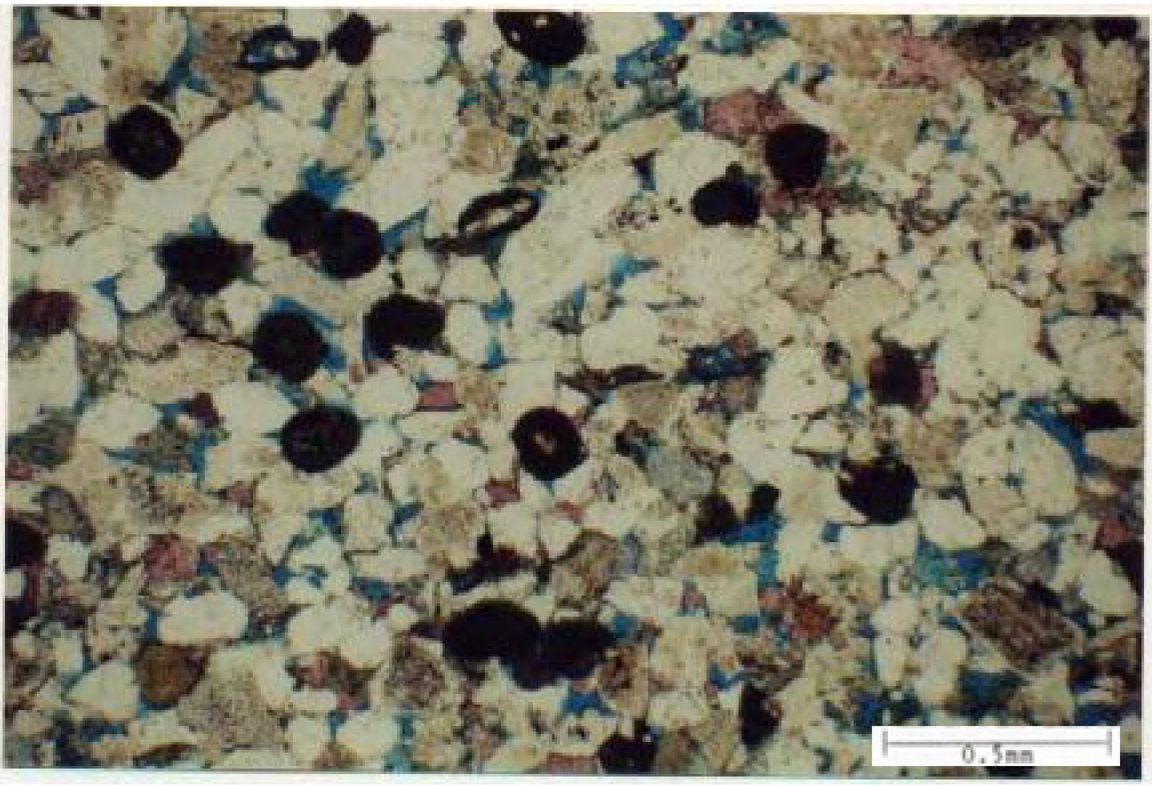

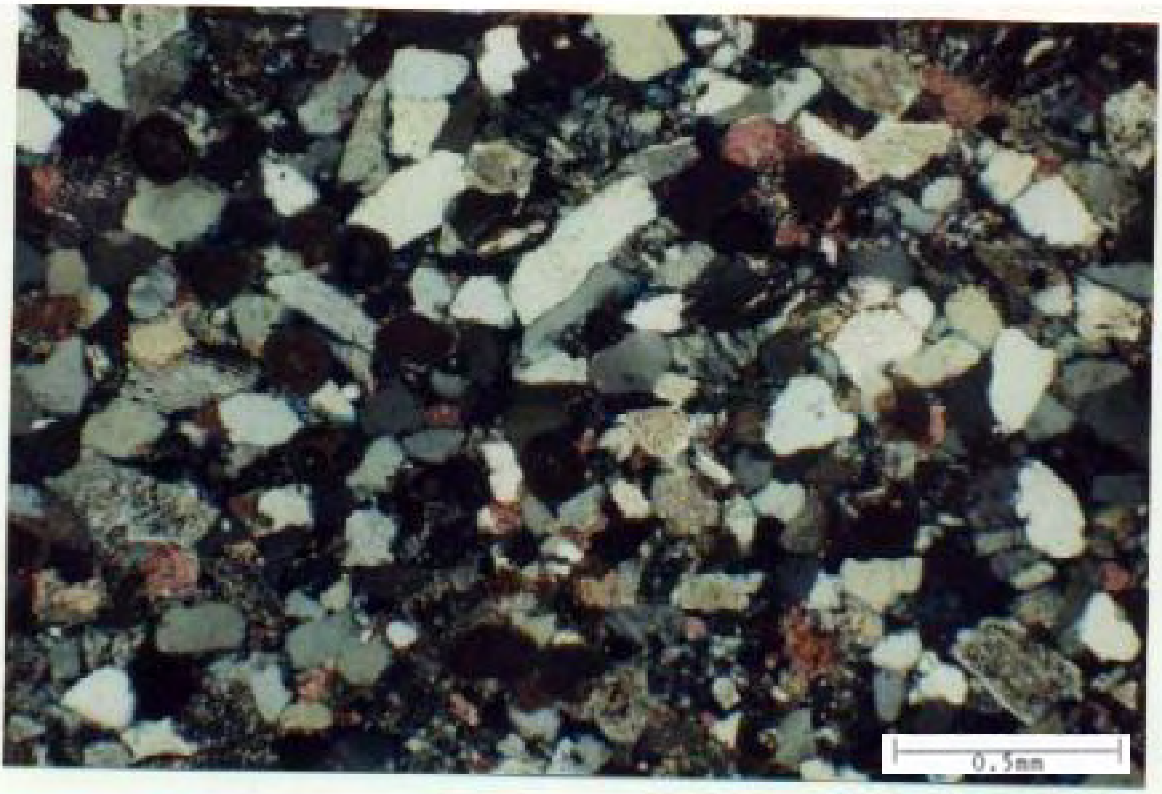

Federal 15-17
43-047-31002
4286 ft
40x

Back

Go to TS 2 100x a

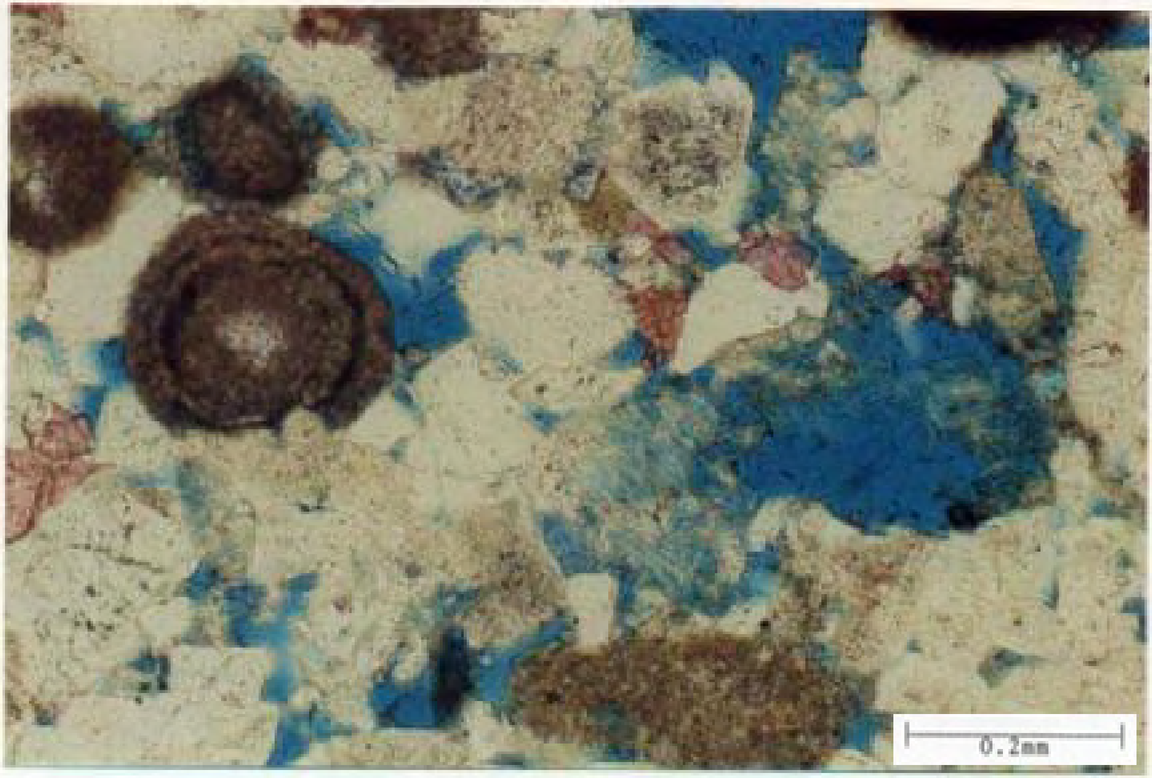

Federal 15-17
43-047-31002
4286 ft
100x

Back to Core Description

Go to TS 2 100x b

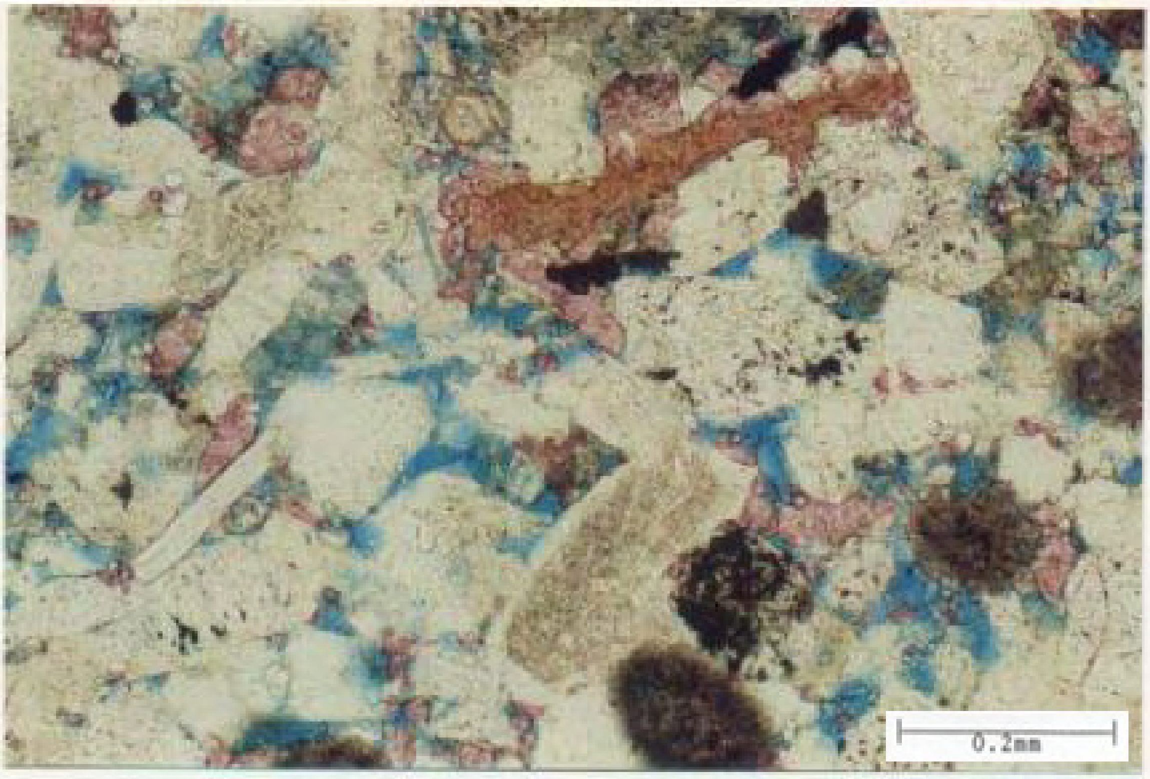

Federal 15-17
43-047-31002
4286 ft
100x

Back

Go to TS 3 40x

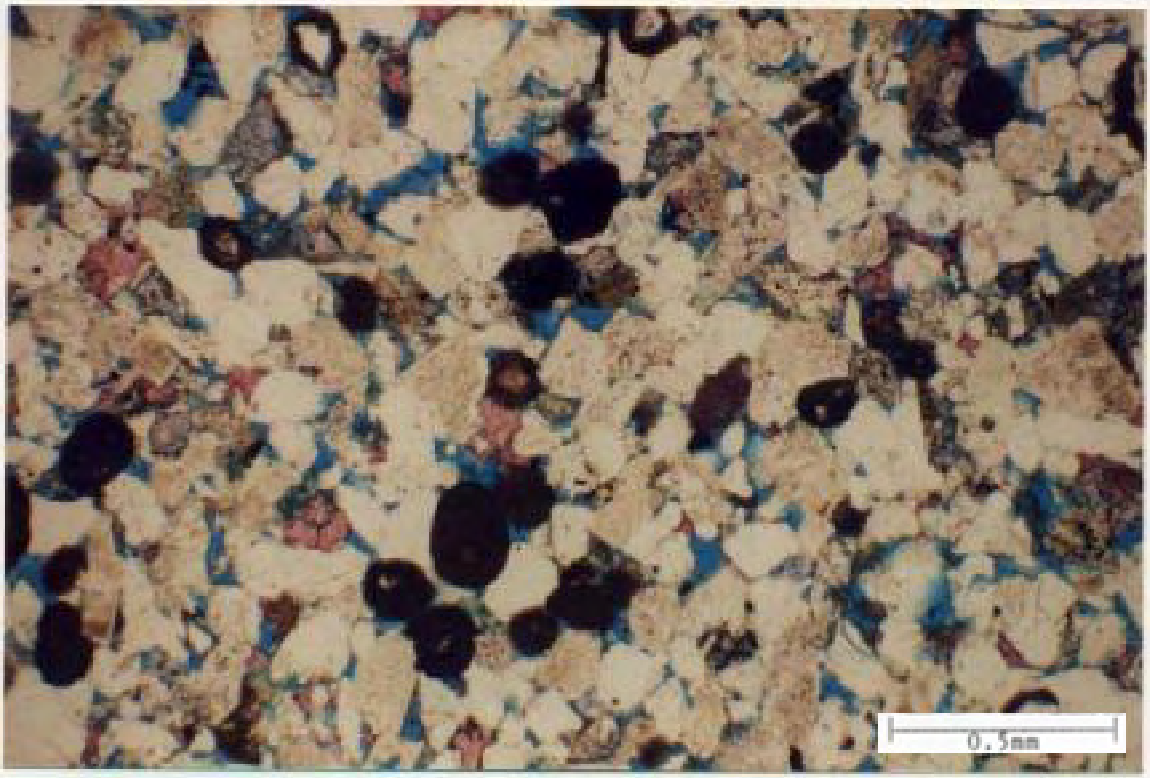

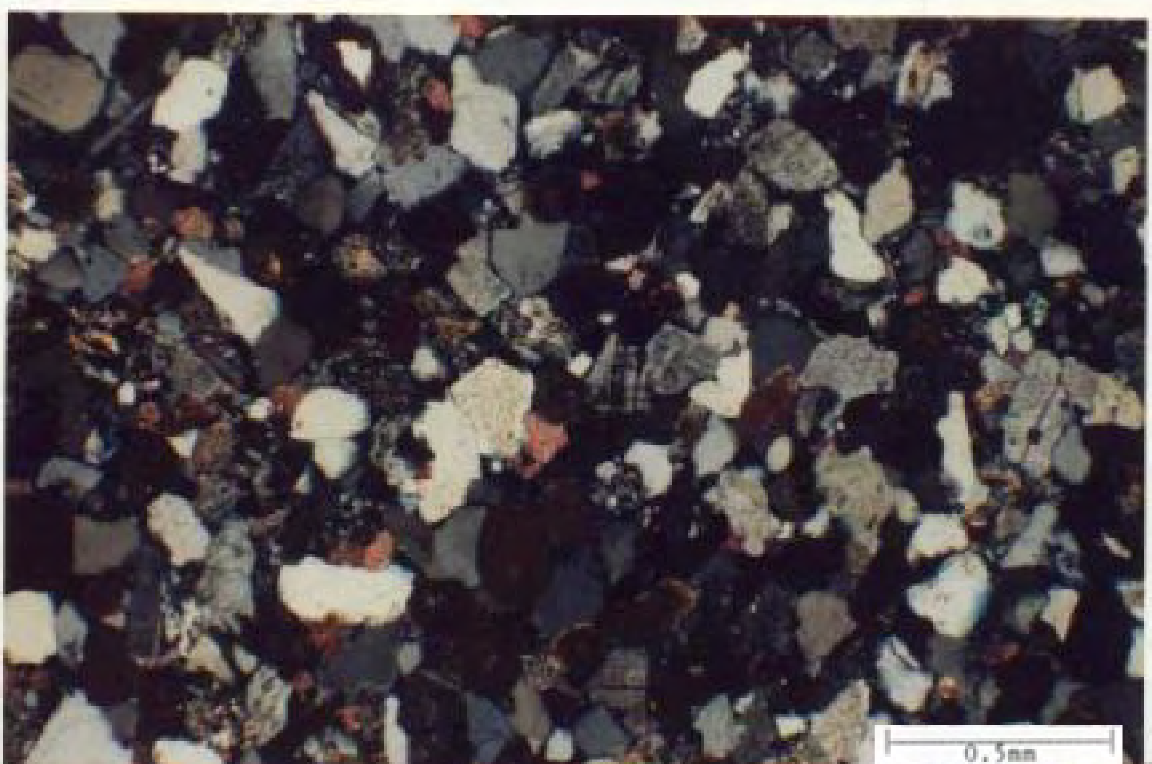

Federal 15-17
43-047-31002
4286.6 ft
40x

Back to Core Description

Go to TS 3 100x a

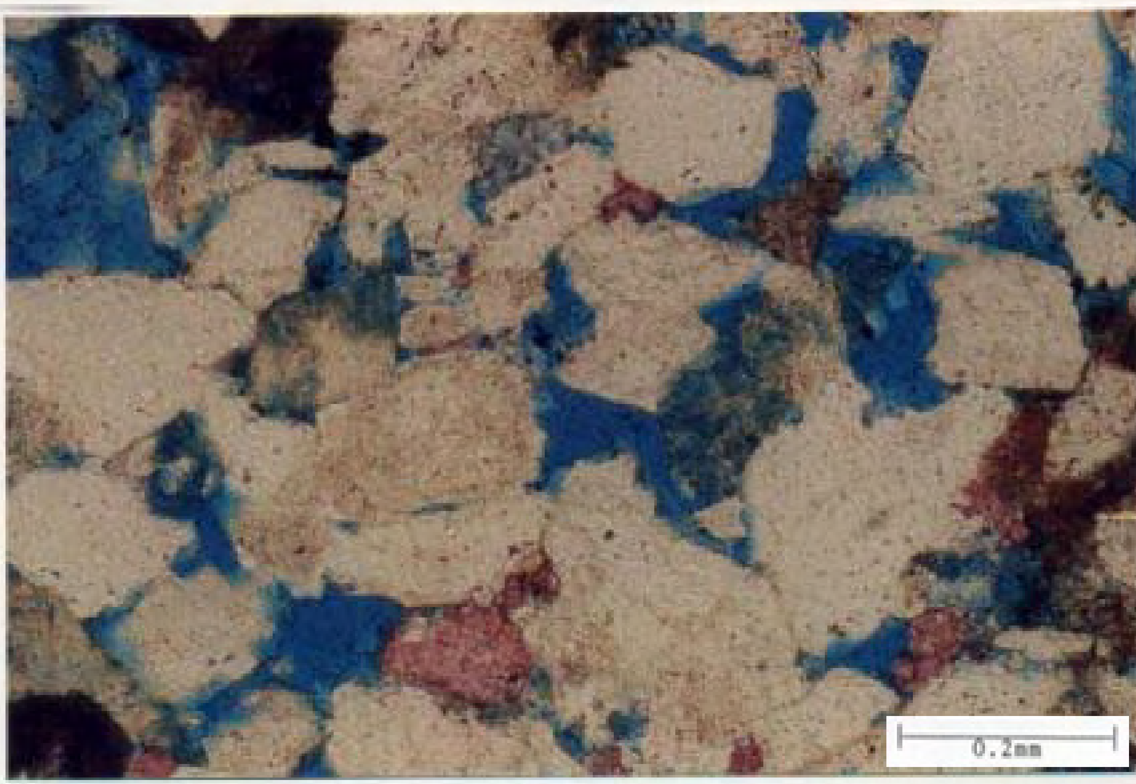

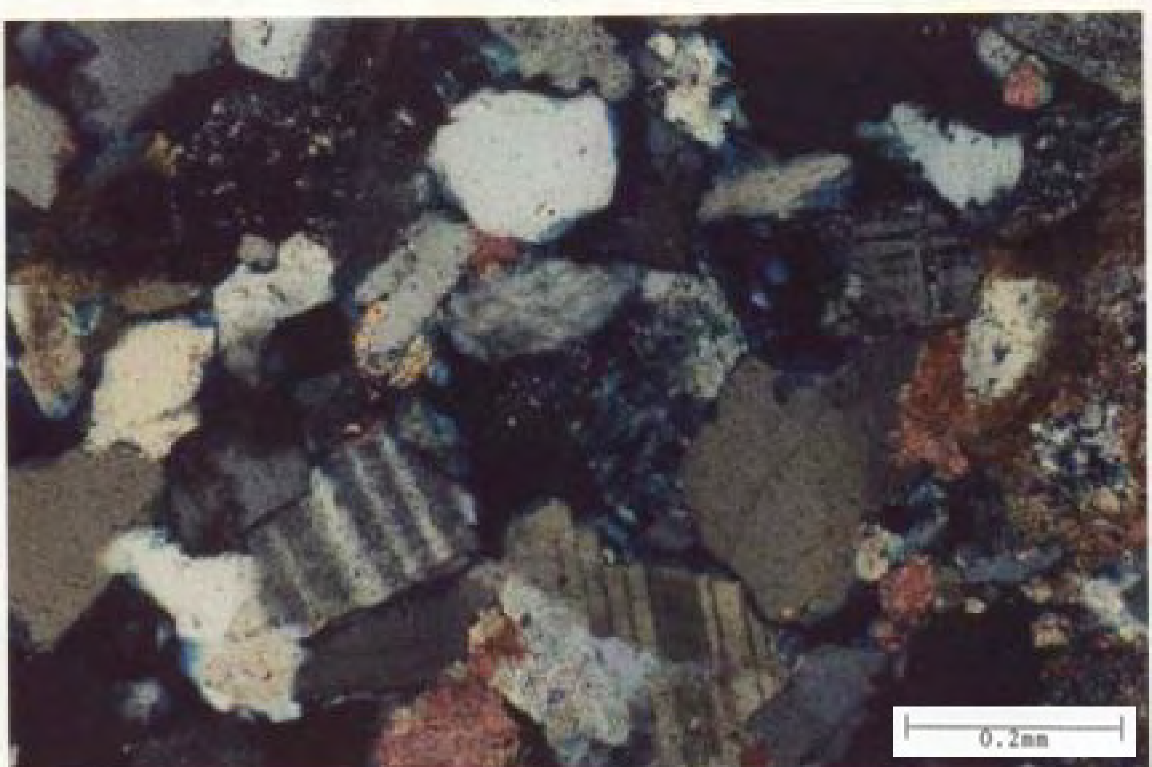

Federal 15-17
43-047-31002
4286.6 ft
100x

Back to Core Description

Go to TS 3 100x b

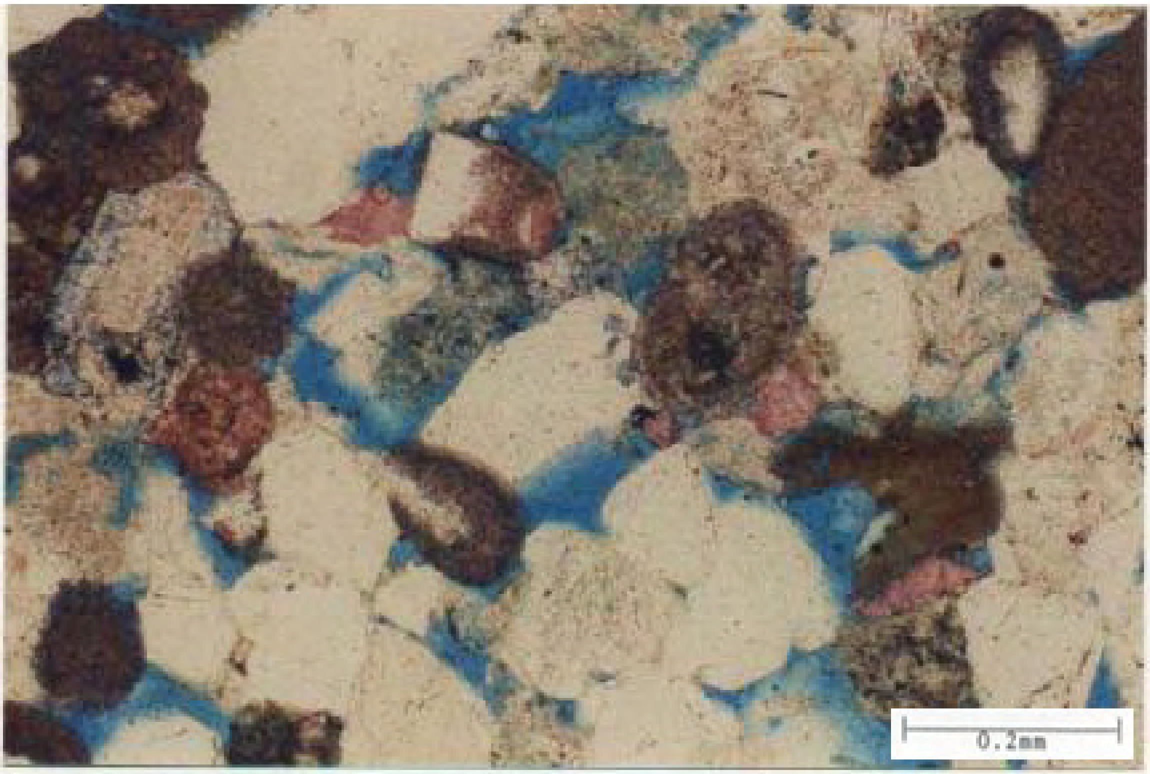

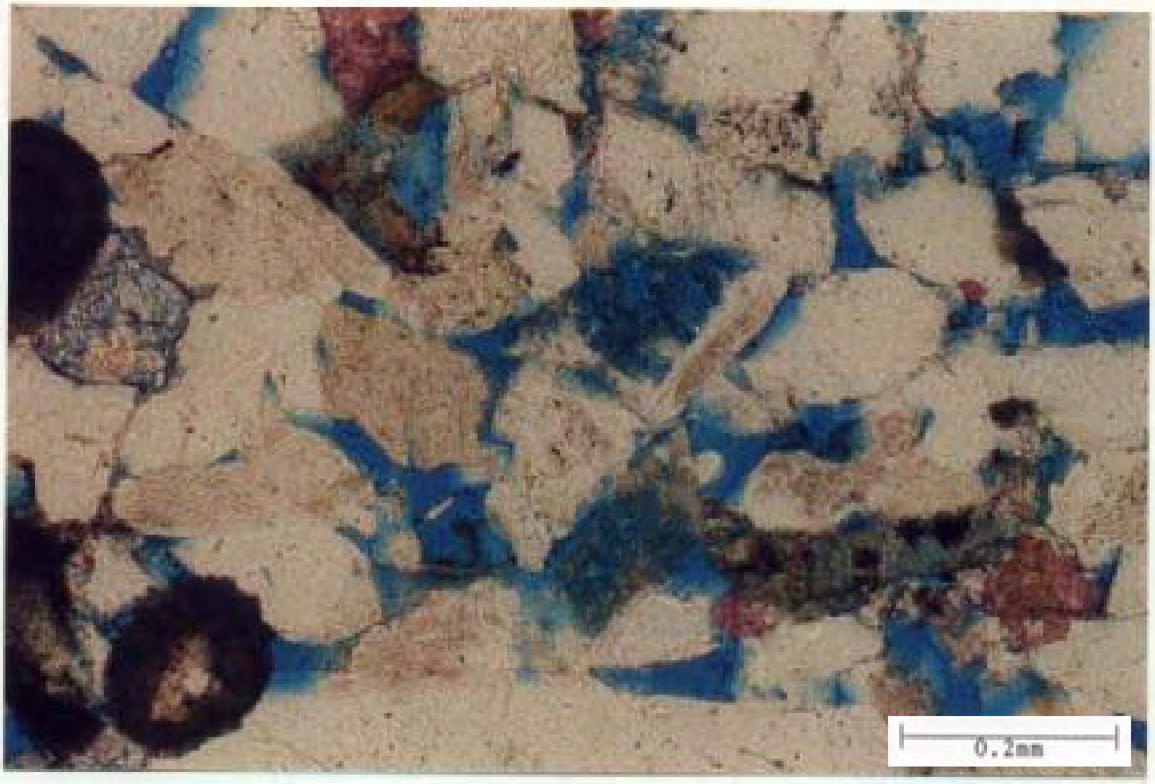

Federal 15-17
43-047-31002
4286.6 ft
100x

Back

Go to TS 3 200x a

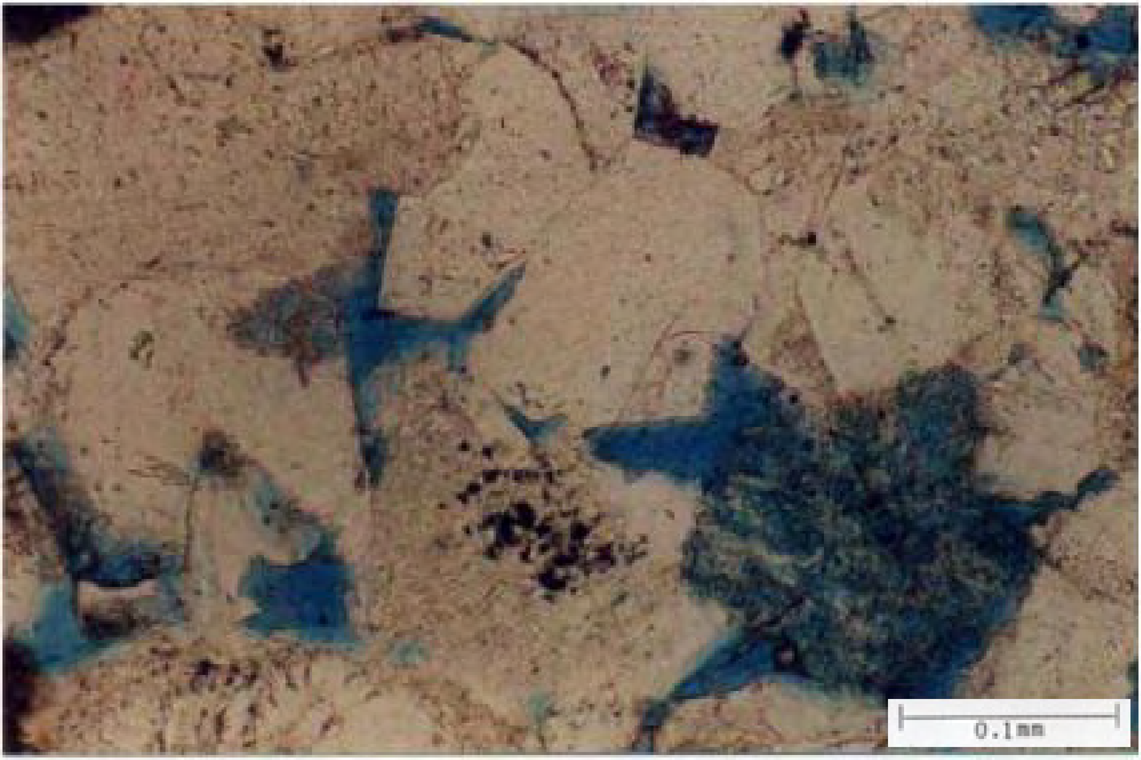

Federal 15-17
43-047-31002
4286.6 ft
200x

Back to Core Description

Go to TS 3 200x b

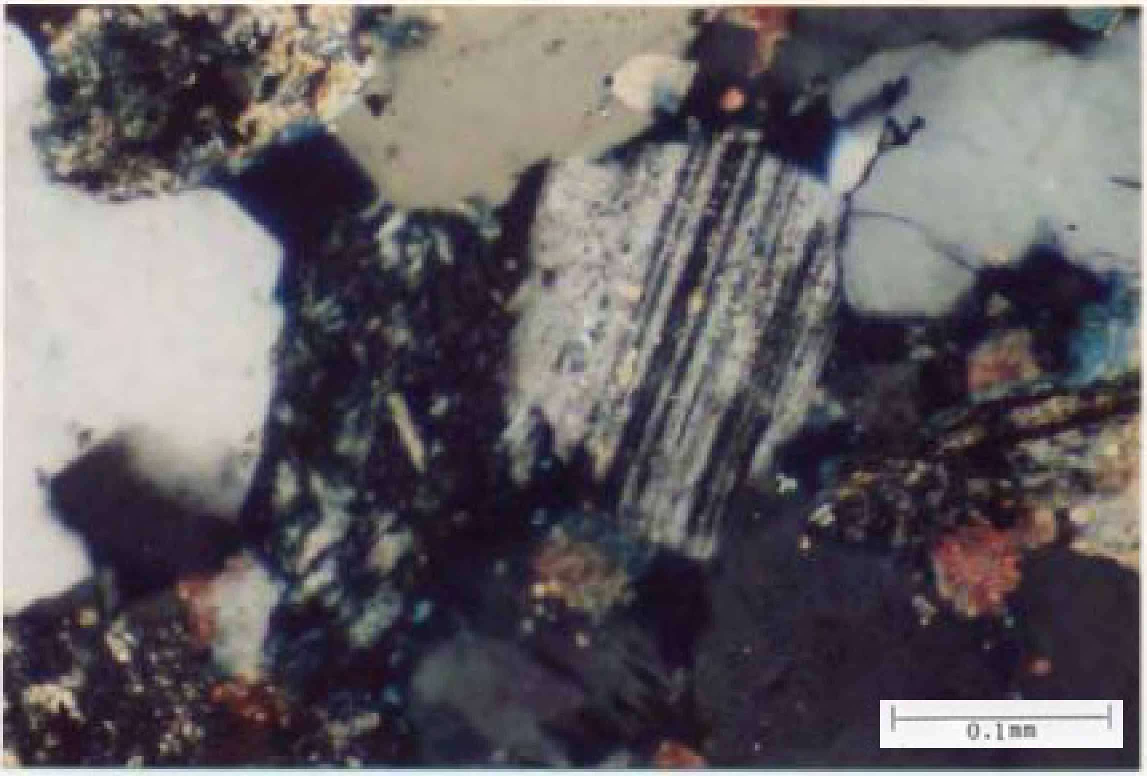

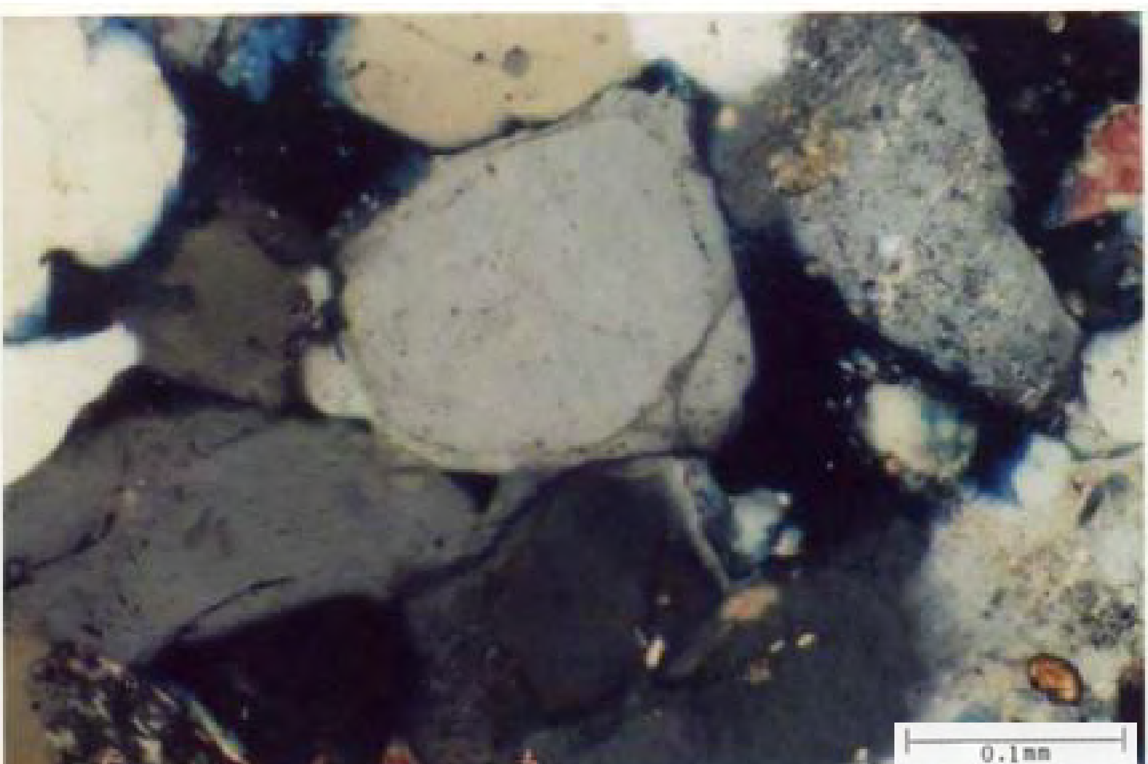

Federal 15-17
43-047-31002
4286.6 ft
200x

Back

Go to TS 3 200x c

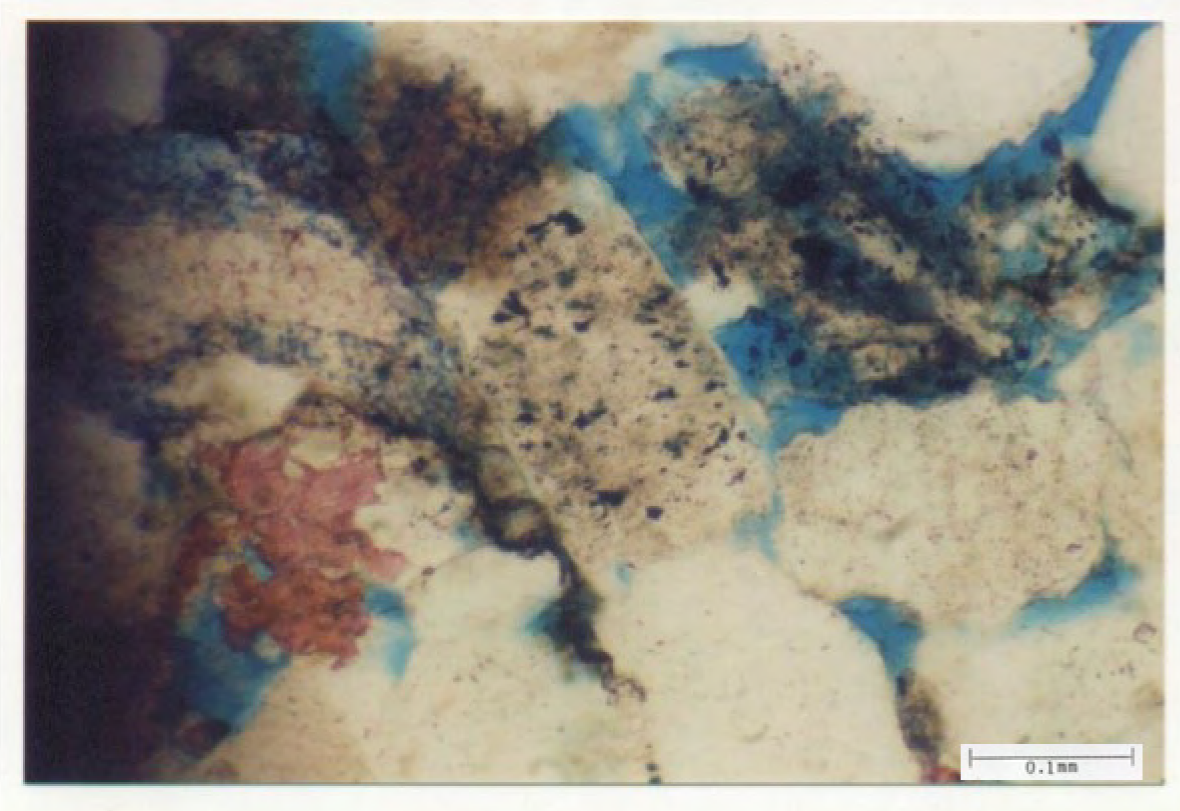

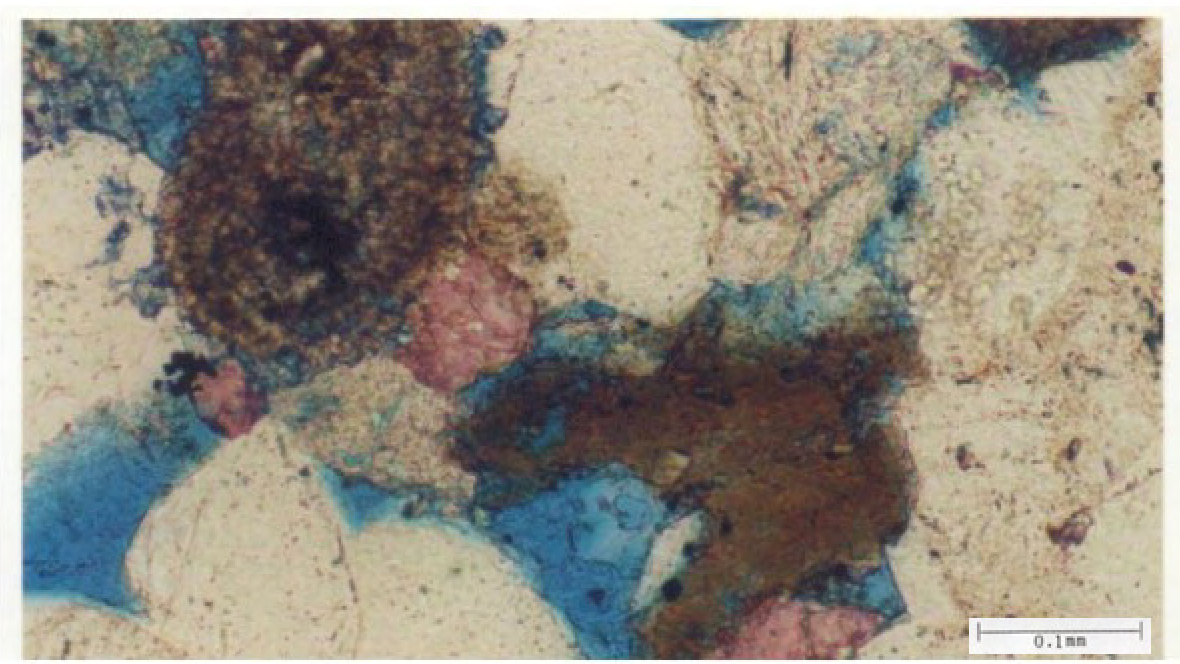

Well 15-17
API 43-047-31002
4286.6 ft
200x

Back

Go to TS 3 200x d

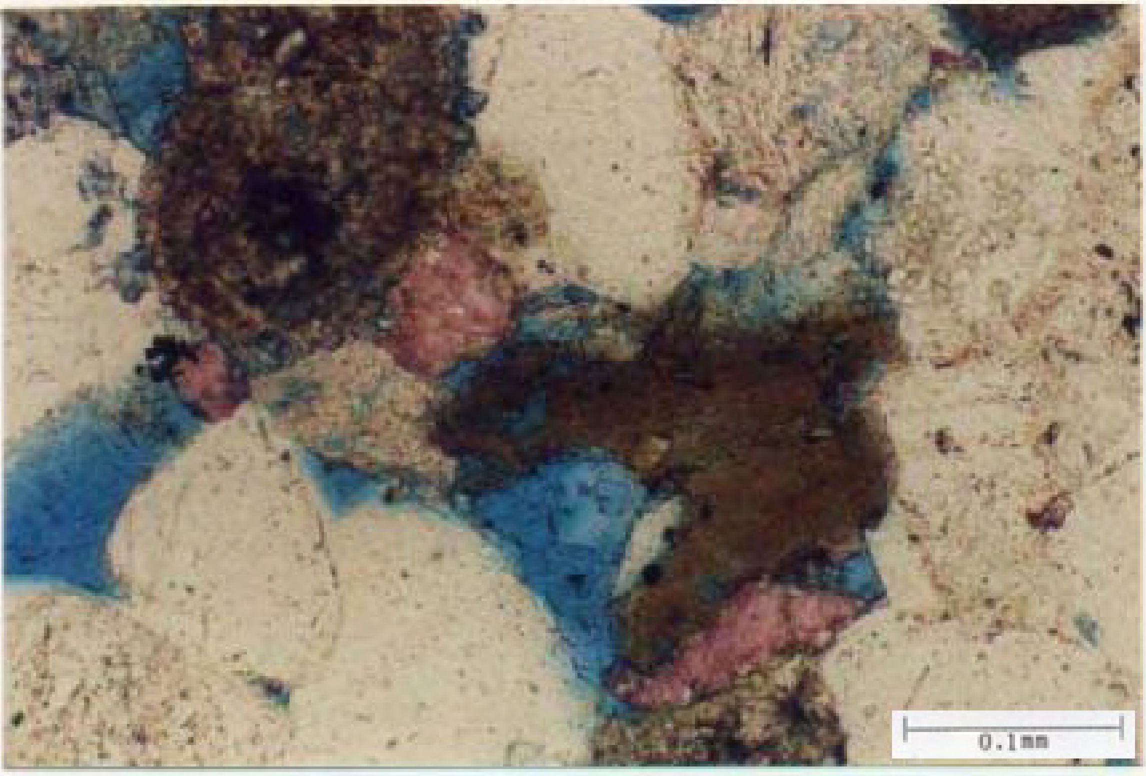

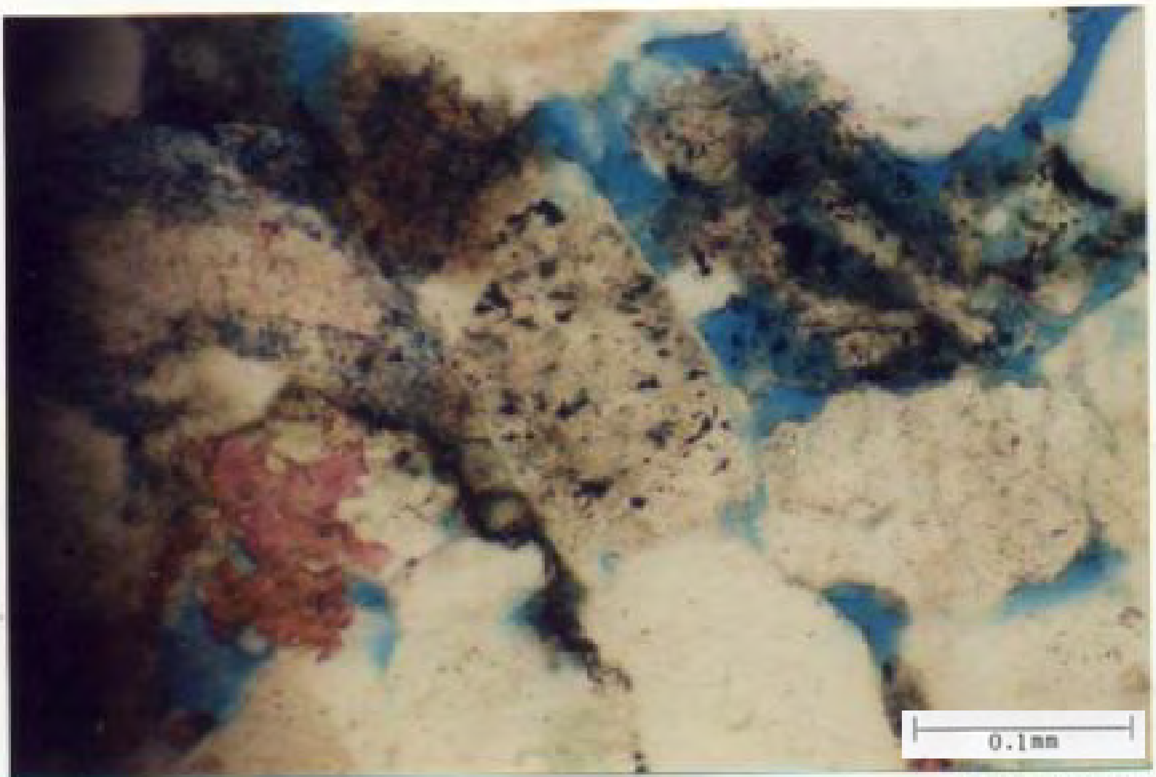

Federal 15-17
43-047-31002
4286.6 ft
200x

Back to Core Description

Back

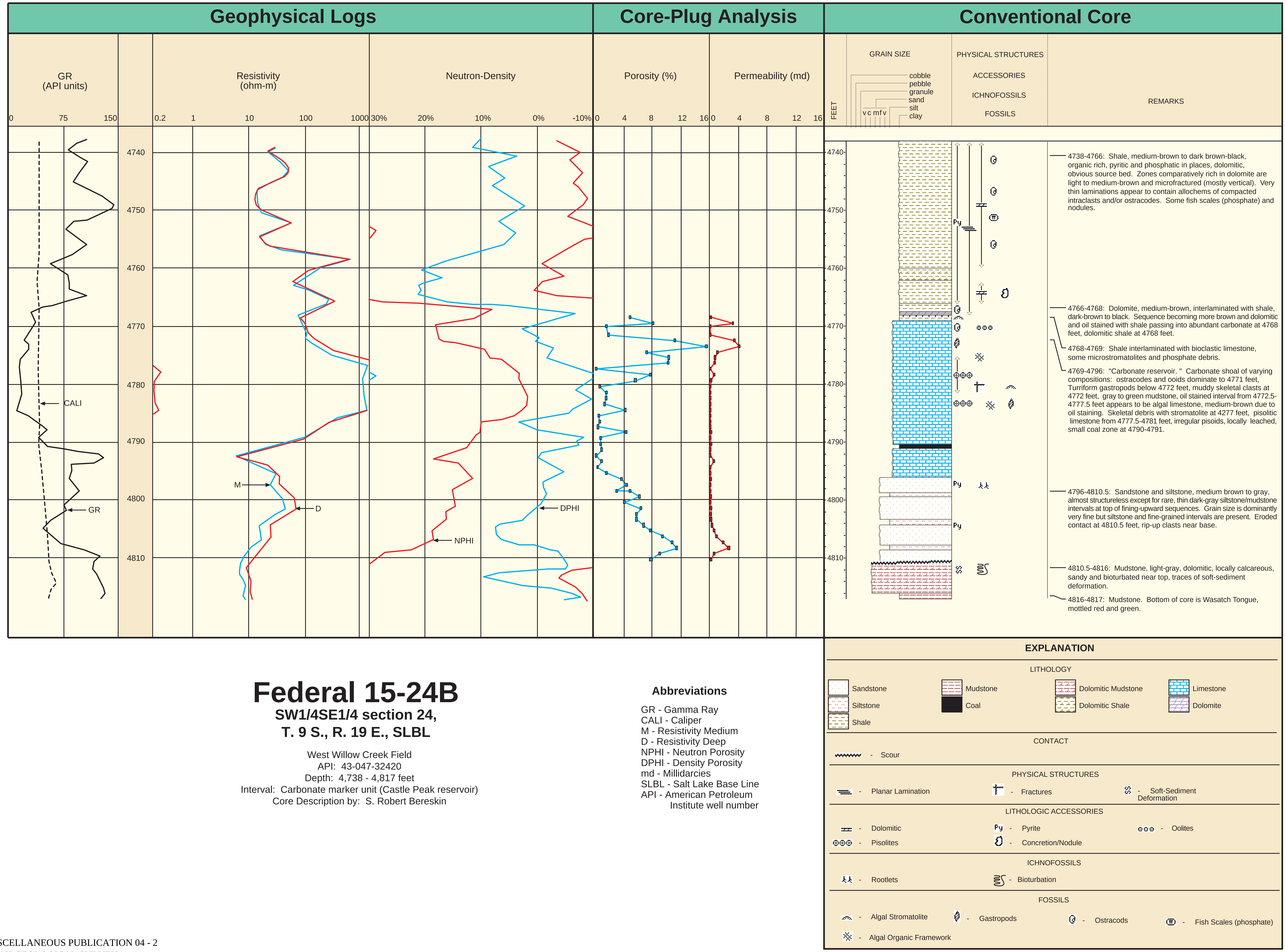

Federal 15-24B

SW1/4SE1/4 section 24, T. 9 S., R. 19 E., SLBL

West Willow Creek Field
API: 43-047-32420
Depth: 4,738 - 4,817 feet
Interval: Carbonate marker unit (Castle Peak reservoir)
Core Description by: S. Robert Bereskin

Abbreviations

GR - Gamma Ray
CALI - Caliper
M - Resistivity Medium
D - Resistivity Deep
NPHI - Neutron Porosity
DPHI - Density Porosity
md - Millidarcies
SLBL - Salt Lake Base Line
API - American Petroleum Institute well number

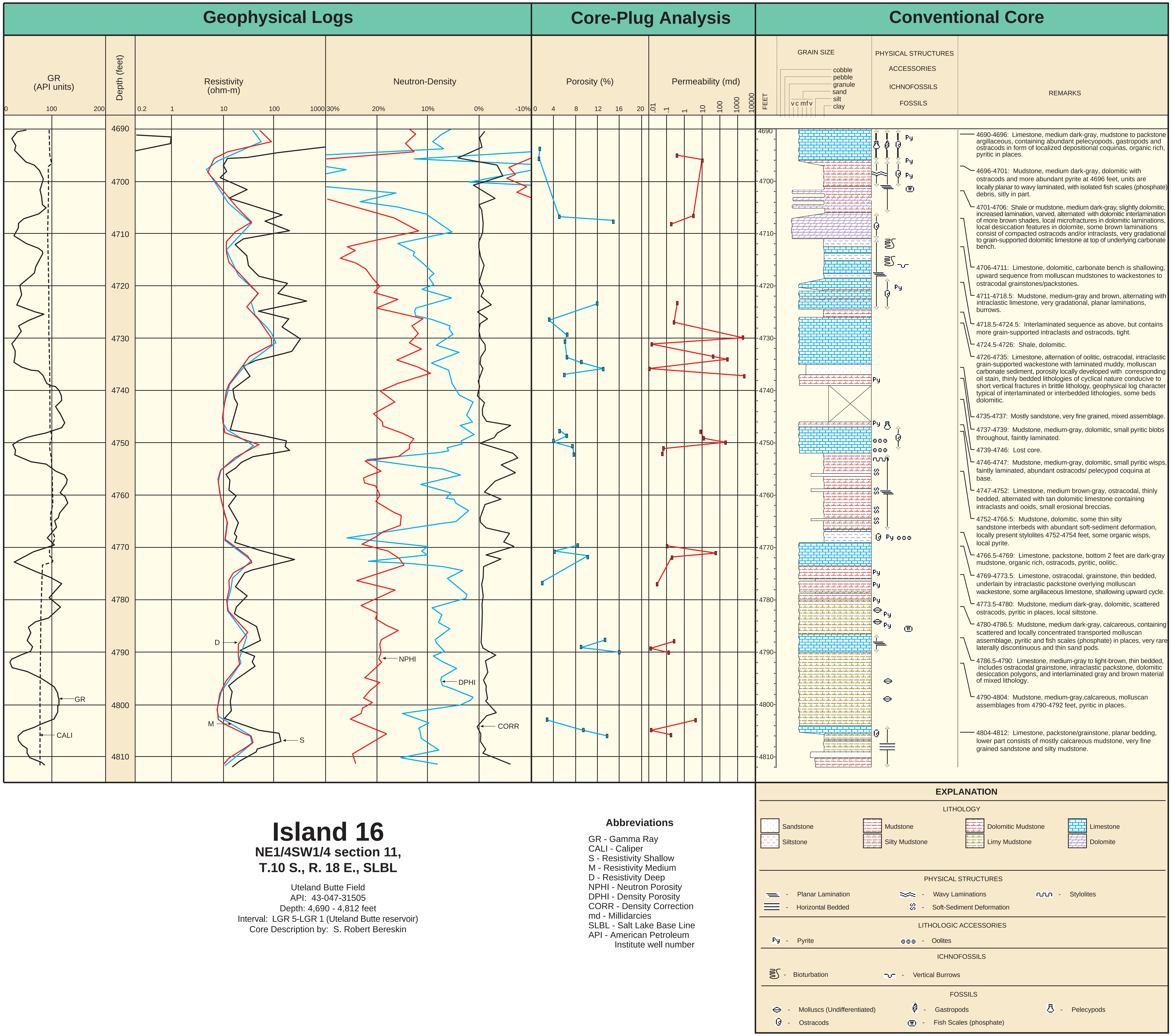

Island 16

NE1/4SW1/4 section 11, T.10 S., R. 18 E., SLBL

Uteland Butte Field
API: 43-047-31505
Depth: 4,690 - 4,812 feet
Interval: LGR 5-LGR 1 (Uteland Butte reservoir)
Core Description by: S. Robert Bereskin

Abbreviations

GR - Gamma Ray
CALI - Caliper
S - Resistivity Shallow
M - Resistivity Medium
D - Resistivity Deep
NPHI - Neutron Porosity
DPHI - Density Porosity
CORR - Density Correction
md - Millidarcies
SLBL - Salt Lake Base Line
API - American Petroleum Institute well number

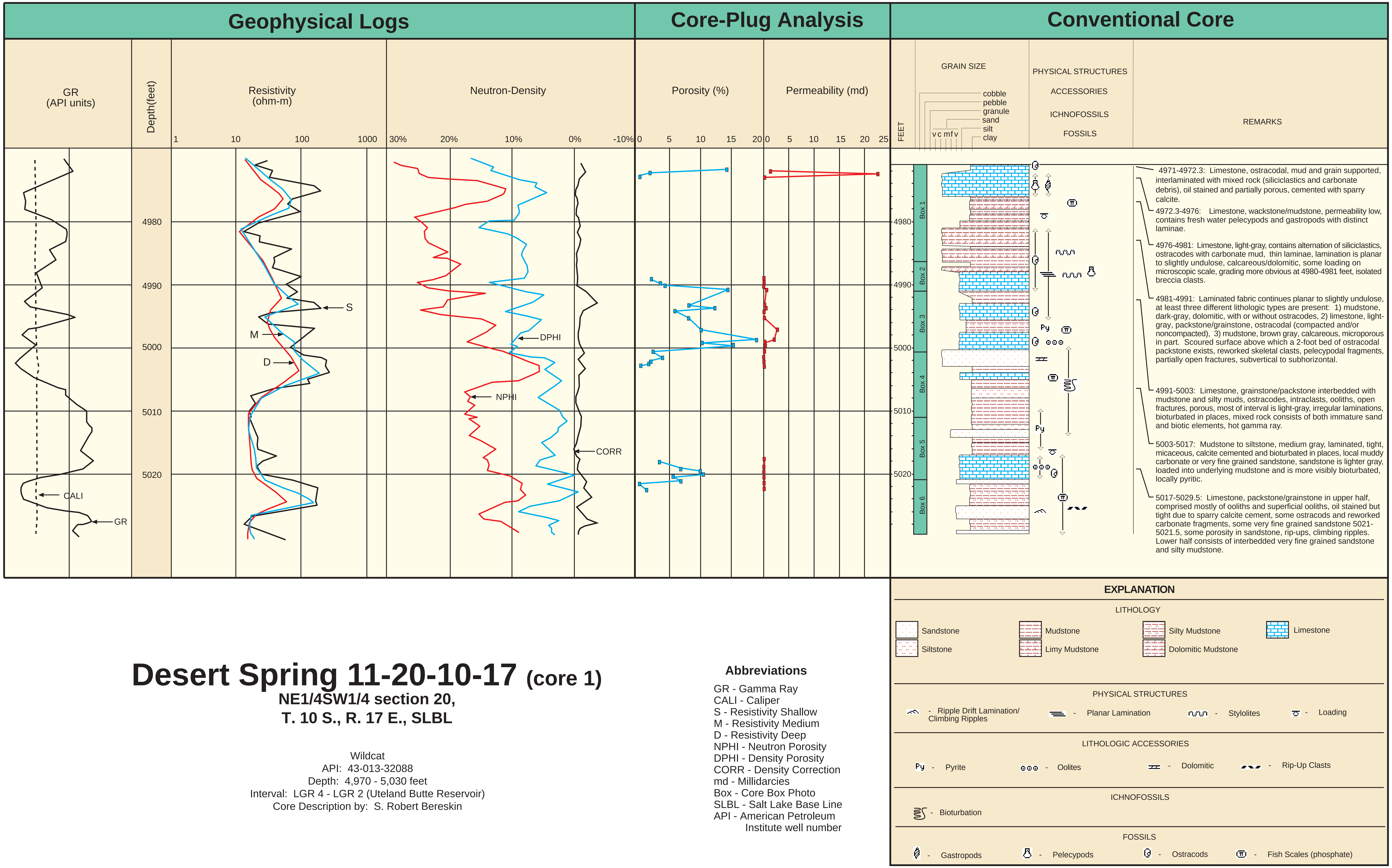

Desert Spring 11-20-10-17 (core 1)

NE1/4SW1/4 section 20,
T. 10 S., R. 17 E., SLBL

Wildcat
API: 43-013-32088
Depth: 4,970 - 5,030 feet
Interval: LGR 4 - LGR 2 (Uteland Butte Reservoir)
Core Description by: S. Robert Bereskin

Abbreviations

GR - Gamma Ray
CALI - Caliper
S - Resistivity Shallow
M - Resistivity Medium
D - Resistivity Deep
NPHI - Neutron Porosity
DPHI - Density Porosity
CORR - Density Correction
md - Millidarcies
Box - Core Box Photo
SLBL - Salt Lake Base Line
API - American Petroleum Institute well number

Back to Core Description

Back to Core Description

Back to Core Description

Back to Core Description

Back to Core Description

Back to Core Description

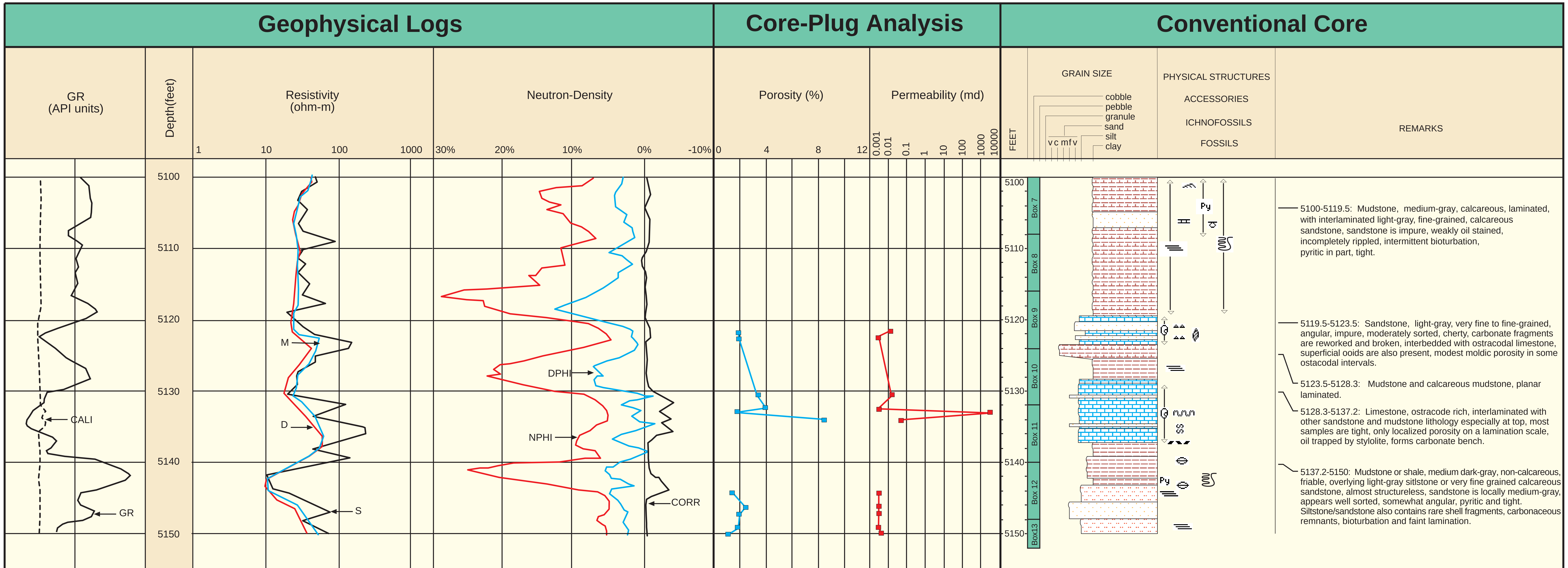

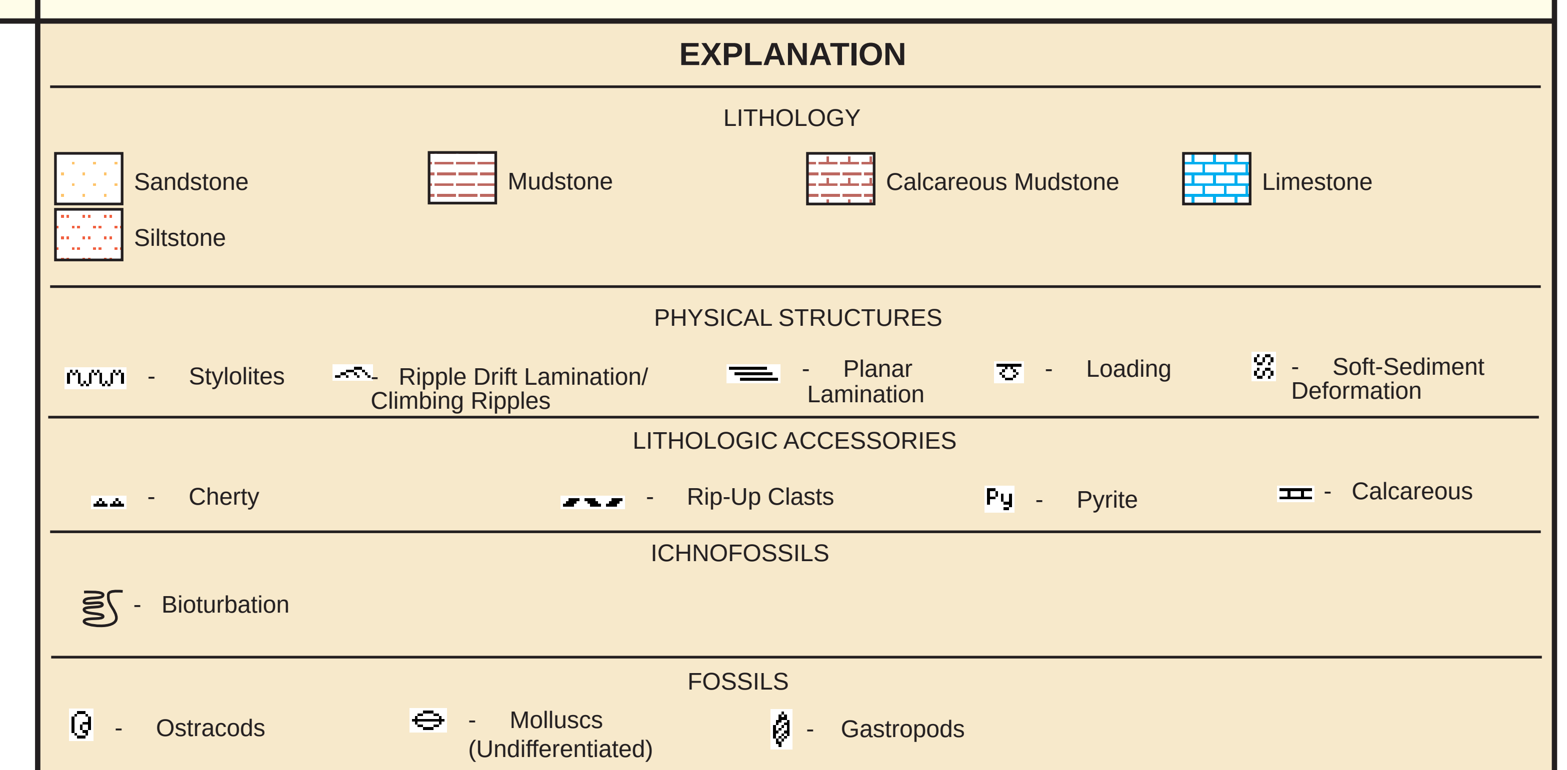

Desert Spring 11-20-10-17 (core 2)

NE1/4SW1/4 section 20,
T. 10 S., R. 17 E., SLBL

Wildcat
API: 43-013-32088
Depth: 5,100 - 5,150 feet
Interval: LGR 1 (Uteland Butte reservoir)
Core Description by: S. Robert Bereskin

Abbreviations

GR - Gamma Ray
CALI - Caliper
S - Resistivity Shallow
M - Resistivity Medium
D - Resistivity Deep
NPHI - Neutron Porosity
DPHI - Density Porosity
CORR - Density Correction
md - Millidarcies
Box - Core Box Photo
SLBL - Salt Lake Base Line
API - American Petroleum
Institute well number

Back to Core Description

Back to Core Description

Back to Core Description

Back to Core Description

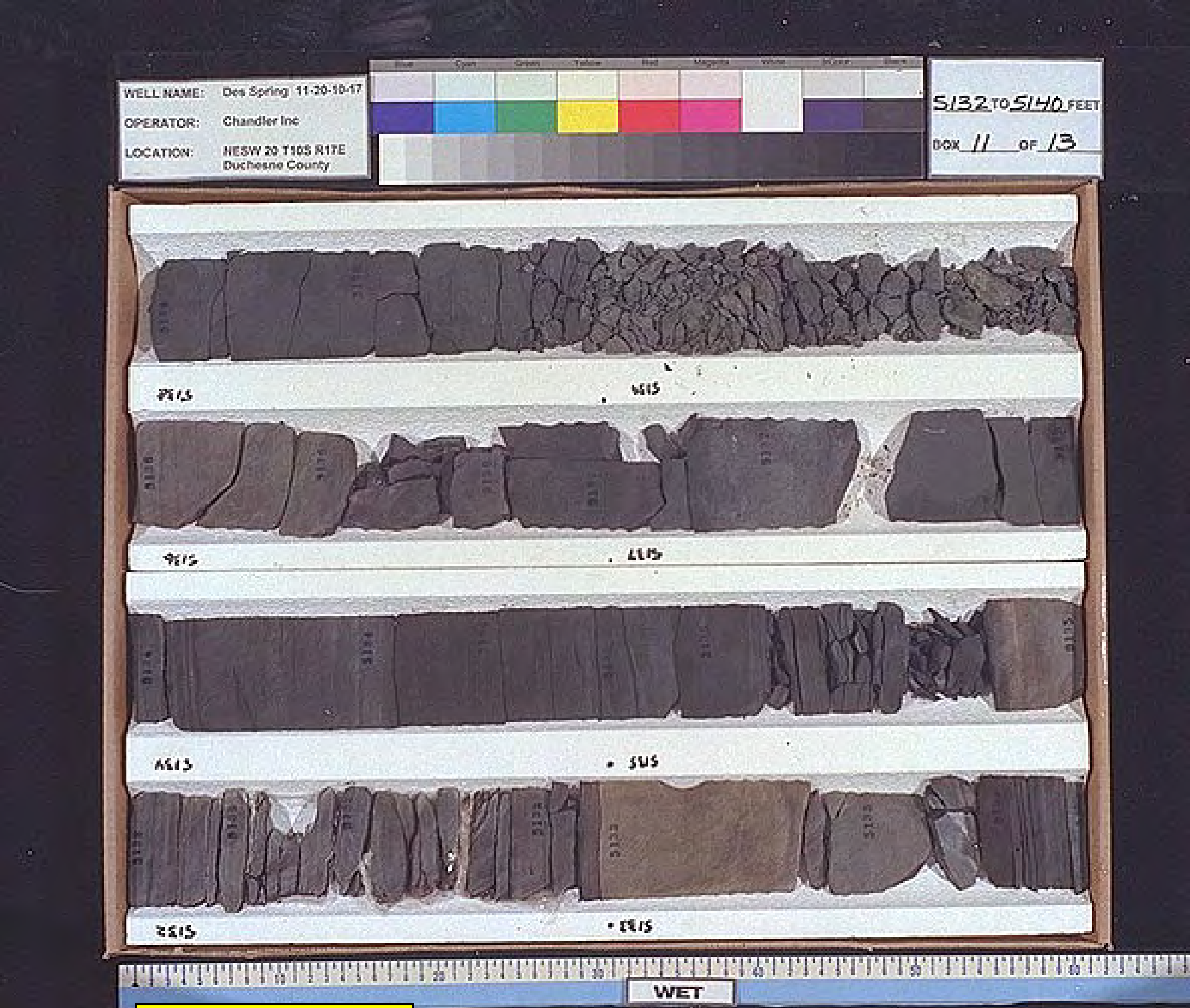

Back to Core Description

Back to Core Description

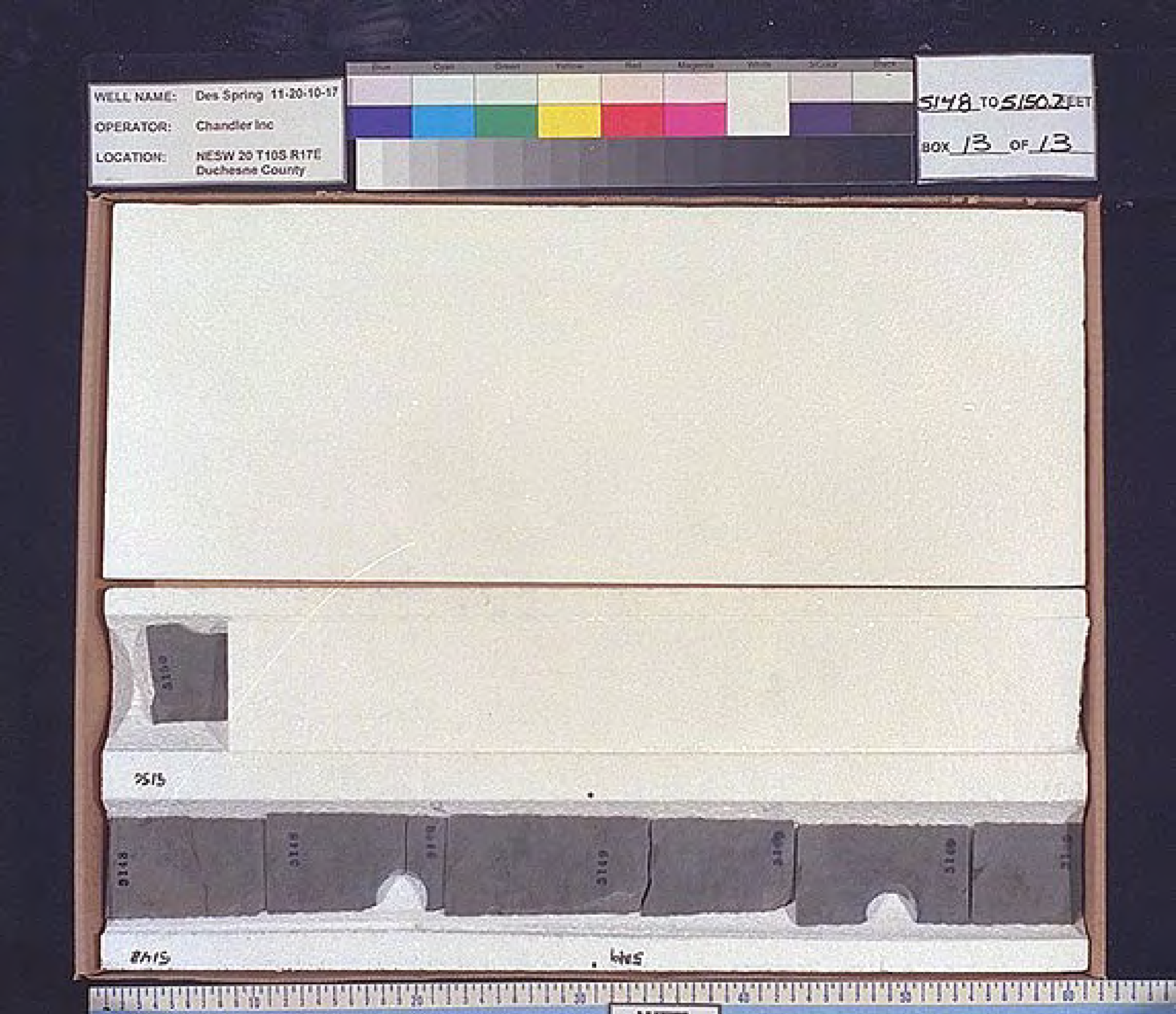

Back to Core Description

APPENDIX B

ROUTINE CORE ANALYSIS DATA

Well location data for the routine core analysis data set. Data from Utah Division Oil, Gas and Mining well records.

Well Number	Location: Section, Township, Range, Salt Lake Base Line and Meridian	API Number	Map Number (figure 1 and table 1)
10-34	Sec. 34, T. 8 S., R. 16 E., SLBLM	43-013-31371	-
11-16H	Sec. 16, T. 9 S., R. 17 E., SLBLM	43-013-30616	-
33-8	Sec. 8, T. 9 S., R. 17 E., SLBLM	43-013-31427	13
34-8	Sec. 8, T. 9 S., R. 17 E., SLBLM	43-013-30778	14
41-8	Sec. 8, T. 9 S., R. 17 E., SLBLM	43-013-30741	-
5-33	Sec. 33, T. 8 S., R. 16 E., SLBLM	43-013-31435	-
1-26	Sec. 26, T. 8 S., R. 16 E., SLBLM	43-013-31767	-
15-24B	Sec. 24, T. 9 S., R. 19 E., SLBLM	43-047-32420	19
2-25	Sec. 25, T. 5 S., R. 5 W., UBLM	43-013-31833	1
9-34	Sec. 34, T. 8 S., R. 16 E., SLBLM	43-013-31407	-
10-34	Sec. 34, T. 8 S., R. 16 E., SLBLM	43-013-31371	-
12-35	Sec. 35, T. 8 S., R. 16 E., SLBLM	43-013-30744	-
12-4	Sec. 4, T. 9 S., R. 16 E., SLBLM	43-013-30699	-
15-17	Sec. 17, T. 9 S., R. 19 E. SLBLM	43-047-31002	18
23-25	Sec. 25, T. 8 S., R. 17 E., SLBLM	43-047-32529	9
33-11J	Sec. 11, T. 9 S., R. 16 E., SLBLM	43-013-31451	11
3A-35	Sec. 35, T. 8 S., R. 16 E., SLBLM	43-013-30608	7
5-33	Sec. 33, T. 8 S., R. 16 E., SLBLM	43-013-31435	-
6-32	Sec. 32, T. 8 S., R. 17 E., SLBLM	43-013-30748	10
6-35	Sec. 35, T. 8 S., R. 16 E., SLBLM	43-013-30751	6
13-32	Sec. 32, T. 8 S., R. 16 E., SLBLM	43-013-31112	-
14A-28	Sec. 28, T. 8 S., R. 16 E., SLBLM	43-013-30792	2
16	Sec. 11, T. 10 S., R. 18 E., SLBLM	43-047-31505	20
34-5	Sec. 5, T. 9 S., R. 17 E., SLBLM	43-047-30721	12
11-20-10-17	Sec. 20, T. 10 S., R. 17 E., SLBLM	43-013-23088	21

Well number	Core depth	Log depth	Core porosity	Horz perm	Vert perm	Core So	Core Sw	Grain density	Log Den porosity	Log D/N porosity	Log interval
10-34	4488	4488	12.3	1.2	-	53.3	22.1	2.66	16.5	18	Beluga
11-16H	4585.5	4585	5.4	0.04	-	62.4	13.4	2.67	2	9	Beluga
11-16H	4355.5	4355	3.4	0.01	-	0	95.3	2.68	6	17	Beluga
11-16H	4354.5	4354	3.6	0.01	-	0	86.6	2.69	7.5	15	Beluga
11-16H	4349.5	4349	1.9	0.01	-	0	91.1	2.77	30	30	Beluga
11-16H	4348.5	4348	1.4	0.01	-	0	73.9	2.67	30	30	Beluga
11-16H	4347.5	4347	1.9	0.01	-	0	52	2.68	20	20	Beluga
33-8	4350	4350	6.6	0.03	-	26.9	41.9	2.67	7.5	8	Beluga
33-8	4315	4315	13.3	3.4	-	51.6	42.7	2.66	13	13	Beluga
33-8	4109	4109	16.9	16	-	45	52.8	2.66	18	18	Beluga
33-8	4114	4114	15.1	8.9	-	46.5	50.6	2.66	17	17	Beluga
33-8	4141.5	4141	13.2	2.5	-	49.6	43.8	2.66	15	15	Beluga
33-8	4142	4142	10.8	0.43	-	42.2	27.6	2.67	16	16	Beluga
33-8	4546	4546	6.1	0.02	-	57.4	26.5	2.68	4	7	Beluga
33-8	4536	4536	11.5	0.31	-	67.6	10.3	2.67	14	14	Beluga
33-8	4401	4401	24.6	122	-	30	63.1	2.77	15.5	19.5	Beluga
34-8	4066.5	4067	2.3	0.01	-	0	73.1	2.67	5	10	Beluga
34-8	4064.5	4065	11.3	11	-	32.3	17.1	2.66	6	12	Beluga
34-8	4071.5	4072	1.2	0.01	-	0	46.1	2.69	9	17	Beluga
34-8	4065.5	4066	9.9	2.35	-	40.7	28.5	2.66	6	10.5	Beluga
34-8	4085.5	4086	12.7	5.34	-	39.4	12.1	2.67	11	13	Beluga
34-8	4086.5	4101	9.1	2.15	-	48.5	24.2	2.66	4	11	Beluga
34-8	4101.5	4102	2.5	0.01	-	0	68.4	2.7	3.5	9.5	Beluga
34-8	4063.5	4064	11	1.04	-	26.7	20.1	2.66	10	13	Beluga
34-8	4062.5	4063	8	0.63	-	33.4	12.5	2.66	13	14.5	Beluga
34-8	4076.5	4077	1.3	0.01	-	0	48.1	2.78	2	11	Beluga
34-8	4077.5	4078	1.8	0.01	-	0	55.6	2.8	0	10	Beluga
34-8	4079.5	4080	4.8	0.01	-	28.5	52.9	2.66	4	11	Beluga
34-8	4080.5	4081	7.1	0.49	-	23.3	54.3	2.66	6	15	Beluga
34-8	4102.5	4103	3.9	0.01	-	0	75.7	2.69	4	9.5	Beluga
34-8	4061.5	4062	12.8	2.52	-	32.7	16.1	2.66	11	15.5	Beluga
34-8	4081.5	4082	9.5	1.67	-	30.4	11.4	2.66	5	14	Beluga
34-8	4058.5	4059	9.8	1.99	-	34.2	34.2	2.67	14	16	Beluga
34-8	4057.5	4058	10.7	0.93	-	40.7	15.4	2.65	15	16	Beluga
34-8	4056.5	4057	12.2	1.83	-	40.3	26.3	2.66	14	15	Beluga
34-8	4055.5	4056	10.5	0.78	-	31.7	26.5	2.65	13.5	15	Beluga
34-8	4054.5	4055	9.9	1.5	-	34.9	20.1	2.65	13.5	15	Beluga
34-8	4053.5	4054	5.5	0.02	-	38	13.1	2.66	12	16	Beluga
34-8	4052.5	4053	4.3	0.05	-	53.5	23.4	2.65	8	13	Beluga
34-8	4051.5	4052	6.9	0.12	-	50.2	13.2	2.65	7	11	Beluga
34-8	4083.5	4084	11.9	2.11	-	29.3	28.1	2.66	7	10.5	Beluga
34-8	4084.5	4085	11.9	2.93	-	30.1	9.5	2.66	5.5	10	Beluga
34-8	4082.5	4083	10	1.58	-	29.3	11	2.65	8	13	Beluga
34-8	4060.5	4061	12.4	3.25	-	34.1	17.1	2.67	10	15	Beluga
34-8	4059.5	4060	13.9	5.12	-	43.1	13.9	2.67	12	15	Beluga
34-8	4050.5	4051	8.4	2.11	-	50.6	16.9	2.66	8	10.5	Beluga
41-8	4113.5	4113	5.9	0.2	-	41.4	35.9	2.66	12.5	14.5	Beluga
41-8	4114.5	4114	8.4	0.5	-	37.3	29.3	2.65	13	14.5	Beluga
41-8	4111.5	4111	6.9	0.01	-	51.1	32.7	2.66	12	15	Beluga
41-8	4127.5	4127	10.5	0.69	-	25	14	2.65	10	12.5	Beluga
41-8	4128.5	4128	9.7	0.7	-	30.8	15.4	2.65	6	12	Beluga

Well number	Core depth	Log depth	Core porosity	Horz perm	Vert perm	Core So	Core Sw	Grain density	Log Den porosity	Log D/N porosity	Log interval
41-8	4129.5	4129	10.2	1.02	-	48.5	15.5	2.65	2	9	Beluga
41-8	4130.5	4130	8.6	1.14	-	50.9	18.5	2.65	0	7	Beluga
41-8	4131.5	4131	7.8	0.62	-	49.3	24.7	2.65	4	8	Beluga
41-8	4132.5	4132	6.2	0.32	-	51.3	25.7	2.65	7	16.5	Beluga
41-8	4133.5	4133	2.5	0.82	-	25.6	61.4	2.66	9	14.5	Beluga
41-8	4134.5	4134	1	0.01	-	41.1	47	2.78	10.5	14	Beluga
41-8	4135.5	4135	0.7	0.42	-	0	86.5	2.68	9	12	Beluga
41-8	4137.5	4137	9.5	1.09	-	34.7	16.2	2.68	12	14	Beluga
41-8	4138.5	4138	11.5	1	-	35.9	12.6	2.67	14	15.5	Beluga
41-8	4112.5	4112	2.6	0.01	-	46.7	35	2.65	11.5	14	Beluga
41-8	4126.5	4126	9.1	0.77	-	36.4	17.3	2.65	11	13	Beluga
41-8	4125.5	4125	9.6	1.1	-	37.8	26	2.65	13	14	Beluga
41-8	4124.5	4124	9.1	0.57	-	41.6	28.6	2.65	13.5	15	Beluga
41-8	4123.5	4123	9	0.67	-	45	25.7	2.65	13.5	15	Beluga
41-8	4122.5	4122	10.6	0.64	-	36.4	20.2	2.66	13.5	15	Beluga
41-8	4139.5	4139	12.2	1.64	-	38.9	10.6	2.66	14	15.5	Beluga
41-8	4140.5	4140	2.8	0.01	-	39.6	28.3	2.66	14	15	Beluga
41-8	4141.5	4141	11.7	0.83	-	32.3	12.7	2.66	14.5	16	Beluga
41-8	4142.5	4142	10.7	0.58	-	29.1	13.7	2.65	15	17	Beluga
41-8	4143.5	4143	11.1	0.84	-	25.5	13.6	2.66	15.5	17	Beluga
41-8	4115.5	4115	9.9	0.26	-	37.3	23.3	2.66	13	15	Beluga
41-8	4121.5	4121	10.2	0.8	-	35.6	25.4	2.66	13	15	Beluga
41-8	4120.5	4120	9	0.63	-	31.6	19.8	2.66	12	14.5	Beluga
41-8	4119.5	4119	10.2	1.12	-	31	19.4	2.66	13	15	Beluga
41-8	4118.5	4118	9.6	0.86	-	34.7	16.3	2.65	13	15	Beluga
41-8	4117.5	4117	10.9	2.36	-	35.7	21	2.67	13	15	Beluga
41-8	4144.5	4144	10.4	0.27	-	46.9	9.4	2.66	14	16	Beluga
41-8	4145.5	4145	12.8	1.69	-	33.6	16	2.66	9	17	Beluga
41-8	4146.5	4146	13.7	3.21	-	49.6	9.4	2.66	10	15	Beluga
41-8	4147.5	4147	15	5.74	-	27.2	19.2	2.66	11.5	13	Beluga
41-8	4148.5	4148	20.5	10	-	35.8	11.9	2.66	13	14	Beluga
41-8	4149.5	4149	2.6	0.01	-	37.1	32.6	2.7	14	15	Beluga
41-8	4150.5	4150	8.1	0.38	-	39.5	31	2.66	14	15.5	Beluga
41-8	4151.5	4151	9.5	0.33	-	36.4	22.8	2.65	13	15.5	Beluga
41-8	4152.5	4152	9.7	0.73	-	31.8	14.4	2.66	13	16.5	Beluga
41-8	4153.5	4153	9.2	0.62	-	36.6	10	2.66	13.5	16	Beluga
41-8	4154.5	4154	9.9	0.46	-	30.4	15.2	2.66	14	16	Beluga
41-8	4155.5	4155	9.8	0.76	-	36.4	12.1	2.66	14	16	Beluga
41-8	4116.5	4116	9.2	0.64	-	44.5	28.8	2.66	13	15	Beluga
41-8	4156.5	4156	12.7	3.78	-	47.2	9.7	2.68	12	14	Beluga
41-8	4157.5	4157	12.6	4.43	-	37.7	11.5	2.67	10	12	Beluga
41-8	4158.5	4158	12.7	5.54	-	43.7	10.9	2.67	8	14	Beluga
41-8	4159.5	4159	11	2.32	-	40.8	9.8	2.66	6	16	Beluga
5-33	4666	4666	12.81	5.775	-			2.65	15.5	16	Beluga
10-34	5880	5880	13.7	9.6	-	34.1	27.6	2.65	15.5	17	CP
10-34	5961	5961	9.7	0.26	-	18	45.3	2.65	11.5	12	CP
10-34	5920	5920	7.9	0.1	-	41.4	32.8	2.69	9	11	CP
10-34	5956	5956	9.2	0.22	-	19.9	46.3	2.66	11	11.5	CP
10-34	5924	5924	9.1	0.12	-	43.4	32.9	2.66	10	12	CP
1-26	5310.5	5310	1.8	126	114	0	90.4	2.71	6	18	CP
1-26	5309.5	5309	2.1	0.001	0.01	0	95.2	2.7	8	19	CP
1-26	5308.5	5308	2.2	0.01	0.001	0	94.9	2.71	10	21	CP

Well number	Core depth	Log depth	Core porosity	Horz perm	Vert perm	Core So	Core Sw	Grain density	Log Den porosity	Log D/N porosity	Log interval
1-26	5296.5	5296	7.4	0.22	0.01	25.3	45.9	2.67	10	12.5	CP
1-26	5295.5	5295	6.9	0.73	0.01	29.5	40.1	2.67	9	12	CP
1-26	5294.5	5294	9.2	274	243	30.3	30.2	2.68	11	13	CP
1-26	5293.5	5293	8.8	0.18	0.06	34.7	30.2	2.66	11	13	CP
1-26	5312.5	5312	2.6	413	365	0	92.1	2.72	6	19	CP
1-26	5307.5	5307	3.9	0.16	0.01	0	94.6	2.71	6	19	CP
1-26	5290.5	5290	8	4.2	0.03	29.9	37.2	2.66	12	14	CP
1-26	5289.5	5289	9.1	0.88	0.21	34.3	29.9	2.66	11	13	CP
1-26	5288.5	5288	8.9	0.22	0.22	34.8	32	2.65	10	13	CP
1-26	5287.5	5287	8.9	14	0.15	35.1	30.7	2.67	11	13.5	CP
1-26	5286.5	5286	7.5	0.12	0.07	26.5	41.1	2.66	12	13.5	CP
1-26	5285.5	5285	9.3	0.23	0.18	32.9	29.2	2.65	11	13.5	CP
1-26	5284.5	5284	10.2	174	0.53	37.8	26	2.67	11	13	CP
1-26	5283.5	5283	9.2	0.19	0.16	32.9	30.1	2.65	10	13	CP
1-26	5282.5	5282	8.6	0.14	0.13	27.7	36.5	2.64	7	13.5	CP
1-26	5273.5	5273	5.7	5.4	0.03	6.7	76.7	2.68	6	13	CP
1-26	5291.5	5291	8.7	0.17	0.1	35.5	32.1	2.65	11	13	CP
1-26	5292.5	5292	7.8	0.21	0.05	37.6	38	2.66	11.5	13	CP
1-26	5276.5	5276	4.4	0.19	0.08	0	93.6	2.68	6	10	CP
1-26	5275.5	5275	4.5	0.95	0.04	0	89.2	2.68	6	9.5	CP
1-26	5281.5	5281	9.2	0.17	0.15	31.8	31.2	2.65	6	12	CP
1-26	5280.5	5280	9.5	0.12	0.13	30.3	34	2.65	7	10.5	CP
1-26	5279.5	5279	8.4	0.06	0.06	26.3	43.1	2.65	8	10.5	CP
1-26	5278.5	5278	8.1	0.06	0.05	22.1	51	2.65	6	10	CP
1-26	5277.5	5277	3.2	0.06	0.001	6.2	91.3	2.67	5	10	CP
1-26	5274.5	5274	5.2	0.06	0.03	7.1	77.1	2.64	6	11	CP
1-26	5272.5	5272	4	0.02	0.01	0	84.7	2.68	4	12	CP
1-26	5271.5	5271	3.8	0.01	0.001	0	72.9	2.69	2	9.5	CP
1-26	5270.5	5270	3.7	0.001	0.001	0	89.3	2.68	2	9.5	CP
1-26	5269.5	5269	3.9	0.01	0.001	0	86.2	2.68	2	9.5	CP
1-26	5268.7	5268	4.3	0.001	0.001	0	89.3	2.71	2	9.5	CP
1-26	5267.2	5267	5.5	0.31	0.08	0	95.5	2.72	3	10	CP
1-26	5266.5	5266	4	1.3	0.001	0	96.4	2.71	6	9	CP
15.24B	4798.5	4796	3	0.01	-	-	-	2.68	0	5	CP
15-24B	4771.5	4769	1.9	0.03	-	-	-	2.71	0	6	CP
15-24B	4810.5	4808	7.8	0.16	-	-	-	2.63	0	12.5	CP
15-24B	4774.5	4772	7.2	1	-	-	-	2.75	0	8	CP
15-24B	4800.5	4798	4.1	0.02	-	-	-	2.69	0	7	CP
15-24B	4772.5	4770	11.2	3.4	-	-	-	2.67	3	10.5	CP
15-24B	4779.5	4777	5.6	0.12	-	-	-	2.67	0	0	CP
15-24B	4789.5	4787	0.8	0.02	-	-	-	2.66	3	6.5	CP
15-24B	4778.5	4776	7.7	0.57	-	-	-	2.64	0	0	CP
15-24B	4775.5	4773	10.3	0.7	-	-	-	2.69	0	4	CP
15-24B	4797.5	4795	4.4	0.03	-	-	-	2.66	0	4	CP
15-24B	4773.5	4771	15.6	4.1	-	-	-	2.68	1	9	CP
15-24B	4799.5	4798	6.2	0.06	-	-	-	2.67	0	7	CP
15-24B	4791.5	4789	0.9	0.03	-	-	-	2.7	0	2	CP
15-24B	4796.5	4794	3.7	0.05	-	-	-	2.54	0	4.5	CP
15-24B	4768.5	4766	4.9	0.05	-	-	-	2.3	16	16	CP
15-24B	4776.5	4774	10.2	0.62	-	-	-	2.69	0	3.5	CP
15-24B	4808.5	4806	11.4	2.6	-	-	-	2.63	7	13	CP
15-24B	4786.5	4784	0.6	0.02	-	-	-	2.7	0	0	CP

Well number	Core depth	Log depth	Core porosity	Horz perm	Vert perm	Core So	Core Sw	Grain density	Log Den porosity	Log D/N porosity	Log interval
15-24B	4785.5	4783	0.5	0.001	-	-	-	2.69	0	0	CP
15-24B	4780.5	4778	0.6	0.02	-	-	-	2.7	0	0	CP
15-24B	4781.5	4779	1.6	0.01	-	-	-	2.74	0	0	CP
15-24B	4769.5	4767	8.1	3.2	-	-	-	2.71	-6	7	CP
15-24B	4783.5	4781	1.3	0.02	-	-	-	2.69	0	0	CP
15-24B	4784.5	4782	4.2	0.04	-	-	-	2.67	0	0	CP
15-24B	4770	4768	1.6	0.03	-	-	-	2.7	0	1.5	CP
15-24B	4787.5	4785	0.4	0.02	-	-	-	2.68	0	0	CP
15-24B	4792.5	4790	0.1	0.02	-	-	-	2.68	0	2.5	CP
15-24B	4803.5	4801	5.8	0.14	-	-	-	2.79	1	8.5	CP
15-24B	4793.5	4791	0.9	0.53	-	-	-	2.69	0	5	CP
15-24B	4788.5	4786	4.3	0.12	-	-	-	2.69	1	5	CP
15-24B	4794.5	4792	0.3	0.02	-	-	-	2.74	0	9	CP
15-24B	4795.5	4793	1.6	0.04	-	-	-	2.54	0	6	CP
15-24B	4790.5	4788	0.8	0.11	-	-	-	2.36	0	2.5	CP
15-24B	4809.5	4807	9	0.57	-	-	-	2.61	5	12	CP
15-24B	4798.5	4797	4.9	0.03	-	-	-	2.65	0	6	CP
15-24B	4777.5	4775	0.1	0.02	-	-	-	2.69	0	3	CP
15-24B	4801.5	4799	6.4	0.1	-	-	-	2.71	0	7	CP
15-24B	4802.5	4800	5.8	0.08	-	-	-	2.72	0	7	CP
15-24B	4807.5	4805	10.8	1.8	-	-	-	2.63	7.5	13	CP
15-24B	4804.5	4802	6.8	0.23	-	-	-	2.69	1	8.5	CP
15-24B	4805.5	4803	7.7	0.56	-	-	-	2.66	2	9.5	CP
15-24B	4806.5	4804	9.4	0.93	-	-	-	2.65	6	12	CP
15-24B	4782.5	4780	1.5	0.02	-	-	-	2.69	0	0	CP
2-25	5536.7	5541	9.7	0.06	-	8.4	45.9	2.66	9.5	11.5	CP
2-25	5533.9	5538	6.3	0.022	-	10.4	46.6	2.67	9	11.5	CP
2-25	5535.4	5540	7.7	0.061	-	9.2	41.6	2.67	9	11.5	CP
2-25	5531.5	5535	6	0.004	-	10.4	52.2	2.67	8	12	CP
2-25	5530.2	5534	7.8	0.042	-	11.2	51.4	2.66	24	19	CP
2-25	5529.1	5533	6.8	0.027	-	15.3	38.3	2.66	28	23	CP
2-25	5532.7	5537	10.3	0.335	-	8.9	28.8	2.66	8	12.5	CP
2-25	5539.8	5544	8.8	0.053	-	7.8	31	2.65	11.5	14	CP
2-25	5538.4	5542	7	0.039	-	11.6	36.4	2.64	11.5	14	CP
2-25	5540.7	5545	4.8	0.014	-	12.5	40.6	2.66	11.5	14	CP
2-25	5528.1	5532	9	0.315	-	13.5	44.3	2.66	14	16	CP
33-8	5458.5	5456	10.4	0.51	0.38	53.6	12.8	2.65	12	12	CP
33-8	5455.5	5453	8.8	0.25	0.17	47.8	18.3	2.68	9	9.5	CP
33-8	5459.5	5457	10	0.39	0.33	52.1	14	2.67	10	11	CP
33-8	5453.5	5451	6.9	0.17	0.01	45.7	27.2	2.71	10	10.5	CP
33-8	5452.5	5450	9.8	0.28	0.17	51.2	14.5	2.68	11	11	CP
33-8	5451.5	5449	10.4	0.53	0.46	50.6	13.3	2.65	10.5	11	CP
33-8	5454.5	5452	10.2	0.51	0.19	49	16.5	2.67	9.5	10	CP
33-8	5448.5	5446	6.5	0.16	0.01	45.6	33.5	2.66	13.5	13.5	CP
33-8	5461.5	5459	4.9	0.1	0.01	44.1	30.6	2.67	10	10.5	CP
33-8	5447.5	5445	9.8	0.46	0.29	52.2	15.3	2.64	13.5	13.5	CP
33-8	5446.5	5444	8.9	0.56	0.08	49.8	21	2.64	12	12	CP
33-8	5445.5	5443	7.6	0.27	0.08	55.5	16.8	2.65	7	9	CP
33-8	5444.5	5442	10.2	0.59	0.49	49.1	15.5	2.64	6	8	CP
33-8	5442.5	5440	11.3	1.3	1	50.5	10.6	2.64	7	7.5	CP
33-8	5440.5	5438	9	0.52	0.96	45.8	22.4	2.65	4	6.5	CP
33-8	5456.5	5454	7.8	0.12	0.01	47.8	19.8	2.69	12	12	CP

Well number	***Core depth***	***Log depth***	***Core porosity***	***Horz perm***	***Vert perm***	***Core So***	***Core Sw***	***Grain density***	***Log Den porosity***	***Log D/N porosity***	***Log interval***
33-8	5457.5	5455	8.4	0.2	0.11	46.8	20.1	2.66	13	13	CP
33-8	5441.5	5439	11	1.4	2.4	49.4	14.9	2.63	5	7	CP
33-8	5443.5	5441	11.5	2.1	1.6	51.9	10.1	2.63	7	8	CP
33-8	5446	5446	6.9	0.77	-	46.1	31.1	2.64	13.5	13.5	CP
33-8	5462	5462	8.3	0.17	-	54	19.6	2.68	12	12	CP
33-8	5455	5455	11.5	0.67	-	43.4	19.1	2.66	13	13	CP
41-8	5487.5	5487	2.9	0.03	-	29.2	38.9	2.66	4	8	CP
41-8	5488.5	5488	2.2	0.01	-	0	87.7	2.68	2	11	CP
41-8	5486.5	5486	5.4	0.11	-	46	23	2.65	6	7.5	CP
41-8	5480.5	5480	4.6	0.01	-	3.8	91.5	2.72	2	15	CP
41-8	5479.5	5479	1.7	0.01	-	3.6	72.5	2.73	2	12	CP
41-8	5478.5	5478	2.8	0.01	-	4.9	87.9	2.69	2	11	CP
41-8	5477.5	5477	2.1	0.01	-	22.6	60.3	2.71	2.5	8	CP
41-8	5485.5	5485	7	0.24	-	40.2	23	2.65	7	9	CP
41-8	5484.5	5484	3.4	0.06	-	45.2	18.1	2.66	8	10	CP
41-8	5476.5	5476	1.9	0.01	-	42	33.6	2.72	2	6	CP
41-8	5475.5	5475	1.7	0.01	-	19.7	52.5	2.71	1	5.5	CP
41-8	5474.5	5474	2.4	0.01	-	37.7	41.9	2.66	2	5.5	CP
41-8	5473.5	5473	2.9	0.09	-	21.3	34.1	2.67	5	7	CP
5-33	5918	5918	10.17	0.683	-	-	-	2.66	3	9	CP
5-33	5922	5922	8.96	0.141	-	-	-	2.65	10	12	CP
5-33	6028	6028	4.24	0.013	-	-	-	2.76	3	8	CP
5-33	5931	5931	9.51	0.108	-	-	-	2.67	9	11.5	CP
5-33	6054	6054	7.33	0.036	-	-	-	2.66	10	12.5	CP
5-33	5993	5993	9.68	0.168	-	-	-	2.66	4	16	CP
9-34	5903	5903	9.7	0.14	-	40.4	35.2	2.68	11	12	CP
9-34	5857	5857	10.6	0.15	-	33.7	37.5	2.67	10	13	CP
9-34	6093	6093	7.7	0.2	-	38.3	55.1	2.68	12	14	CP
9-34	5862	5862	14	5	-	34.3	36.4	2.65	11.5	13.5	CP
9-34	5858	5858	10	0.17	-	33.7	30.3	2.68	10	13	CP
10-34	5007	5007	14	5.5	-	36	39.4	2.66	14	16	MB
10-34	4998	4998	13.3	1.2	-	37.6	48.5	2.66	4	12	MB
10-34	5006	5006	12.2	0.6	-	47.3	17.4	2.66	15	17	MB
10-34	4989	4989	5.8	0.04	-	39.9	18.8	2.67	16	17.5	MB
11-16H	4641.5	4641	1.5	0.02	-	0	29.2	2.68	6	15	MB
11-16H	4636.5	4636	1	0.01	-	0	28.7	2.67	4	14	MB
11-16H	4634.5	4634	1	0.01	-	0	52.4	2.68	8	16	MB
11-16H	4633.5	4633	1.2	0.01	-	0	26.1	2.69	12	18	MB
11-16H	4631.5	4631	0.7	0.01	-	0	57.7	2.68	2	11	MB
11-16H	4630.5	4630	0.7	0.01	-	0	61.1	2.69	2	13	MB
11-16H	4611.5	4611	1.9	0.01	-	0	60.4	2.68	6	14	MB
11-16H	4610.5	4610	2.8	0.01	-	0	80.8	2.67	4	13	MB
11-16H	4586.5	4586	1.5	0.01	-	0	51.4	2.72	4	11	MB
11-16H	4587.5	4587	0.9	0.01	-	0	64.4	2.7	5	12	MB
11-16H	4609.5	4609	0.9	0.01	-	22.6	52.8	2.66	1	11	MB
11-16H	4608.5	4608	1	0.01	-	0	50.8	2.68	3	7.5	MB
12-35	5009.5	5006	16.4	119	-	41.7	9.1	2.65	18	20	MB
12-35	5022.5	5019	3.3	0.01	-	21.6	5.6	2.69	14	15	MB
12-35	5020.5	5017	8.7	0.28	-	46.2	15	2.65	14	14	MB
12-35	5019.5	5016	10.3	0.13	-	45.5	13.3	2.64	14	14	MB
12-35	5023.5	5020	3	0.001	-	31.1	51.9	2.66	14	14	MB
12-35	5019.5	5014	9.1	0.61	-	38.1	21.4	2.67	8	12	MB

Well number	*Core depth*	*Log depth*	*Core porosity*	*Horz perm*	*Vert perm*	*Core So*	*Core Sw*	*Grain density*	*Log Den porosity*	*Log D/N porosity*	*Log interval*
12-35	5018.5	5015	10.3	0.66	-	44.5	16.2	2.65	14	15	MB
12-35	5005.5	5002	9	0.47	-	37.9	11.8	2.66	12	13.5	MB
12-35	5006.5	5004	3.9	0.001	-	48.1	26.2	2.68	10	15	MB
12-35	5021.5	5018	5	0.01	-	48.8	19.6	2.65	12	12	MB
12-35	5008.5	5005	16.5	127	-	31.6	12.1	2.64	12	20	MB
12-35	5024.5	5021	2.5	0.001	-	33.9	52.2	2.68	12	12	MB
12-35	5010.5	5007	9.6	2.2	-	44.8	8.5	2.66	18	19	MB
12-35	5011.5	5008	9.4	2.4	-	40.1	11.5	2.66	15	15	MB
12-35	5007.5	5004	4.4	0.001	-	0	86	2.71	7	18.5	MB
12-35	5012.5	5009	9	0.33	-	45.9	11	2.66	14	14	MB
12-35	5016.5	5013	5.6	0.01	-	26.7	57.9	2.72	7	10.5	MB
12-35	5015.5	5012	6.8	0.12	-	57.3	17.9	2.65	7	10	MB
12-35	5014.5	5011	2.8	0.001	-	58	21	2.66	5	11.5	MB
12-35	5013.5	5010	2.8	0.001	-	38.6	49.7	2.74	8	12	MB
12-4	4895.5	4895	2.1	0.01	-	35.2	56.3	2.7	13	14.5	MB
12-4	4894.5	4894	1.2	0.01	-	70.2	20	2.68	14	15	MB
12-4	4876.5	4876	2.6	0.01	-	4.5	90	2.64	6	13	MB
12-4	4875.5	4875	2.7	0.01	-	9.5	85.2	2.65	7	12.5	MB
12-4	4874.5	4874	3.2	0.01	-	27.2	66.4	2.66	6	11	MB
12-4	4893.5	4893	4.6	0.03	-	54.6	13.7	2.66	14	15.5	MB
12-4	4892.5	4892	6.8	0.49	-	30.3	15.2	2.66	12	16	MB
12-4	4891.5	4891	7.4	0.04	-	46.1	25.9	2.67	9	15	MB
12-4	4890.5	4890	8.2	0.6	-	53.8	28.3	2.68	8	12	MB
12-4	4889.5	4889	7.6	0.06	-	47.4	27.1	2.68	10	12	MB
12-4	4888.5	4888	7.6	0.06	-	40.8	29.9	2.66	13.5	13.5	MB
12-4	4887.5	4887	6.9	0.03	-	38.5	31.3	2.66	10	14	MB
12-4	4886.5	4886	11	0.49	-	37.1	16.9	2.65	7	12.5	MB
12-4	4885.5	4885	9.4	0.1	-	38.6	21.4	2.68	7.5	11.5	MB
12-4	4884.5	4884	7.5	0.29	-	38.3	29.8	2.68	8	12	MB
12-4	4883.5	4883	2.6	0.01	-	28.9	47	2.67	7	11.5	MB
12-4	4882.5	4882	6.2	0.29	-	59.7	18.6	2.67	5.5	12	MB
12-4	4881.5	4881	7.5	0.13	-	36.7	20.6	2.67	5.5	12.5	MB
12-4	4880.5	4880	6.9	0.06	-	32.5	23.8	2.65	6	13	MB
12-4	4879.5	4879	6	0.09	-	45.1	35.5	2.65	6.5	11	MB
12-4	4878.5	4878	5.9	0.07	-	50.5	33.7	2.65	6.5	11	MB
12-4	4877.5	4877	4	0.02	-	50.4	19.2	2.66	6	13.5	MB
12-4	4873.5	4873	3	0.01	-	26.5	64.9	2.65	4	8	MB
12-4	4872.5	4872	2.8	0.01	-	31	55.1	2.67	3	9.5	MB
12-4	4871.5	4871	2	0.01	-	9.4	84.5	2.67	3	11	MB
15-17	4304.5	4313	5.1	0.01	5.1	0	85.6	2.69	4	12	MB
15-17	4302.5	4311	10.5	0.22	10.5	0	71.6	2.67	3.5	11.5	MB
15-17	4300.5	4309	3.6	0.01	3.6	0	61.1	2.67	4	7.5	MB
15-17	4287.5	4296	13	40	17	29.1	37.8	2.68	13	16.5	MB
15-17	4286.5	4295	12.6	29	11	23.2	42.7	2.68	16	18	MB
15-17	4285.5	4294	12.8	21	31	29.2	29.3	2.67	15	18.5	MB
15-17	4284.5	4293	12.5	4.11	1.65	29.4	35.3	2.68	15	19	MB
15-17	4283.5	4292	11.7	1.66	0.45	7.6	69.1	2.67	14	17.5	MB
15-17	4281.5	4290	14.4	27	22	29.1	31.8	2.66	16	19.5	MB
15-17	4280.5	4289	15.8	42	28	29.5	29.5	2.65	19	21	MB
15-17	4279.5	4288	15.8	49	44	29	30.3	2.65	20	21.5	MB
15-17	4278.5	4287	16.7	42	49	28.8	36.3	2.65	21.5	23	MB
15-17	4277.5	4286	15.6	28	21	26.8	40.7	2.65	20.5	23	MB

Well number	*Core depth*	*Log depth*	*Core porosity*	*Horz perm*	*Vert perm*	*Core So*	*Core Sw*	*Grain density*	*Log Den porosity*	*Log D/N porosity*	*Log interval*
15-17	4276.5	4285	13.5	8.4	1.42	28.4	45.2	2.65	20.5	23	MB
15-17	4275.5	4284	16.1	17	15	28.3	34.3	2.66	18.5	21.5	MB
15-17	4274.5	4283	15.4	8.7	9.02	19.5	46.7	2.66	18.5	21	MB
15-17	4273.5	4282	15.5	8.51	6.34	23.6	38.6	2.66	17.5	20	MB
15-17	4272.5	4281	14.6	8.21	4.78	26.6	38.1	2.66	17.5	20	MB
15-17	4271.5	4280	14.6	5.4	3.7	20.6	47.7	2.65	19.5	21	MB
15-17	4270.5	4279	13.6	2.57	0.84	23.6	40.4	2.67	17.5	20	MB
15-17	4269.5	4278	14.7	7.87	2.41	22.8	40.2	2.66	13.5	18	MB
15-17	4268.5	4277	14.3	4.98	1.58	26.2	39	2.66	13.5	18	MB
15-17	4267.5	4276	15.7	11	8.52	26.2	42.7	2.65	15.5	19	MB
15-17	4266.5	4275	14.7	4.8	1.49	22.4	45.6	2.65	16.5	20	MB
15-17	4265.5	4274	16.2	17	12	23.7	39.4	2.64	17.5	19	MB
15-17	4264.5	4273	15.7	16	9.25	23.4	41.4	2.65	18	19	MB
15-17	4263.5	4272	17.1	30	20	24.4	40.2	2.65	17.5	19.5	MB
15-17	4262.5	4271	12.1	5.56	1.42	27.4	31.4	2.66	16.5	20	MB
15-17	4261.5	4270	10.4	1.12	0.75	29.8	29.1	2.66	12	19	MB
15-17	4260.5	4269	13.3	23	18	24.4	35.6	2.66	9.5	15	MB
15-17	4282.5	4291	5.5	0.03	0.04	12.7	77.1	2.71	13	17	MB
23-25	5170.5	5165	12.3	2.59	0.209	24	31.8	2.67	14.5	14.5	MB
23-25	5171.5	5166	12.5	2.12	1.97	26.3	32	2.67	14	15	MB
23-25	5173.5	5168	15.3	6.28	0.833	36.3	25.9	2.67	17	17.5	MB
23-25	5172.5	5167	13.4	5.58	1.97	33.5	29.6	2.67	14	15.5	MB
23-25	5175.5	5170	13.8	4.29	0.638	34.2	28.7	2.66	17.5	17.5	MB
23-25	5176.5	5171	14.3	1.37	0.775	29.8	27.8	2.66	17	17	MB
23-25	5177.5	5172	14	7.41	0.349	29	31.1	2.66	16.5	16.5	MB
23-25	5174.5	5169	15.2	6.2	1.91	39.3	26.1	2.67	18	18	MB
23-25	5179.5	5174	13	8	0.345	30	30.8	2.67	15.5	16	MB
23-25	5180.5	5175	11.9	1.38	0.117	21.9	34.9	2.67	14	15	MB
23-25	5181.5	5176	10.5	1.85	1.85	20.4	36	2.66	14	15	MB
23-25	5182.5	5177	6.4	0.125	0.0001	1.5	63	2.66	10	12	MB
23-25	5183.5	5178	6.2	0.143	0.128	2.5	62.8	2.65	8	10	MB
23-25	5184.5	5179	4	0.027	0.002	0	90.5	2.71	7	9.5	MB
23-25	5178.5	5173	12.7	2.34	0.268	27.5	32.4	2.66	16	17	MB
23-25	5164.5	5159	7.6	2.69	0.002	15	52.5	2.68	6	12.5	MB
23-25	5169.5	5164	12.6	0.847	0.001	24	34.1	2.66	15	15	MB
23-25	5168.5	5163	12.8	1.02	0.375	26.3	32.4	2.67	15	15.5	MB
23-25	5167.5	5162	12.8	1.71	0.141	26.5	34.1	2.66	15	15.5	MB
23-25	5166.5	5161	13.4	2.46	1.12	34.2	29.4	2.87	14	15	MB
23-25	5165.5	5160	12.7	4.82	0.805	16.6	37	2.67	10	13	MB
33-11J	4856.5	4861	10	0.46	0.21	27.5	12.4	2.65	12	14	MB
33-11J	4855.5	4860	7.2	0.04	0.01	31.7	39.1	2.66	8	13	MB
33-11J	4854.5	4859	7.9	0.01	0.001	0	87	2.69	7	13	MB
33-11J	4859.5	4864	9	0.08	0.05	38	23.3	2.66	4	12	MB
33-11J	4863.5	4868	9.7	0.14	0.04	28.2	29	2.66	13	15	MB
33-11J	4864.5	4869	10.3	0.99	0.13	43.1	14.8	2.66	3	9	MB
33-11J	4869.5	4874	13.8	19	1.9	37.2	14.6	2.65	4	12	MB
33-11J	4865.5	4870	12.3	1.1	0.26	0.5	16.5	2.66	4	14	MB
33-11J	4866.5	4871	10.6	2.2	0.2	39.1	20.3	2.65	3.5	11.5	MB
33-11J	4867.5	4872	12.9	7.2	0.17	38.8	21.5	2.68	10	16	MB
33-11J	4858.5	4863	8.3	0.06	0.02	37.5	21.7	2.66	6	11.5	MB
33-11J	4857.5	4862	11	1.1	0.82	31.6	14.4	2.65	11	13	MB
33-11J	4860.5	4865	8.1	0.01	0.001	0	82.6	2.68	6	12.5	MB

Well number	*Core depth*	*Log depth*	*Core porosity*	*Horz perm*	*Vert perm*	*Core So*	*Core Sw*	*Grain density*	*Log Den porosity*	*Log D/N porosity*	*Log interval*
33-11J	4868.5	4873	4.5	0.03	0.001	24.8	27.2	2.66	12	18	MB
33-8	4656.5	4656	14.7	7.8	3	49.3	13.4	2.65	13	13	MB
33-8	4657.5	4657	14.9	19	19	52.1	12.7	2.66	15	15	MB
33-8	4658.5	4658	14	11	7.4	59.6	6.9	2.66	16	16	MB
33-8	4655.5	4655	13.9	8.7	3.8	59.6	6.2	2.64	6	9	MB
33-8	4659	4659	15.3	569		36	57.3	2.66	6	12	MB
33-8	4645.5	4645	6.4	0.04	1186	43	38.2	2.65	5	7	MB
33-8	4659.5	4659	12.2	7	2.2	45.1	12.6	2.65	16	16	MB
33-8	4644.5	4644	6.7	0.02	79	28.1	56	2.67	7	8.5	MB
33-8	4655	4655	4.4	0.02	-	54.3	34.2	2.66	4	11	MB
33-8	4654.5	4654	12.7	2.8	0.72	48.8	9.7	2.64	5	7	MB
33-8	4648.5	4648	4.8	0.07	0.01	5.9	68.7	2.66	4	9	MB
33-8	4653.5	4653	9.9	0.4	0.02	43.9	19	2.65	6	8	MB
33-8	4650.5	4650	3.7	1.1	0.1	39.6	31.9	2.66	7	9.5	MB
33-8	4643.5	4643	5.3	0.1	24	42.5	64.3	2.67	7	9	MB
33-8	4642.5	4642	5.2	0.02	0.01	37.8	42.5	2.65	6	8	MB
3A-35	4991.4	4986	11.3	0.615	-	17.5	18.1	2.64	12	20	MB
3A-35	4992.9	4988	12.7	2.67	-	16.5	14.2	2.63	12	21	MB
3A-35	4994.4	4989	13.2	3.21	-	12.2	11.3	2.64	5	17	MB
3A-35	5000.5	4996	13.9	9.4	-	12.3	9.5	2.67	3.5	11	MB
3A-35	5002.2	4997	11.6	2.02	-	19.7	19	2.64	3.5	9.5	MB
3A-35	4997.5	4995	13.3	2.57	-	13.4	12.2	2.64	3.5	11	MB
5-33	5040	5040	4.93	0.031	-	-	-	2.66	4	12	MB
5-33	5035	5035	10.62	0.912	-	-	-	2.65	5	14.5	MB
5-33	5033	5033	9.48	0.203	-	-	-	2.65	1.5	11	MB
5-33	5028	5028	12.28	0.755	-	-	-	2.65	7.5	14.5	MB
5-33	5023	5023	5.35	0.022	-	-	-	2.66	6	9	MB
6-32	5051-52	5055	9.6	0.25	-	42.6	9.8	2.64	5	7.5	MB
6-32	5047-48	5051	5.5	0.15	-	49.7	9.1	2.65	8	11	MB
6-32	5048-49	5052	11.3	8.5	-	47.8	9.7	2.65	8.5	10	MB
6-32	5050-51	5054	11.5	1.9	-	48	7.9	2.64	7	10	MB
6-32	5049-50	5053	10.2	0.64	-	41.4	8.9	2.64	8	9.5	MB
6-32	5043-44	5047	4.3	0.01	-	0	83.5	2.65	12.5	14	MB
6-32	5052-53	5056	9.8	0.25	-	45.7	9.1	2.64	5.5	7.5	MB
6-32	5042-43	5046	5.3	0.09	-	40.4	22.4	2.67	13	15	MB
6-32	5046-47	5050	4.1	0.08	-	0	90.8	2.71	6	13	MB
6-35	5041	5044	12.5	28	-	42.9	10.5	2.66	12	14.5	MB
6-35	5040	5043	11.9	14	-	37.4	14.2	2.72	14	17	MB
6-35	5039	5042	15.8	155	-	41.7	13.2	2.69	16	19.5	MB
6-35	5036	5039	16.9	124	-	36.5	15.4	2.67	15	19	MB
6-35	5035	5038	13.6	9.6	-	37.5	13.4	2.66	14	17	MB
6-35	5047	5050	4.2	0.01	-	49	18.4	2.66	6	10	MB
6-35	5033	5036	12.6	7.5	-	43.3	11.4	2.66	12	17	MB
6-35	5032	5035	8.6	0.27	-	34.9	15.5	2.67	13	16.5	MB
6-35	5031	5034	13.3	4.7	-	36	16.6	2.66	15	17	MB
6-35	5030	5033	14	6.5	-	40.4	15.5	2.66	15	17.5	MB
6-35	5029	5032	13.8	4.1	-	37.8	13.7	2.67	12	17.5	MB
6-35	5028	5031	14.1	7	-	40.7	17.8	2.66	9	18	MB
6-35	5026	5029	14.1	5.9	-	33.5	21.3	2.67	12	16.5	MB
6-35	5038	5041	17.3	170	-	33.5	17.9	2.66	18	21	MB
6-35	5037	5040	17.3	118	-	33.4	15.7	2.66	17	20.5	MB
6-35	5034	5037	13	4.4	-	38.4	13.5	2.65	15	19	MB

Well number	***Core depth***	***Log depth***	***Core porosity***	***Horz perm***	***Vert perm***	***Core So***	***Core Sw***	***Grain density***	***Log Den porosity***	***Log D/N porosity***	***Log interval***
9-34	4994	4994	6.3	0.04	-	55	34.9	2.66	10.5	10.5	MB
9-34	5004	5004	11	0.45	-	50.1	20.2	2.65	13	15.5	MB
9-34	5006	5006	13.5	1.7	-	51.5	12.5	2.66	15	16	MB
10-34	5810	5810	10.6	0.15	-	48.2	16.4	2.69	15	17.5	Travis
10-34	5800	5800	14.8	0.43	-	41.8	25.9	2.67	16.5	19	Travis
10-34	5514	5514	11.8	0.09	-	49.2	25.6	2.66	12.5	16.5	Travis
10-34	5510	5510	12	0.09	-	50.7	22.6	2.66	12.5	16	Travis
13-32	5600	5600	15	6.27	-	-	-	-	16.5	18	Travis
13-32	5584	5584	13	1.73	-	-	-	-	14.5	17	Travis
13-32	5540	5540	9.9	0.63	-	-	-	-	11	14	Travis
14A-28	5639	5336	9	0.46	0.5	49.6	34.2	2.66	12.5	16.5	Travis
14A-28	5598	5595	16.6	13	0.43	70.7	16.4	2.65	18	20.5	Travis
14A-28	5638	5635	11.7	0.77	0.99	40.5	20.2	2.66	12	16	Travis
14A-28	5615	5612	12.5	0.14	0.07	29.1	44.2	2.66	12.5	17	Travis
14A-28	5595	5592	14.8	3.5	0.07	67	20.4	2.65	16.5	19	Travis
16	4805.5	4805	13.8	0.17	0.001	82.3	10	2.73	12	15	Travis
16	4694.5	4694	1.5	0.38	0.11	72.3	20.6	2.67	20	20	Travis
16	4804.5	4804	9.5	0.01	0.001	69.8	23.3	2.69	12	16	Travis
16	4802.5	4802	2.9	3.9	1	79	12.3	2.69	6	14	Travis
16	4789.5	4789	16.1	0.13	0.001	23	33.5	2.81	8	14	Travis
16	4788.5	4788	9.1	0.01	0.001	49.6	37	2.69	8	14	Travis
16	4787.5	4787	13.5	0.26	0.09	27.6	55.3	2.77	8	13	Travis
16	4776.5	4776	2	0.03	0.03	7.4	59	2.69	6	14	Travis
16	4771.5	4771	10.3	0.2	0.17	82.1	12.1	2.78	17	17	Travis
16	4770.5	4770	4.2	57	15	81	12.2	2.69	11	14	Travis
16	4769.5	4769	8.3	0.11	0.001	67.9	15.9	2.71	10	12	Travis
16	4751.5	4751	7.7	0.06	0.04	74	12.1	2.72	6	10	Travis
16	4750.5	4750	7.5	0.07	0.08	73.8	13.6	2.76	6	10	Travis
16	4749.5	4749	4.1	270	52	70.5	18.3	2.71	2	8	Travis
16	4748.5	4748	6.5	13	2.3	80.7	8.7	2.68	1	7	Travis
16	4747.5	4747	5.1	8.3	0.56	59.1	22.8	2.75	2	10	Travis
16	4736.5	4736	6	2396	1.1	30.2	60.4	2.67	6	8	Travis
16	4735.5	4735	13	0.01	0.001	59.4	28.1	2.71	8	10	Travis
16	4734.5	4734	9.1	0.27	0.001	39.1	20.4	2.75	10	12	Travis
16	4733.5	4733	6.4	256	0.01	61	20.3	2.73	8	12	Travis
16	4730.5	4730	6.1	0.01	0.001	47.3	13.5	2.71	8	11	Travis
16	4729.5	4729	6.5	1923	0.26	55.8	33.1	2.73	6	10	Travis
16	4726.5	4726	3.2	0.26	0.07	65.8	19.7	2.69	6	9	Travis
16	4723.5	4723	11.9	0.4	0.28	57.7	8.4	2.75	12	16	Travis
16	4707.5	4707	14.9	0.19	0.17	54.1	30.3	2.73	6	9	Travis
16	4706.5	4706	5	3.2	9.32	62.2	19.2	2.64	12	16	Travis
16	4695.5	4695	1.4	9.9	0.43	74.8	14.7	2.67	24	24	Travis
33-11J	5204.5	5209	2	0.03	0.01	2	36.8	2.68	6	11	Travis
33-11J	5203.5	5208	2.8	0.02	0.02	27.2	57.9	2.67	14	15	Travis
33-11J	5202.5	5207	5.6	0.03	0.001	48.6	16.4	2.68	15	16.5	Travis
33-11J	5201.5	5206	5.5	0.01	0.02	63.5	9.4	2.66	16	18	Travis
33-11J	5200.5	5205	6.2	0.1	0.001	56.7	3	2.66	14.5	12	Travis
33-11J	5199.5	5204	15.3	9.4	5.6	45.1	12.8	2.66	15.5	17.5	Travis
33-11J	5198.5	5203	13.7	5.7	2.1	42	8.6	2.64	16	18	Travis
33-11J	5197.5	5202	13.3	4.3	1.4	40.6	4	2.64	16	18	Travis
33-11J	5196.5	5201	14.2	8.3	5	66.7	12	2.65	13	15	Travis
33-11J	5195.5	5200	14.4	8.2	4	48.7	12.1	2.65	10	13.5	Travis

Well number	*Core depth*	*Log depth*	*Core porosity*	*Horz perm*	*Vert perm*	*Core So*	*Core Sw*	*Grain density*	*Log Den porosity*	*Log D/N porosity*	*Log interval*
33-11J	5194.5	5199	12.3	1.3	0.06	50.1	6.7	2.65	9	13	Travis
33-11J	5193.5	5198	11.2	1.4	0.59	50.9	2.8	2.66	9	13.5	Travis
33-11J	5192.5	5197	8.4	0.1	0.11	58.8	4.3	2.66	8.5	15	Travis
33-11J	5191.5	5196	7.7	0.03	0.001	67	19	2.67	9.5	13.5	Travis
33-11J	5190.5	5195	9.1	0.001	0.001	57.7	23.2	2.67	10	13	Travis
33-11J	5189.5	5194	5.8	0.05	0.03	47.7	11.7	2.65	12	15	Travis
33-11J	5188.5	5193	6.7	0.21	0.09	57.7	6.3	2.67	14	16.5	Travis
33-11J	5187.5	5192	9.2	0.43	0.22	49.6	4.8	2.65	13	16	Travis
33-11J	5186.5	5191	11.5	1.1	0.72	50	5.4	2.64	11	14.5	Travis
33-11J	5185.5	5190	11.5	0.75	0.2	54.3	7.4	2.65	10	13	Travis
33-11J	5184.5	5189	11.4	0.55	0.5	51.4	4.6	2.65	6	13	Travis
33-11J	5183.5	5188	8.3	0.04	0.02	54.8	10.2	2.67	5	11.5	Travis
33-11J	5182.5	5187	7.6	0.01	0.04	52.6	13.1	2.67	5	10	Travis
33-11J	5181.5	5177	5.7	0.01	0.001	10.9	62.7	2.69	6	10	Travis
33-11J	5171.5	5176	2.5	0.001	0.001	24.7	59.9	2.69	4.5	9	Travis
33-11J	5170.5	5175	3.8	0.16	0.001	28.3	55.3	2.69	3	8.5	Travis
33-11J	5168.5	5173	5	0.28	0.02	50.3	11.8	2.67	3	8.5	Travis
33-8	5275	5275	10.5	787	-	54.5	11.7	2.47	15	21	Travis
33-8	5171	5171	9.5	0.25	-	56.1	15.7	2.67	13	13.5	Travis
33-8	5077	5077	10.1	0.28	-	52.5	12.4	2.68	13	13	Travis
33-8	5041	5041	6.9	0.03	-	61.4	26.4	2.67	9	10	Travis
33-8	5013	5013	5.7	0.02	-	59.8	34.3	2.65	7	8	Travis
34-5	5007.5	5007	2.1	0.01	-	73.6	16.4	2.67	6	14	Travis
34-5	5011.5	5011	4	0.01	-	58.9	31.4	2.65	4	11	Travis
34-5	5012.5	5012	4.3	0.01	-	50.8	36.3	2.66	5	10	Travis
34-5	5013.5	5013	4.5	0.03	-	48.9	32.6	2.66	5.5	10.5	Travis
34-5	5014.5	5014	4.8	0.03	-	46.9	33.8	2.66	7	11.5	Travis
34-5	5015.5	5015	5.3	0.05	-	48	30.7	2.67	9	13	Travis
34-5	5016.5	5016	5	0.02	-	57.2	20.2	2.66	9.5	13	Travis
34-5	5017.5	5017	6.1	0.12	-	67.1	14.9	2.65	9.5	13	Travis
34-5	5018.5	5018	8.5	0.11	-	62.1	16.3	2.65	9.5	12.5	Travis
34-5	5019.5	5019	8.1	0.16	-	65.4	15.7	2.66	8	11	Travis
34-5	5020.5	5020	5.5	0.08	-	57.5	16.9	2.66	8	12	Travis
34-5	5021.5	5021	4.8	0.01	-	51.6	28.9	2.7	12	17	Travis
34-5	5022.5	5022	4.5	0.05	-	67.5	14.5	2.67	14	15	Travis
34-5	5023.5	5023	3	0.02	-	54.6	15.6	2.74	6	11	Travis
34-5	5024.5	5024	15	21	-	40.8	9.4	2.67	12	15.5	Travis
34-5	5025.5	5025	15.8	32	-	44.7	8.7	2.68	13.5	17	Travis
34-5	5026.5	5026	10.4	53	-	38.5	8.7	2.66	12	15.5	Travis
34-5	5027.5	5027	8.6	2.73	-	51	9.4	2.66	8	13	Travis
34-5	5028.5	5028	3.8	0.01	-	62.1	16.6	2.66	5	13.5	Travis
41-8	5252.5	5252	11.8	2.22	-	60.4	5.5	2.65	11	15.5	Travis
41-8	5011.5	5011	3.7	0.01	-	36.6	31.4	2.66	5	18	Travis
41-8	5256.5	5256	8.9	0.79	-	45.5	5.4	2.65	14	17.5	Travis
41-8	5255.5	5255	3.3	0.01	-	58.8	7.4	2.66	10	15	Travis
41-8	5254.5	5254	9.7	1.03	-	58.1	5.5	2.65	10	15	Travis
41-8	5253.5	5253	11.9	1.68	-	55.1	6.4	2.66	11	15.5	Travis
41-8	5251.5	5251	9.9	0.61	-	56.6	9.8	2.66	12	16	Travis
41-8	5250.5	5250	11.8	0.96	-	56.9	10.9	2.65	15	18	Travis
41-8	5249.5	5249	10.1	0.79	-	52.1	11.8	2.65	16.5	19	Travis
41-8	5248.5	5248	9.7	0.06	-	71.6	9.5	2.64	16	18.5	Travis
41-8	5247.5	5247	8.9	0.67	-	56	5.9	2.66	16.5	19	Travis

Well number	*Core depth*	*Log depth*	*Core porosity*	*Horz perm*	*Vert perm*	*Core So*	*Core Sw*	*Grain density*	*Log Den porosity*	*Log D/N porosity*	*Log interval*
41-8	5246.5	5246	9.5	1.13	-	58	5.8	2.65	17	19	Travis
41-8	5245.5	5245	10.1	0.63	-	60.5	6	2.65	16	18.5	Travis
41-8	5244.5	5244	9	0.55	-	54.7	5.2	2.66	14.5	18	Travis
41-8	5243.5	5243	10.2	0.64	-	61.1	13.3	2.65	14.5	18	Travis
41-8	5242.5	5242	11.1	1	-	62	12.4	2.65	14.5	17.5	Travis
41-8	5241.5	5241	10.6	0.91	-	63.6	13.6	2.65	14.5	17	Travis
41-8	5240.5	5240	12	0.68	-	66.8	12.1	2.67	14.5	17	Travis
41-8	5239.5	5239	11.4	1.14	-	66.4	36.4	2.65	15	17.5	Travis
41-8	5238.5	5238	11.6	0.93	-	53.2	24.8	2.67	15	17.5	Travis
41-8	5237.5	5237	11.2	1.09	-	61.8	21.8	2.67	15	17.5	Travis
41-8	5236.5	5236	9.8	0.62	-	58.6	20.7	2.66	15	17.5	Travis
41-8	5235.5	5235	6.6	0.04	-	57.2	14.3	2.65	15	18	Travis
41-8	5234.5	5234	6.3	0.02	-	75.2	9.4	2.67	15	18	Travis
41-8	5233.5	5233	3.4	0.29	-	64.6	6.2	2.64	14	16.5	Travis
41-8	5232.5	5232	2.5	0.01	-	48	16.9	2.67	11	15	Travis
41-8	5231.5	5231	8.3	0.03	-	36.6	16.3	2.66	10	14.5	Travis
41-8	5230.5	5230	8.6	0.18	-	44	7.3	2.65	9	14.5	Travis
41-8	5229.5	5229	5	0.55	-	38.8	7.1	2.65	8	15	Travis
41-8	5228.5	5228	2.4	0.01	-	5.3	30.5	2.67	8	16	Travis
41-8	5227.5	5227	20.5	34	-	71.5	17.3	2.65	8	15	Travis
41-8	5226.5	5226	19.7	39	-	81.5	9.1	2.65	7	13.5	Travis
41-8	5225.5	5225	19.4	22	-	76.7	6.1	2.65	8	14	Travis
41-8	5224.5	5224	20.4	45	-	41.5	5.9	2.65	20	22	Travis
41-8	5001.5	5001	14.8	9.2	-	34.3	9.1	2.67	13	21	Travis
41-8	5002.5	5002	7.7	1.39	-	45.1	12	2.66	15	23	Travis
41-8	5003.5	5003	2.2	0.01	-	19.8	62.2	2.68	8	18	Travis
41-8	5004.5	5004	4.1	0.03	-	31.2	40.1	2.66	4	14	Travis
41-8	5005.5	5005	5.5	0.01	-	46.2	22.7	2.66	8	12	Travis
41-8	5006.5	5006	3.4	0.02	-	0	76.3	2.68	8	14	Travis
41-8	5007.5	5007	7.1	1.7	-	39.8	22.8	2.65	6	14	Travis
41-8	5008.5	5008	6.6	0.39	-	43.8	21.9	2.66	7	19	Travis
41-8	5009.5	5009	6.7	0.11	-	43.4	25.2	2.66	6	18	Travis
41-8	5010.5	5010	5.9	0.14	-	37	24.6	2.66	5	18	Travis
5-33	5304	5304	14	2.282	-	-	-	2.65	3	9.5	Travis
5-33	5464	5464	10.75	0.14	-	-	-	2.65	4	15	Travis
5-33	5458	5458	12.45	1.562	-	-	-	2.65	10	12	Travis
5-33	5456	5456	12.37	1.315	-	-	-	2.66	14	16.5	Travis
9-34	5651	5651	13.1	0.63	-	69.4	12.3	2.66	17	19	Travis
9-34	5650	5650	9	0.11	-	64.8	37.4	2.67	14	17.5	Travis
9-34	5356	5356	10.4	0.16	-	57.5	20.2	2.69	11.5	14	Travis
9-34	5344	5344	3.8	0.03	-	75.1	18.7	2.67	7	9	Travis
9-34	5338	5338	14.4	0.8	-	55.7	20.7	2.66	16	18	Travis
11-20	4993.5	4998	12.3	0.447	-	52	4.9	2.74	8	11	UB
11-20	4999	5003	10.3	0.233	-	69.5	9.9	2.7	4	5	UB
11-20	4998.5	5002	18.9	2.07	-	87	2.1	2.74	10	10	UB
11-20	4997	5001	10.1	2.7	-	62.2	4.6	2.74	9	10	UB
11-20	4995	4999	8.1	0.068	-	59.7	24.1	2.74	10	13	UB
11-20	4993.1	4997	8.3	0.133	-	50.7	7.2	2.75	5.5	9	UB
11-20	4990.5	4995	14.4	0.509	-	79.3	0.8	2.77	20	15.5	UB
11-20	4990	4994	4.3	0.004	-	77	9.3	2.75	9	16	UB
11-20	4989.5	4994	3.6	0.012	-	44.7	44.3	2.75	9	16.5	UB
11-20	4988.9	4993	2.2	0.017	-	41.4	12.8	2.75	5	13	UB

Well number	Core depth	Log depth	Core porosity	Horz perm	Vert perm	Core So	Core Sw	Grain density	Log Den porosity	Log D/N porosity	Log interval
11-20	4972.5	4976	0.4	0.005	-	28.5	60.5	2.71	4.5	8	UB
11-20	4972	4976	2	22.6	-	33.5	51.8	2.54	4.5	8	UB
11-20	4971.5	4975	14.2	1.317	-	53.6	5.7	2.76	6	8.5	UB
11-20	4999.5	5004	15.3	0.393	-	54.9	5.3	2.76	5	5.5	UB
11-20	5000.5	5005	2.4	0.022	-	79.8	16.7	2.74	4	5.5	UB
11-20	5001.5	5006	4.1	0.017	-	85.2	14.6	2.67	2	7	UB
11-20	5002	5006	2	0.005	-	44.9	21.9	2.68	2	7	UB
11-20	5132.3	5136	3.9	0.003	-	27.5	71.2	2.72	4	6.5	UB
11-20	5132.9	5137	1.7	3025	-	29	13.7	2.7	4	7	UB
11-20	5133.9	5138	8.5	0.042	-	79	10	2.75	0	4	UB
11-20	5002.8	5007	0.5	0.005	-	26.7	16.2	2.67	3	10	UB
11-20	5017.9	5122	3.4	0.101	-	90.4	5.8	2.76	2	3.5	UB
11-20	5144.2	5148	1.4	0.003	-	62.1	4.9	2.67	3	5	UB
11-20	5146.2	5150	2.4	0.003	-	59.6	9.2	2.71	3	4	UB
11-20	5147.2	5151	1.9	0.003	-	54.9	44.3	2.73	2	4	UB
11-20	5149.2	5153	1.8	0.003	-	60.5	36.2	2.72	4	5	UB
11-20	5150.2	5154	1	0.004	-	51.7	44.8	2.69	4	4.5	UB
11-20	5019.5	5024	10	0.026	-	68.2	18	2.78	0	4	UB
11-20	5020	5024	10.4	0.033	-	48.8	34.6	2.77	0	4	UB
11-20	5020.5	5025	5.7	0.009	-	79.1	17.6	2.76	2	6.5	UB
11-20	5021	5025	6.9	0.029	-	64.6	17.3	2.76	2	6.5	UB
11-20	5021.5	5026	0.3	0.021	-	69.1	29.4	2.66	7	10	UB
11-20	5022.6	5027	1.5	0.003	-	57.6	39.9	2.72	9	12	UB
11-20	5121.3	5126	1.8	0.013	-	54	25	2.71	7	13.5	UB
11-20	5122	5126	1.8	0.003	-	65.3	24.9	2.73	7	13.5	UB
11-20	4994	4998	5.9	0.028	-	73.8	6.8	2.75	8	11	UB
11-20	5002.4	5006	1.8	0.005	-	88	11.5	2.68	3	10	UB
11-20	5019	5023	6.8	0.01	-	81.9	11.6	2.77	2	5	UB
11-20	5130.5	5134	3.3	0.015	-	89.3	6.8	2.76	0	2.5	UB

Horz perm = horizontal permeability
Vert perm = vertical permeability
Core So = core determined oil saturation
Core Sw = core determined water saturation
Grain density in g/cc
Log Den porosity = porosity derived from the density log
Log D/N porosity = porosity derived from averaging the density and neutron log values
Log interval = correlation intervals (see figure 2)

CP = Castle Peak
MB = Monument Butte
UB = Uteland Butte

APPENDIX C

SCANNING ELECTRON MICROSCOPY ANALYSIS REPORT TO THE UTAH GEOLOGICAL SURVEY

by
TerraTek

Salt Lake City, Utah
July 10, 2003

Scanning Electron Microscopy Analysis

Introduction and Analytical Procedures

Scanning electron microscopy (SEM) analysis was conducted on six samples representing selected core intervals of the Green River Formation, obtained from various wells in the Uinta Basin, Utah. A sample information summary is presented below:

Table 1. SEM Sample Information

SEM Sample No.	Well No.	Depth (feet)	General Lithology
1	33-8	4657	quartz-cemented sandstone
2	33-8	5456	clay-rich sandstone
3	9-34	5344	tight, calcareous sandstone/siltstone
4	2-33	5647.3	laminated, argillaceous sandstone/siltstone
5	2-33	5649.7	laminated, argillaceous sandstone/siltstone
6	5-33	5993	arkosic sandstone with clay

A small, freshly broken portion of each sample was mounted on a standard SEM mount and coated with gold-palladium. The sample was then placed in a Hitachi S-450 scanning electron microscope equipped with a Kevex energy dispersive x-ray spectrometer (EDX), examined, and photographed at a range of magnifications to document the morphology of the rock fabric and the pore system. Pore-lining and pore-filling substances were identified wherever possible.

Discussion

The six selected samples exhibit a broad range of reservoir quality properties, cement types, porosity classes, and clay distributions. A brief summary of the typical characteristics of each samples are presented below:

Sample 1 exhibits the best reservoir quality in the group and contains the least amount of secondary or detrital clay. Although somewhat reduced in size by silica and ankerite cements, intergranular pores are comparatively open and "clean". Additional effective pore types include moldic and dissolution voids. Minor diagenetic clays comprise moderately crystalline illite flakes, well-crystalline chlorite grain coatings, and trace pore-filling kaolinite. Microporous (sedimentary) rock fragments are also commonly encountered.

Sample 2 displays poor to fair reservoir quality and abundant pore-reducing cement and clay. Secondary ankerite and silica overgrowths are largely responsible for porosity degradation. In addition, diagenetic clay, predominantly well-crystalline illite, typically lines or fills remaining pore space. Minor grain-coating and pore-lining chlorite is also recognized. Microporous voids are abundant in the pore network, although patches of dissolution-related porosity provide locally better reservoir quality.

Sample 3 exhibits exceptionally poor reservoir quality because of pervasive calcite cementation. Microporous voids dominate the pore network and include intragranular micropores in partially leached or weathered feldspars and rock fragments, as well as voids in secondary clay structures. Later authigenic clays include patchy, moderately crystalline illite and chlorite.

Abundant detrital clay in **Samples 4 and 5** contributes to poor porosity development and comparatively low reservoir potential in these intervals. Compacted illite and mixed-layer clays fill nearly all intergranular pores. Additionally, secondary illite clay is commonly associated with the detrital matrix. Scattered dissolution pores, more common in **Sample 4**, mark sites of feldspar or carbonate cement leaching. Poorly effective micropores are abundant throughout both samples.

Sample 6 offers modest to good overall reservoir quality. Intergranular porosity is reduced by quartz overgrowths, patchy carbonate cements, and authigenic clay, although significant pore space remains. *Well-crystalline, secondary illite fibers are pervasive throughout the sample fabric and commonly coat detrital grains and bridge intergranular pores and pore throats*. Delicate illite fibers loosely attached to grains are highly susceptible to breakage and migration through the pore system. Additionally, abundant illite will certainly affect gamma ray and resistivity log responses.

Scanning Electron Microscope Photomicrographs

PLATE 1
Sample 1, Well No. 33-8
Depth: 4657 feet

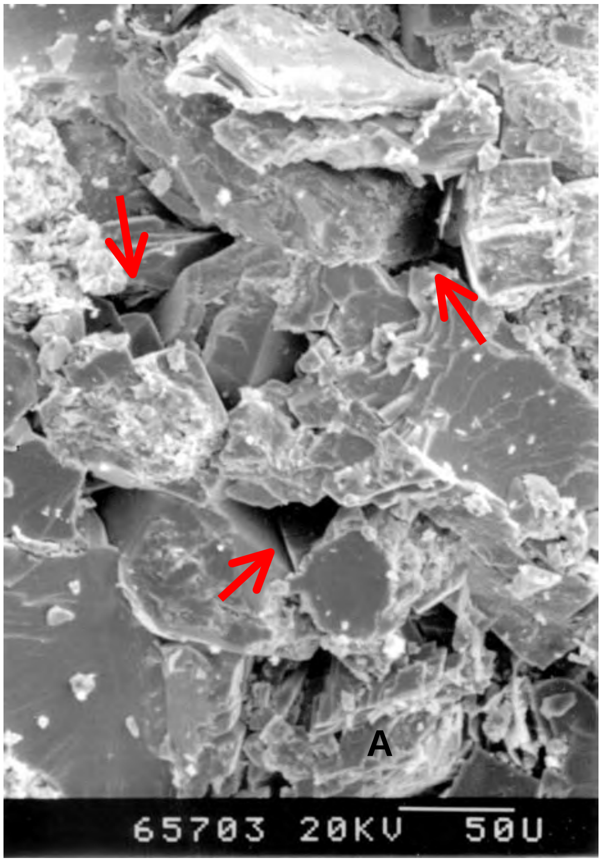

Low-magnification overview includes several reduced, but "clean" intergranular voids (arrows). Quartz overgrowth cement has reduced intergranular pore size somewhat, although overall reservoir quality remains comparatively good. Authigenic clays are minor, and ankerite (A) is a patchy pore filling. Scale bar = 50 microns. (300×)

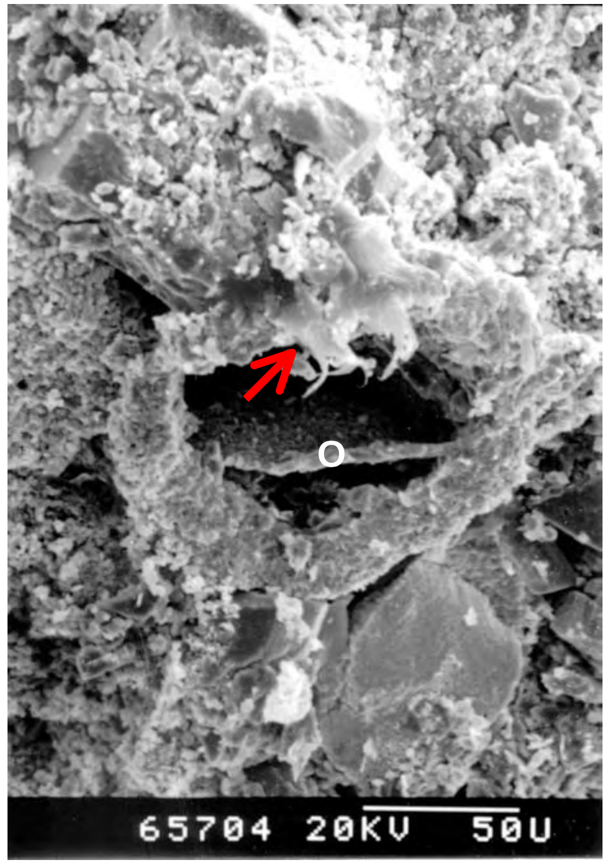

Another low-magnification photomicrograph highlights an irregular, compacted ooid (O) with internal moldic porosity and poorly crystalline structure. Larger pore types throughout this sample are dissolution enhanced. Also note adjacent intergranular pores and secondary illite flakes at arrow. Scale bar = 50 microns. (400×)

PLATE 2
Sample 1, Well No. 33-8
Depth: 4657 feet

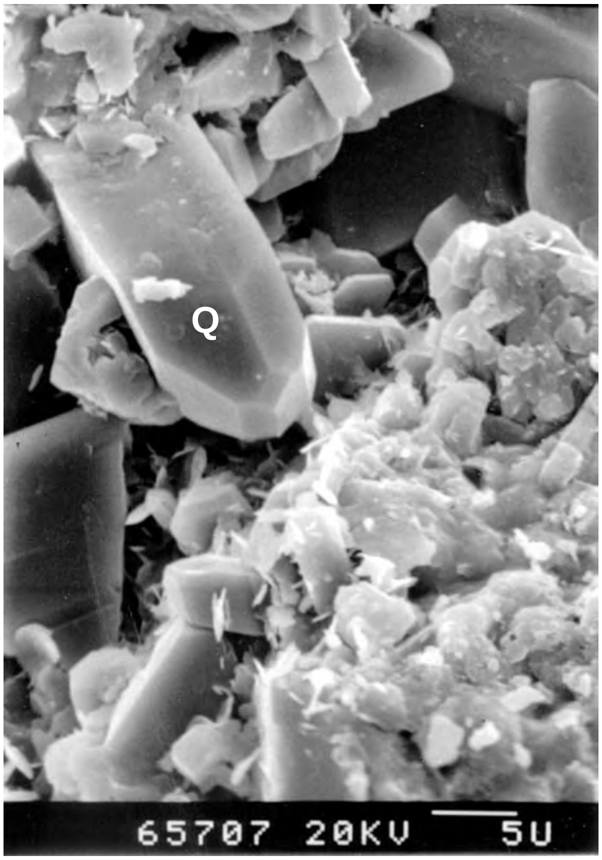

Textural detail illustrates typical authigenic mineralogy. Euhedral quartz overgrowths are common throughout the sample and likely precipitated in several diagenetic "pulses". Small overgrowth prisms shown here (Q) are pore lining and pore filling. Microcrystalline clays visible on the grain surfaces are early-formed chlorite plates. Scale bar = 5 microns. (2200×)

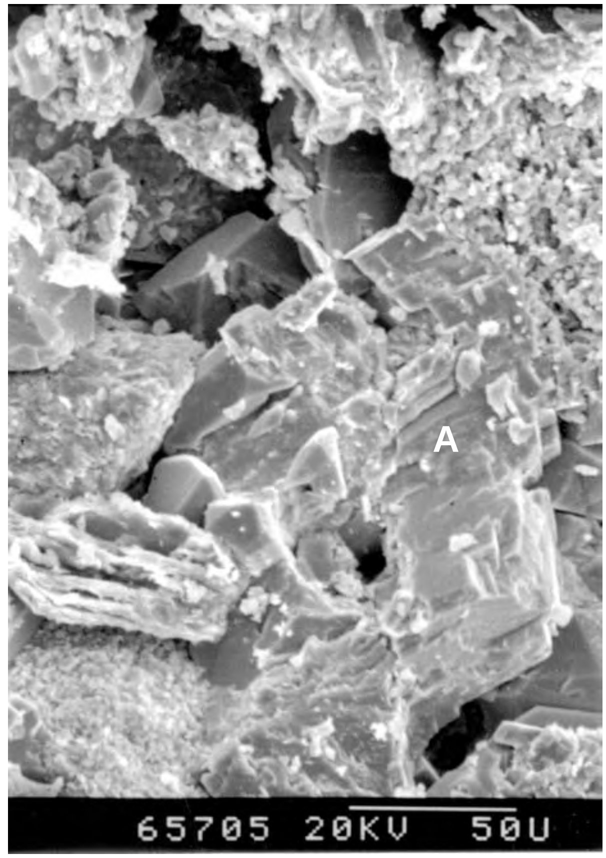

Secondary cements and pore types are shown at medium magnification. Coarse, well-crystalline ankerite (A) and quartz overgrowths commonly occlude large secondary or dissolution-enhanced voids, whereas minor clays form grain coatings and pore linings. Also note remaining open porosity, as well as a weathered biotite grain at lower left. Scale bar = 50 microns. (440×)

PLATE 3
Sample 1, Well No. 33-8
Depth: 4657 feet

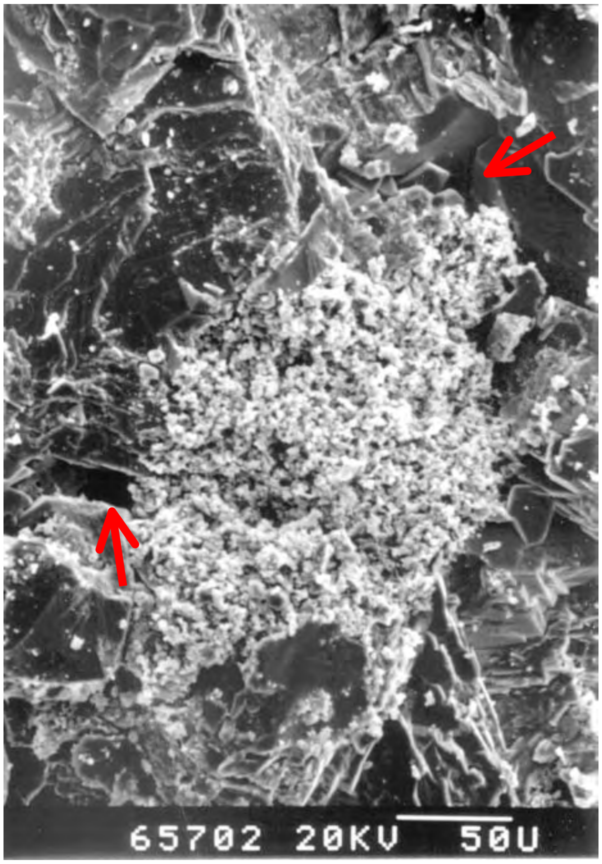

A microporous sedimentary rock fragment at low magnification. Also visible are several reduced intergranular pores (arrows) and extensive silica overgrowth cement. Scale bar = 50 microns. (300×)

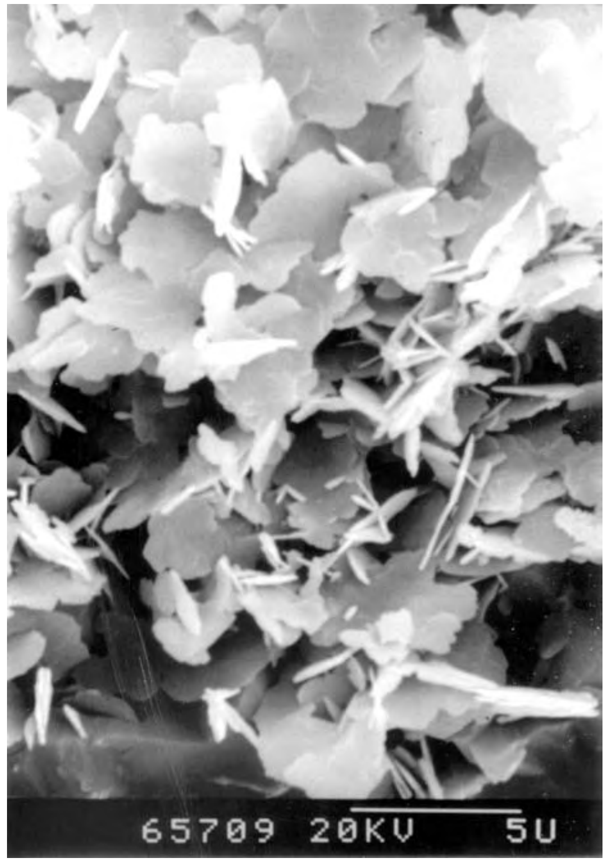

Platy, secondary clays form grain coatings and pore linings. Clay morphology and EDX signature identify this clay as well-crystalline chlorite. Several microporous voids, typically less than 5 microns in size, are also visible throughout the clay structure. Scale bar = 5 microns. (4400×)

PLATE 4
Sample 2, Well No. 33-8
Depth: 5456 feet

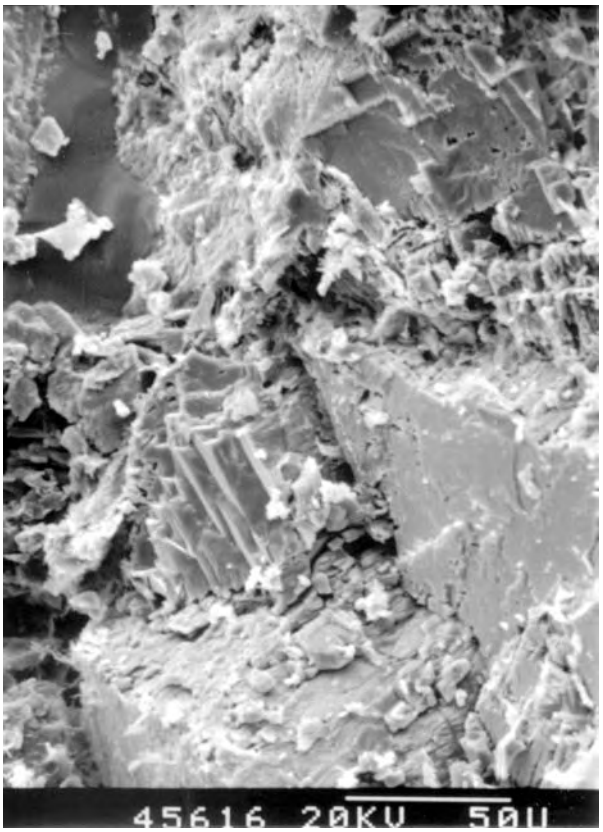

Low-magnification photomicrograph reveals highly reduced intergranular porosity, pervasive ankerite cement (center and upper right) and more abundant clays. Scale bar = 50 microns. (430×)

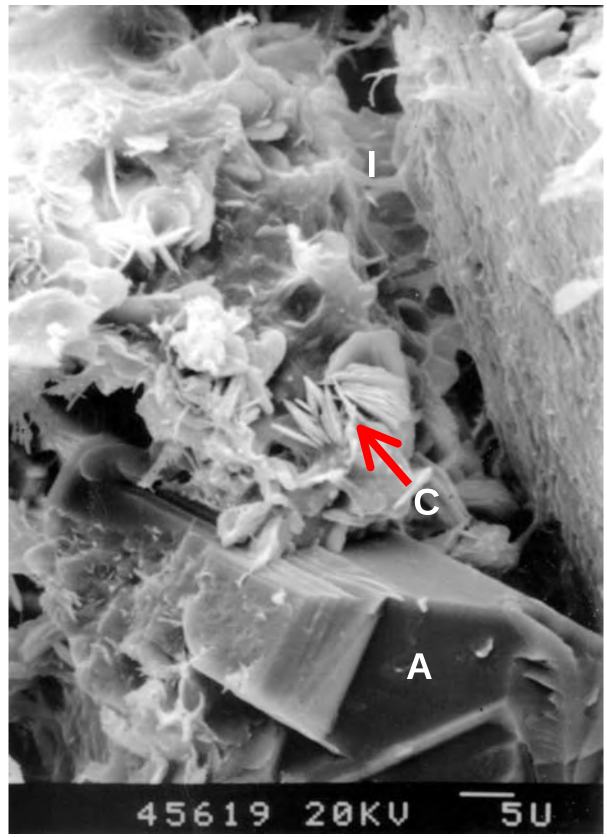

Several authigenic minerals are visible at high magnification. In addition to conspicuous ankerite pore fillings (A), secondary illite is abundant as pore linings and pore bridges (I) and chlorite (C) is locally present as grain coatings and pore linings. Intergranular pore space is greatly reduced and micropores associated with clays are abundant. Scale bar = 5 microns. (1400×)

PLATE 5
Sample 2, Well No. 33-8
Depth: 5456 feet

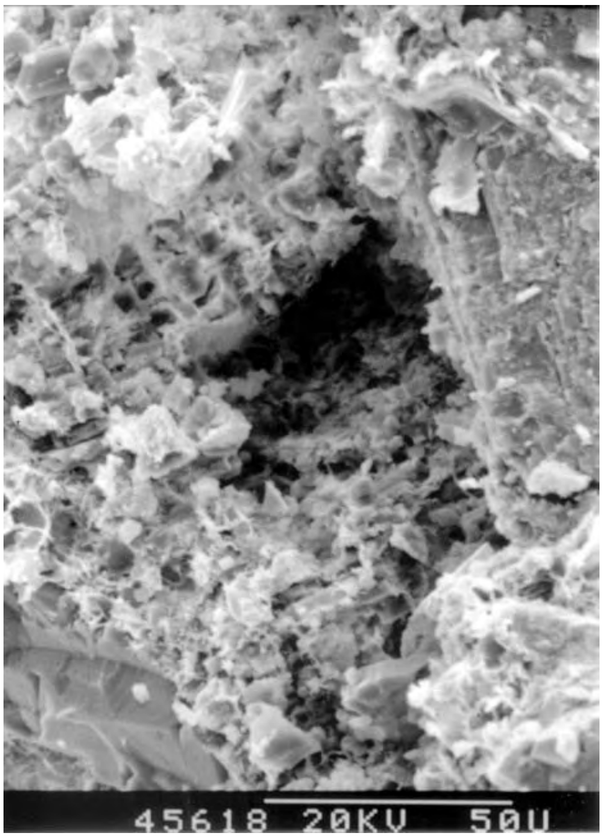

Medium-magnification view of a reduced intergranular pore (center). In contrast to the previous sample, this sample includes well-crystalline illite as extensive pore linings and grain coatings. Scale bar = 50 microns. (650×)

More detailed view of secondary illite and associated micropores. EDX peaks for Si, Al, and K confirm illite composition. Delicate, well-formed illite fibers and flakes are highly susceptible to breakage and migration through the pore system. Concentrations of illite at pore throats can significantly reduce permeability is areas of high flow velocity. Scale bar = 5 microns. (1100×)

PLATE 6
Sample 2, Well No. 33-8
Depth: 5456 feet

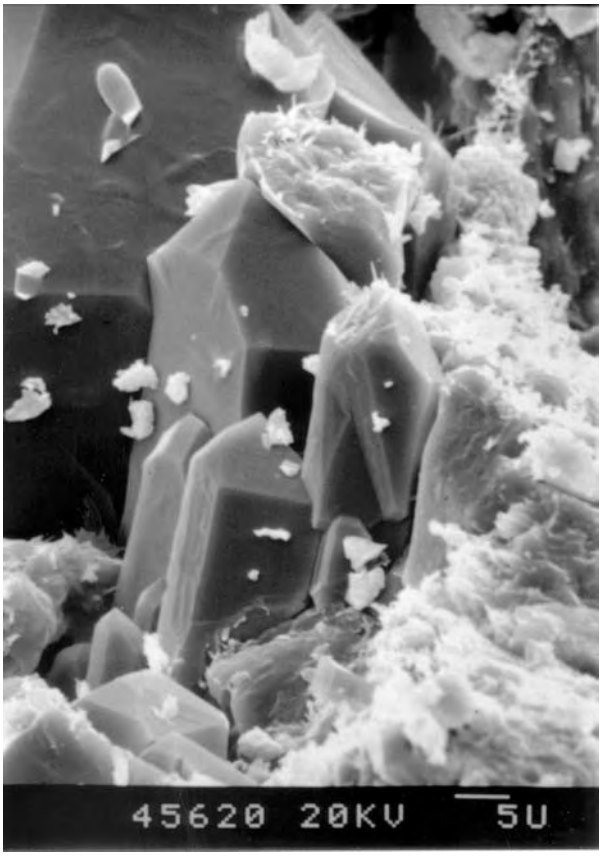

Pore-reducing mineral cements also include quartz overgrowths. Here, a “family” of variably sized overgrowth prisms extends into intergranular pore space. Also present are microcrystalline illite flakes, which likely precipitated after quartz. Scale bar = 5 microns. (1400×)

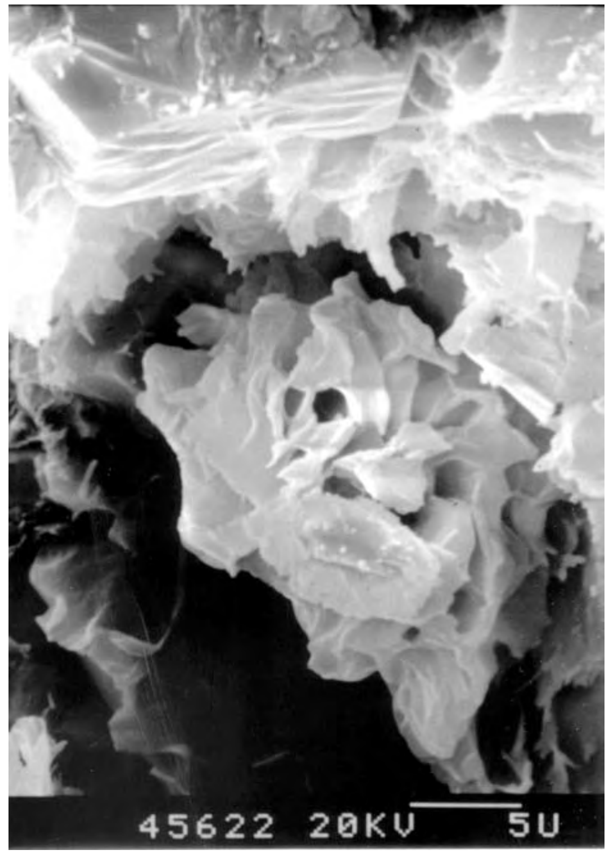

Unusual pore-lining clay structure at high magnification. Microporous clay is likely a combination of mixed-layer illite/smectite and illite. Scale bar = 5 microns. (2800×)

PLATE 7
Sample 3, Well No. 9-34
Depth: 5344 feet

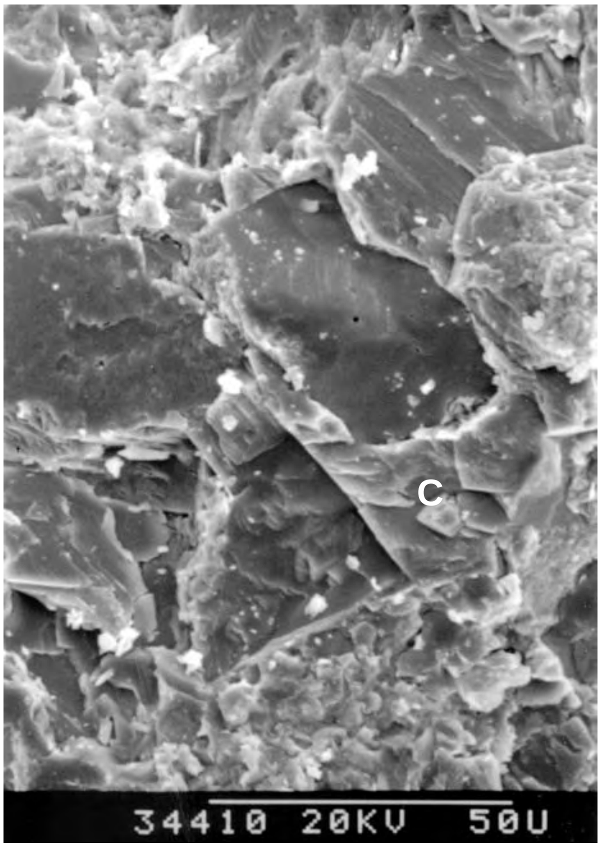

Low-magnification photomicrograph reveals very tight, well-cemented fabric and poor interparticle porosity. Coarse, pervasive calcite cement (C) is primarily responsible for porosity reduction. EDX spectrum includes prominent peaks for Si, Al, and Ca, confirming the presence of calcite. Scale bar = 50 microns. (790×)

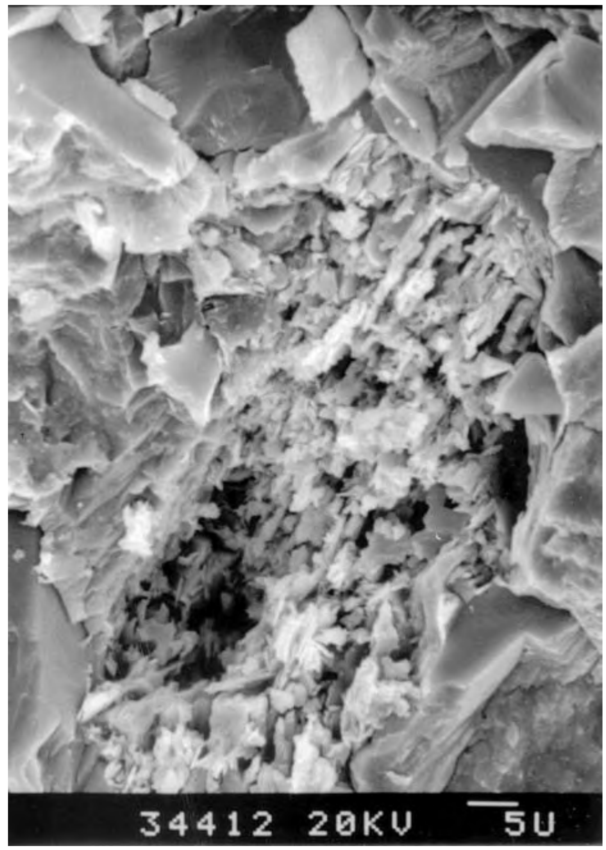

Minimal porosity at this depth is concentrated in partially leached grains and patches of secondary or replacive clay. Here, a partially dissolved feldspar grain hosts internal microporosity along remnant cleavage and twin planes. Replacive illite is also visible. Scale bar = 5 microns. (1300×)

PLATE 8
Sample 3, Well No. 9-34
Depth: 5344 feet

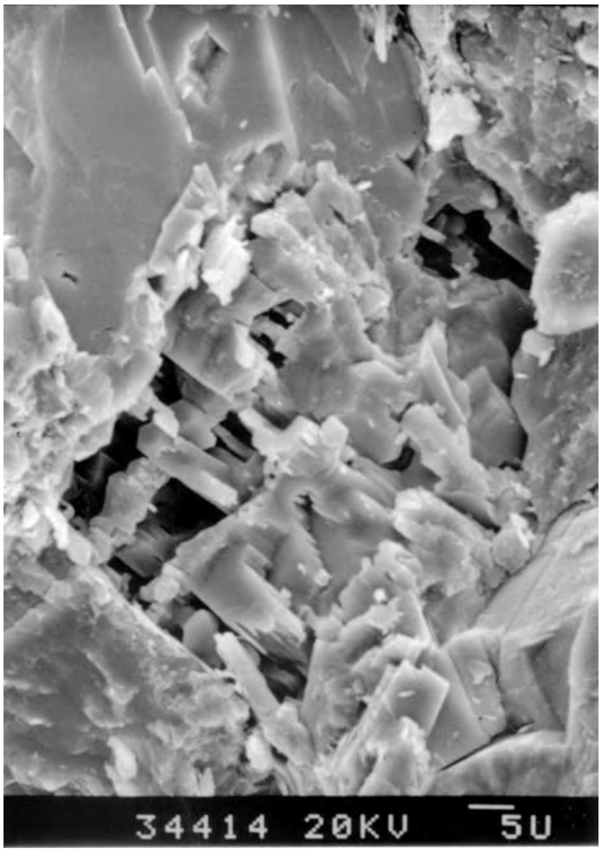

Another view of secondary dissolution porosity in plagioclase feldspar (center). Pore size is 5-10 microns and pore effectiveness and interconnectivity is low. EDX spectrum includes peaks for Si, Al, Ca, Na, K, and Fe, confirming the presence of plagioclase and calcite, with possible illite. Scale bar = 5 microns. (1200×)

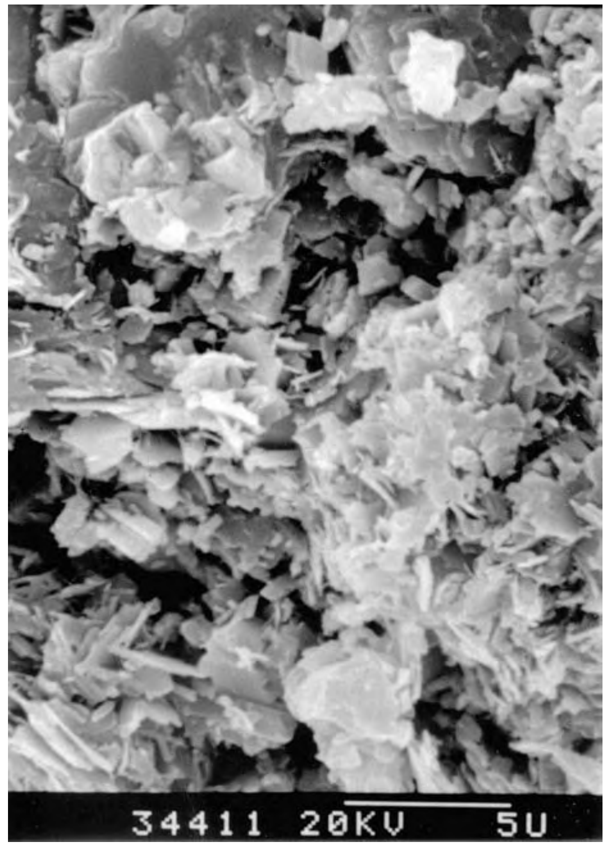

High-magnification image of microporous, pore-filling and replacive clays. Platy clay morphology and EDX signature that includes Fe and Mg peaks indicate a chlorite composition. Chlorite crystallinity is poor to moderate. Also note that pore size here is less than 5 microns. Scale bar = 5 microns. (4300×)

PLATE 9
Sample 4, Well No. 2-33
Depth: 5647.3 feet

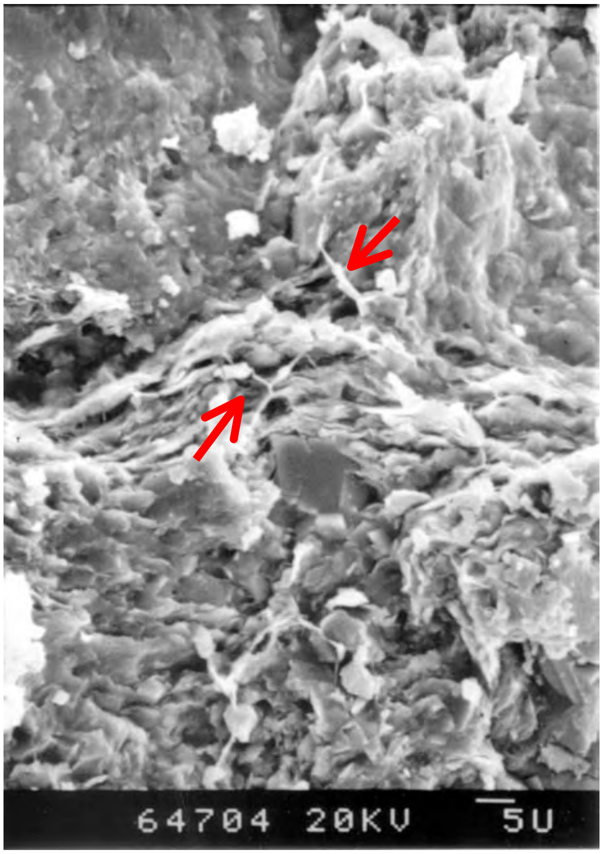

Clay-rich texture at medium magnification. Close inspection of flattened detrital clay at center reveals secondary illite extensions (arrows). Not surprisingly, the dominant porosity types in this argillaceous sample are microporous voids hosted by detrital and authigenic clays, compacted pseudomatrix, and sedimentary rock fragments. Scale bar = 5 microns. (1000×)

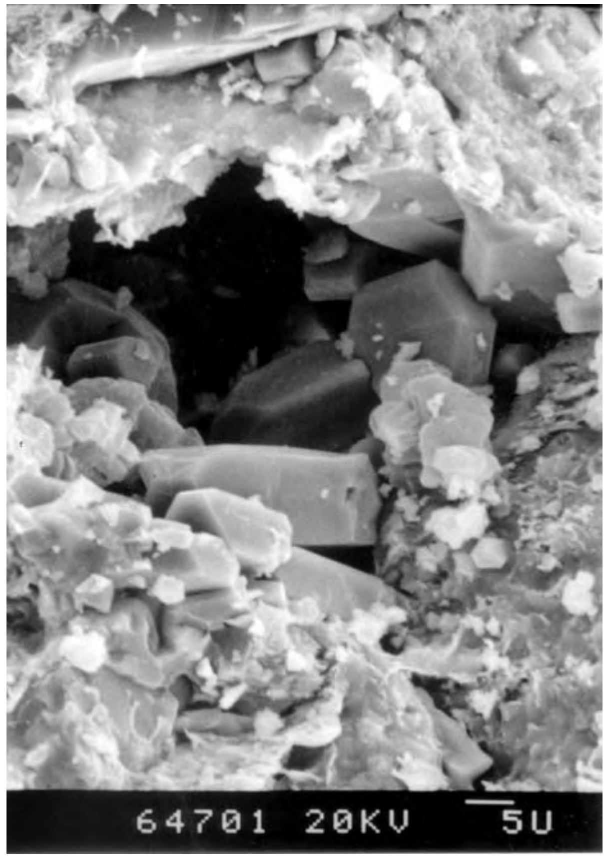

Rare macropore shown at high magnification. Open porosity is likely the result of localized secondary dissolution. Also note partial occlusion by euhedral quartz overgrowths and pore lining illite. Scale bar = 5 microns. (1300×)

PLATE 10
Sample 4, Well No. 2-33
Depth: 5647.3 feet

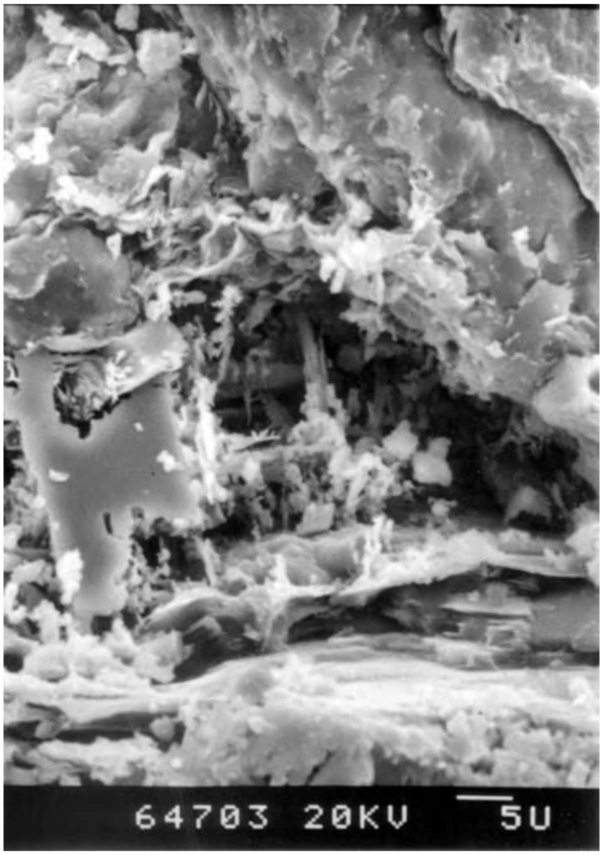

Other isolated pore types include dissolution voids created by partial to complete grain leaching. Grain at center (likely a feldspar) has been partially dissolved and replaced by secondary illite. Compacted detrital clays and micropores are also visible. Scale bar = 5 microns. (1500×)

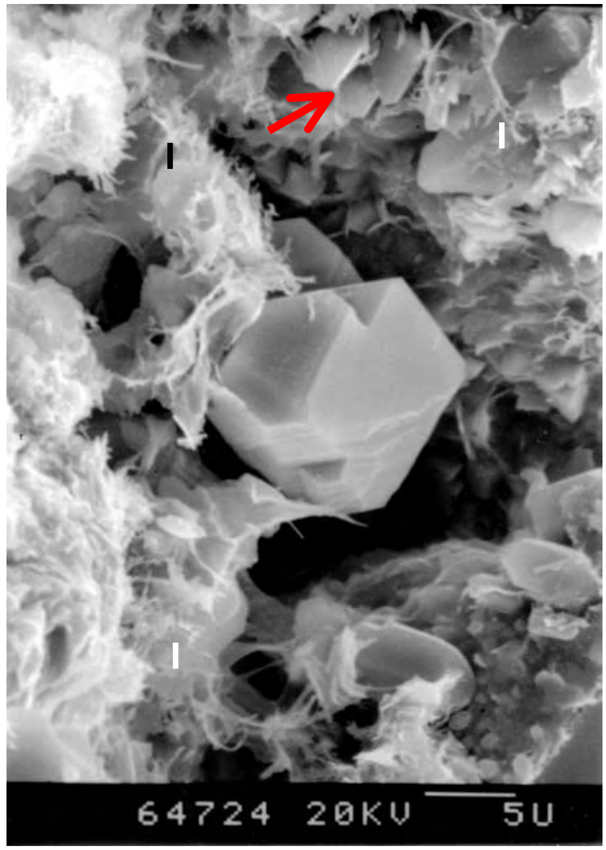

Small intergranular pore at high magnification. Delicate secondary illite fibers and flakes (I) thickly line the pore walls and bridge pore throats. Illite is accompanied by possible grain-coating chlorite plates (arrow) and carbonate cement (center). Some open intergranular porosity remains and abundant micropores are found in open clay structures. Scale bar = 5 microns. (2400×)

PLATE 11
Sample 5, Well No. 2-33
Depth: 5649.7 feet

Low-magnification overview of textural characteristics. As in the previous sample, a laminated, clay-rich texture hosts pervasive microporosity and few open macropores. In fact, larger dissolution pores are even more rare than in the previous sample. Compacted detrital clays form pore-filling pseudomatrix between framework grains and are commonly accompanied by secondary clay (illite). Scale bar = 50 microns. (300×)

Higher-magnification image highlights typical detrital clay partially supporting the silty/sandy framework (note grain at right). Flattened, flaky clay morphology is characteristic of a low-expandable illite/smectite matrix. Micropores hosted by detrital clay matrix are largely ineffective. Scale bar = 5 microns. (3000×)

PLATE 12
Sample 5, Well No. 2-33
Depth: 5649.7 feet

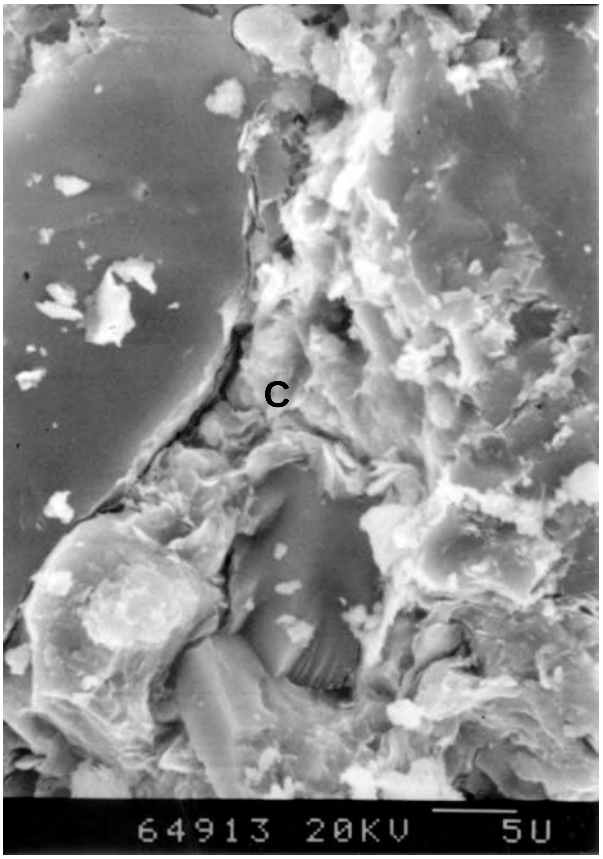

Textural detail highlights compacted detrital clays (C) filling intergranular pore space. In many cases, detrital clay exhibits overgrowths or extensions of secondary illite fibers and flakes. Little or no microporosity is visible. Scale bar = 5 microns. (2200×)

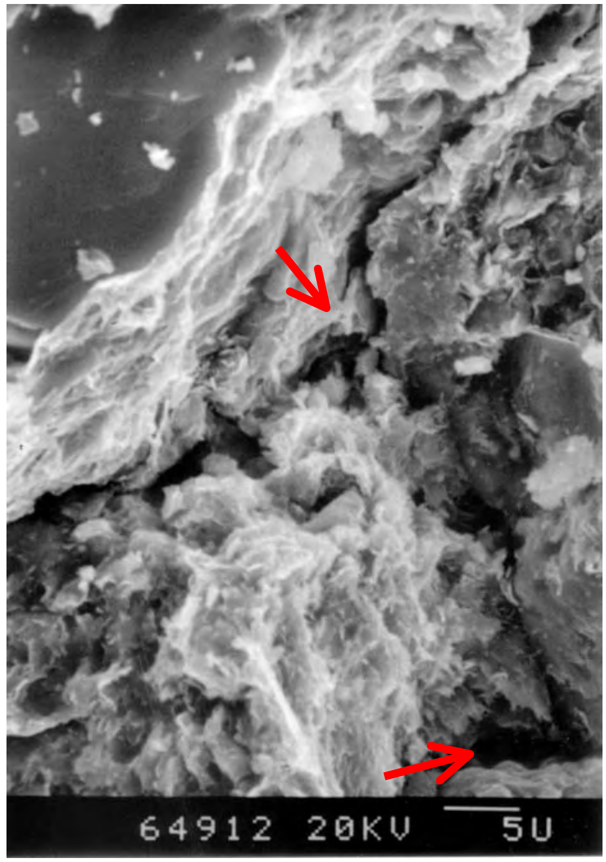

High-magnification view, similar to that at left, illustrates clay-filled intergranular pore space and obstructed pore throats (arrows). Detrital clay is predominantly illite-rich illite/smectite with minor secondary illite extensions. Also note microporosity associated with clays. Scale bar = 5 microns. (2000×)

PLATE 13
Sample 6, Well No. 5-33
Depth: 5993 feet

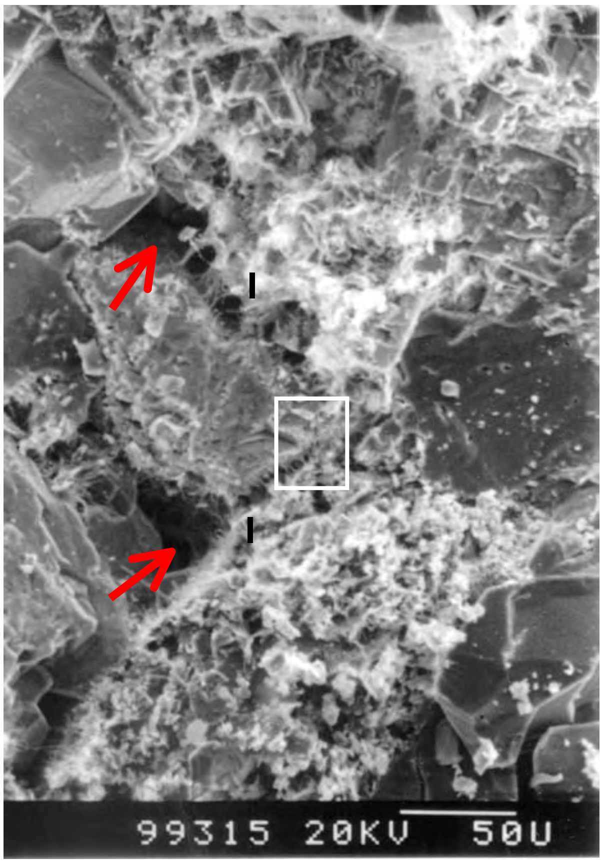

Textural overview of moderately porous sandstone with conspicuous secondary clay. Both quartz overgrowth cement and well-crystalline illite reduce intergranular voids, although visible intergranular pore space remains (arrows). Pore-bridging illite (I) is visible even at low magnification. Scale bar = 50 microns. (300×)

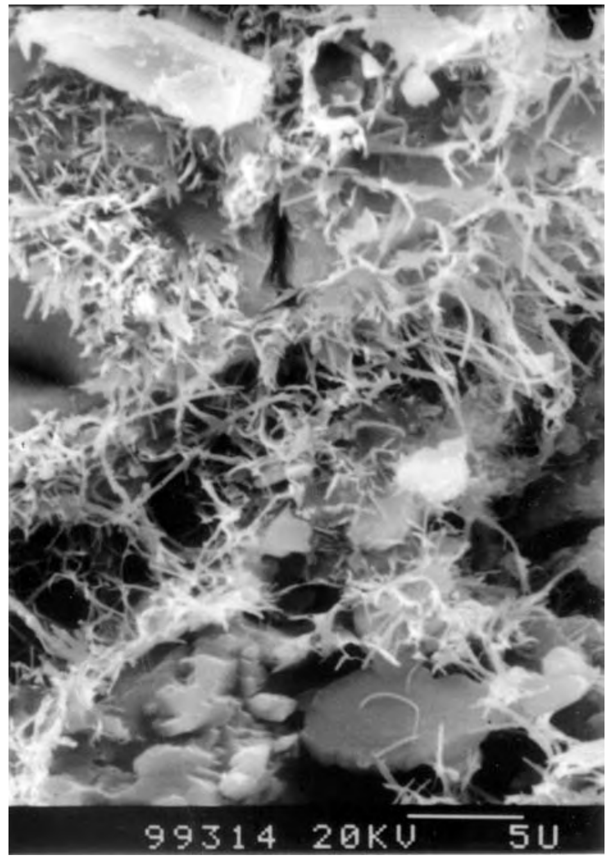

High-magnification view of boxed area at left. Fragile, well-formed illite fibers are pervasive and commonly form secondary pore linings, pore bridges, and grain coatings. These delicate clay structures are particularly vulnerable to breakage and migration as fines. Grain at bottom of view is partially dissolved and replaced by clay. Scale bar = 5 microns. (3000×)

PLATE 14
Sample 6, Well No. 5-33
Depth: 5993 feet

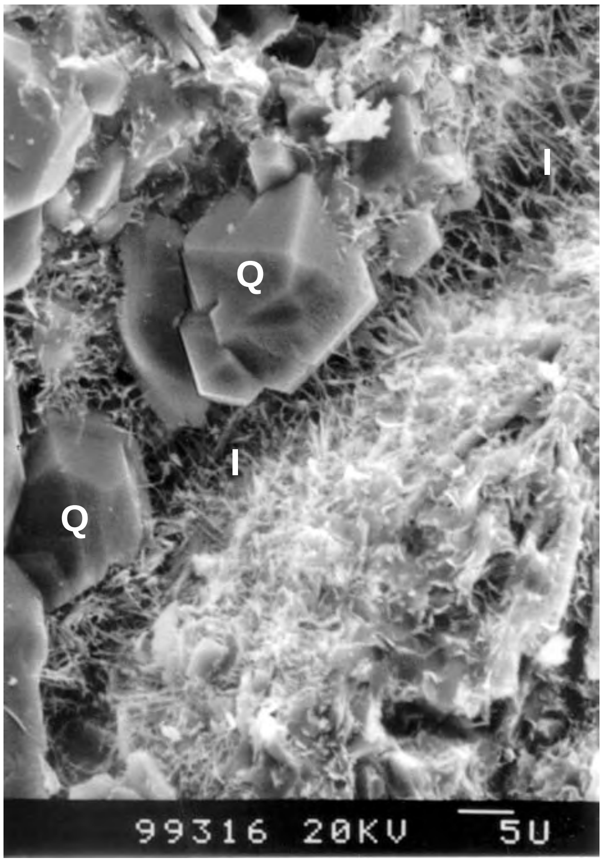

Medium-magnification view of grain surfaces highlights the two dominant authigenic minerals: euhedral quartz overgrowth cement (Q) and well-crystalline illite fibers (I). Secondary illite likely precipitated after quartz overgrowth formation. Also note delicate clay morphology and micropores hosted by clay structures. Scale bar = 5 microns. (1500×)

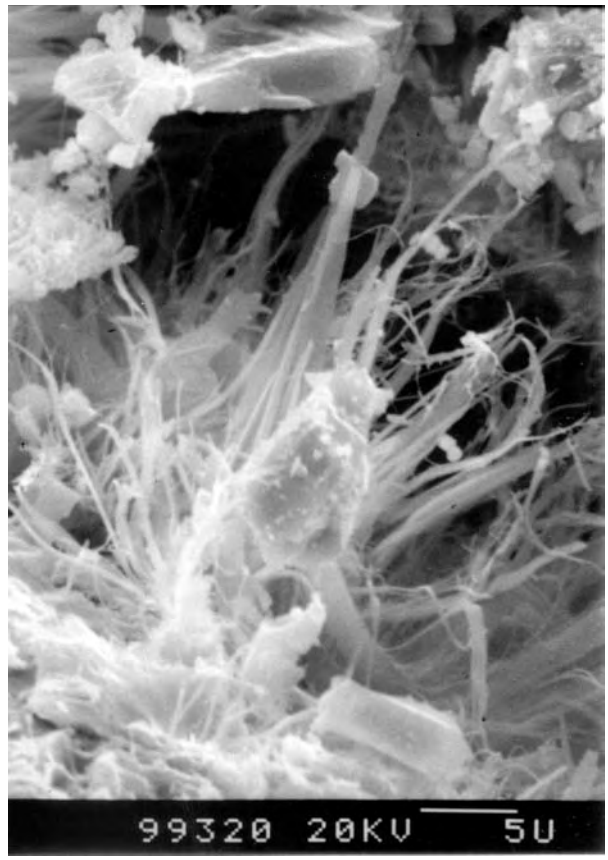

High-magnification image illustrates a “textbook” example of authigenic illite hairs extending into intergranular pore space. Not only do illite fibers reduce intergranular pore and pore throat size, delicate hairs are susceptible to breakage, migration, and accumulation at pore throats. Pervasive illite at this depth will also certainly affect resistivity and gamma log properties. Scale bar = 5 microns. (2500×)

PLATE 15
Sample 6, Well No. 5-33
Depth: 5993 feet

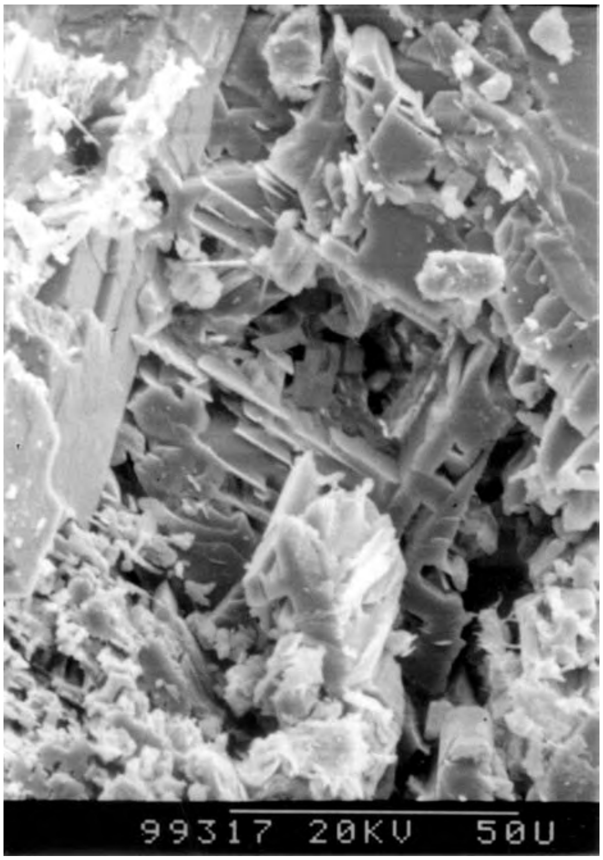

Dissolution porosity in weathered feldspar is especially common in this arkosic sandstone. Here, a weathered and partially leached potassium feldspar hosts internal dissolution porosity along twinning and cleavage lamellae. Minor replacive illite clay is also visible. Scale bar = 50 microns. (760×)

Adjacent to the grain shown at left is another feldspar exhibiting intragranular dissolution porosity. In this case, the cross-hatched twinning pattern and EDX signature indicate that the grain is microcline. These internal micropores in the 5-10 micron size range are largely ineffective pore types. Scale bar = 5 microns. (1000×)

PLATE 16
Sample 6, Well No. 5-33
Depth: 5993 feet

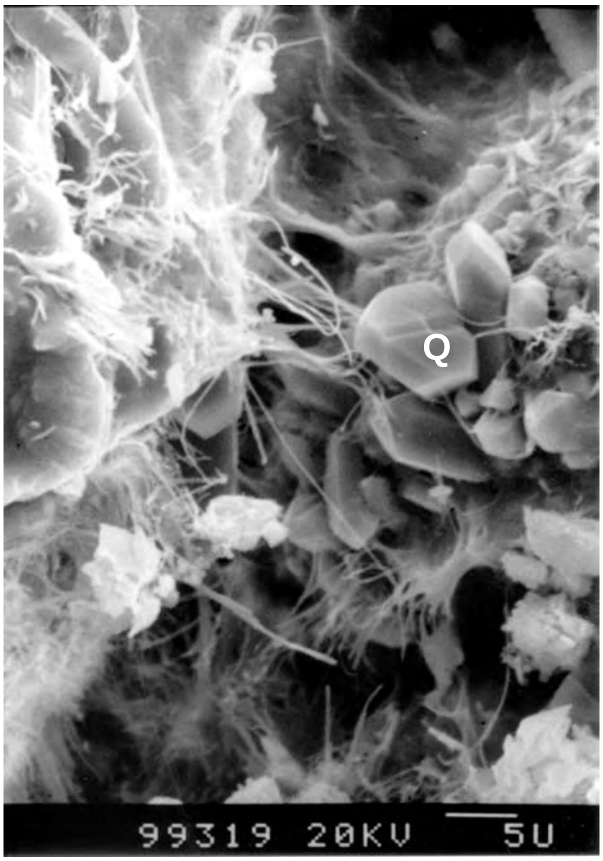

Grain-to-grain contact at high magnification reveals ubiquitous pore-bridging illite (center) and small, euhedral quartz overgrowth prisms (Q). Individual illite hairs extend to lengths of 15-20 microns in places. Scale bar = 5 microns. (1900×)

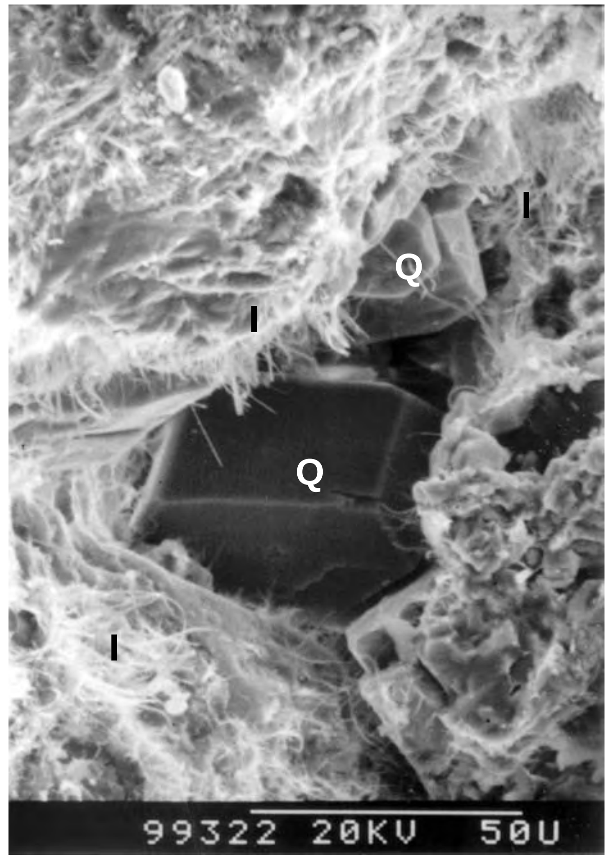

A medium-magnification view looking into an intergranular pore. Blocky quartz overgrowths (Q) partially occlude porosity, and authigenic illite fibers (I) commonly extend into remaining pore space. Scale bar = 50 microns. (710×)

APPENDIX D

X-RAY DIFFRACTION DATA

Federal 14A-28

Travis 2-33

Travis 6-33

Monument Federal 9-34

Provided by Sue Lutz, Energy and Geoscience Institute, University of Utah, Salt Lake City, Utah

Mineralogy, Approx. Wt.% [X] (or) Relative Abundance [ ]

Fed #14A-28 Sample No.	Quartz	Plagioclase	K- Feldspar	Siderite	Calcite	Dolomite	Pyrite	Chlorite	Illite+ Mica	Mixed-layer illite-smectite	Amorphous/ Below Detect.	% smectite in illite-smectite	
5595.0-96.0 Bulk	49	32	7		3	4		2	3		-		
Clay								26	74				
5598.0-99.0 Bulk	48	32	6	1?	3	5	Tr	3	2		-		
Clay								25	75				
5615.0-16.0 Bulk	46	26	6	Tr?	5	6	1	4	2	4	-		
Clay								27	28	45		10	illite-rich illite-smectite
5638.0-39.0 Bulk	51	21	6	Tr	14	4	Tr	2	2		-		
Clay								25	75				
5639.0-40.0 Bulk	43	21	5		3	10	3	3	4	8	-		
Clay								9	35	56		10	

MM = Predominant M = Major m = Minor Tr = Trace ? = Tentative Identification

SUMMARY OF X-RAY DIFFRACTION ANALYSIS

Lower Douglas Creek Sandstone
Well 2-33
Travis Unit,
Greater Monument Butte field

Mineralogy, Approx. Wt.% [X] (or) Relative Abundance [ ]

Sample No.	Quartz	Plagioclase	K- Feldspar	Siderite	Calcite	Dolomite	Pyrite	Chlorite	Mixed-layer Chlor-smectite	Illite+ Mica	Mixed-layer Illite-smectite	Smectite	Amorphous/ Below Detect	% smectite in illite-smectite
5648 core Bulk	36	15	12		2	8	1	2	tr	4	20		-	
Clay								13	4	10	73			15
5650.5 core Bulk	43	14	5	2	20	5		4	tr	2	5		-	
Clay								7	9	14	69	1		15
5656 core Bulk	43	19	6	tr	20	3		2		1	5		-	
5659 core Bulk	40	17	6	tr	3	5	tr	4		5	19		-	
5666 core Bulk	42	17	8	1	7	7	tr	3		2	13		-	
5668 core Bulk	20	9	4	2	3	3		2		4	53		-	15
5672 core Bulk	16	6	5		4	3	3	2		3	58		-	15

MM = Predominant M = Major m = Minor Tr = Trace ? = Tentative Identification

SUMMARY OF X-RAY DIFFRACTION ANALYSIS

Lower Douglas Creek
Well 6-33 Core
Travis Unit,
Greater Monument
Butte field

Mineralogy, Approx. Wt.% [X] (or) Relative Abundance [ ]

Sample No.		Quartz	Plagioclase	K- Feldspar	Siderite	Calcite	Dolomite	Ferroan Dolomite	Pyrite		Chlorite	Mixed-layer Chlor-smectite	Illite+ Mica	Mixed-layer illite-smectite		Amorphous/ Below Detect.					% smectite in illite-smectite	
5596 Bulk		15	6	4			13		5		tr	2	3	52		-					~20	
5601 Bulk		30	11	4				5	3		3	1	5	38		-						
5604.5 Bulk		26	9	5			5		4		1	tr	2	48		-						
5605 Bulk		29	12	7			4	2	1		2	tr	3	40		-						
5606 Bulk		16	9	4	2		8		2		1		1	48		9						
5613 Bulk		23	12	5			4		12		2	2	4	36		-						

MM = Predominant M = Major m = Minor Tr = Trace ? = Tentative Identification

SUMMARY OF X-RAY DIFFRACTION ANALYSIS

Monument Federal #9-34. Core plugs of marker beds Sample No.		Quartz	Plagioclase	K- Feldspar	Calcite	Siderite	Dolomite	Ferroan Dolomite	Pyrite		Chlorite	Mixed-layer Chlor-smectite	Illite+ Mica	Mixed-layer illite-smectite	Smectite		Amorphous/ Below Detect.				% smectite in illite-smectite	
		Mineralogy, Approx. Wt.% [X] (or) Relative Abundance [ ]																				
3188 Bulk		17	8	11		1	22						8	15	8		10				20	
3214 Bulk		36	22	6	2		24		tr				3	5	2		-					
4994 Bulk		36	30	8	14		4				4	tr	2	2	tr		-					
5004 Bulk		48	27	7	4		6		tr		3	1	2	2			-					
5006 Bulk		45	35	4	2		3				3		2	6			-					
5338 Bulk		41	26	13	7		4				5	1	3	tr			-					
5344 Bulk		26	28	5	34		3				2		2				-					
5356 Bulk		37	30	9	3		4				8	1	3	5			-					
5650 Bulk		33	25	5	3	1	5				4		5	19			-				15	
5651 Bulk		43	26	7	3		5				4		3	9			-					
5857 Bulk		47	22	5	1		5	8	1		1		2	8			-				<10	
5858 Bulk		47	20	5	1		6	8			1		5	7			-				<10	
5862 Bulk		61	17	7	1		2	3	tr		tr		3	6			-					
5903 Bulk		47	27	5	5	1	2	4			tr		3	6			-					
6092 Bulk		37	17	8	2		4	3	tr		3		4	22			-				20	

MM = Predominant M = Major m = Minor Tr = Trace ? = Tentative Identification

SUMMARY OF X-RAY DIFFRACTION ANALYSIS